UNIVERSITY OF THESSALY

SCHOOL OF ENGINEERING

DEPARTMENT OF MECHANICAL ENGINEER

THESIS

FAILURE DIAGNOSTICS AND RECYCLING OF SPENT LITHIUM ION BATTERIES

by

MARGONIS DIMITRIOS

PETSAS IOANNIS

Supervisor: Prof. Panagiotis Tsiakaras

Submitted in partial fulfillment of the requirements for the master's degree of diploma in Mechanical Engineering at the University of Thessaly

Volos, 2023

ΠΑΝΕΠΙΣΤΗΜΙΟ ΘΕΣΣΑΛΙΑΣ

ΠΟΛΥΤΕΧΝΙΚΗ ΣΧΟΛΗ

ΤΜΗΜΑ ΜΗΧΑΝΟΛΟΓΩΝ ΜΗΧΑΝΙΚΩΝ

ΔΙΠΛΩΜΑΤΙΚΗ ΕΡΓΑΣΙΑ

ΑΣΤΟΧΙΕΣ ΔΙΑΓΝΩΣΗ ΚΑΙ ΑΝΑΚΥΚΛΩΣΗ ΤΩΝ ΕΞΑΝΤΛΗΜΕΝΩΝ ΜΠΑΤΑΡΙΩΝ ΙΟΝΤΩΝ ΛΙΘΙΟΥ

υπό

ΜΑΡΓΩΝΗΣ ΔΗΜΗΤΡΙΟΣ

ΠΕΤΣΑΣ ΙΩΑΝΝΗΣ

Επιβλέπων: Καθ. Παναγίωτης Τσιακάρας

Υπεβλήθη για την εκπλήρωση μέρους των απαιτήσεων για την απόκτηση του

Μεταπτυχιακού Διπλώματος Μηχανολόγου Μηχανικού

Βόλος, 2023

Members of Examination Committee:

First Examiner (Supervisor)
Dr. Panagiotis Tsiakaras
Professor
Department of Mechanical Engineering
University of Thessaly

Third Examiner
Dr. Athanasios Papathanasiou
Professor
Department of Mechanical Engineering
University of Thessaly

Second Examiner
Dr. Angeliki Brouzgou
Assistant professor
Department of Energy Systems,
Faculty of Technology
University of Thessaly

ABSTRACT

With the increasing demand for energy storage systems, significant progress has been made in various electrochemical devices, with lithium-ion batteries being the most important. However, a significant portion of environmental impacts are occurred by the failures of lithium-ion batteries, and their non-recycling is a concern to a large part of the scientific community.

This paper focuses on the environmental consequences of energy production, followed by a discussion of the implications of lithium mining and the life cycle of a lithium-ion battery. Subsequently, various electrochemical devices for energy conversion and storage are reported.

The operating principle and components of lithium-ion batteries will be discussed in the following chapters. Failures that might occur and how to diagnose them will be addressed. The benefits and drawbacks of the numerous methods for recycling spent lithium-ion batteries will be highlighted.

Finally, some prospects for cathode and anode materials, as well as other components, will be gone through, and future data will be mentioned.

ΠΕΡΙΛΗΨΗ

Με την αυξανόμενη ζήτηση για συστήματα αποθήκευσης ενέργειας, σημαντική πρόοδος έχει σημειωθεί σε διάφορες ηλεκτροχημικές συσκευές, με τις μπαταρίες ιόντων λιθίου να είναι οι πιο σημαντικές. Ωστόσο, ένα σημαντικό μέρος των περιβαλλοντικών επιπτώσεων προκύπτει από τις αστοχίες των μπαταριών ιόντων λιθίου και η μη ανακύκλωσή τους απασχολεί μεγάλο μέρος της επιστημονικής κοινότητας.

Αυτή η εργασία εστιάζει στις περιβαλλοντικές συνέπειες της παραγωγής ενέργειας, ακολουθούμενη από μια συζήτηση των επιπτώσεων της εξόρυξης λιθίου και του κύκλου ζωής μιας μπαταρίας ιόντων λιθίου. Στη συνέχεια αναφέρονται διάφορες ηλεκτροχημικές συσκευές μετατροπής και αποθήκευσης ενέργειας.

Η αρχή λειτουργίας και τα εξαρτήματα των μπαταριών ιόντων λιθίου θα συζητηθούν στα επόμενα κεφάλαια. Οι αποτυχίες που μπορεί να προκύψουν και ο τρόπος διάγνωσής τους θα αντιμετωπιστούν. Θα επισημανθούν τα οφέλη και τα μειονεκτήματα των πολυάριθμων μεθόδων ανακύκλωσης χρησιμοποιημένων μπαταριών ιόντων λιθίου.

Τέλος, θα εξεταστούν ορισμένες προοπτικές για υλικά καθόδου και ανόδου, καθώς και άλλα εξαρτήματα και θα αναφερθούν μελλοντικά δεδομένα.

ACKNOWLEDGMENTS

Words cannot express our gratitude to our supervisor professor Tsiakaras Panagiotis, for his invaluable patience and feedback. His knowledge and experience helped us complete our thesis and we could not have undertaken this journey without his generous commitment.

Furthermore, we are grateful to Balkourani Georgia, who provided us with all the necessary feedback and for applying her knowledge to improve our work. We gratefully acknowledge the three-member examination committee consosting of Tsiakaras Panagiotis, Pappathanasiou Athanasios, and Brouzgou Aggeliki. In addition, we would like to acknowledge the University of Thessaly for providing us with the opportunity to join this wonderful master's degree program ''Analysis and Management of Energy Systems'' in which the cooperation with the professors and classmates were extraordinary.

We are also grateful to our parents Margonis Georgios, Hontou Fotini and Petsas Georgios, Tzianopoulou Eleni, who, with their mental and financial support, helped us complete both our undergraduate studies and our postgraduate studies at the University of Thessaly. Their belief in us has kept our spirit and motivation high during this process.

ΕΥΧΑΡΙΣΤΙΕΣ

Τα λόγια δεν μπορούν να εκφράσουν την ευγνωμοσύνη μας στον επιβλέποντα καθηγητή μας κ. Τσιακάρα Παναγιώτη για την ανεκτίμητη υπομονή και τις υποδείξεις του. Οι γνώσεις και η εμπειρία του μας βοήθησαν να ολοκληρώσουμε τη διπλωματική μας εργασία και δεν θα μπορούσαμε να εκπληρώσουμε αυτό το ταξίδι χωρίς τη γενναιόδωρη προσφορά του.

Επίσης είμαστε ευγνώμονες στη Μπαλκουράνη Γεωργία, η οποία μας παρείχε όλες τις απαραίτητες υποδείξεις αλλά και για την εφαρμογή των γνώσεών της ώστε να βελτιώσουμε την εργασία μας. Θα θέλαμε να ευχαριστήσουμε την τριμελή επιτροπή αποτελούμενη από τους Τσιακαρά Παναγιώτη, Παππαθανασίου Αθανασίου, και Μπρούζγου Αγγελική. Επιπλέον, θα θέλαμε να ευχαριστήσουμε το Πανεπιστήμιο Θεσσαλίας που μας έδωσε την ευκαιρία να συμμετάσχουμε σε αυτό το υπέροχο μεταπτυχιακό πρόγραμμα «Ανάλυση και Διαχείριση Ενεργειακών Συστημάτων» στο οποίο η συνεργασία με τους καθηγητές και τους συμμαθητές ήταν εξαιρετική.

Τέλος, θέλουμε να ευχαριστήσουμε τους γονείς μας Μαργώνη Γεώργιο, Χόντου Φωτεινή και Πέτσα Γεώργιο, Τζιανοπούλου Ελένη, οι οποίοι με την ψυχική και οικονομική τους υποστήριξη, μας βοήθησαν να ολοκληρώσουμε τόσο τις προπτυχιακές όσο και τις μεταπτυχιακές σπουδές μας στο Πανεπιστήμιο Θεσσαλίας. Η πίστη τους σε εμάς κράτησε το πνεύμα και το κίνητρό μας ψηλά κατά τη διάρκεια αυτής της διαδικασίας.

TABLE OF CONTENTS

LIST OF FIGURES

LIST OF TABLES

CHAPTER 1

Introduction

Alessandro Volta's battery, also known as a voltaic pile, was an early battery invented by Alessandro Volta in the late eighteenth century (**Figure 1.1**). It consists of a stack of alternating copper and zinc discs separated by layers of cardboard soaked in saltwater. The copper and zinc discs act as positive and negative electrodes, respectively, and the saltwater allows electric current to flow between them. The electric current produced by the voltaic pile is relatively weak. However, it was the first successful use of electricity as a power source and was a significant stepping stone in the development of modern batteries [1].

Figure 1.1. Illustration of the first battery [2].

After numerous phases and different kinds of batteries in 1985, Akira Yoshino developed an ion-lithium battery prototype. Then, Sony and Asahi Kasei developed a commercial Li-ion battery in 1991. The beginning of revolution in the sector of the battery has just begun. Long lifespan and the ability to recharge make them the primary source of energy for different small appliances. Even though there was expanded significant research on batteries over the years, its

objectives have remained constant. All battery scientists are required to preserve safety while keeping costs as low as possible while reducing the weight and size of the battery. Recent reviews on LIBs have given a comprehensive review of the technical and historical difficulties that we have to face on LIBs [3]. Lithium-ion batteries are the primary energy storage in our routine because of their variety of usage, even for electric cars. The future and their evolution will play a key role in improving the quality of people's life by reducing the usage of hydrocarbons in many energy sectors [1].

The significant rise in carbon emissions is a result of globalization and industrialization [4]. The massive carbon emissions harm our climate, causing harmful environmental changes and health problems. Over the coming decades, fossil fuels will continue to be necessary. How quickly, though, can we increase the use of alternative energy sources to combat climate change? [5].

Increased e-mobility and the ability to store renewable energy are two ways to address our difficulties in transitioning to a low-carbon economy [6]. Over the past two decades, lithium-ion batteries have proven to be a promising technology for practical energy storage [7]. The advantages of lithium-ion batteries over conventional rechargeable batteries include their high operating voltage, high specific energy, and long lifespan [8].

Although storing energy in lithium-ion batteries has many positive environmental effects, a rise in battery production will make waste management more difficult and stress the recycling infrastructure that already exists. Taking a preventative approach to managing future waste streams of used batteries is crucial. Battery recycling is essential as the lithium-ion batteries market expands to obtain valuable and scarce raw materials [9]. The current state of battery recycling is characterized by high costs and a lack of efficient technology [7]. In addition, because of the complexity of their component composition, lithium-ion batteries are more challenging to recycle than traditional batteries. Due to their classification as various hazardous materials, it is critical to follow all regulations [10]. An ideal recycling system from a sustainability perspective would enable a closed loop in which old batteries are used to create new ones [8].

Today, about 95% of lithium-ion batteries are landfilled after reaching the end of their useful lives, demonstrating that the recycling sector lags [11]. A competitive and sustainable industrial battery recycling sector will be needed to meet the rising demand for lithium-ion batteries. Currently, recycling companies are struggling to collect lithium, in particular, to

complete the supply chain for raw materials [12]. At the same time, battery manufacturers are under pressure from European regulations that mandate recycling 50% of the average battery weight [13].

In chapter 2, the current environmental impact of energy production will be discussed. An overview of energy sources' risk factors and environmental concerns will be referred to. Furthermore, an electrochemical overview and different electrochemical devices will be mentioned.

Afterwards, in chapter 3, the principle operation of batteries will be described. Battery chemistry, basic components of a typical battery and their importance in the operation of LIBs will be discussed. Moreover, different ways about the performance improvement of cathode materials, such as doping, and their results, will be stated.

In chapter 4, failures and diagnostics will be alluded to. Failures will be classified as internal and external, and the root of the cause will also be mentioned. In addition, the importance of BMS in the diagnostics of batteries and the principle operation will be referred to.

In chapter 5, the recycling process will be defined. The different methods of recycling, function and a comparison will be presented.

In chapter 6, future materials and prospects of LIBs will be discussed. Depending on the component of LIBs, different materials will be identified. Projections about supply demand and various other data will be examined as well.

Finally, in chapter 7, a summary of conclusions about using LIBs in our daily life, performance, and availability will be noted.

CHAPTER 2

Environmental impacts of energy production & electrochemical devices for energy conversion & storage

2.1 Introduction

Pollutants, dangers, accidents, and the deterioration of the environment's quality and natural ecosystems are only a few of the environmental issues linked to energy use. Our concerns, formerly primarily local or regional problems, have grown in scope over the past few decades due to increased energy use, with a growing understanding of the international and global scope of the most significant energy-related environmental challenges. Emerging environmental issues are becoming more noticeable, particularly in developing or recently industrialized nations where energy growth rates are frequently exceptionally high. Environmental management still needs to be appropriately integrated into the infrastructure. These can sometimes be chronic issues that are worsening, but they frequently signify acute or severe crises. Due to the minimal contribution of developing nations, industrialized nations are primarily accountable for air pollution, ozone depletion, and carbon emissions. Because energy use in underdeveloped countries is far less efficient than in more industrialized countries, there is a significant potential for energy efficiency. Significant adjustments must be made to how energy is produced and used. The promotion of the energy transition; improvement of energy efficiency in terms of conservation; support for renewable energy technologies; and support for environmentally friendly transportation systems are just a few examples of national and international programs that are taken into consideration [14].

2.1.1 Environmental Impacts of the Electricity System

Almost every component of the energy system has the potential to have an impact on the environment, and the severity of these effects will vary depending on where and how the electricity is produced. The environmental impacts can generally be broken down into the following categories:

• Emissions of greenhouse gases and other air pollutants, particularly when a fuel is burned; and

• Use water resources to generate steam, provide cooling, and perform other functions.

• Pollution discharged into bodies of water, particularly thermal pollution (water that is hotter than the actual temperature of the body of water).
• The generation of hazardous waste, which could also be solid.
• The use of land for the development of power plants, transmission lines, and distribution networks.
• The effects on plants, animals, and ecosystems are caused by air, water, waste, and land pollution.

Some of these environmental factors may also impact people's health, particularly if they expose individuals to toxins in the air, water, or soil [15].

2.1.2 Comparative overview—renewable vs. non-renewable energy sources

How fully committed are we to the significant important hydrocarbon energy source? The requirement for resources grows when people grow even more quickly than the average rate of 2%. While wealthy developed economies, which account for 25% of the world's population, consume 75% of the world's energy supply, high living standards and energy consumption rise together [16].

Environmental pollution, acid rain, depletion of the ozone layer, habitat loss, and nuclear releases are all issues related to energy consumption and supply. If society is to have a bright future with electricity that has minimal adverse effects on the environment, these issues must be tackled collectively. There is ample evidence that the future would suffer if people continued to try to change the climate. Specific environmental problems have been receiving more attention from the public and oil businesses. The notion that consumers are accountable for emissions and costs is becoming more widely accepted. Prices of these natural products have increased in many nations over the last one to two decades to offset environmental costs partially. The global population is expected to double by the middle of the twenty-first century, and economic growth will almost certainly continue to accelerate. By 2050, it is anticipated that the world's energy consumption will rise while primary oil production will expand 1.5–3-fold [17].

In the meantime, the issue will undoubtedly worsen energy-related environmental problems like acid rain, stratospheric ozone depletion, and climate change [18]. Increased usage of renewable energy resources and technology is one answer to the unavoidable lack of electricity. Infrastructure practicality, performance, applicability, environmental factors, material shortages, and public acceptance of the infrastructure will all be considered appropriately. The energy from all sources of power is constant. The moon, sun, and geothermal activity brought on by a significant soil decline produce tidal rise and fall. Although the concept is unknown, there

are potential energy sources. To develop a workable engineering solution, research funding is being invested in the project [19].

The easy part of understanding the mechanism from a scientific standpoint is comprehension; engineering is challenging to execute. Considering the claims above, we should learn that one of the crucial issues in debates on sustainable development is energy. There were many different ideas of sustainable development, with the following one in particular: "growth that meets present demands without compromising future generations [20]. A lot of reasons will contribute to the long-term expansion of the revolution. One of these essentials is the requirement for an entirely renewable energy supply. It is generally acknowledged that having a reliable energy source is necessary but insufficient for community development. The number of energy resources available determines the ability of a system to develop sufficiently frequently (freely and sustainably accessible for an affordable price in the long run, and that can be used for all essential purposes without negative social consequences), as well as how effectively and productively those resources are used. Renewable energy sources and environmental sustainability are starting to have a personal tie.

Table 2.1 Risk factors depending on the various types of renewable energy source [21].

Renewable Source	Pollution	Habitats lose/diversity	Invasive- alien species fauna	Overexploitation	Climate change
Wind	1	3,4	2	2	2
Solar	1	3	2	2	3
Hydro	1	1,3	3	3	3
Biofuels	1	1	3	3	1
Biomass energy	1	1	1	3	1
Ocean Energy	1	3,4	2	2	2
Geothermal	1	1,4	2	2	2

In **Table 2.1**, we describe the Risk factors of different renewable sources. Number 1 refers to ‘’Strong references for the existence of causality’’, number 2 refers ‘’Insignificant or weak references for the existence of causalities’’, 3 refers to ‘’ Contextual or inconclusive references about causalities (theoretically)’’ and 4 ‘’Sound, light, and heat pollution, including other non-chemical pollutants’’. As illustrated in **Figure 2.1**, many potential solutions to environmental challenges exist, and renewable energy technologies are essential for a sustainable future.

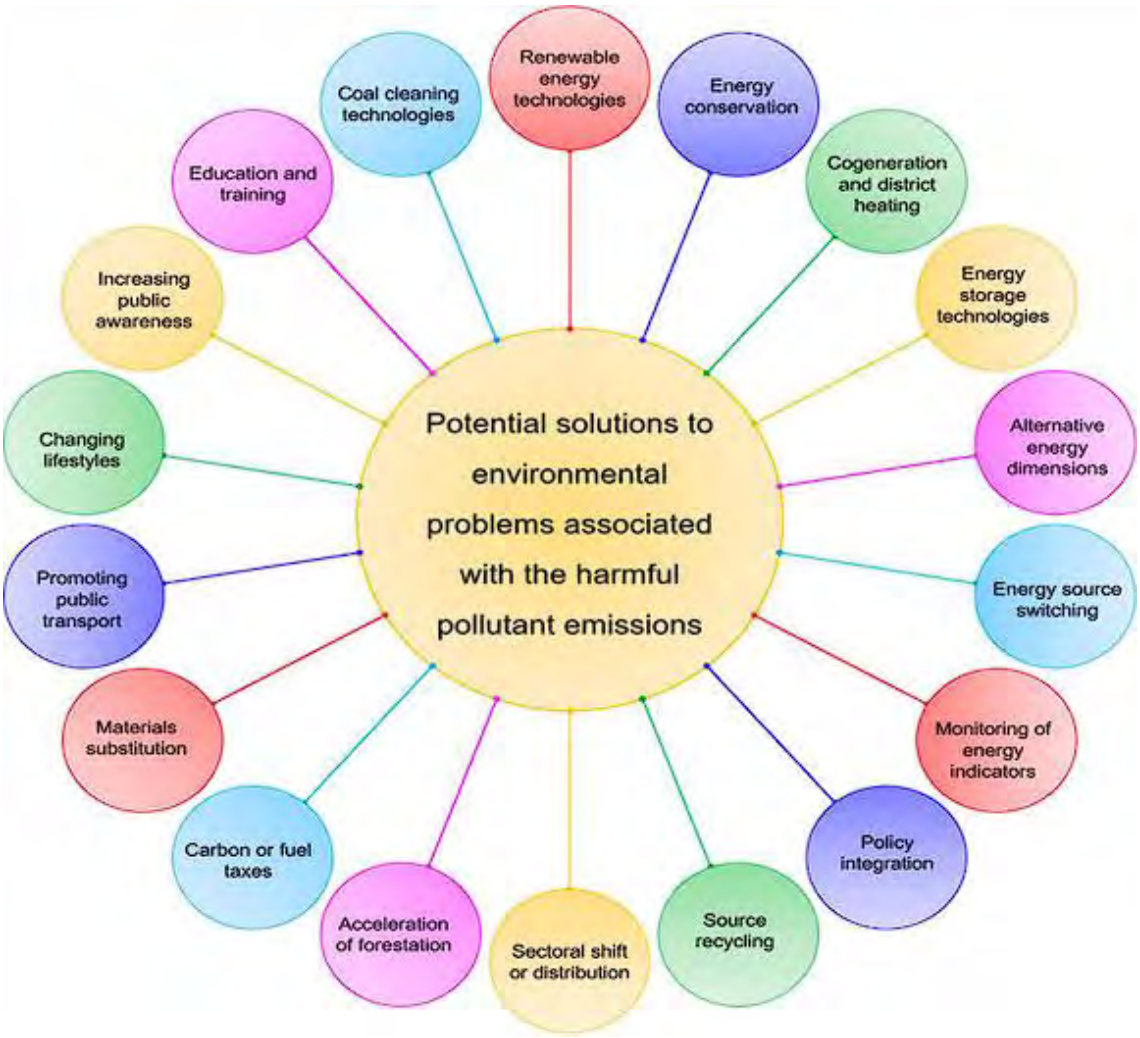

Figure 2.1. Potential solutions to environmental problems associated with the harmful pollutant emissions [21].

2.2 Environmental impact of libs

2.2.1 Introduction

Because of how lithium batteries are utilized now, there are significant economic and environmental issues. The tremendous demand for lithium and heavy metals like cobalt and nickel for energy storage and the anticipated future increase in demand have led to problems like natural resource strain and pollution caused by the exploration and processing of metals. The amount of readily available lithium may soon run out, and its price will increase if demand continues at its current rate. Even rare metals like lithium, cobalt, and nickel are in comparable

condition. These and other environmental problems brought on by the exploration, use, and disposal of LIBs are discussed in the following parts. Additionally, recycling tactics will be covered, providing several solutions to the economic and environmental problems caused by LIBs. For each of the significant LIB components, the previously investigated recycling procedures are presented, with an analysis of their benefits and drawbacks.

2.2.2 Environmental concerns of LIBs

Environmental concerns are connected to the extraction and processing of lithium sources. Still, pollution from the reckless disposal of lithium batteries—which contain toxic chemicals like heavy metals like nickel and cobalt—is even more significant [22]. Going back to lithium, its a metal that is in great demand and is a scarce resource. The economic and environmental issues mentioned above will become more severe when lithium resources are depleted. Over time, higher lithium prices will make it more desirable to extract low-concentration resources. This may still be more practical and accessible than recycling. Still, the mining, extraction, and purifying processes—which rely on energy use and industrial waste generation—could cause additional or substantial environmental harm [23,24]. As shown in **Figure 2.2**, lithium prices started to stabilize in 2019. However, over the following years, its price is expected to be increased further [25].

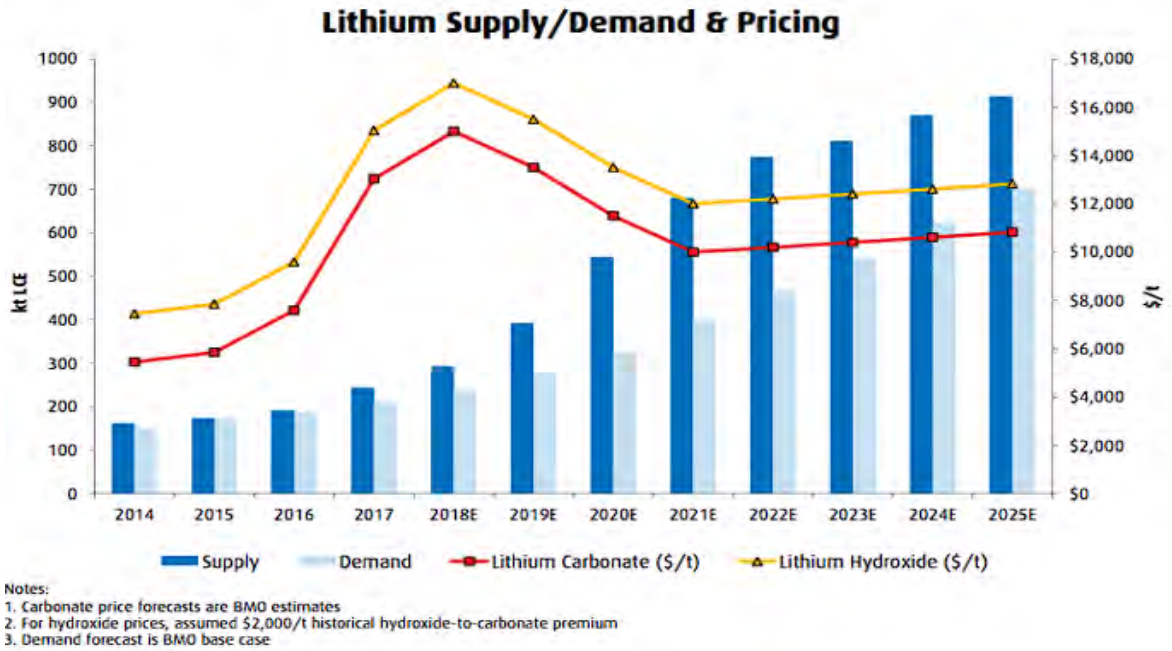

Figure 2.2. Lithium Supply/Demand and Pricing [26].

Despite the urgent need to utilize lithium and other metals needed by LIBs more effectively, only 10% of this sort of equipment and materials are recycled globally, which means that the other 90% ends up in landfills, rendering valuable materials unrecoverable.

Because the natural lithium reserves alone cannot supply the demand in the near future, this scenario needs to be corrected. The transition to the electric mobility concept, which aims to replace conventional internal combustion engine vehicles (ICEVs) with more environmentally friendly EVs, will be the key factor driving this demand. A European Commission study has demonstrated that an EV's emissions are much lower than those of an ICEV. This is especially true when the charge of the EV is done using renewable energy sources. As shown in **Figure 2.3**, around 12 GHG is produced when the wind is used as an energy source, followed respectively by a European mix of 20 GHG [27].

These findings, which are a direct result of an EV's substantially reduced component count compared to an ICEV, consider the environmental costs associated with the development and disposal of the batteries used in EVs.

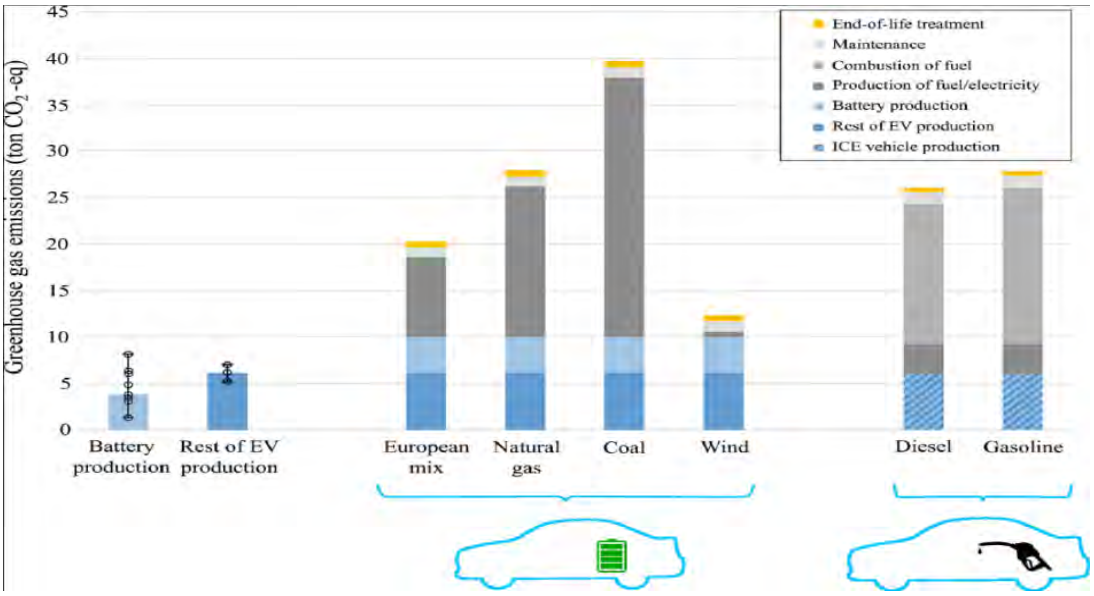

Figure 2.3. GHG emissions from the lifecycle of a mid-sized 24 kWh battery EV and ICE car. The vehicle's estimated operational lifetime is 150 000 km [27].

When battery manufacture is considered, EV production is more carbon-intensive than ICE vehicle production. Still, EVs can compensate for this at the use stage by using a higher renewable energy-based electrical mix. An estimated 0.4 Gt CO_2 reduction can be achieved by switching to batteries from ICEVs. By 2030, this reduction in CO_2 emissions might reach 2.2 Gt

CO_2 if renewable energy sources are also used [27]. Due to the factors mentioned above, it is anticipated that the demand for LIBs in the automotive industry will increase along with the expected growth of the EV market, which will increase the urgency of recycling used batteries to meet production chain demands and decrease spent battery disposal.

Although they have benefits, LIBs have a variety of environmental impacts, particularly during manufacture and towards the conclusion of their life cycle. Recycling and renewable energy sources can reduce the LIB industry's environmental impact. Recycling primarily safeguards the environment in two ways: by recovering valuable and rare materials. First, recovering metal cuts down on the need for mining and refining. Second, recycling reduces the amount of waste that is frequently harmful or non-biodegradable (due to toxic metals and some acids) [28].

Because they may be used several times, LIBs are superior to primary batteries for preserving natural resources because they prevent the extraction of additional resources to create new devices. However, the energy stored in batteries should also come mainly from renewable sources to manufacture truly ecologically acceptable LIBs. The economy must be decarbonized to lower greenhouse gas emissions. This can only be done by using clean and efficient energy sources. With such systems, batteries may be charged during times of high production and drained subsequently during times of higher demand. The most significant environmental implications of LIB manufacturing, use, deconstruction, and disposal are covered in this section.

A summary of the many stages considered in a LIB life cycle assessment. Life Cycle Assessment of LIBs (**Figure 2.4**) is a helpful tool in the product development phase to identify potential risks, environmental consequences, and key stages in the product life cycle [29]. The interactions between the various phases are displayed while taking into account the phases' production, use, and end-of-life cycles, as well as the additional opportunities that recycling and second-life utilization bring to the life-cycle assessment [30-32]. It enables the modulation of many theoretical scenarios, introducing various pertinent variables and comparing the outcomes potentially used in practice. Life Cycle Assessment also allows evaluation of the effects of multiple production chains and forecasts future industrial effects under various scenarios [33]. LCA demonstrates how many processes and parts contribute to each device's environmental impact, which opens the door to their replacement with more environmentally friendly ones and lessens the battery's overall ecological impact [34]. There are significant differences between LFP and LMO active materials in terms of how they affect the environment, particularly during the manufacturing phase, at the level of acidification and

eutrophication [26]. Assessing the effects on human health at various phases of a battery's life is also pertinent. However, getting all the necessary data might be challenging, so certain critical assumptions must occasionally be made, which can result in erroneous predictions [35].

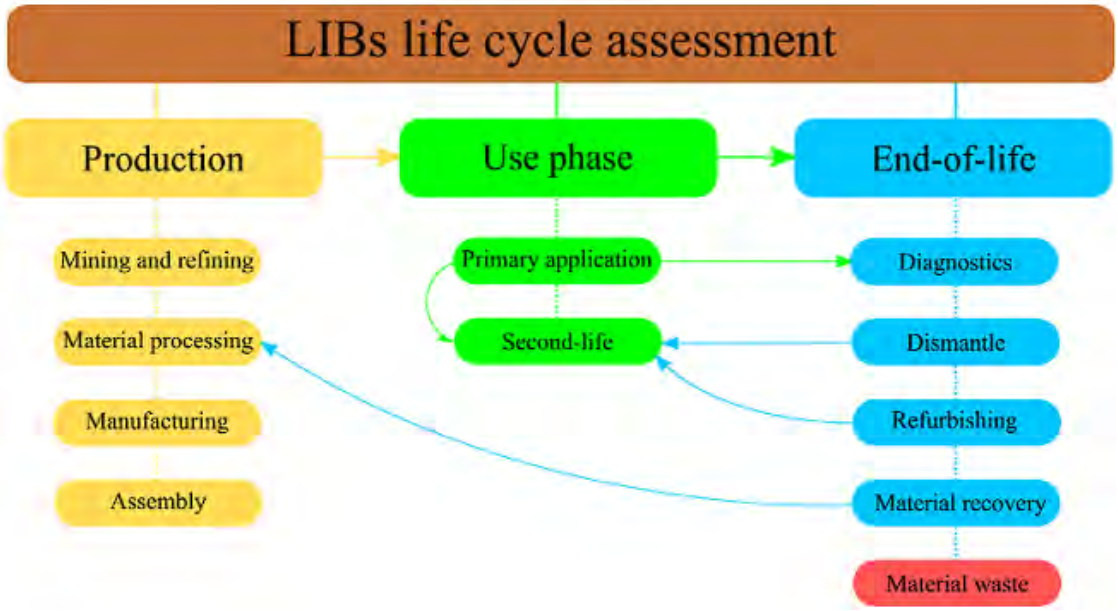

Figure 2.4. Diagram of a LCA analysis [36].

The life cycle of lithium-air batteries, for example, has been examined from the production of raw materials to the recycling process to assess the significant environmental impacts compared to those of other battery types and investigate their potential for a sustainable wide range of applications. The research demonstrates that the production stage has the most significant effects. However, fewer cells are produced as a result of increased cell efficiency. The new scenario's key impact factor is energy losses in the form of heat during the battery charge and discharge process. Lithium-air batteries have a 4–9 times lower environmental impact than the most advanced battery technologies. Recycling can reduce the environmental impact of manufacturing by 10% to 30%. However, as lithium-air batteries are no longer commonly utilized, there are currently no large-scale recycling techniques [37].

When comparing the advantages of recycling to mining and processing lithium and rare metals, it is essential to note that as demand for lithium rises; prices will increase as well, making it profitable to explore less accessible sources. Exploiting those inferior reserves, however, will negatively affect the explored areas. Finding alternatives to diversify energy storage systems and stop the intense exploitation of natural resources is consequently crucial. Future battery recycling

predictions predict a 50% reduction in our reliance on natural resources. Natural resources will still be required because not all items can be recycled [32,38].

When used in a circular economy setting, the disposal of used LIBs has a great deal of potential to reduce the amount of energy used to create new gadgets. This effect may be further amplified using wasted LIBs in stationary energy storage systems. However, it is not always economical to recycle and repurpose the resources from used LIBs. The recovery cost may be greater than the extraction cost of fresh materials depending on the battery type, and the components used [39].

The synthesis of materials, fabrication techniques, and waste management provide hazards and environmental problems in producing LIBs, just like in every other industrial operation. In a method called selective extraction, cathode waste from the commercial manufacture of LIBs can be processed to recover pure metals like Co, Ni, and Li. This method optimizes the use of mineral resources while considerably reducing the environmental impact of industrial battery production [40].

In addition, LIBs raise concerns about ecotoxicity and human health. Mistakes, overcharging, or overheating in malfunctioning or improperly operated LIBs can cause fires and explosions. Safety tests have been created to prevent these occurrences over the course of the battery life. However, the wide variety of devices used in these tests, each with a unique composition and set of features, leads to varying findings. As a result, occasionally, events still occur despite these safety procedures [41].

Additionally, many battery models have higher cobalt, copper, and nickel levels than recommended. In other cases, lead and thallium are even present, significantly increasing the ecotoxicity of LIBs. Other compounds used in LIBs include lithium manganese oxide and lithium cobalt oxide, both of which have been shown to have long-term chronic effects on particular populations of crustaceans [42].

The recycling capacity of LIBs has been compared to the current lead-acid and nickel-metal-hydride battery recycling systems. Secondary batteries are more easily recovered due to their similar composition and design, which enables the recovery of high-quality materials using essentially the same procedures, despite having environmental and operational advantages over them. However, many distinct types of LIBs and a wide variety of materials are involved, making it impossible to create "universal" recycling systems. Different methods have been suggested to recover certain materials from various battery types [10].

2.2.3 Lifetime environmental impacts

Based on an average of all LIB chemistries, supplying over the battery's lifespan, 1 kWh of electricity requires 0.26 kWh of energy from fossil fuels and results in 74 g. of GHG emissions only due to the production of the battery without considering internal efficiencies. Further research would also be needed regarding the impact of battery life on the vehicle's lifetime. The need for a battery replacement in an older electric vehicle might not be financially beneficial and be considered a constructive total loss and thus decrease vehicle lifetime. This could result in an even greater significance of battery lifetime.

2.3 Electrochemical Devices for Energy Conversion & Storage

2.3.1 Introduction

The two most important fields that have attracted a lot of interest from the scientific community that have emerged are energy harvesting and energy storage. Relying solely on fossil fuels confines generating energy to a particular field. Therefore, quick action is required to materialize the prospect of exploring several potential energy productions and harvesting possibilities. In this instance, recently, there has been a lot of interest in renewable energy sources. New technologies have been used for decades to improve the entire effectiveness of energy carrier generation, transmission, and distribution between industrial sectors and household customers. However, the difficulty persists since renewable energy sources are such covert resources. As it is shown in **Figure 2.5**, some common devices are fuel cells, batteries and supercapacitors [43].

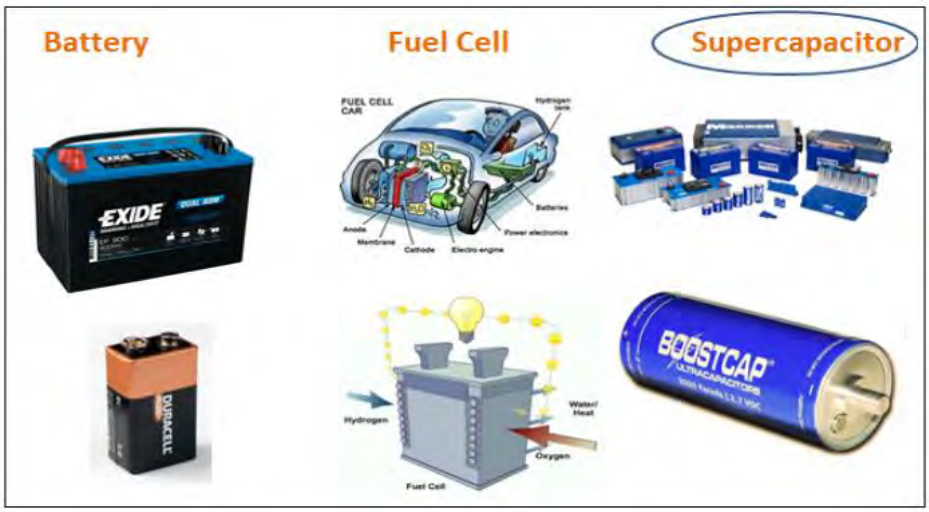

Figure 2.5. Types of electrochemical energy storage devices [43].

Consequently, numerous laboratory-scale techniques have been developed to consume dangerous gases like CO and CO_2, etc., to create synthetic fuels. It should be noted that, as these synthetic fuels need to reach a specific energy threshold before becoming useful, catalysts are typically used to get around this. Modern catalysts exist that can efficiently produce oxygen and hydrogen or convert carbon dioxide to organic fuels that can be recycled multiple times in the system. But because these state-of-the-art catalysts contain precious metals, scaling is limited. On the other hand, if the world wants to phase out fossil fuels in the future entirely, energy storage is a crucial factor to consider. This is feasible if dependable and stable energy storage technologies can be created along with energy harvesting. Electrical energy storage (EES) has been the main focus of research for the past few years because most energy sources generate electricity as the final form of energy carrier, which is subsequently distributed locally or transferred to distant sites. Due to the limited supply of lithium in the earth's crust, batteries, particularly Li-ion batteries currently used for electrical energy storage, are likely to be a short-term solution for EES. Many new materials, like gadolinium-doped barium cerates (Gd-doped $BaCeO_3$—BCG), which are solid electrolytic materials, are tested in electrochemical devices due to their strong protonic conductivity in hydrogen and water-containing atmospheres at temperatures between 600 and 900 °C. However, there are many issues with how these materials are prepared [44].

2.3.2 Electrochemistry overview

Electrochemistry illustrates the fundamental ideas of the presence and mobility of bulk electrons and the interfaces between Ionics, electronics, semiconductors, photonics, and dielectric materials. These concepts have implications for various scientific fields, including chemistry, engineering, biology, materials science, and environmental science. It performs the inverse as well of previously stated: the electrolytic removal of electricity from energetic compounds. In connection with the ion-containing electrolytic phase, the anode and cathode electrodes instantly conduct electricity in traditional electrolytic procedures. Anode and cathode electrodes produce specified chemical changes (oxidation and reduction, respectively) without using any hazardous chemicals, typically in settings similar to ambient temperature and pressure. For synthesis, separation, characterization, and pollution management, electrolysis can be cost-effective, computer-controllable, convenient, and selective. To help us with our high level of technological skill, sophisticated electrochemical cells and cell components are easily accessible on the market.

Furthermore, humans are bio-electrochemical machines that employ an electrochemical process to convert the sun's stored energy in food into muscular power. The electrochemistry area is separated into the following groups based on the prevalence of electrolytic phenomena in technology and gadgets. All of these technologies share the same underlying concepts, but their practical applications might vary considerably. For instance, cell designs, electrode materials and sizes, electrolytes, and separators may all be tailored to a specific application's requirements. Electrolysis should be favored in contrast to competing chemical routes since redox species are continually regenerated, and trace quantities of redox reagents are required without creating stoichiometric byproducts. A significant drawback of electrochemical technology is the high solubility of the reactants needed for a practical current density [45-48].

2.3.3 Electrochemical Rechargeable Batteries and Supercapacitors

An electrochemically rechargeable battery, sometimes called a secondary battery [10], is an energy storage device that uses electricity produced elsewhere to produce an electrochemical reaction (upward, positive G) at two electrodes, which is then released naturally, and this energy goes down. A wide assortment of rechargeable batteries is available from a variety of commercial sources. They can be used repeatedly to stabilize an electrical distribution network and are available in various sizes, forms, and energy/weight and energy/volume ratios. Batteries are good at providing high levels of energy. However, the energy they can store per unit of weight (50–1000 W kg-1) is no more important than that of fuel cells because batteries can, at best, consume all the material on their plate.

In contrast, all the chemical fuel available to fuel cells is converted into energy in fuel cells. Depending on how they are used, batteries have a different shelf life. Their use in applications like car starters, portable gadgets, light vehicles (such as electric wheelchairs, scooters, e-bikes, Etc.), equipment, and provide sustained energy to internal artificial organs (cardiac pacemakers, hard-of-hearing aid devices, Etc.) has had a transformative impact on our way of life. Industrial rechargeable batteries are utilized in grid energy storage facilities for load levelling, which is storing electric energy for times of high load. A capacitor is commonly known for providing large amounts of power but with a low capacity for energy storage, while a battery is typically used as a source of energy that has a lower output of power but a higher amount of energy storage.

A capacitor composed of two conducting plates and a dielectric, an insulator that allows current to flow through it ionically but not electrically [49].

2.3.4 Lead-Acid Batteries

French physicist Gaston Plante invented lead-acid batteries in 1959, revolutionizing the portable power industry [47]. Each cell's interior features a lead dioxide cathode, a metallic lead sponge anode, and a solution comprising 37% weight percent sulfuric acid as the electrolyte. They are made up of six cells with a nominal voltage of 2 volts.

At the anode, its primary discharge reaction is:

$$Pb + HSO_4^- \rightarrow PbSO_4 + H^+ + 2e^- \quad (2.1)$$

The reaction that occurs at the cathode when a discharge takes place is:

$$PbO_2 + 3H^+ + HSO_4^- + 2e^- \rightarrow PbSO_4 + 2H_2O \quad (2.2)$$

The total cell reaction has a thermodynamically reversible potential of 1.93 V, requiring fewer cells to reach a given potential. Lead-acid batteries with intermittent loads tend to be bulky and heavy, reduce their cycle life, and typically have a maximum available power of 50% Depth of Discharge for more powerful applications. These batteries have become the best choice for vehicle applications such as starting, lighting, and ignition due to their durability, resistance to abuse, and cost-effectiveness. The market for lead-acid batteries used as starting batteries for internal combustion engines is enormous. They rarely last longer than 4 years and can be recharged 300–400 times despite having reduced energy/weight ratios (35–40 $Wh\,kg^{-1}$) but better power/weight and energy/volume ratios. They are dangerous because of the heavy metals used in their construction, and if disposed of improperly, they could harm the environment [50,51].

2.3.5 Li-Ion Batteries

A LIB is a form of rechargeable battery that was invented by M. S. Whittingham of Binghamton University and Exxon in the 1970s. It uses lithium metal as the anode and titanium (II) sulfide as the cathode. Anode, cathode, and electrolyte are the main functional elements of LIBs [47]. Instead of having metallic lithium act as the anode in a lithium-ion battery, intercalated lithium compounds such as Li in porous carbon or graphite are used. Lithium ions move from the negative electrode to the positive electrode via the separator diaphragm and nonaqueous electrolyte during discharge and reverse the direction of travel during charging.

The cathodic half reaction of LIB is:

$$LiCoO_2 \leftrightarrow Li_{1-x}CoO_2 + xLi^+ + xe^- \quad (2.3)$$

The anodic half reaction of LIB is:

$$xLi^+ + xe^- + 6C \leftrightarrow Li_xC_6 \quad (2.4)$$

Recently, innovative architectures made with nanotechnology have been used to boost LIB performance. The basic properties of the electrode material are chemistry, performance, cost, and safety. Due to their high energy/weight ratios, lack of memory effect, and gradual loss of battery charge level when not in use, lithium-ion batteries (LIBs) are the most popular choice for power storage today. Because of their high energy density and increased interest in military, electric car, and aerospace applications, LIBs are becoming more and more attractive for use in portable devices.

The internal resistance of LIBs is higher than that of other rechargeable batteries, such as NiMH and NiCd batteries, and it rises with use and ages, decreasing the cell's capacity to provide current. High levels of charging combined with high temperatures (either from charging or the ambient air) will lead to a quicker decrease in battery capacity. Charging creates electrolyte deposits that prevent ion transport. The expected open-circuit voltage for a lithium iron phosphate cathode and graphite anode lithium-ion battery is 3.2V, while the usual charging voltage is 3.6V [52,53].

2.3.6 Zinc–Air Batteries

Zinc-air batteries [54] have certain characteristics with fuel cells, such as the consumption of zinc electrodes as fuel and the ability to regulate the reaction rate by changing the airflow. George W. Heise and Erwin A. Schumacher of the National Carbon Company created these cells in 1932, which marked the start of commercial manufacturing (US patent 1899615(A) dated January 28, 1933).

A zinc-air battery utilizes a carbon-based porous air electrode (cathode) that absorbs atmospheric oxygen. This oxygen is guided inside a gas-permeable yet liquid-tight membrane, which functions as a catalyst, to the zinc electrode (anode). This oxidation of the zinc releases electrons and generates a current, which in turn produces ZnO. The 1960s and 1970s were when these batteries were first invented, as shown in **Table 2.2**, in which other important characteristics such as cost of materials, valuable electrolytes depending on the type of battery and theoretical voltage and energy density are referred to.

Table 2.2. Comparison of Different Types of Metal-Air Batteries [55].

Battery Systems	Fe-Air	Zn-Air	Al-Air	Mg-Air	Na-Air	K-Air	Li-Air
Year Invented	1968	1878	1962	1966	2012	2013	1996
Cost of metals ($\$\ kg^{-1})^a$	0,40	1,85	1,75	2,75	1,70	~20	68
Theoretical Voltage (V)	1,28	1,65	2,71	3,09	2,27	2,48	2.96
Theoretical energy density ($Wh\ kg^{-1})^b$)	763	1086	2796	2840	1106	935	3458
Electrolyte for practical batteries	Alkaline	Alkaline	Alkaline or Saline	Saline	Aprotic	Aprotic	Aprotic
Practical Voltage (V)	~1,0	1,0-1,2	1,1-1,4	1,2-1,4	~2,2	~2,4	~2,6
Practical Energy Density ($Wh\ kg^{-1}$)	60-80	350-500	300-500	400-700	Unclear	Unclear	Unclear
Primary (P) or electrically rechargeable	R	R	P	P	R	R	R

At the Cathode (porous air-carbon electrode):

$$O_2 + 2H_2O + 4e^- \rightarrow 4OH^-(E_0 = 0{,}4\ V) \quad (2.5)$$

At the Anode:

$$Z_n + 4OH^- \rightarrow Z_n(OH)_4^{2-} + 2e^-(E_o = 1{,}25\ V) \quad (2.6)$$

The Fluid reaction:

$$Zn(OH)_4^{2-} \rightarrow Z_nO + H_2O + 2OH^- \quad (2.7)$$

The Overall reaction:

$$2Z_n + O_2 \rightarrow 2Z_nO\ (E_o = 1{,}65\ V) \quad (2.8)$$

Based on zinc active material, ZABs have a high gravimetric energy density of 1350 Wh/kg and a theoretical cell voltage of 1.65 V. To achieve longer lifetimes, practically all designs are tuned for 1.4 or 1.3 V. The foregoing reactions are reversed during the charging process, with oxygen released at the positive air electrode, and zinc oxide transformed back to zinc at the negative anode. When zinc is discharged, it is turned into zinc oxide (ZnO) and needs to be replenished by mechanical charging, which involves exchanging depleted zinc cartridges with new ones. As the charge-discharge cycles are repeated, the pores of the air electrode become slowly filled with liquid electrolytes, suppressing the air electrode's oxygen reactions. Due to the comparatively high stability and reversibility of zinc material, particularly in alkaline electrolytes, and its affordability and safety, zinc-air batteries (ZABs) have technological benefits over other metal-air battery systems. They can be designed into more useful large-scale (VE and fixed grid storage) and small-scale (portable and wearable devices) applications. However, the secondary (rechargeable) ZAB's commercialization has been hampered by issues with capacity retention and cycle life, primarily caused by zinc dendrite formation, shape

change during zinc regeneration, and subpar air electrode issues performance. Recent developments at Eos Energy Storage and Zinc Nyx Energy Solution, Inc. resulted in various long-life rechargeable zinc-air flow batteries that are predicted for use in various applications, including grids and VEs [56]. In addition, due to the sluggish four electrons, not fast kinetics of OER, a huge overpotential is important to start the reaction. A significant key role in the decrease of overpotential reaction is catalysis. However, due to the high price of Ir and Ru, which are used as efficient OER catalysis, different transition metal-based materials have a good effect on OER. The most well-researched metal that have replaced noble metals for OER is cobalt, but other methods, such as using W_2CoB_2 as an electrode material, have also been investigated. Zn -air batteries using W_2CoB_2-PT/C catalysis indicate a power density of 116.5 mW cm^{-2} and a long-life cycling stability of 200 h. In summary, Zn-air batteries play a significant role as an innovative technology for future energy demands due to their great theoretical energy density (1086 Wh kg^{-1}) [57-61].

2.3.7 Liquid Redox Batteries

A beta-alumina oxide ceramic ion conductor is used to separate molten anode and cathode materials, allowing for the formation of liquid-metal batteries. They are excellent for grid-scale storage, have a low cost of production, and have an incredibly high-power density. The 1980 invention of sodium-sulfur batteries (**Figure 2.6**) [62], which prime example of this type of technology is a cell with a molten sodium anode and a molten sulfur cathode that are separated from a conductive ceramic electrolyte made of sodium beta-alumina, a combination of eleven parts aluminum oxide Al2O3 and one part sodium oxide NaO with a melting point of 2100 °C.

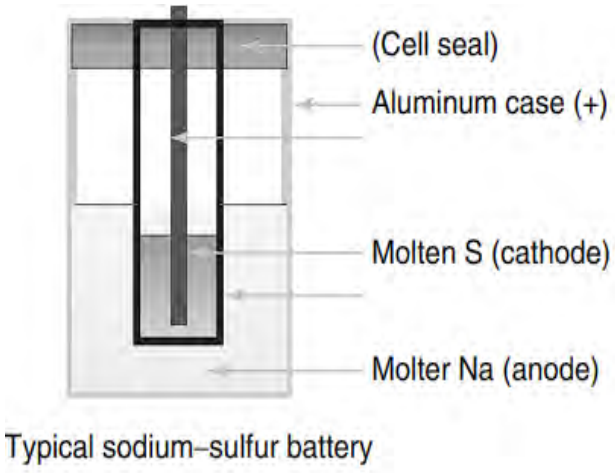

Figure 2.6. A diagram illustrating a standard sodium-sulfur battery as a liquid redox battery [62].

While sodium and sulfur melt at 98 °C and 113 °C, respectively, the operational temperature is around 350 °C. The sodium atoms' electrons are stripped during discharge, passing from the external load and toward the sulfur cathode. The sodium ions, which have a positive charge, go through the electrolyte, and interact with sulfur and electrons to create sodium polysulfide. Sodium polysulfide is stripped of its electrons during recharge, turning them back into sodium ions. Now that the sodium ions have crossed the electrolyte, they can form sodium atoms by reuniting with their lost electrons in the sodium. The sodium-sulfur battery can produce a huge amount of energy and power destiny (50–200 Wh/kg and 100–200 W/kg, respectively), but it only has a short shelf life (usually 2–5 years). While the solid electrolyte is vulnerable to mechanical deterioration due to the changing phase that appears as the sodium ions are decreased to the metallic state during cycling, batteries with liquid electroactive materials have the advantage of offering infinite life cycles to the active materials due to the lack of morphological changes.

2.3.8 Sensors

In our days, there are a various type of sensors that are necessary for example numerous technical processes in metallurgy, petrochemistry, and construction material manufacture take place at high temperatures. To lower the high power-intensity of those same processes, power inputs must be reduced, and fuel firing regimes optimized. The improvement of various fuel firing processes necessitates a dependable composition management of exhaust gases, particularly the presence of oxygen and incomplete combustion products. Stabilized zirconia gas sensors are widely utilized in transportation, industry, and scientific research. These instruments can test gas mixtures at high temperatures, including heavily dusty exhaust gases from thermal power plants, across a wide range of oxygen concentrations with high accuracy, pace, and without the need for sample preparation. These types of sensors based on YSZ solid electrolyte are conventionally used for gas analysis. Electrochemical oxygen sensors are divided into two main kinds: the potentiometric and type amperometric [63-71]. Some important characteristics for solid state sensors are:

- Transportation properties
- Ceramic properties
- Long term and chemical stability
- Thermomechanical properties [64].

Amperometric sensors can detect the concentration of gases for instance oxygen, hydrogen, water vapor, carbon monoxide, certain hydrocarbons, ammonia, and even in a variety of gas combinations [72]. Amperometric sensor is dependent on the measurement of electric current in which is related with the diffusion flow of the analyzed gas on the electrode [73]. In addition, a combination of amperometric and potentiometric sensor based on the $BaCe_{0.72}Zr_{0.1}Y_{0.2}O_{3-\delta}$ has been examined in which can be used for a hydrogen analysis at temperature range of 450 – 500 °C [67].
Glucose sensor, which is challenging for scientists today, and they play a key role in the measurement of glucose. The crucial prerequisites for the progress of any high-performance enzyme-less electrochemical sensor are:

- The existence of a large number of active sites as possible on the electrocatalytic surface area for the adsorption and diffusion of as many reactant molecules as possible,
- The high electrocatalytic active sites' capacity for the evolution of a multi-step electrooxidation reaction,
- Fast charge transfer [74,75].

Other types of sensors are electrochemical biosensors are biocatalytic which have enzymes and its role is to identify the target-analyte producing electroactive and affinity sensors which are dependent on the intercalation among a bioreceptor and the production of an electrical signal [76-78].

2.3.9 Light Fuel Generation and Storage

Experts in various fields have been keenly interested in light-fuel hydrogen as a potential clean energy source because it can generate energy without producing any pollutants and has one of the highest energy densities, with a value per mass of 140 MJ/kg. Most of the hydrogen utilized by industries comes from water splitting or fossil fuels. Only 4% of industrial hydrogen is produced by electrolysis, the least expensive method. Most industrial hydrogen demand is met by traditional sources such as coal, oil, and natural gas, producing about 10% carbon dioxide (CO_2) and hydrogen gas. It is critical to cultivating hydrogen technology by effectively producing hydrogen from renewable sources like solar and wind power through water splitting. Electrolysis for water splitting calls for the utilization of a costly proton exchange membrane (PEM) together with a liquid electrolyte (KOH), or a thermochemical process which necessitates a temperature in the range of 700-1000 ^{o}C.

It is well known that the steam reforming reaction can make hydrogen in a fuel processor from commonly available fuels (CnHmOp). The choice of technology is heavily influenced by the availability of feedstock, cost, and process byproducts (such as the quantity, quality, and purity of the steam produced). Alcohols are one of many fuels that can be converted to hydrogen. They are especially promising as fuel for fuel cells because they easily degrade in water and produce a hydrogen-rich mixture. Due to its easy production from renewable resources and comparatively high hydrogen concentration, bioethanol is particularly crucial [79].

2.4 Water Electrolysis

Alessandro Volta created the voltaic pile in 1800 for the electrolysis of water. Finally, Gramme machine, developed from Zenobe Gramme in 1869, made the electrolysis of water a low-cost method of hydrogen creation. Dmitry Lachinov created an industrial process for electrolyzing water in 1888 [80] that produced hydrogen and oxygen. The issue of resource scarcity and environmental degradation is getting worse as society's economy develops, and it is a direct threat to human life and advancement. The development of new renewable energy is imminent. Due to its lack of pollution, high energy density, and sustainability, hydrogen is regarded as the most viable replacement for non-renewable fossil fuels [81]. Synthesizing cost-efficient and robust bifunctional electrocatalysts for neutral and alkaline water splitting is highly desired but remains a significant challenge due to the sluggish hydrogen/oxygen evolution reaction (HER/OER) kinetics [81]. Water electrolysis is one of the most efficient methods for producing hydrogen at room temperature [82,83]. Two reactions are involved in the electrolysis of water: the oxygen evolution reaction (OER) at the anode and the hydrogen evolution reaction (HER) at the cathode [84,85]. One method to improve the performance of the HER is to place a three-dimensional metal network electrocatalyst consisting of a worm-like S-doped RhNi alloy (S-RhNi) [86]. Another simple method for creating a catalyst with high efficiency and low cost that is encapsulated is using carbon nanotubes grown in situ. The description of Ni particles on nickel foam should encourage more research into transition metal catalysts for hydrogen evolution in acidic settings [87]. Not all the electrical energy used in water electrolysis is converted to hydrogen's chemical energy. The four-electron oxidation of water to oxygen at the anode in a well-designed cell (**Figure 2.7**) required the highest overpotential. An efficient and affordable electrocatalyst has yet to be created to speed up this reaction. The standard state-of-the-art for this oxidation is platinum alloys. Pt and its alloys exhibit the best electrocatalytic activity with the highest exchange current density out of the many accessible catalysts. However, the large-scale generation of hydrogen faces significant obstacles

due to its high cost and limited supply. Numerous efforts have been made to create non-Pt electrocatalysts in response, including developing metal alloys, carbides, phosphides, borides, sulfides, and nitrides [88-94].

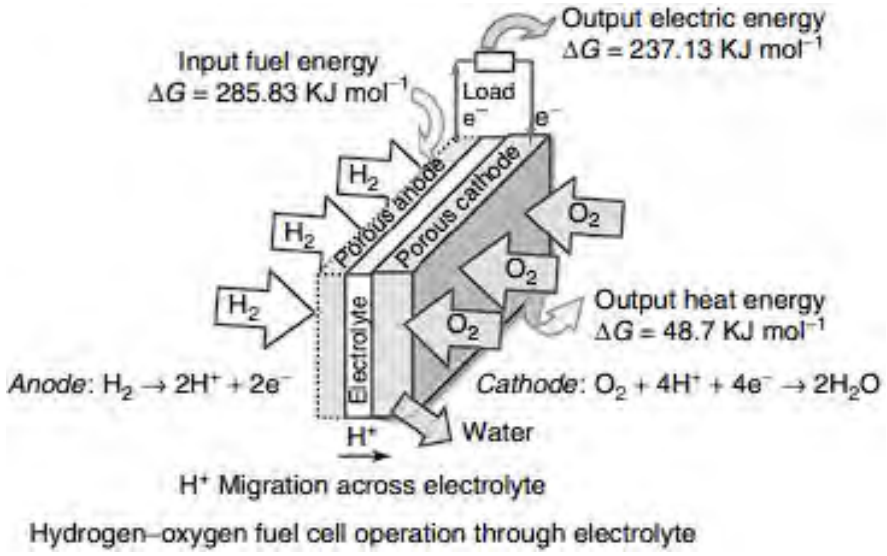

Figure 2.7. A Hydrogen-oxygen fuel cell uses electrolysis to separate water into hydrogen and oxygen, with chemical and energy processes at the electrodes and an electrolyte to help the process [95].

2.4.1 Electrochemistry of Water Splitting

An external electrical power source connects two electrodes the anode and the cathode, in a correctly designed water electrolysis cell. Hydrogen is produced at the cathode (the negatively charged electrode, where electrons reduce the water), and oxygen is produced at the anode (the positively charged electrode, where oxidation occurs) in a 2:1 ratio. The effectiveness of electrolysis can be improved by introducing an electrolyte (e.g., a Nafion solid polymer membrane, a strong acid such as H_2SO_4, or a strong base like NaO or KOH) and electrocatalysts. When combined with a unique catalyst on either side of the membrane, a solid polymer electrolyte like Nafion can split a water molecule with just a 1.8V power supply.

Reaction at the Anode:

$$2H_2O(1) \rightarrow 4H^+(aq) + 4e^- + O_2(g) \uparrow (E_A = -1{,}23\ eV) \quad (2.9)$$

Reaction at the Cathode:

$$2H^+(aq) + 2e^- \rightarrow H_2(g) \uparrow (E_c = 0{,}00V) \quad (2.1.1)$$

The water electrolysis cell has a standard potential of -1.23 V at 25° C at pH 0. This endothermic reaction, which can be quantified using the Nernst equation, will maintain -1.23 V

at 25 ºC even when the pH is 7. The change in Gibbs free energy for this reaction is ΔG = +2.46 eV or 237.2 kJ/mol. There is more Gibbs free energy present than usual in the electrolysis of water, as evidenced by the negative voltage. Supplying the system with energy in the correct amounts is necessary for both the breaking down of water, and the formation of gases. CoNi oxyhydroxide nanosheet catalysts, which provide high performance and stability in alkaline conditions, are another cost-effective method of water splitting [96].

2.4.2 Photoelectrochemical and Photocatalytic H2 Generation

Three basic steps are involved in a photocatalytic reaction: The photocatalyst draws in more energy from sunlight than the material's band gap energy, and this causes the photogenerated electrons and holes to separate and move to other areas of the photocatalyst's surface without recombining. This results in the reduction of water to produce H_2 and the oxidation of water to yield O_2.

Figure 2.8 illustrates a photocatalyst reaction to three different systems, particulate photocatalytic (PC) water splitting system, photoelectrochemical (PEC) water splitting system, and (C) photovoltaic-photoelectrochemical hybrid (PV-PEC) system indicated. Due to the huge single-plant photoproduction of pure hydrogen fuel, photoelectrochemical water splitting technology is financially beneficial for water electrolysis for electricity generation. Although titanium (TiO_2) was the first substance to be described as a photoelectrochemical water-splitting catalyst, it can function under UV light due to its large band gap of 3.2 eV. In 1972, Fujishima and Honda described an electrochemical cell for photoelectrochemical water splitting that consisted of an n-type TiO_2 (rutile) anode and a Pt black cathode [97,98].

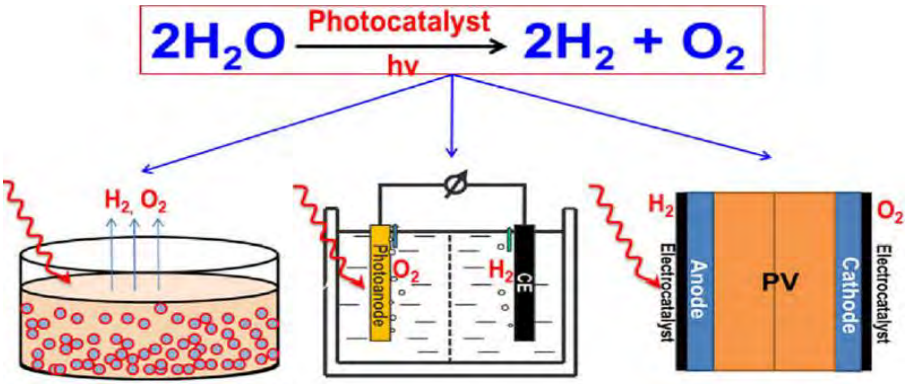

Figure 2.8. The solutions for solar hydrogen via water splitting. (A) Particulate photocatalytic (PC) water splitting system, (B) photoelectrochemical (PEC) water splitting system and (C) photovoltaic-photoelectrochemical hybrid (PV-PEC) system [99].

2.5 Fuel Cells: Fundamentals to Systems

Fuel cells are small electrical energy generators that use fuel (chemical energy) by oxidizing fuel (such as hydrogen, methanol, and hydrocarbons) at the anode and reducing oxygen (which is typically taken from the air and stirred into a solution) like an oxidant at the opposite cathode upon immersion in the electrolyte. The electrolyte is made precisely to permit ion passage but not electron passage. The electrical current is produced as the free electrons move through a wire. Fuel cells have a unique advantage over other energy-generating technologies. The free, very dense energy is instantly converted into pollution-free electrical energy without contributing to global warming. Fuel cells do not produce any unwanted byproducts (CO_2, SO_2, nitrogen oxides of nitrogen, or particulates) that are typically linked to the oxidation of fossil fuels in conventional energy conversion systems because no combustion reactions are engaged in them. Fuel cells are, therefore, eco-friendly. However, compared to batteries, which need to be recharged after use, fuel cells have the added benefits of being lighter, quieter, cleaner, and vibration-free. They are favored options for usage as complements to batteries because of these factors. Fuel cells have the potential to be a viable replacement for internal combustion engines in cars due to their energy efficiency, cleanliness, and the fact that they can run on different fuels. Moreover, direct fuel cells, victual hydrocarbons into the fuel cell stack without needing a reformer to produce hydrogen [100-102].

Fuel cells can be sorted into two types based on their operating temperature and the electrolyte they use. Low-temperature fuel cells include alkaline, proton exchange membrane fuel cells (PEMFC), direct methanol fuel cells (DMFC), and solid oxide fuel cells. High-temperature fuel cells consist of phosphoric acid (PAFC), molten salt, and solid oxide fuel cells. This categorised is illustrated in **Figure 2.9**. Metal-organic frameworks (MOFs), also known as coordination polymers (CPs), are a new class of functional materials in catalysis, chemical separation, sensors, gas storage, nonlinear optics, etc. They are constructed from metal centers and organic linkers that extend "infinitely" in at least one dimension. MOFs have advantages due to their surface area, controlled structure, and clearly defined and organized linkages. A unique self-sacrifice template method for preparing carbon materials for electrochemical energy applications has recently emerged through the pyrolysis of porous MOFs. The benefits of the carbon materials made from MOFs include:

i) Atom-level compositional control: uniform atom distribution in heteroatom-doped carbon as a result of regular organic linker crystallization and distinct MOF precursor structure

ii) Pore structure: due to tuneable morphology and uniformly dispersed metal or metal oxide as pore-forming agents, large specific surface areas and hierarchical mesopores are formed.

When creating non-Pt electrocatalysts for the oxygen reduction process (ORR), these characteristics may have favorable effects on both the kinetics and mass transfer [103].

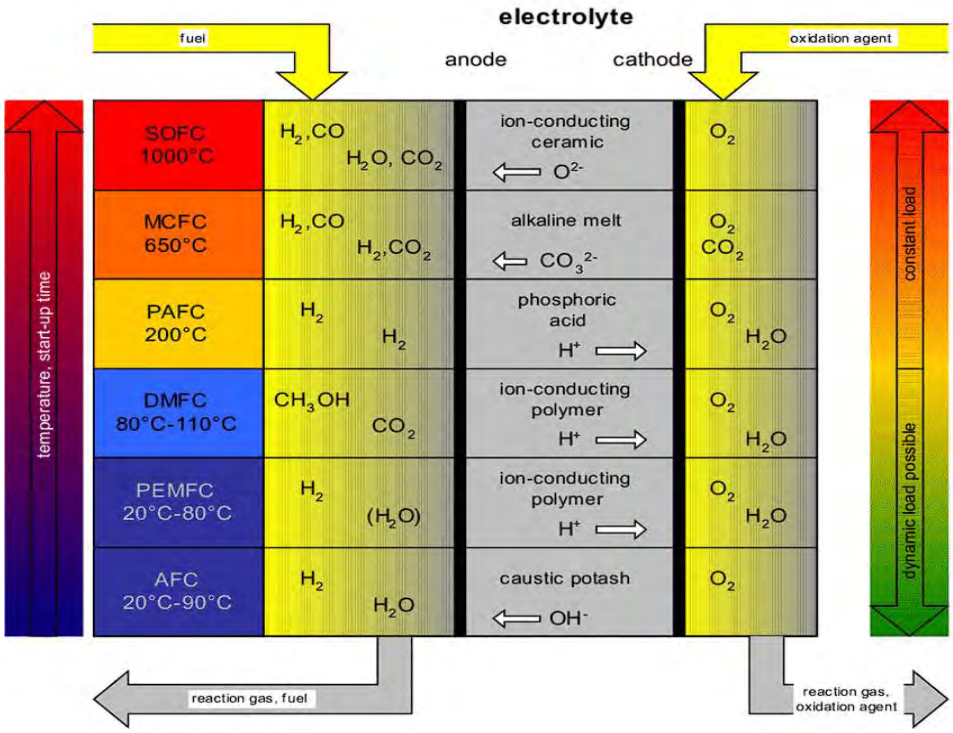

Figure 2.9. Overview of the various types of fuel cell technology [104].

2.5.1 Low temperature fuel cells

2.5.1.1 Alkaline Fuel Cells

Alkaline fuel cells are economical to provide power from 10-100 kW and require only basic solutions such as electrolytes. They also work optimally at 80°C and have a 60-70% cell efficiency. However, for fuel cells that use acid solutions or high temperatures, only noble metals can be used as electrode materials, whereas alkaline fuel cells have a wide range of electrode catalysts available (which are relatively). In contrast to intermediate- and high-temperature cells, which require an additional power source to start and warm up, they may provide roughly 25% of the power needed at optimal temperature when they are first turned on. The disadvantage of AFCs is that CO_2-free air is utilized in cells since air containing CO_2 and O_2 creates carbonates in an alkaline solution and obstructs the pores of porous electrodes. AFCs, which only need H_2 and O_2, were the bacteria cells employed in the Apollo lunar project [105]. Due to its high alkaline

hydroxide conductibility, liquid potassium hydroxide (KOH) electrolyte solutions are used in AFCs, as shown in **Figure 2.10** [106].

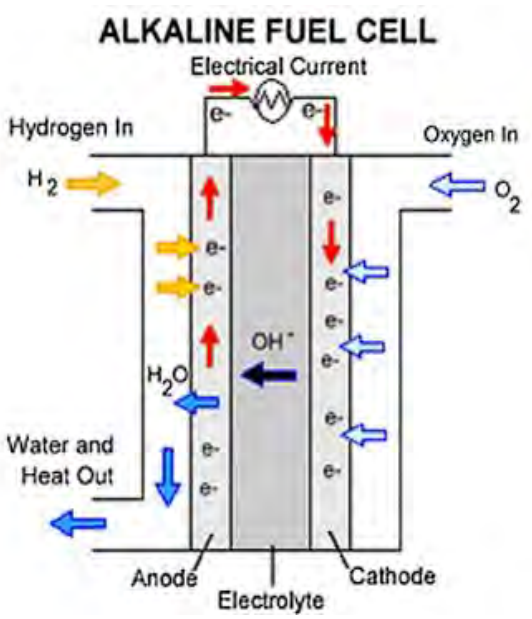

Figure 2.10. Schematic representation of an alkaline fuel cell [106].

2.5.1.2 Proton Exchange Membrane Fuel Cells

The proton-conducting electrolyte, which divides the anode and cathode sides in the classic PEMFC design, was first referred to as a "solid polymer electrolyte fuel cell" (SPEFC) in the early 1970s before the proton exchange process was fully appreciated. The bipolar electrode plates in a standard membrane electrode assembly (MEA) are often constructed of noble metals, nickel, or carbon nanotubes and coated with a catalyst for greater efficiency (such as platinum, nanoiron particles, or palladium) [107,108]. As an encouraging alternative to their costlier Pt-containing equivalents for the oxygen reduction process, Fe-N-C-based electrocatalysts (ORR) have been created [109]. They are separated from the electrolyte using carbon sheets. PEMFCs have a cell efficiency of about 40–70% and can generate 100–500 kW of electricity at temperatures as low as 50–120 °C (for Nafion) and as high as 120–220 °C. Currently, fuels generated from either natural gas or biomass, including ethanol, butanol, hydrogen, and methanol. PEM devices use stored hydrogen gas to operate, but they are still considered the most common choice. As part of Project Gemini, a NASA space mission, PEM systems made their first significant advancement. Their distinctiveness lies in their slim profile, lightweight construction, quick start-up and employment of a solid electrolyte instead of a liquid one [108].

Using a solid electrolyte instead of a liquid makes it simpler and less expensive to seal the anode and cathode gases. This can extend the cell's life span and stack, as solid electrolytes are less vulnerable to corrosion than other types of electrolytes. Other advantages include compact design, lightweight, and rapid start-up. Low operation temperatures of about 80 °C, which are insufficient for effective cogeneration, are the main drawbacks of PEM, though.

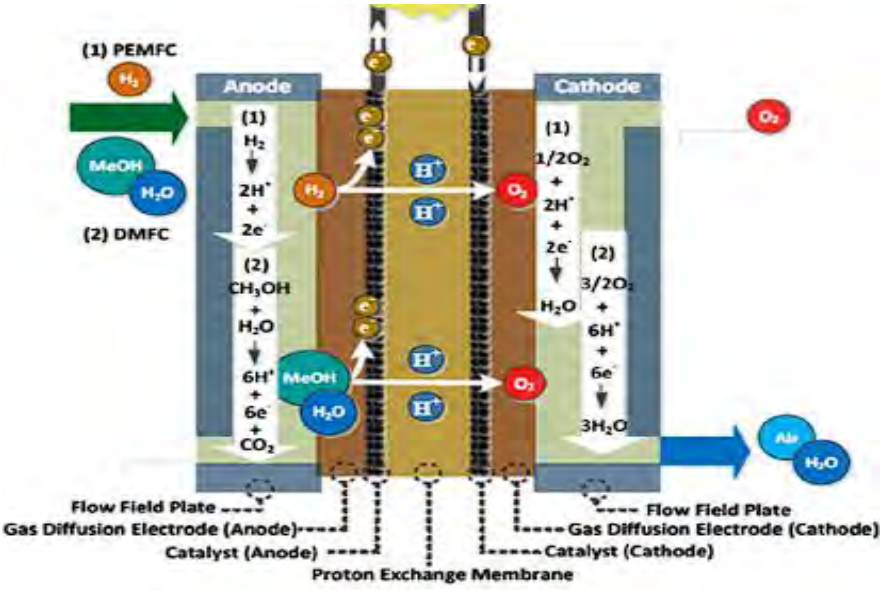

Figure 2.11. Schematic representation of a proton exchange membrane fuel cell (PEMFC) (1) and Direct Methanol Fuel Cells (DMFCs) (2) [110].

For the cell to operate optimally, the electrolyte is necessary to saturate with water; if not, the membrane will break, resulting in the breakdown of the cell. Controlling and managing the humidity levels in the anode and cathode streams is essential. **Figure 2.11** shows a schematic representation of a PEMFC [111]. Direct methanol fuel cells (DMFC) and hydrogen fuel cells are the two different forms of proton exchange membrane fuel cells that both use proton exchange membrane to transport protons [108,112-114].

2.5.1.3 Direct Methanol Fuel Cells

DMFCs have the ability to generate a minimal amount of power for a long time. These fuel cells are able to generate between 100 mW and 1 kW of power with a 20-30% efficiency. The DMFCs were a great choice for very small to medium-sized applications. That’s because they have a high energy density, operate almost at room temperature, operate longer than rechargeable batteries, instantly recharge by merely changing the disposable fuel cartridge, are non-toxic to discard, are

lightweight, and have a high energy density [94,115]. Direct Methanol Fuel Cells systems are used to provide energy for a variety of applications, such as smaller vehicles like forklifts and tuggers, mobile energy sources for domestic purposes, cellular devices, digital imaging tools, notebook computers, audio systems, soldier-mounted operational tools, battery rechargers, and independent energy sources for testing and instruction equipment [116,117]. In Direct Methanol Fuel Cells (**Figure 2.11**, (2)), the methanol [102] and water solution is delivered to the anode, where the catalyst internally reforms it and oxidizes it to release electrons and protons [114,118,119].

2.5.2 High temperature fuel cells

2.5.2.1 Phosphoric Acid Fuel Cells (PAFCs)

Approximately 100 MW of electricity may be generated using molten phosphoric acid (H_3PO_4) fuel cells at an operating temperature of 150–220 °C and 80% cell efficiency. When utilized as the electrolyte in PAFCs, pyrophosphoric acid ($H_4P_2O_7$), a polymer of phosphoric acid typically generated at around 150 °C, causes an ionic solution with a significantly higher conductivity than the parent acid. In Proton Exchange Membrane Fuel Cells (PEMFCs), the hydrogen injected at the anode is split into protons and electrons, with the protons serving as the charge carriers. Water is created when oxygen, typically obtained from air, is combined with protons that have moved through the electrolyte to the cathode. Electrons are also directed to the cathode, which can be used via an external circuit. In the fuel cell, the series of processes described below result in heat production as a byproduct and electricity [120,121].

2.5.2.2 Molten Carbonate Fuel Cells

According to **Figure 2.12**, MCFCs are high-temperature fuel cells that use an electrolyte made of a molten salt mixture of carbonates (salt of sodium or magnesium carbonate) floating in a porous, chemically inert ceramic lithium aluminum oxide ($LiAlO_2$) matrix. When the electrolytes in MCFCs are heated, salts melt at 650 °C, conducting carbonate ions (CO_3^{2-})from the cathode to the anode [122]. A hydrogen oxidation reaction involving carbonate ions and the anode results in the production of water and carbon dioxide, and the release of electrons to the external circuit. In the cathode, oxygen is reduced to carbonate ions by combining carbon dioxide and electrons from the external circuit.

These cells operate at a high temperature, which reduces damage from carbon monoxide poisoning and allows waste heat to be recovered to produce more electricity [123]. Durability is

the main drawback of the present MCFC technology. High operating temperatures and corrosive electrolytes cause accelerated component deterioration and cell life. Scholars are exploring designs of fuel cells that could prolong their lifespan without compromising output and corrosion-resistant materials to construct components [124].

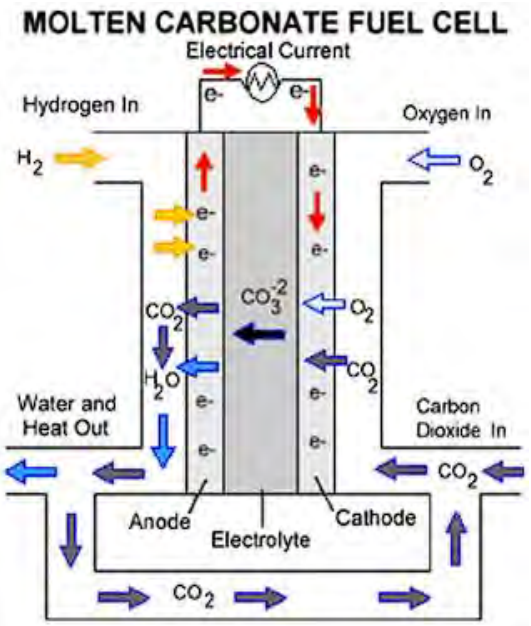

Figure 2.12. Schematic representation of a Molten Carbonate Fuel Cell [124].

2.5.2.3 Solid Oxide Fuel Cells

Solid oxide fuel cells (SOFCs) are well-known electrochemical systems that directly transform the chemical energy of a fuel into electricity. Due to their independence, high efficiency, variety of fuels (which includes the ability to use biogas and natural gas, among others), and environmental safety, SOFCs have a significant advantage over conventional energy production systems. Based on SOFCs, significant efforts have been made to create commercially feasible generators with low costs and long-term stability. By decreasing the operating temperature to the intermediate temperature (IT) range of 400–750 ^{o}C, this issue can be successfully resolved while allowing the use of less expensive electrode and interconnector materials and inhibiting stack degradation [125,126].

The ideal applications for solid oxide fuel cells (SOFCs) are large-scale stationary power generators that can supply electricity to communities and enterprises [127]. As seen in **Figure 2.13**, the electrolyte for SOFCs is often a hard ceramic metal compound, like calcium oxide or

zirconium oxide [128]. The active fuels in SOFCs can be hydrogen [129] or carbon monoxide. The predicted efficiency of SOFCs in converting fuel to electricity is between 50% and 60%.

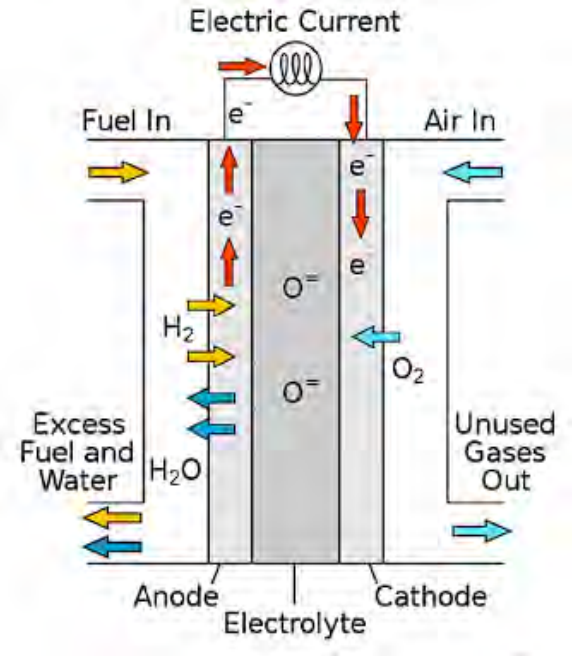

Figure 2.13. Schematic representation of a Solid Oxide Fuel Cell [124].

Creating novel electrolyte types with sufficient conductivity and stability at lower temperatures is necessary to lower the operating temperature of SOFCs. Thus, novel techniques for their preparation are also needed. Due to their excellent protonic conductivity at lower temperatures than O_2 conducting electrolytes like YSZ [101], proton conducting conductors like $BaCeO_3$, $SrZrO_3$, and $BaZrO_3$ are seen as good options for intermediate temperature SOFC electrolyte materials [129].

CHAPTER 3

Principal Operation of Lithium-Ion Batteries

3.1 Introduction

There has been a rapid increase in energy need for more efficient, cost-effective, environmentally friendly, and long-term energy storage solutions. Li-ion batteries have been the piler for the digital electronic revolution in today's mobile society, solely employed in consumer devices, including smart phones and laptops, drawing international attention [130,131].

LIBs have ruled the global market for electronic products, particularly laptops and mobile phones, since their commercial beginnings in the 1990s [130,131]. In addition, LIBs can be used in Electric cars, electric-powered undersea vehicles, and aircraft [132]. As seen in **Figure 3.1**, Bloomberg New Energy Finance noted that the use of LIBs has grown significantly and is projected to continue to rise [133].

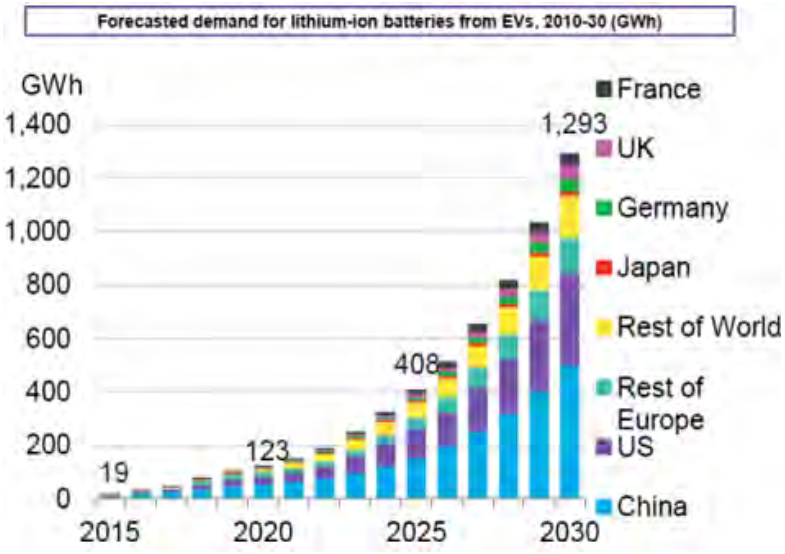

Figure 3.1. Prediction of lithium-ion battery usage [133].

Substantial research is required to comprehend faults and fatigue damage of LiBs to enhance durability, trustworthiness, and reduced replacement price with substantial improvement of characteristics such as higher specific energy and volume energy density, cyclability, charging rate, stability, and safeness [134]. Indeed, stronger Li-ion batteries with increased endurance and

cheaper costs are already in high demand due to the rising capability of mobile gadgets and the expanding market for electric cars.

Compared to other conventional rechargeable batteries, LiBs have a few key benefits. First, because of its low reduction potential, Li gives the maximum cell potential for Li-based batteries. Furthermore, because Lithium is the third lightest element, Li-based batteries have a significant gravimetric and volumetric capacity [135]. **Figure 3.2** depicts the energy densities of several existing batteries, demonstrating LiBs' advantage; although Lithium batteries offer a higher energy density than LiBs, their low recharging capability and safety issues are significant negatives [133].

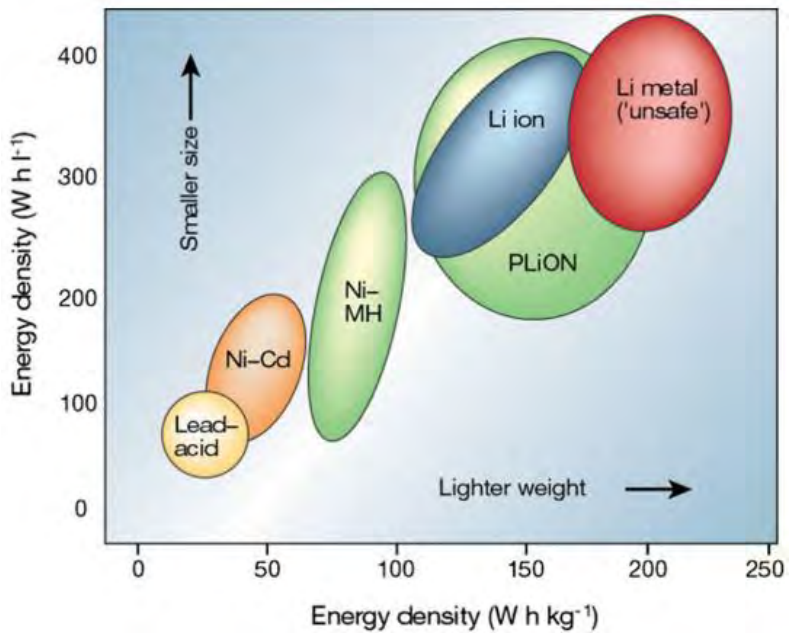

Figure 3.2. Energy density of different batteries [133].

For a more incredible view, reviewing the evolution of Li-ion batteries during the last 30 years may be helpful. Whittingham suggested lithium batteries at Exxon in the 1970s [52]. The electrode materials that Whittingham used were titanium and lithium metal. However, this rechargeable lithium battery was not a commercial success because of the expensive cost of titanium and some other safety concerns [136]. Bernhard Lithium suggested bidirectional intercalation of Lithium in graphite and intercalation in cathodic oxides as Lithium cells in 1974 - 1976 [137-140]. The primary limitations for the battery's lifetime were electrolyte breakdown and solvent intercalation into graphite [141,142]. In 1979 and 1980, Godshall and Goodenough & Mizushima devised and demonstrated a Lithium cell with voltage through Lithium metal as

the anode and Lithium Cobalt oxide as the cathode. Lithium batteries became economically viable due to advancements in cathode material [143,144].

In 1980, the reversible electrochemical intercalation of Lithium in graphite was demonstrated by Yazami, making it the most preferred electrode in commercial LiBs [145]. In 1982, Godshall was granted a US Patent for using $LiCoO_2$ as cathodes [146]. In 1983 Thackeray et al. expanded the manganese spinel as a cathode material. Due to its low cost, superior electrical lithium-ion conductivity, and 3D structure, manganese spinel cathode material was promising because of its structural stability and optimal performance[147]. Yoshino created a Li battery cell in 1985 using carbonaceous compounds where lithium-ions may be injected as one electrode.

Furthermore, $LiCoO_2$ is stable in the air [148]. $LiCoO_2$ enabled industrial-scale manufacture and is often considered the origin of the present Li-ion battery. Yoshino's breakthrough has been hailed as a watershed moment in commercial Li-ion battery development [149]. In 1991, Sony and Asahi Kasei introduced the first LiBs that were able to find on the market. In 1996, Goodenough suggested using lithium iron phosphate ($LiFePO_4$) as positive electrode material [150]. In 2016, LiBs represented 83% of all recently launched energy storage system capacity globally [151].

3.2 Principal operation of Lithium-ion Batteries

Before we start explaining the operation of LIBs, we have to ask: What is a battery? A battery is a device that produces electricity by using the chemical energy inside it. This conversion happens by using the phenomenon of electrochemistry in which electrical equipment such as electrode anodes and cathodes take advantage of those chemical reactions inside the battery [49].

3.3 Battery chemistry and charging/discharging

The main components that a lithium-ion battery has are the negative electrode (anode), a positive electrode (cathode) and the electrolyte. Between the two electrodes, anode, and cathode, is the electrolyte which includes a solution of lithium salts allowing Li-ion transport between them. An external load is used to send electrons from the anode to the cathode during discharging. In **Figure 3.3**, Li electrons flow from the anode to the cathode in the electrolyte simultaneously. The charging process is reversed, with electrons moving from cathode to anode and Li ions moving in the same direction across the electrolyte. This method will store incoming

energy as chemical energy in the anode and cathode. Usually, for construction of a lithium-ion battery, a typical element that is used in the cathode materials is Lithium molybdenite $LiMO_2$ reactions with M as a transition metal by the chemical reaction pathway described below [152],

$$LiMO_2 \Leftrightarrow xLi^+ + xe^- + Li_{1-x}MO_2 \quad (3.1)$$

The formula for the carbon materials in negative electrode (anode) is expressed by:

$$xLiC_6 \Leftrightarrow xLi^+ + xe^- + XC_6 \quad (3.2)$$

The total formula for a completed Lithium-ion battery is expressed by:

$$LiMO_2 + C_6 \Leftrightarrow Li_{1-x}MO_2 + Li_xC_6 \quad (x = 0.5 - 3.7\ V) \quad (3.3)$$

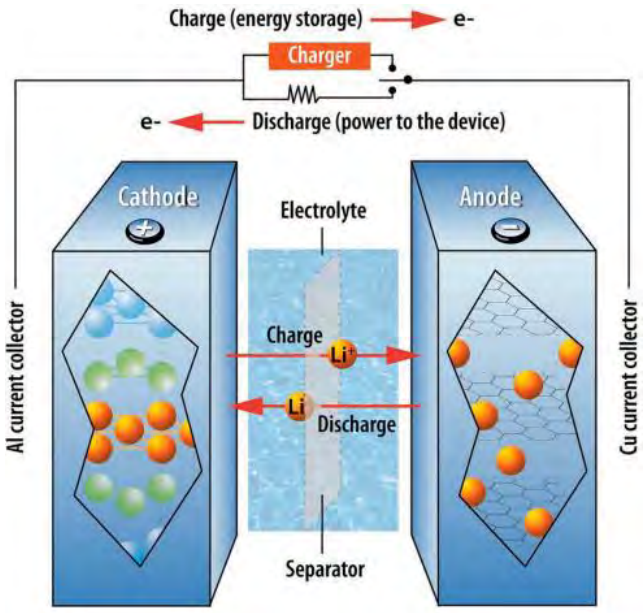

Figure 3.3. Operation of a Lithium-ion Battery [153].

3.4 Cell Structure

3.4.1 Anode

The anode is a critical component of a rechargeable battery, and its characteristics and shape significantly impact the battery's total operation. Graphite is utilized in the majority anode market because of its distinctive hierarchical structure. Once lithium ions are embedded in graphite, the relatively broad interstice among two adjacent layers of carbon atoms provides entry places for the lithium ions, keeping the anode material's form, diameter, and structure from altering during the charged-discharge process. Other unique pathways for lithium-ion exchanges

have been investigated in addition to the usual mode. Displaced reactions in alloy anodes and redox reactions are examples of such processes [154,155].

Other carbon-based compounds that have received much interest include buckminsterfullerene, graphene, and nanotubes (see **Figure 3.4**). Specific carbon nanotubes (CNTs) have been discovered to have extraordinarily high electrical conductivity and other unique properties linked to the structure or aligning of the nanotubes [156,157].

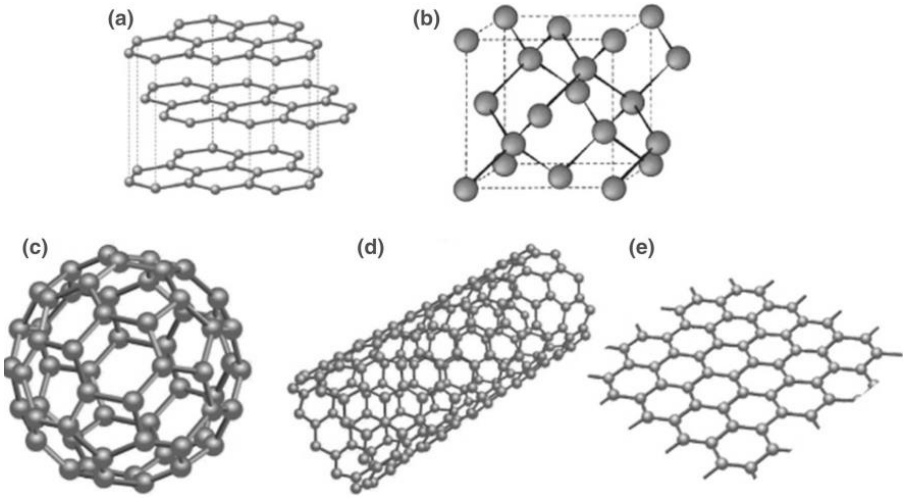

Figure 3.4. Various carbon ordered structures a) graphite, b) diamond, c) 0 D, buckminsterfullerene (C60), d) nanotube and e) graphene [158].

To measure and evaluate battery efficiency, specific characteristics are highlighted in LIB experiments. These are examples of rate capacity, coulombic efficiency, and reversible/irreversible capacity. Previously, it was considered that the exceptional rechargeable properties of LIBs were attributable to the bidirectional recycling of lithium ions. However, multiple losses occur in the actual intercalation/de-intercalation cycle [155]. Some of the direct losses are caused by forming a layer known as the Solid Electrolyte Interface (SEI). This happens during the initial charge-discharge cycle and results from the electrolyte-electrode compound reaction. Furthermore, SEI is not wholly detrimental to the functioning of LIBs since it helps to ensure the ability to move freely of the lithium ions while limiting the implantation of the solution inside the electrode. However, because SEI production depletes many lithium ions mainly from the system and SEI layers ultimately result in an irreversible capacity loss in batteries, drastic steps must be implemented to reduce or alleviate the degradation of reversible capacity in LIBs.

Some other essential factor in the design process of LIBs is coulombic performance. The percentage of lithium removal capacity to acquire additional lithium in the same cycle is known as Coulombic efficiency. This indicates that the charging capacity of the cathode compound is divided by its discharging capacity and conversely for the anode compound. Electrolyte dissolution and chemical or physical alterations in electrode active materials can affect coulombic efficiency. LIB capacity changes according to the current. Because high capacity is usually acquired at low currents, discharge capacity at high currents, often called rate capacity, can become a significant consideration.

It is important to remember that overcharging and discharging lithium-ion batteries will cause irreparable damage to the cathode and anode electrodes. Power density, volumetric and specific capacity, is a significant aspect to consider. Studies have shown that decreasing the electrodes' thickness to a minimal level may be a compelling and efficient approach to boosting the battery's power density, even reducing current density and resistivity. Additionally, increasing production techniques and efficiency is crucial to fulfilling the expanding market need for phones, inexpensive and tiny electric and electronic devices [159,160].

3.4.2 Cathode

A suitable cathode and anode electrode need to be thermostable and a great conductor of ions and electrons, while the electrolyte must be less reactive to the electrodes but also have strong ionic conductivity [161,162]. The cathode material is the most important component of LIBs, accounting for over half of the total cost. Scientists have been gradually synthesizing the cathode materials using the chemical to make them more stable and less expensive. The cathode electrode is complicated, resulting in abrupt structure and phase transitions. The major qualities of the battery that have drawn the most attention from researchers are its energy and power density, stability, and so on.

The electrochemistry of the cathode and anode electrodes determines the efficiency of the Li^+-ions. The main criteria for electrode materials include:

a) Reduced anode and strong cathode standard redox potential,
b) High charge density,
c) A greater degree of tunability,
d) Ecological friendly,
e) Reliability and cost effectiveness [163,164].

The electrode materials are crucial in determining the total efficiency of batteries. The continuity formula is used to compute the specific energy of a battery cell [165] .

$$E = \frac{V_{cathode} - V_{anode}}{\frac{1}{C_{cathode}} + \frac{1}{C_{anode}}} \quad (3.4)$$

Where,

C (mAh/g) is the theoretical specific capacity

V is the average working voltage

As demonstrated in **Figure 3.5**, outstanding and increased cathode materials performance has been the major focus and assessment of operating voltage and actual capacity of various cathode materials utilized in LIBs [166].

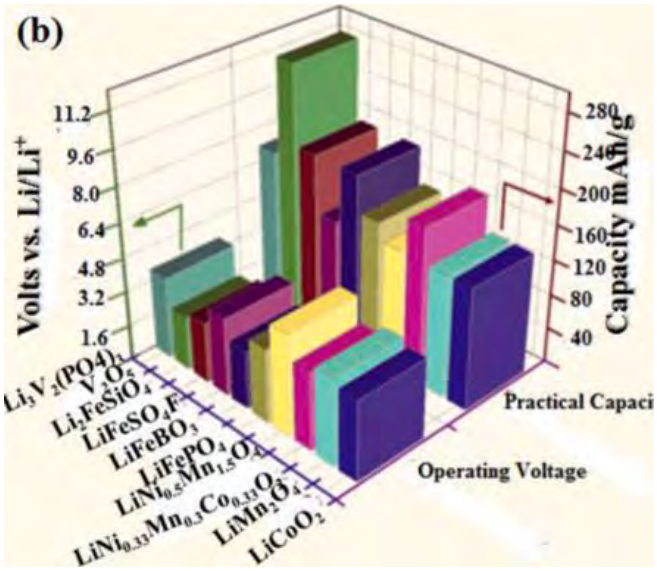

Figure 3.5. Various types of cathode materials that are used in LIBs [166].

Because of the lithium-free anode, lithium is the primary component of LIBs. The cathode electrode's property is primarily determined by its conductivity and high integrity. Because dispersion is important in the cathode, it needs to support reversible intercalation and deintercalation of Li^+-ion, just like the anode. The formulation of components with enhanced effectiveness, large capacity, safeness, and availability will successfully inspire the widespread application of LIBs. Compared with the other cell components of LIBs (anode, electrolyte, separator), the cathode or positive electrode is the heaviest and most costly component. The most desirable characteristics of cathode materials are:

1. The Fermi level needs to be as low as possible.
2. The potential energy of the cathode electrode needs to be high.
3. It must be easy to formulate.
4. Cost-effective and friendly to the environment.
5. Excellent thermal properties and high compatibility with the electrolyte avoid burst.
6. The dispersion properties of Li-ions should be rapid.
7. Great electronic and ionic conductivity.
8. Great reversibility of Li-ions intercalation and deintercalation [167,168].

3.4.3 Separators

The separator is an important component that precludes precise interaction between anodes and cathodes and allows lithium ions to move through the two electrodes. Furthermore, the separator is important in ensuring battery safety [169]. Because of the abuse, separators may be unable to stop the cathode and the anode from contacting each other under certain conditions, resulting in an internal short circuit. Several factors contribute to the breakdown of separators; when subjected to mechanical and electrical abuse, separators fail due to extrusion and puncture, whereas separators collapse due to thermal stress [170].

Various attempts have been made in the last few years to build high-performance separators for LIBs with a high level of safety (**Figure 3.6**).

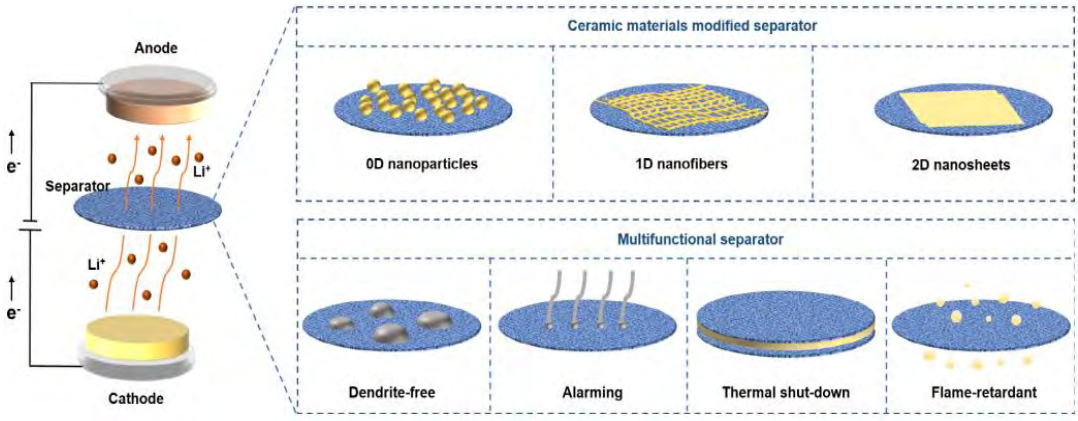

Figure 3.6. Structure of separator for high-safety Lithium-ion Batteries [171].

Altering conventional separators with ceramic materials or organic polymers are among the most efficient ways to enhance separators' thermal stability. Multifunctional separators are also designed to separate dendrites intelligently, including dendrite-suppressing, dendrite-

detecting, thermal shutdown, and flame-retardant separators. LIBs' safety can be improved by reducing the likelihood of thermal runaways and lowering the risks [172,173].

Characteristics of a basic separator

A suitable porosity is required for the separator to preserve sufficient liquid electrolyte for Li+ -ion spread. The regular separator has an appealing porosity of 40-60% [174]. When the separator has low porosity, it absorbs inadequate liquid electrolyte, increasing the internal resistance of the batteries and decreasing ionic conductivity and chemical efficiency.

In comparison, a separator with excessive porosity reduces the structural properties of the separator and shrinks at extreme temps, compromising battery safety. The porosity of the separator is defined as the ratio of void volume to obvious geometric volume, with the void implied to be wholly engaged only by liquid electrolyte, and the following equation can describe it:

$$Porosity\ (\%) = \frac{W-W_0}{\rho_L V_0} X100 \quad (3.5)$$

Where:

W and W_0 is the weight of seperator before and after the immersion inside of liquid electrolyte

ρ_L is the Electrolyte density

V_0 is the Seperator volume

Separators depend greatly on pore size and spread. Pores must be tiny to avoid big active material particles and dendrites from penetrating and causing an internal short circuit. The pore diameter is generally in the sub-micrometer (1 μm) range. The defined pore spread promotes a homogeneous Li^+ flow rate and current density distribution, resulting in fewer dendrites.

The separator's great wettability against liquid electrolytes is a significant feature determined by the component, porosity, pore size, and pore bending. Liquid electrolytes must wet the separator to obtain minimum internal resistance and fast ion transfer. Poor hydration of the separator could result in heterogeneous Li plating and the formation of dendrites [175]. The contact angle of liquid electrolytes on the separator can be used to determine wettability.

The cycle life of batteries, performance, and capacity are affected by ionic conductivity, which is described by the separator's wettability and porosity. A great ionic conductivity is a must and ideal number for powerful batteries. The following equation is described ionic conductivity:

$$\sigma = \frac{L}{A * R_b} \quad (3.6)$$

σ is the ionic condutivity

R_b is the bulk resistance

A is the area of separator

L is the thickness

Characteristics of a High–Safety Separator

The separator is critical to battery efficiency and reliability. The separator's essential duty is to separate the anode and cathode to avoid an internal short circuit. As a result, at different temperatures, the separator must not dwindle. Creating a separator with a strong mechanical structure and thermal stability is a viable solution for increasing battery safety in many uses. Overall, the specifications for high-safety separators are inversely related to those for high-performance separators.

The separator must have excellent mechanical properties and adaptability. The separator must be sufficient to withstand the strain in the winding production process for cylindrical batteries when assembled. Furthermore, the separator should have a high perforated power to preclude the infiltration of metal dendrites and active particles during normal or harsh procedures. Mechanical strength usually has an opposite relation with ionic conductivity. A relatively thick separator with lower porosity has a stronger mechanical structure but poor ionic conductivity.

Another factor to consider when evaluating the separator's safety is its thermal stability. Under abusive conditions, for instance, overcharging or overheating, a sequence of prospective thermal runaway interactions occur in LIBs, resulting in heat concentration and increased temperature. The separator must preserve structural stability at high temperatures to avoid interaction between the cathode and anode. Differential scanning calorimetry (DSC) can be used to assess the thermal stability of the separator. Over a specific temperature, the separator shrinks, resulting in an internal short circuit and battery burst. The separator's thermal shrinkage when heated at 100 °C for 1 hour is needed to be 5%.

The thermal shrinkage of the separator is measured by the difference in dimensions before and after heat treatment at a specific temperature, as illustrated in Equation (3.7).

$$Thermal\ shrinkage\ (\%) = \frac{D_i - D_f}{D_i} X100 \qquad (3.7)$$

Where,

$D_i\ area\ of\ separator\ before$

$D_f\ area\ of\ separator\ after$

For excellent mechanical strength and great thermal conductivity, the pores must be shuttered and blocked when overheating or a short circuit happens. The shut-it-down impact should occur before sacrificing mechanical stability that could protect electrode interaction and thermal runaway. Moreover, the separator must be equipped with a fire retardant. When a thermal runaway occurs, the fire-retardant separator can stop the fire, preventing an explosion. However, it is hard to fulfill all these factors, but a balance between the efficiency and safety of separators should happen [176].

3.4.4 Electrolyte

An electrolyte is a substance that helps the flow of lithium ions between the cathode and the anode and increases the conductivity. The usual electrolyte composition is $LiPf_6$ (lithium hexafluorophosphate) or $LiBF_4$ (lithium tetrafluoroborate), which are dissolved by a combination of propylene carbonate and diethyl carbonate [177].

Because it interacts with the other materials in the battery, such as the positive and negative electrodes, the electrolyte determines the current density, temporal stability, and reliability of the battery. Furthermore, because the electrolyte interfaces with the cathode and anode, its chemical stability criteria severely limit the material's useable range. The chemical compatibility of passive layers is caused by the solid electrolyte interface. This kind of layer's creation and physical features depend on the characteristics of the electrode (particularly the negative), meaning that electrolyte research cannot be readily separated from electrode research. As a result, an increasing amount of attention has been dedicated to analyzing the electrolyte, which serves as the vehicle for transporting charges in a battery. The electrolyte is inside the battery and should provide stability between two electrodes. In addition, the electrolyte should not affect the battery's chemistry, and all the Faradaic reactions should happen by anode and cathode. In general, a desirable electrolyte might satisfy the next minimum requirements:

1. The electrolyte has to be a great ionic conductor and electronic insulator, allowing for easy ion (Li) transport while minimizing self-discharge.
2. A large electrochemical gap should exist because, in this way, the electrolyte corrosion will not happen in the range of working potentials in the positive and negative electrodes.
3. It has to be inactive to other cell components like separators and electrode layers.
4. In the case of liquid electrolytes, a criterion of thermal stability should be considered; the melting and boiling points should be considered beyond the operating temperatures.

5. It has to be environmentally friendly, has minimal toxicity, and be effective to other ecological criteria.
6. It has to be founded on renewable chemistries, which means that the elements must be plentiful, and the formation methods should have minimal impacts as feasible.
7. It has to be cost-effective for the materials and production that are required.

For room temperature lithium-ion batteries, the electrolytes are categorized into:

- Non-aqueous electrolytes in which they have lithium salts being dissolved in an organic solvent or solvent mixture.
- Aqueous electrolytes in which they have lithium salts being dissolved in water.
- Ionic liquids electrolytes in which organic salts dopped in lithium salts.
- Polymer electrolytes consist of a solid and gel polymer.
- Hybrid electrolytes [178].

3.4.5 Safety Vents

A safety vent is inserted in a Li-ion battery to slow overheating and protect the battery from breakage and explosion [179,180] . Therefore, venting should take place at the early phases of heat dissipation to remove enough produced gases, slow overheating, lower pressure, and avoid a burst. The conventional vent design includes an architecturally weak spot in the system that permits an escape in circumstances that could contribute to or suggest the onset of overheating.

Depending on several original designs, **Figure 3.7** depicts a common vent layout for a cylindrical Li-ion battery.

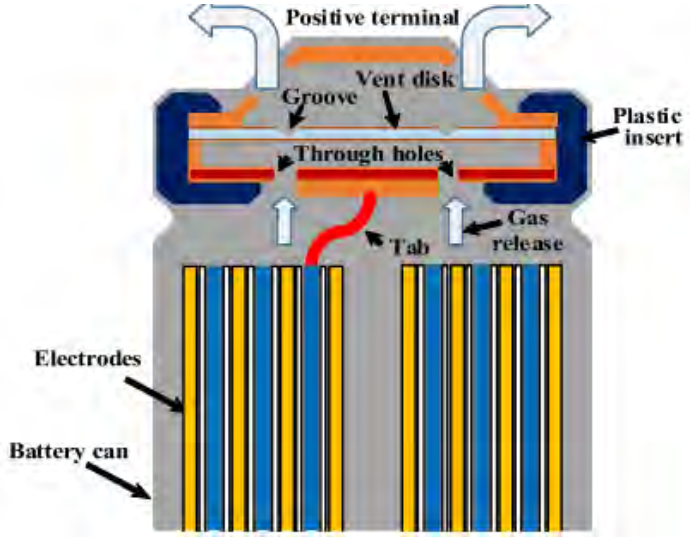

Figure 3.7. Pattern Illustration of a Safety Vent [181].

As previously stated, the venting mechanism in cylindrical batteries is typically comprised of three components: a positive terminal, an upper plate with groove (scored or circular arc form), and a bottom plate level [179], [182-184]. The positive terminal has two openings that let gases/fluids pass. The upper plate is a barrier between the battery's inner structure and the surrounding environment. The upper disk prevents the gas from escaping until the pressure differential supplied to the top disk is large enough to bust an aperture. The groove concentrates stress locally and will break when the pressure is increased dramatically, enabling gases to escape [185].

A well-designed vent must let gas be quickly evacuated from the battery. Overheating will happen if the vent is not opened in time. If the vent aperture is not large enough to appropriately alleviate pressure gets blocked, the internal pressure will continue to rise, resulting in battery breakage and burst [132], [186].

In summary, the most important cell components of Li-ion batteries are indicated in **Figure 3.8**.

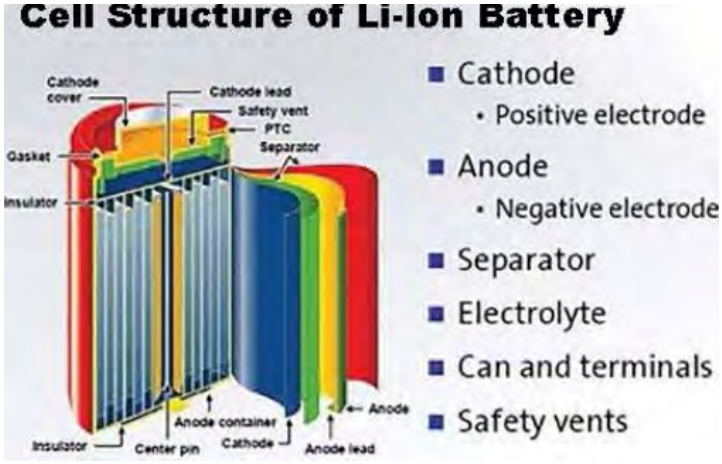

Figure 3.8. Cell structure basic components [187].

3.5 Performance of cathode materials

3.5.1 Cathode modification by surface coating

Since most positive electrode materials have low conductivity and rapid capacity fading throughout cycles, researchers are attempting to tackle this issue through several modification approaches. Surface coating is considered one of the greatest success strategies for improving cathode materials' thermal and structural properties since it not only increases particle layer function but also gives new physical, electrochemical, and mechanic characteristics [188]. At the moment, the design of surface coating compounds is mostly divided into two types:

1. One method is to cover the layer of the cathode compound particle with a thin layer of a heterogeneous material **Figure 3.9(a)**.
2. The alternative method is to cover the cathode compound with various components in various layers to build a composite structure **Figure 3.9(b)**.

It has been discovered that the majority of the oxide coating contributes to the structural stability of the electrode materials and prevents the contact of the electrode and electrolyte; therefore, the electrochemical performance of Lithium-ion batteries is increased. Furthermore, Zhang et al. demonstrated that the composite coating has a cooperation impact on cathode alteration, for instance, coating oxides and conductive compounds (carbon). By this, the conductivity and stability of the positive electrode compounds resulted in an improved performance rate of Lithium-ion batteries [189].

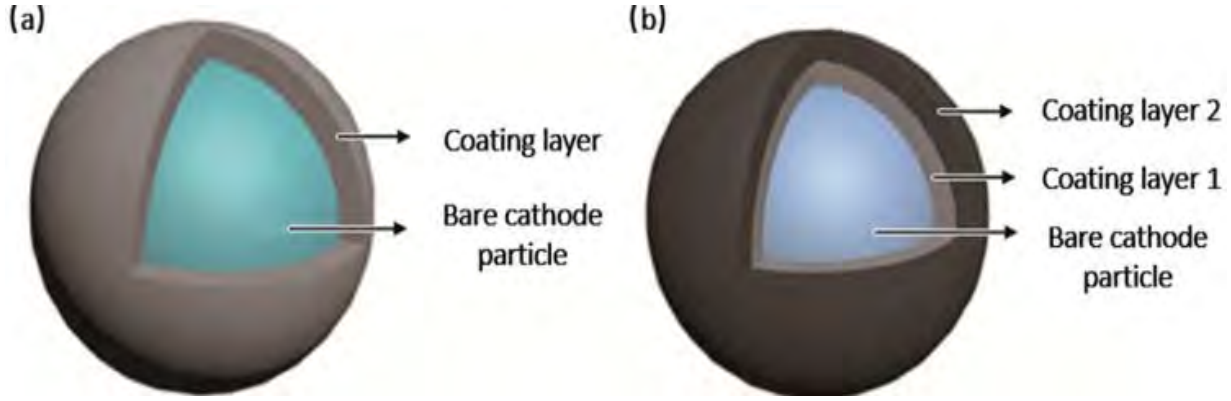

Figure 3.9. Positive electrode structure by coating a) single-layered coating, b) composite coating [167].

Surface coating is strongly connected to positive electrode compounds efficiency. Different coating innovations might also impact the positive electrode characteristics: a denser coating layer may include improved particle safeguards, but the disadvantage is that the transportation of ions and electrons is reduced. A light coating layer is challenging to generate and complicated to reach the required preventive role. Furthermore, coating processes – for example (dissolving or sintering) - can potentially disrupt the surface morphology of cathode materials. As a result, the homogeneity and maneuverability of cathode surface coatings substantially impact their performance. It is critical to use optimal coating materials and a suitable coating process to produce high-performance cathode materials. Some well-known methods of surface coating are chemical vapor deposition (CVD), atomic layer deposition (ALD), radio frequency (RF), organic pyrolysis technology, Co-precipitation coating, and Sol-gel method [190-195].In **Table 3.1** elecrochemistry performance of coated and

uncoated with $LiNi_{0.80}$ $Co_{0.15}$ $Al_{0.05}$ O_2 are illustrated and in **Table 3.2** the advantages and disadvantages of surface coating methods.

Table 3.1. Electrochemistry performance of coated and uncoated $LiNi_{0.80}Co_{0.15}Al_{0.05}O_2$ cathodes (C = current ratio, CR=capacity retention) [196-209].

Synthesis Method	Characteristics	Electrochemical Performance
Solid-state reaction sintered at 720 ˚C for 28 h	Microspheres	180 mAh g^{-1} at 0.2 C; CR of 87% after 76 cycles at 1 C
Two-step coprecipitation sintering in O_2	Microrods, SSA of 0.5 m^2 g^{-1}	218 mAh g^{-1} at 0.1 C; CR of 93% after 100 cycles at 1 C in range 2.7–4.3 V
Coprecipitation with 5-sulfosalicylic acid as chelating agent	Secondary spherical particle 8 μm dia.	203 mAh g^{-1} at 0.1 C; CR of 93.3% after 200 cycles at 1 C in range 3.0–4.3 V
Coprecipitation heated at 750 ˚C under O_2 stream	0.5–1.5 μm particle size agglomerates of 20 μm 0.23% cation mixing	177 mAh g^{-1} at 0.1 C; CR of 82% after 500 cycles at 2 C rate in range 3.0–4.1 V
Coprecipitation sintered at 750 ◦C	400–600 nm particle size polyhedral shape	200 mAh g^{-1} at 0.2 C; 92% CR after 60 cycles at 1 C
Ball milling with LATP Sintered At 750 ◦C in O_2	10 μm spherical particle 200 nm thick coating	180 mAh g^{-1} at 0.1 C; CR of 88% after 100 cycles at 2 C rate in range 2.8–4.3 V
Coprecipitation, sintered at various O_2 pressures optimized for 0.1 MPa	Sphere-like 15 μm dia.	166 mAh g^{-1} at 0.1 C; CR of 87% after 100 cycles at 1 C rate in range 2.8–4.3 V
Polysiloxane coating Hydrolysis condensation	Spherical agglomerates 20 μm dia.	184 mAh g^{-1} at 0.1 C; CR of 96% after 150 cycles at 1 C rate in range 2.8–4.3 V
Li_2O-$2B_2O_3$ coating by a solution method	Commercial LCA	169 mA g^{-1} at 360 mA g^{-1}; CR of 94.2% after 100 cycles in the range 3.0–4.3 V
LiAlO2 coating by milling	Spherical agglomerates 20 μm dia.	172.3 mAh g^{-1} at 1 C; CR of 94.67% after 100 cycles at 1 C in the range 3.0–4.3 V
$Li2TiO_3$ coating by near-equilibrium deposition	Spherical agglomerates 6–8 μm dia.	187.5mAh g^{-1} at 0.5 C; CR of 93.5% after 200 cycles at 0.5 C in the range 2.8–4.3 V
$LiTiO_2$ coating by hydrolysis	Spherical agglomerates 3–15 μm dia.	164.1 mAh g^{-1} at 1 C; CR of 90.8% after 100 cycles at 1 C in the range 2.8–4.3 V
Dual coating Sb-doped SnO_2 and $Li2TiO_3$	Spherical agglomerates 10 μm dia.	153 mAh g^{-1} at 5 C; CR of 88.56% after 200 cycles at 1 C at 60 ◦C in the range 3 - 4.3 V

Table 3.2. Summary of different coating methods with advantages and disadvantages [210].

Surface Coating Method	Advantages	Disadvantages	Ref
Wet chemical routes (Sol–gel, hydro/solvothermal etc.)	Simple and economical one-pot procedure improves structural stability of cathode by surface doping with foreign metal ion	Non-uniform coating on particle surface Physical protection cannot be completely reduced	[211]
Chemical polymerization routes	Improves surface electronic conductivity	Non-uniform coating on particle surface Long-term thermal instability Multifunctional polymer coating is required	[212,213]
Deposition techniques (Sputtering, PLD, ALD, etc.)	Uniform coating on particle surface. Adjustable and precise thickness	Expensive Difficult in uniformed growth of films	[214,215]

3.5.2 Doping NCA - Doping NCM

Doping NCA. Doping NCA is also an approach utilized to boost cycle ability. Although the coating has minimal influence on the structure compound's stability and functions by insulating the surface layer from electrolyte chemical changes and oxygen depletion over cycling, doping helps to stabilize the bulk structure [216].

Remarkably, little effort has been taken to enhance the Li-rich layer NCA positive electrode by combining the synergistic action of ionic doping and surface functionalization. By combining degraded NCA with $MgHPO_4$ preparation and heating at 750 ºC, Mg^{2+} surface doping and Li_3PO_4 coating are both achieved concurrently. Consequently, the quantity of surface remaining lithium compounds and the level of Li/Ni cation mixture was decreased [217]. In **Table 3.3**, electrochemistry properties for the LCA method are illustrated.

Doping NCM. Lattice doping with different cations is another method of stabilizing the structure of NCM. Current examples include niobium and Nd^{3+} doping of $LiNi_{0.5}Co_{0.2}Mn_{0.3}O_2$ Weigel et al. established a "top-down" technique to dope with Mg^{2+}, Al^{3+}, Si^{4+}, Ti^{4+}, Zr^{4+}, and Ta^{5+} in $LiNi_{0.8}Co_{0.1}Mn_{0.1}O_2$. Doping using calcium and molybdenum has been used to reduce the material's volume change and deterioration [218-222]. In **Table 3.4**, electrochemistry properties for the $LiNi_{0.76}Co_{0.09}Mn_{0.15}O_2$ method are illustrated.

Table. 3.3 Doped $LiNi_{0.80}$ $Co_{0.15}$ $Al_{0.05}$ O_2 cathode material's electrochemistry properties (C = current ratio, CR=capacity retention) [216,223-231].

Dopant	Electrochemical Properties
K	217 mAh g^{-1} at 0.1 C; CR of 87.4% after 150 cycles at 1 C (2.8–4.6 V)
Zr	133.6 mAh g^{-1} after 100 cycles at 250 mA g^{-1} (2.5–4.6 V)
Fe	138.9 mAh g^{-1} at 1 C with CR of 88.4% at 1 C after 350 cycles (2.8–4.3 V)
Cu and Fe	Initial discharge 143 mAh g^{-1} at 10 C; 168 mAh g^{-1} after 100 cycles at 1 C (2.8–4.3 V)
Ti	179.6 mAh g^{-1} after 200 cycles at 1 C; CR at 97.4% (3.0–4.5 V)
Mn	174.0 mAh g^{-1} at 2 C, with CR of 81% after 900 cycles at 2 C (2.8–4.3 V)
Te (1 wt.%)	159.2 mAh g^{-1} at 10 C, 205 mAh g^{-1} at 1 C; CR of 81.4% after 100 cycles at 1 C (2.7–4.5 V)
Na	170.1 mAh g^{-1} at 1 C, CR of 90.7% after 200 cycles at 1 C (2.8–4.3 V)
Concentration gradient of Al	116mAh g^{-1} at 10 C, 214 mAh g^{-1} at 0.1 C (2.8–4.4 V) full cell: 195 mAh g^{-1} at 1 C with CR at 99% after 500 cycles (3–4.2 V)
Concentration gradient of Al	198.1 mAh g^{-1} at 0.1 C; CR of 70.9% after 500 cycles at 1 C (3–4.3 V)

Table 3.4. $LiNi_{0.76}Co_{0.09}Mn_{0.15}O_2$ electrochemical properties (C = current ratio, CR=capacity retention) [232-240].

Dopant	Electrochemical Properties
Zr	172 mAh g^{-1} at 1 C; CR of 83.2 % after 200 cycles at 1 C (2.8–4.5 V)
Ti	165.02 mAh g^{-1} at 1 C; CR of 77.01% after 150 cycles at 1 C (2.8–4.3 V)
Ti	160.6 mAh g^{-1} after 200 cycles at 1 C; CR of 95.03% (2.8–4.3 V)
Al	154 mAh g^{-1} after 200 cycles at 1 C; CR of 85.32% (2.8–4.3 V)
Mg	147 mAh g^{-1} after 200 cycles at 1 C; CR of 82.07% (2.8–4.3 V)
Al	171.71 mA h g^{-1} at 1 C; CR of 96.15% after 100 cycles at 1 C (3.0–4.3 V)
Al-doped gradient	203 mAh g^{-1} at 0.5 C; CR of 95% after 100 cycles at 0.5 C CR of 95% after 1000 cycles at 1 C in full cell (graphite anode) (3.0–4.2 V)
Al-doped gradient	213.6 mAh g^{-1} at 0.1 C; Cr of 89.5% after 200 cycles at 0.1 C (3.0–4.5 V) 145 mAh g^{-1} at 10 C
P and F coating	162.3 mAh g^{-1} after 100 cycles at 0.5 C, CR of 94.4% (3.0–4.3 V)
Y	189.4 mAh g^{-1} at 0.5 C; CR of 98.4% after 100 cycles at 0.5 C (2.8–4.5 V)
La	192 mAh g^{-1} at 1 C; CR of 90.1% after 200 cycles (2.75–4.5 V)

3.5.3 Coating NCM

Surface modifications of $LiNi_{0.8}Co_{0.1}Mn_{0.1}O_2$ are considered necessary. Since a 3 nm size cation-mixing nanolayer with rock-salt construction is generated on the cathode layer, it could be referred to as a similar coating technique, thus preventing additional structural deterioration. Nonetheless, this monolayer is an insulator, and a more conductive substance must be coated to boost rate capability [241]. In **table 3.5**, the electrochemistry performance for $LiNi_{0.8}Co_{0.1}Mn_{0.1}O_2$ electrodes is illustrated.

Table 3.5. $LiNi_{0.8}Co_{0.1}Mn_{0.1}O_2$ electrode's electrochemical performance (C = current ratio, CR=capacity retention) [242-260].

Coating	Preparation	Electrochemistry Performance
Li_2SiO_3	Solvothermal method using Si $(OC_2H_5)_4$ and LiOH	133 mAh g^{-1} after 52 cycles at current density of 100 mA g^{-1} in the voltage range 3.0–4.6 V
Li_2TiO_3	Nanobelts obtained from reaction between MC2O4·xH_2O and Ti$(OC_4H_9)_4$	150 mAh g^{-1} at 0.5 C in the voltage range 3.0–4.3 V; CR of 92% after 100 cycles at 2 C rate
$Li3VO_4$ (3 wt.%)	Wet chemistry using V_2O_5 and LIOH·H_2O	164 mAh g^{-1} at 0.1 C in the voltage range 2.0–4.3 V; CR of 83% after 100 cycles at 1 C rate
MoO_3 /Li2MoO_4 (3 wt.%)	Dry coating method using (NH_4) 6Mo7O_{24}·$4H_2O$	200 mAh g^{-1} at 0.1 C rate in the voltage range 2.8–4.3 V; CR of 94.8% after 100 cycles at 1 C
Li_3PO_4	In situ coating in $NH_4H_2PO_4$ solution	176 mAh g^{-1} at 0.1 C rate in the voltage range 2.9–4.2 V; CR of 89.6% after 250 cycles at 1 C
Li_3PO_4 -PPy co-coating	Two-step: wet-coating for Li_3PO_4 /chem. polymer. PPy	159 mAh g^{-1} at 10 C rate in the voltage range 2.8–4.5 V; CR of 95.1% after 50 cycles at 0.1 C
Li_3PO_4 -$AlPO_4$ co-coating	Al $(H_2PO_4)_3$ added to ethyl alcohol	182.8 mAh g^{-1} at 1 C in the range 2.8–4.3 V; CR of 91.79% after 100 cycles at 1 C
Li_3PO_4-$AlPO_4$-$Al(PO_3)_3$ coating	Al $(PO_3)_3$ in ethanol reacting with NCM811	201.8 mAh g^{-1} at 0.1 C in the range 3.0–4.3 V; CR of 85.4% after 50 cycles at 0.1 C
$FePO_4$	Sol–gel method	151.4 mAh g^{-1} at 5 C in the voltage range 2.74–4.5 V; CR of 86% after 400 cycles at 0.2 C
$LiAlF_4$	ALD	184 mAh g^{-1} at 50 mA g^{-1} in the voltage range 2.74–4.5 V; CR of 76% after 300 cycles
LiF-LaF_3	Polyvinyl pyrrolidone-assisted wet coating process	173.6 mAh g^{-1} at 5 C in the voltage range 2.8–4.6 V; CR at 81.8% after 100 cycles at 5 C
SiO_2	Aqueous solution method using Na_2SiO_3·$9H_2O$	185 mAh g^{-1} at 1 C rate in the voltage range 2.8–4.3 V; CR of 90% after 300 cycles
$LaAlO_3$ (3 wt.%)	Solid method, using La $(NO_3)_3$·$6H_2O$ and Al (CH (CH_3)2O)$_3$	155 mAh g^{-1} at 1 C rate in the voltage range 2.7–4.3 V; CR of 84.5% after 200 cycles at 1 C
$LaPO_4$	Wet chemistry aqueous solution with La $(NO_3)_3$·$6H_2O$ + $NH_4H_2PO_4$	200 mAh g^{-1} at 0.1 C rate in the voltage range 3.0–4.3 V; CR of 91.2% after 100 cycles at 1 C
$AlPO_4$ (0.5 wt.%)	Ethyl alcoholic solution with $Al(H_2PO_4)_3$ at 50°C	150 mAh g^{-1} at 10 C rate
Co_3O_4 (0.6 wt.%)	Sonication in ethanol solution with Co $(OH)_2$	186 mAh g^{-1} at 1 C rate after 100 cycles
WO_3 (0.25 wt.%)	Wet process in alcohol using WO_3 dissolved in H_2O	189 mAh g^{-1} at 0.2 C rate in the voltage range 2.8–4.3 V; CR of 70% after 100 cycles at 1 C
$Li_{1.5}Al_{10.5}Zr_{1.5}(PO_4)_3$ (1 wt.%)	Sol–gel method	179.3 mAh g^{-1} at 1 C in the voltage range 2.8 4.5 V; CR at 84.8% after 200 cycles at 1 C
PANI-PEG	One step wet-coating method	156.7 mAh g^{-1} at 10 C in the voltage range 2.8–4.3 V; CR of 88.4% after 100 cycles at 2 C
PEDOT-coated $LiNi_{0.85}Co0_{.1}Mn0_{.5}O_2$	CVD process	178 mAh g^{-1} at 1 C rate in the voltage range 2.7–4.3 V; CR of 91% after 100 cycles at 1 C
Pyr-2D	Reaction of amine and ketone in presence of NCM	175 mAh g^{-1} at 1 C rate; CR of 88.8% after 100 cycles at 1 C; voltage range 2.8–4.5 V

3.5.4 Types of Lithium-ion batteries

Lithium-ion batteries play a key role today. Their advantages over other secondary batteries are increasing so much in popularity nowadays. An innovative type of lithium battery is non-aqueous Li-O_2 which has a significantly great theoretical energy density, almost ten times greater than usual Lithium-ion batteries. For better battery performance, a valuable way is to improve the electrochemical properties of air cathode material because the battery is dependent on the slow kinetics of oxygen evolution and reduction reactions and, as a result, is the battery's weakness as well [261-263].

Another innovative type is Li-S, which is expected to be the backup plan of commercial Lithium-ion batteries because of their great reserves, significant theoretical specific capacity, and eco-friendly properties. Unfortunately, some disadvantages are low conductivity, shuttle effect, and volume expansion. However, different materials have been tested to enhance its performance with the most effective way of using carbon porous as a host of S [264]. In **Table 3.6**, different types of lithium batteries are indicated.

Table 3.6. Typical uses of lithium-ion batteries [265].

Chemical Name	Material	Short Form	Notes
Lithium Cobalt Oxide	$LiCoO_2$	Li-Cobalt	Uses for cameras, laptops, cell phones. Higher capacity.
Lithium Manganese Oxide	$LiMn_2O_4$	Li-manganese, spinel	Safer, high specific power and long life but lower capacity than Lithium Cobalt batteries
Lithium Iron Phosphate	$LiFePO_4$	Li-Phosphate	
Lithium Nickel Manganese Cobalt Oxide	$LiNiMnCoO_2$	NMC	
Lithium Nickel Aluminum Cobalt Oxide	$LiNiCoAlO_2$	NCA	Gaining importance in electric power-train and grid storage
Lithium Titanate	$Li_4Ti_5O_{12}$	Li-titanate	

CHAPTER 4

Failures – Diagnostics

4.1 Introduction to Failures

Several incidents and breakdowns have been reported due to the increasing demand for lithium-ion batteries in daily life, such as smartphones, laptops, and electric automobiles. Temperature, pressure, and overcharging are just factors that influence how these batteries work. Consequently, scientists learn how to recognize these issues, and lithium battery technology improves yearly [130,131].

While Li-ion batteries are recognized for their extended service life, their service life is heavily influenced by environmental factors and operating mode. Battery aging happens during operation and invariably results in performance decline and system failure, which causes discomfort and risks significant repercussions like a thermal runaway or even fire and explosion [266,267].

Furthermore, mechanical deterioration has been identified as one of the major reasons for battery aging or failure. Materials deform and create thermal stresses when atoms migrate and reorganize if limited. This might lead to degradation or damage in the components, such as fracturing or void formation. Furthermore, the mechanical stresses created can substantially impact other processes throughout the battery process [268].

4.2 Types of common failures

The types of failures are categorized into two different sectors inside and outside failures.

4.2.1 Internal Failures

Internal problems are a concern since lithium-ion batteries are still in development. Internal faults can cause voltage drops, SOC drops (state of charge drops), temperature increases, resistance increases, and battery instability [269].

4.2.1.1 Overcharge

Overcharging can cause a variety of issues that harm lithium-ion batteries. For example, it can cause dangerous circumstances like increased pressure and thermal runaway, creating gases that

can burst the battery and shorten its life because of incorrect BMS voltage and current estimations [270,271]. Furthermore, when the temperature rises, the thickness of the solid electrolyte decreases, which might result in an internal short circuit in the battery. Finally, electrolyte degradation and metal dissolution can generate fire and excessive thermal runway [272].

4.2.1.2 Over discharge

Improper state of charge estimates, wrong voltage, and current measures could be occurred by over discharge similar to overcharge. [270]. Copper distancing could be occurred on electrodes because of over-discharge, as the results have shown by the microscopy of scanned electrons and X-ray diffraction. [273]. Electrochemical impedance spectroscopy (EIS) investigations further show that during battery over discharge, the anode's impedance is substantially lower than the cathode's, implying that the anode's SEI change is much greater than the cathode's, resulting in capacity loss and current collecting corrosion [271]. Over discharge can reduce a Li-ion cell's lifetime and thermal stability and cause significant swelling [272]. During over discharge, the anode potential also rises abnormally, which might lead the Cu inside the cell to oxidize to Cu^{2+} ions. The dissolved Cu^{2+} ions may migrate to the separator, resulting in an internal short circuit [274].

4.2.1.3 Internal Short Circuit

Lithium-ion batteries could have two types of short circuits internal and external. When the separator layer between the electrodes collapses, an internal short circuit result [275-277]. This separator failure can be related to melting because of an increased temperature, cell deformation, dendritic development, or compressive stress. A contact between electrodes and an internal short circuit could be a result of these separators' failures in which a penetration to its surface can make the electrons move from the anode to electrolyte towards the cathode. As a consequence, thermal runaway can happen, and then the electrolyte starts getting damaged. [278]. Thermal runaway is mostly occured by temperature buildup produced by a short circuit. High-capacity cells, in general, are more susceptible to thermal runaway due to internal short circuits than standard-capacity cells [279].

4.2.1.4 Effects of dendrite growth

Dendrites are merely concentrations of different metal ions. Consider the Li system: throughout the charging process, the Li metal ions settle uniformly on the anode surface,

generating regular metal deposition, and this occurs at a very low overpotential (0.1 V/Li). This kind of deposition generates an epitaxial-like area immediately above the anode surface at extremely low overpotential. So, when salt concentration on the anode surface decreases owing to kinetic constraint, the overpotential (0.5-3.5 V/Li) rises, causing uneven deposition and the production of whisker or needle dendrites. These whiskers intertwine and develop a mossy (bush-like) shape as they expand [280-283]. This moss dendritic form obstructs the surface of the microporous separator because the tip's development rate is quicker than the radial growth rate, and the dendrite's shape is a one-dimensional fibrous structure. Finally, as ion concentrations near the anode surface approach zero, the potential surface drops to + 1V/Li, and fractal development begins to create tree-like dendrites (**Figure 4.1**).

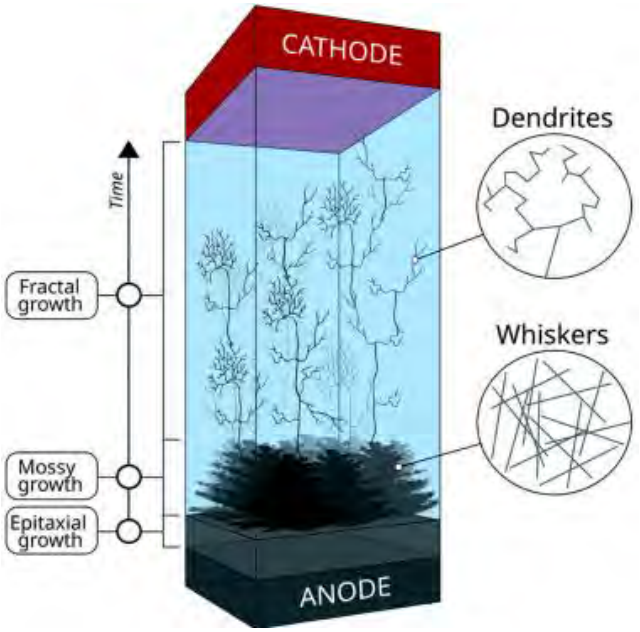

Figure 4.1. Illustration of dendrite growth formation [283].

Consequently, it is characterized as a single crystal generated by non-uniform metal ion deposition), which is commonly utilized for the fractal form, penetrating the separator and creating thermal runaway and short circuits [284-286].

There are several reasons for the formation of dendrite that is affected by the operating conditions, such as:

- Temperature
- Pressure

- Current density and substrate
- Electrolyte
- Electrolyte additive and concentration
- Electrolyte type
- Interphase [287].

4.2.1.5 External Short Circuit

There are several reasons for the formation of dendrite that is affected by the operating conditions, such as: When the tabs are linked via a low resistance channel, an external short circuit develops [280]. Another reason is electrolyte leakage from cell enlargement caused by gas production during overload [288]. It may also happen as a result of water immersion and collision deformation. An external short circuit occurs when an external heat-conducting component makes simultaneous touch with the positive and negative terminals, resulting in an electrical connection between the electrodes [289]. According to one research, thermal runaway occurs when the Li-ion diffusion in the negative electrode is limited owing to an external short circuit and the heat created by the electrolyte breakdown in the positive electrode [288]. The cell's energy can also be discharged abnormally by an external short circuit.[279].

4.2.1.6 Overheating

Increased temperature can happen to a lithium-ion battery when the voltage regulator on an alternator fails, delivering a large amount of power back to the battery and generating overheating [290]. External and internal short circuits can also induce overheating [291]. Overheating the battery promotes cathode deterioration and increases SEI at the anode. There is a significant capacity loss as a consequence of overheating. Overheating a Li-ion battery can cause the components inside of the battery to degrade and form gas bubbles, which, in most circumstances, leads the battery to enlarge and possibly explode [292]. When the heat is increased above a limit, it results overheating, and the disadvantage of that is that it is not easy to extinguish or reduce as it is created [293].

4.2.1.7 Thermal Runaway

Thermal runaway can be connected to the already-mentioned internal battery problems. Increased temperatures and excessive current while the battery is charged can also be associated

with it. A strong reaction could occur if the heat reaches the melting point of lithium[294]. Another reason for thermal Runaway is restricted air movement [295]. Galushkin et al. discovered that the amount of charging/discharging cycles can increase the chance of thermal runaway.[296]. The research also discovered that thermal runaway is linked to various exothermic events in batteries. Also, it is connected with various exothermal events. The first one is the breakdown of the solid electrolyte interface, which significantly increases the heat generation at the start of thermal runaway. During this process, the positive electrode produces O_2 through a changeover phase, and the lithiated negative electrode absorbs this O_2. In addition, it can raise the pressure and heat of lithium-ion cells, resulting in the breakdown of content and generating combustible hazardous gas emissions. When a battery deals with a failure like that, it usually overheats and explodes [296].

4.2.1.8 Temperature effect in LIBs

Most of the temperature impacts are caused by chemical processes in the batteries and materials utilized in the batteries. Regarding chemical reactions, the link between the rate of chemical and temperature reaction follows the Arrhenius equation, and temperature variations can cause changes in the electrochemical reaction rate in batteries [297]. Temperature influences the ionic conductivities of electrodes and electrolytes in addition to chemical processes. For instance, the ionic conductivity of lithium salt-based electrolytes at low temperatures diminishes [298].

Low-temperature effects

LIBs' performance degrades at conditions below 0 °C [299,300]. In 2001 a demonstration showed that the power and energy densities of Panasonic 18650 LIBs were 800 W/L and 100 Wh/L at 25 °C, respectively, and these values decreased by 98.75% and 95% to 10 W/L and 5 Wh/L at 40 °C [301]. Another study discovered that when the operating temperature was reduced from 25 °C to -15 °C, a LIB's state of charge (SOC) is characterized by the ratio of the current residual capacity to the total available capacity, which declined by 23% [302,303].

With the complicated material system operated in LIBs, performance decline at low temperatures can be attributable to various factors. Initially, the low temperature will change the electrolyte's properties. As the temperature drops, the viscosity of the electrolyte rises, reducing ionic conductivity. The internal resistance will rise as the impedance of chemical ion movement increases. Low freezing point electrolytes were investigated to counteract this effect and other electrolyte additions [303-307]. During their study on LIBs for space applications, Bugga et al.

[303] developed a guideline for designing formulas for low-temperature electrolytes. The enhanced electrolytes have a more comprehensive working range of temperature (**Figure 4.2A**) and are helpful in aircraft batteries [305]. Li et al.b [305], have reported an improved electrolyte formulation including 1.0 M $LiPF_6$ in ethylene carbonate (EC), propylene carbonate (PC), and ethyl methyl carbonate (EMC) (1:1:8 by weight). For the batteries tested at 40 °C, this formulation allowed for capacity retention of 68%, whereas the standard formulation only allowed capacity retention of 20%. (**Figure 4.2B**). Specific electrolyte additions, such as lithium fluorophosphate ($LiPO_2F_2$), have also been shown to improve LIB performance at low temperatures (**Figure 4.2 C**) [307].

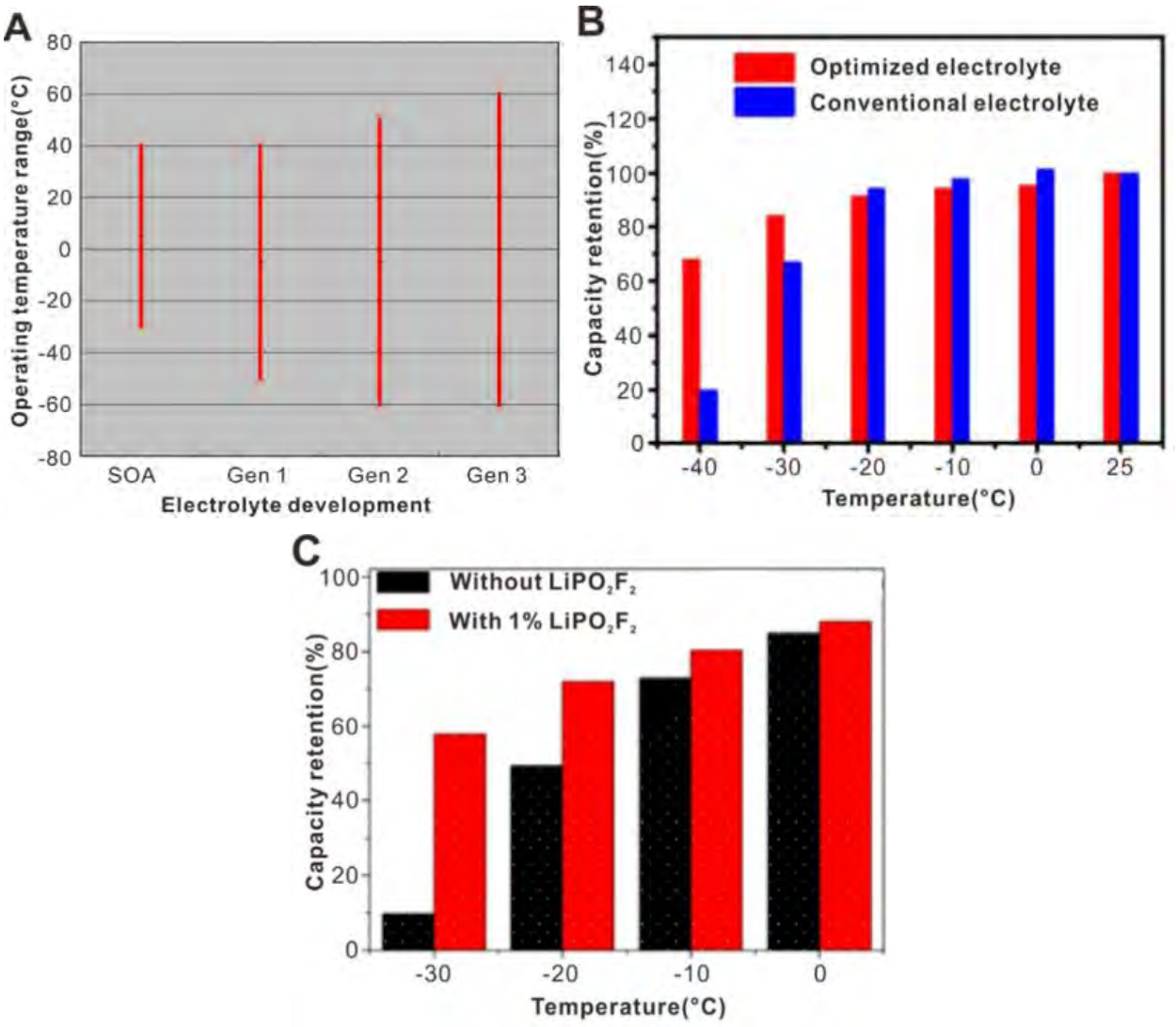

Figure 4.2. A) Different generations of electrolytes [298], B) Capacity retention of optimized and conventional electrolytes [308], C) Importance of using $LiPO_2F_2$ as addictive in electrolyte [307].

The rise in charge-transfer impedance in LIBs is another essential component contributing to low-temperature performance loss. At -20 °C, the charge-transfer impedance of $LiFePO_4$-based cathodes was three times greater than at ambient temperature. The kinetics of batteries are greatly influenced by such high charge-transfer resistance [309]. Zhang et al. examined the performance of LIBs at low temperatures and revealed that the charge-transfer impedance rose dramatically as the temperature dropped. A depleted battery's charge-transfer resistance is often significantly more excellent than a charged battery [310]. As a result, charging a battery at low temperatures is more complex than draining it. Furthermore, the low-temperature performance loss is linked to the sluggish transport of lithium ions within electrodes. This slowing can be minimized by using electrode components with low activation energy [311].

Therefore, lithium plating is a common phenomenon at low temperatures. The cold situation will cause anode polarization and bring the potential of graphite and other carbon-based anodes closer to that of lithium metal, slowing down lithium-ion interrelation with the anodes during the charging process. As a result of the accumulated lithium ions being placed on the surface of the electrodes, the battery capacities are reduced. Furthermore, lithium plating can be found as dendritic, that pierces the separators and causes an internal short-circuit [312-316].

High-temperature effects

High-temperature impacts are far more complicated than low-temperature effects. Heat is created inside the batteries during LIB function and knowing the heat generation is crucial in limiting the high-temperature impacts in LIBs [294]. A theoretical illustration of overheating effect can be shown in **Figure 4.3** [317].

Figure 4.3. Thermal runaway effect on battery [317].

Heat Generation

At average temperatures, heat generation within LIBs is connected with charge transfer and chemical processes during charging and discharging. In LIBs, heat is produced in either reversible or irreversible processes [318-321]. **Figure 4.4** depicts the potential heat production within LIBs. The heat produced in the reversible reaction, also called entropic heat, is caused by a change in reversible entropy during electrochemical processes [294].

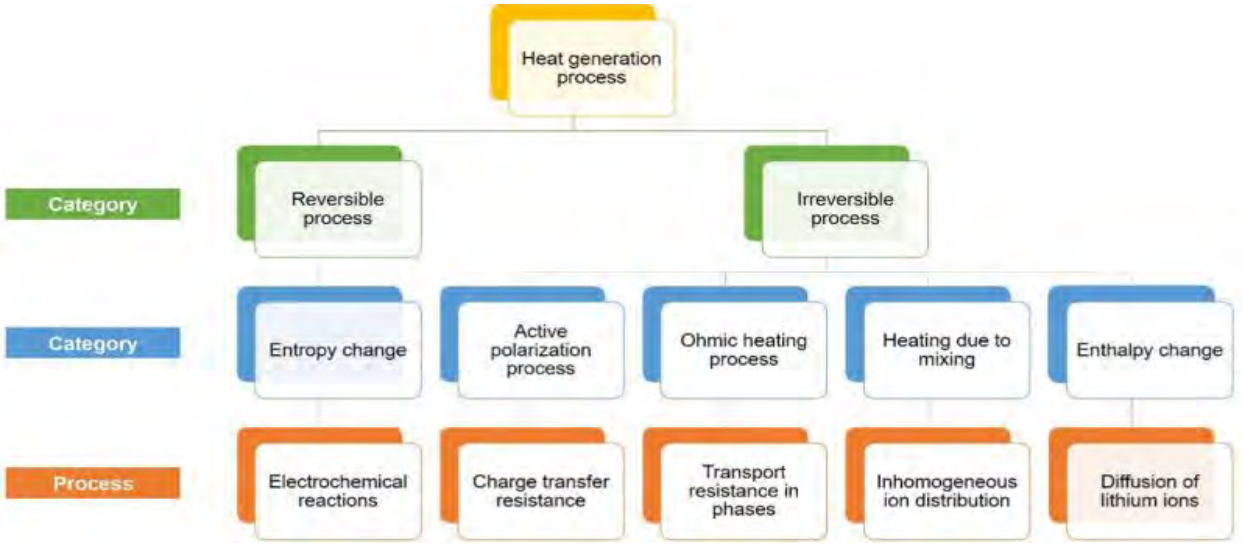

Figure 4.4. Categorized heat generation process in Lithium-ion batteries [322].

Several irreversible phenomena can create heat, including dynamic polarization, ohmic heating, mixing heating, and enthalpy change. Polarization is caused by an overpotential between the batteries' operational and open circuit potentials [323-325]. It causes an increase in charge transfer resistance at the electrode-electrolyte interface, also known as the Solid Electrolyte Interface (SEI). Heat is created once lithium ions surpass this resistance at the contact for intercalation/deintercalation [326]. The electrode and the electrolyte suffer from ohmic heating. The impedance of electrodes and electrolytes prevents charges from being transported [225,327]. When the LIBs are in function, either charging or discharging, the ion distribution turns inhomogeneous, which might result in ion mixing and heat generation during mixing [331,340] [328,329]. Another type of irreversible heat-generating process is the enthalpy change caused by a phase shift in cathodes, predominantly caused by the diffusion of lithium ions [294].

4.2.1.9 Approaches for internal temperature monitoring of LIBs

The heat transfer at the surface of batteries is simple to get using typical temperature measuring methods, such as thermocouples and thermal imaging devices [330]. However, using these technologies to monitor the internal temperature of LIBs takes much work. The self-production of heat while operating can raise the internal temperature of LIBs. Because of the multilayered architectures and low indices of heat transfer of battery components, heat transmission from the inside to the outside of batteries is challenging. The internal temperature distribution is similarly asymmetric [331-333].

Scientists attempted to investigate several techniques for monitoring the interior temperature of LIBs in light of their sealed nature and the electrochemical reactions of LIBs during functioning. As shown in **Figure 4.5**, these methodologies are divided into two categories: contact measurement and contactless measurement.

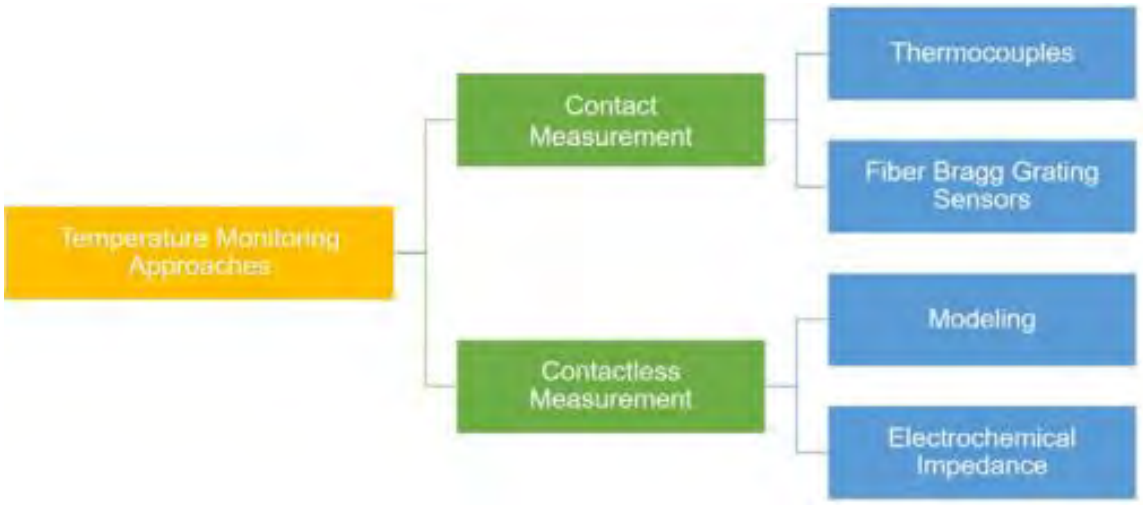

Figure 4.5. Strategies for monitoring the inner temperature of LIBS [322].

Temperature sensors such as thermocouples and Fiber Bragg Grating (FBG) are put inside LIBs to monitor the temperature in contact measurement directly. In contrast, the interior temperature of the batteries was measured indirectly in the contactless measurement. Two primary contactless techniques are modeling simulation and electrochemical impedance. Electrochemical and thermal models were developed in the simulation to evaluate the operation of LIBs in various scenarios and theoretically predict the internal temperature. Another contactless way is to predict interior temperature using electrochemical impedance. The

electrochemical impedance of LIBs varies with temperature. The inner temperature of LIBs may be estimated by developing calibration curves showing the relationships between impedance and temperature. In this part, we will go through the current methodologies for measuring the LIB's interior temperature using touch and contactless methods [294].

4.2.1.10 Aging

Aging is a side effect of using LIBs at high temperatures. LIBs' lifespan is reduced as they age, not just their performance [334,335].LIB aging, in general, encompasses cycle aging and calendar aging. Due to the complicated composition and functioning method of LIBs, these two forms of aging always occur together [330]. Raising the operating temperature of LIBs over the optimum range accelerates the aging process and causes LIB deterioration. The majority of study in this field focuses on the aging of the different components within the battery or the battery system [336-339].

Most research on the thermal aging impact on specific components focuses on electrodes and electrolytes. Gabrisch and colleagues investigated the capacity variation of $LiCoO_2$ and $LiMn_2O_4$ cathodes [337]. The $LiCoO_2$ and $LiMn_2O_4$ cathodes were thermally aged for 10 and 6 days, correspondingly, at 75 °C. The discharge characteristics of these two cathodes revealed a significant loss of capacity following age treatment (**Figure 4.6A** and **B**). According to scientists, the thermal-induced crystallographic alteration led to the permanent interrelation of lithium ions in cathode lattices, resulting in cathode capacity loss [340]. Handle et al.[339] investigated the heat breakdown of lithium hexafluorophosphate ($LiPF_6$), a typical conductive salt in electrolytes. At high temperatures, the breakdown of $LiPF_6$ is accelerated by the presence of proton impurities. The breakdown pathway of $LiPF_6$ in a combination of ethylene carbonate (EC) and diethylene carbonate (DEC) (1:2, v-v) at 60 °C which resulted in the synthesis of difluorophosphoric acid as the primary decomposition product.

Research of the complete battery system gives more thorough evidence of the high-temperature aging effects of LIBs than research on individual components. Bodenes et al. investigated the aging of Li (Ni, Mn, Co) O_2 (NMC)-based LIBs [336]. According to **Figure 4.6A**, the capacity reduction of the studied battery was 7.5% after being cycled at 85 °C and 22% after being cycled at 120 °C.

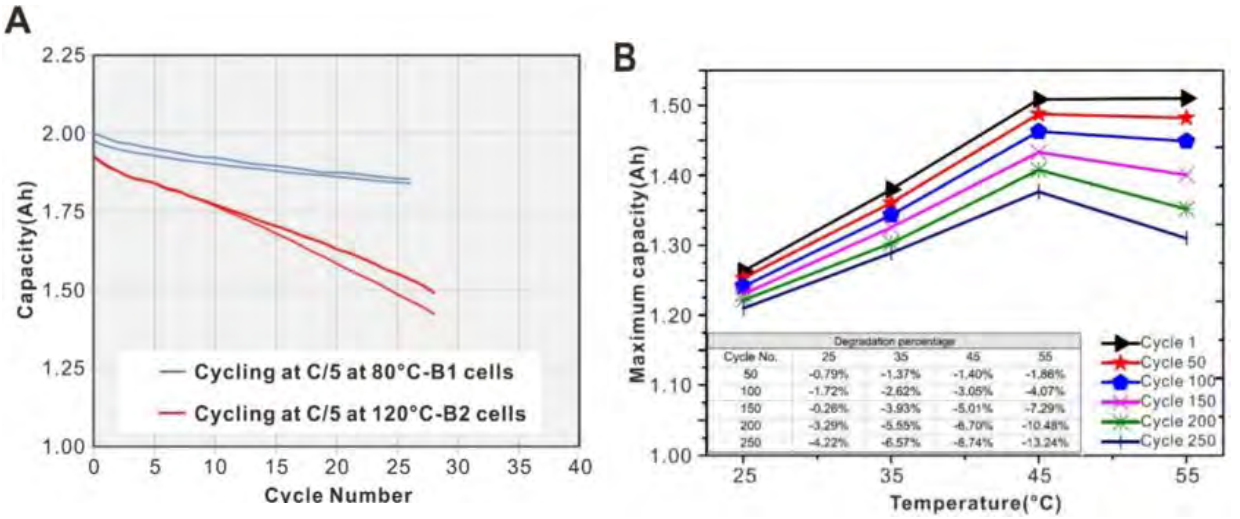

Figure 4.6. A) Capacity alteration [333], B) Maximum capacity alteration and the amount of degradation [337].

They suggested two plausible explanations for aging deterioration by assessing the alteration of binder and SEI during the aging process using different characterization techniques. On the contrary, the polyvinylidene fluoride (PVDF) binder moved to the anode surface and prevented lithium-ion intercalation. Additionally, carbonate species decreased at high temperatures, and inorganic species rose at the SEI layers, causing a rise in resistance within the batteries. Leng et al. [337] examined the temperature influence on the rate of capacity deterioration of a Sony Prismatic LIB after aging from 25 °C to 55 °C using an electrochemistry-based electrical (ECBE) model (**Figure 4.6B**). Trying to elevate the temp in the examined range partially enhanced the capacity of the battery. However, it also increased the rate of capacity loss during cycling, as seen in **Figure 4.6B.** The increase in deterioration rate was mainly attributed to electrode degradation, where phase shift and surface functionalization were exacerbated at high temperatures [341].

4.2.1.11 Accelerated Degradation

Cell degradation is a typical feature among most batteries and can be caused by several factors, including age and self-discharging processes [342]. On the other hand, accelerated deterioration is abnormal and can pose severe difficulties in Li-ion battery applications. A deterioration procedure is getting quicken when stored to high temperatures [343,344]. Outer deterioration is additionally enhanced by increased impedance, greater cycle frequency, change in SOC, and voltage rates. Corrosion of current collectors alters electrode material, and interactions within electrodes and electrolytes are examples of rapid degradation mechanisms.

Rapid degradation can reduce the battery's lifespan, which can be a significant concern in uses like EVs. It can also create surface layers and contact degradation, leading to electrode degradation, material disintegration, and lithium loss. These occurrences can induce transport barriers to penetrate the separator, resulting in an internal short circuit and, eventually, a thermal runaway [345].

4.3 External failures

External battery failures can substantially impact the BMS's other operations and induce internal battery issues. External faults are classified as temperature, voltage, current sensor, cell connection, and cooling system faults. A common problem is the cooling system fault, which causes heat failures, since the mechanism breaks down to generate appropriate chilling [346].

4.3.1 Sensor Fault

A reliable sensor fault diagnosis mechanism is required to maintain battery safety and performance. It also aids in the prevention of internal defects such as overcharging, overcharging, overheating, outer and inner short circuits. In addition there are temp, voltage, and current sensor failures. Vibration, impact electrolyte leakage, and other physical conditions cause sensor malfunctions. They might also be caused by faulty battery connections or corrosion surrounding the battery sensor [347]. A sensor malfunction can hasten battery deterioration, impede BMS functions owing to the inaccurate state assessment, and create other internal battery issues [348].

Temperature Sensor

The temperature sensor is an essential component of the Li-ion battery system since it provides battery management systems with crucial heat measurements to regulate the performance efficiently of battery. When the system fails, then it might cause inaccurate data at BMS, leading to further issues owing to poor thermal management [296]. Imprecision in the BMS thermal management function can significantly reduce battery’s lifespan. Aging, overheating, short-circuiting, capacity fading owing, and thermal runaway can occur if the system fails as well [349]. **Figure 4.7A** illustrates a pattern of temperature sensors and **Figure 4.7B** a realistic temperature sensor.

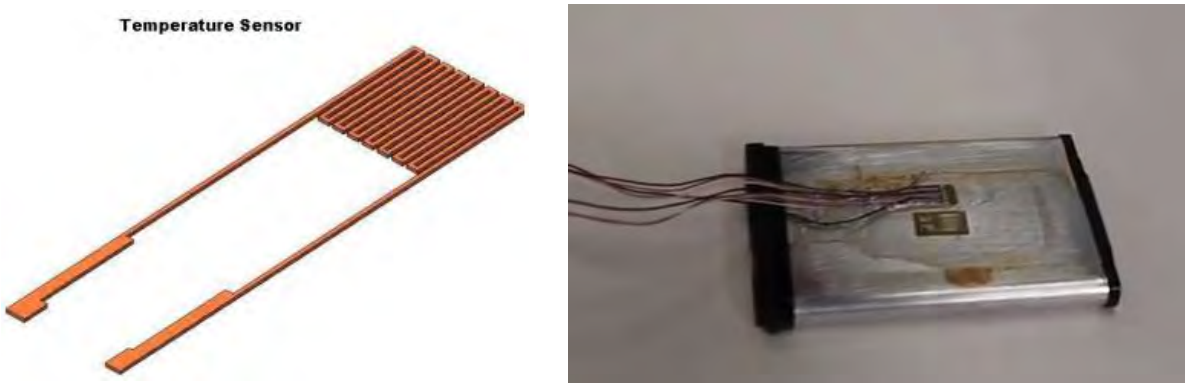

Figure 4.7. A) Temperature sensor pattern [350], B) Temperature sensor on a Lithium-ion Battery [270].

Voltage Sensor

The voltage sensor measures the voltage of the cells in the battery pack. The cell voltage can be measured on a battery pack with this sensor. Overcharge and over-discharge are a result of the defection of this sensor that can cause the cell or complete pack to exceed the manufacturers' voltage highest/lowest limits [351]. A faulty voltage sensor causes erroneous SOC and SOH calculation, leading to an internal issue when the battery suffers from overcharge and over discharge [352].

Current Sensor

The current that passes through and leaves the battery to the battery management system is measured and transmitted by the current sensor. Subsequent issues can be created if the current sensor is not working properly. The current might skip the sensor, resulting in inaccurate measurements. A faulty current sensor also causes erroneous assessment of SOC and other parameters, which affects the BMS management actions and leads the cell to overcharge, over-discharge, or overheat [352].

4.3.2 Cooling System Failure

This system is responsible for the heat treatment of the battery. The battery temperature is maintained within the proper limits, and the heat from the battery pack is extinguished with the help of this system, as illustrated in **Figure 4.8**. If there is a fan or motor breakdown or it is not working correctly, there is a system failure which can be occurred by damaged wires of the fan or temperature sensor or a blown fuse [353,354]. The temperature sensor and cooling system malfunction are inextricably linked since they rely on a temperature range [348]. A cooling

system issue is one of the most severe errors since it causes the battery to overheat and eventually thermal runaway. As a result, it is critical to detect it as soon as possible.

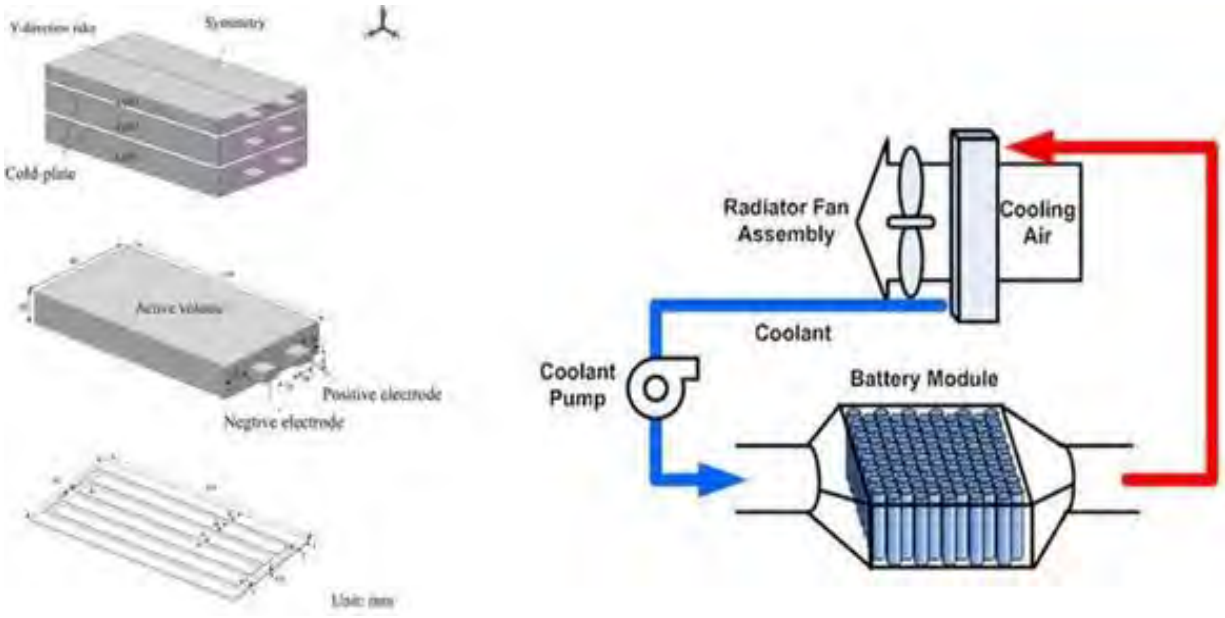

Figure 4.8. A) Illustration of liquid cooling system, B) a common cooling system [354].

4.3.3 Cell Connection Fault

This system fault occurs from an incorrect wire connection among the cell terminals, which can become loose over time due to vibration or corroded by contaminants [355]. When this defect develops, cell resistance might skyrocket, resulting in cell imbalance from unequal current or overheating of the malfunctioning cell [356]. This defect is easy to identify using voltage and temperature sensors. However, if left unresolved, it can lead to more severe repercussions like an external short circuit or thermal runaway.

4.4 Battery management system

A battery management system is responsible for the proper operation of a battery pack in, which can monitor and improve the performance of a battery. In the case of an abnormal state, the BMS can command the module(s) to be disconnected from the system. It increases battery performance by incorporating appropriate safety measures into a system. BMS is used in power system applications to monitor, manage, and supply battery power at optimal efficiency [357].

4.4.1 Software Design

The BMS software design allows for multitasking. Initially, it was not feasible to work on two activities simultaneously; one activity had to be put on hold while the other was completed. Various actions may be carried out concurrently in the modern BMS system design without disruption. To guarantee BMS safety, the early responsibilities of a BMS software design, for instance, measurement of voltage and current, over the protection of current and voltage, temperature monitoring, and protective relay actuation, must be completed immediately. The design of BMS software is depicted in **Figure 4.9** [358].

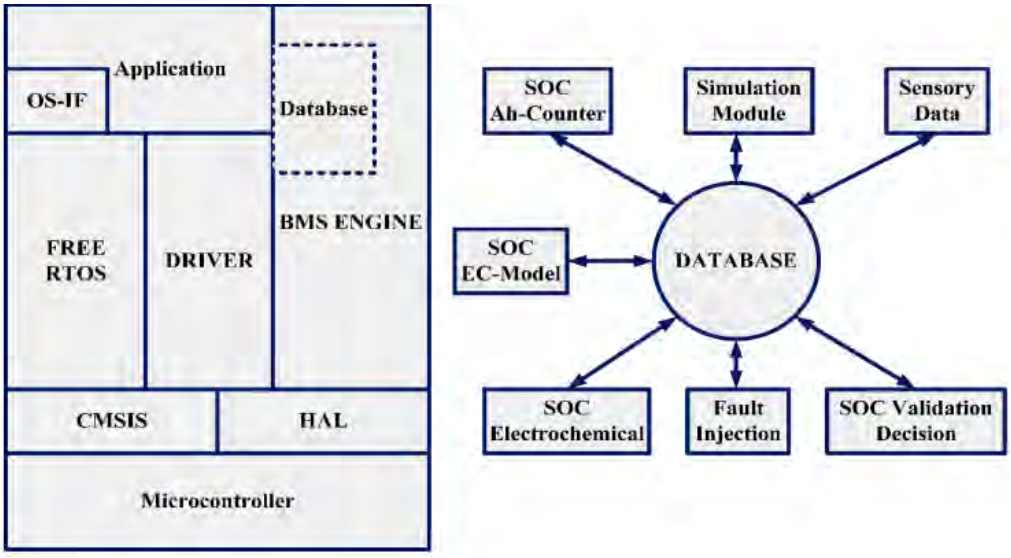

Figure 4.9. BMS software design [359] .

4.4.2 Operation

A battery management system is responsible for the proper operation of a battery pack in, which can monitor and improve the battery's performance. These measurements are essential because the state of charge, state of health, depth of discharge, and critical functional factors of the cells/battery packs are calculated. In addition, the aid of the measurement in increasing battery life and keeping up with the existing power network's demand needs. These main variables can be used to maximize battery life:

1. The system that is rensponsible for energy management includes a user interface for controlling-analyzing the efficiency of battery systems in various system blocks.
2. Efficiency and safety characteristics of the battery pack
3. Operating system resilience under various incident situations.

4. Monitoring and controlling the energy management system by using internet-of-things (IoT)

BMSs are created by combining operational unit blocks with different planning approaches. Depending on cell needs various uses will aid in determining the right design, functional unit blocks, and associated electrons. In addition, BMS plays a vital role in the pure battery's operation related to cell life and accuracy. The various methods of modeling BMS applications can improve the accuracy of the state of charge. Another significant advantage of BMS is the accuracy of cell balancing, which operates in the service of energy performance. As a result, the efficiency improvement of batteries has occurred through these proper measures.

Furthermore, an extended battery life can happen by controlling the battery's power with BMS a maximum efficiency. The management of charging and discharging has a substantial influence on cell life. Battery managmenent system have profitable benefits as well. Include increased battery lifespan, increased precision, and cheaper costs. Functions of BMS are depicted in **Figure 4.10.**

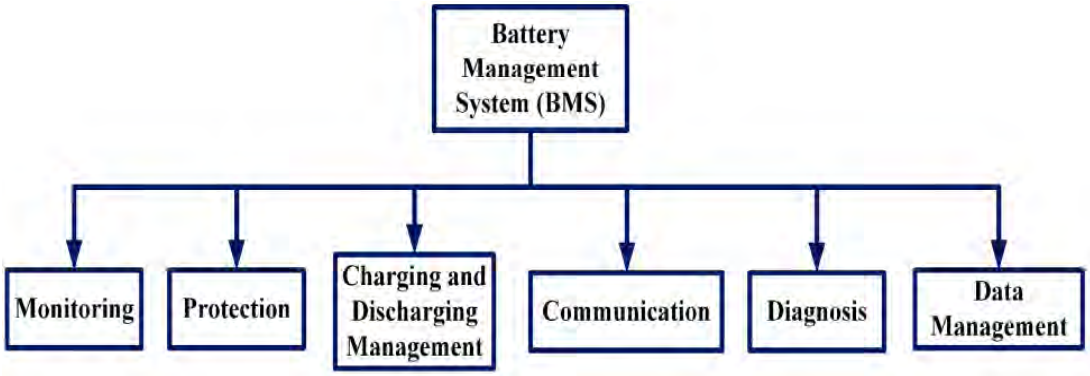

Figure 4.10. BMS operations [359].

BMS substantially affects the structure and function of batteries, particularly in terms of lowering the ecological consequences of battery systems. Because the surrounding environment of the battery pack generates variations in the cell/pack characteristics, BMS can safeguard the battery system from external occurrences. For BMS safety, the battery pack can manage two kinds of heats: electrochemical reaction heat and cell surrounding heat. BMS keep those two kinds of battery temps within their acceptable limits. BMS can deal with possible risks associated with battery system functioning. It guards against cell chilling and the mislaying of cell heating controls.

Furthermore, overload and heat effects could be minimized by charging/discharging cycles in which they are affected by the battery management system. As a result, it could affect the

surrounding. All of them could reduce the environmental impact of power plants and other systems, reducing air pollution and improving human health measurements and consequences.

4.4.3 Advantages of BMS

The technical benefits of utilizing (see **Table 4.1**) BMS include preventing damages by over or under voltage and balancing cells. The functional advantages are security, dependability, capability, and it can reduce the possibility of thermal runaway in powerful batteries. In addition, it detects defective batteries connected to parallel and series. It can provide profitable benefits by extending battery life and cutting costs. For instance, for a 22 kWh mid-size EV cell pack, BMS contributes just 8% of the overall battery pack cost [359,360].

Table 4.1. Benefits of BMS [359].

Environmental impact	Technical Efficiency Impact
Decrease of CO_2 emissions: When batteries are operated by a BMS to collect clean power to supply peak demand, CO_2 emissions can be reduced by 40%.	**SOH estimation:** BMS allows the exact prediction of battery's state of health (SOH). It has a favorable influence on the operation's and performance's safety quality.
Greenhouse gas advantages: Combining BMS and greater utilization of clean off-peak power, batteries' greenhouse gas (GHG) advantages might be doubled.	**Ideal Charging:** According to the design criteria, the goal is to provide less time-consuming, super-efficient, effective, and more safety solutions.
Advantages of the impacts of running out of metals: Effective to managing charge/discharge cycles and frequent operation. It affects the components used, which have a significant impact to surrounding and energy.	**Quick Analysis:** It supports state of charge and health. State of current is described as utilizing a full cycle of information, while state of healt is characterized depending on the amount of data cycles.
Advantages of the impacts of temperature control: BMS can manage two kinds of temperatures in the battery pack: electrochemical reaction and environment temperature.	**Self-analysis:** BMS supports SOC and SOH. SOC is described as utilizing a complete information cycle, whereas SOH is characterized depending on the number of data cycles.

4.4.4 Safeguarding

A BMS shall safeguard the battery system from every potential risk. Identifying the operating condition, defining failure criteria, verifying and recognizing the system, forecasting cell over voltage and current, estimating the segration failure, and monitoring raised/reduced

heat, are all part of BMS safety. Because of the external factors, the battery pack generates variations in the cell/pack parameters, and the system must be protected from these factors [359].

4.4.5 Management of the charging/discharging process

Battery's SOC has a considerable influence on its longevity. The quantity of charge/discharge cycles of every battery varies, and its lifespan is decreased as the quantity of these cycles is increased. The battery management system has to identify a better technique of charge/discharge. In addition, it has to support the state of charge because it plays a crucial role in longevity. BMS manages the region by monitoring the current of the charger turning the controllers on or off between the cell and charger, establishing power limitations, and performing stability [359].

4.4.6 BMS in diagnosis

BMS measures and forecasts SOC, the battery's energy capacity, battery life, DOD and SOF, the time required for a charging process, the temperature of the cell, and the internal impedance of current and cell potential for a pure and efficient operation of the battery. Moreover, BMS is in charge of identifying defects like flames, burst and mitigating failure effects impacts. As a result, defect diagnostics is a crucial BMS capability.

The depth of discharge measurement is required to determine the optimal battery cycle. The greater the DOD, the shorter the battery life will be. Lead-acid batteries, for instance, have a shorter lifespan if the depth of discharge is greater than 50%. To minimize unanticipated dangers, the depth of discharge must be kept in the BMS. The SOC is a variant of the same depth of discharge estimation. The quantity of energy that may be retrieved from a battery is indicated by its capacity. The battery capacity often measures the collected charge. The capacity of a battery is proportional to the temperature of the cell. At room temperature, batteries operate optimally. As the temperature drops, the inner impedance of the battery rises, reducing battery capacity. Besides other tests, the state of fitness evaluates the battery's ability to be paired with the system [359].

As already mentioned, the BMS's primary duty is to reduce the hazards related. Defects are the most significant common source of dangerous circumstances, and the BMS's safety operations can reduce the likelihood and severity of these faults. Sensors and insulators are popular safety elements added to battery systems. Additional operating limitations for voltage, current, and temp are measured via sensors attached to the cells [361]. Unfortunately, as the BMS design gets more complex, battery problems can become more intricate, and these safety precautions need to be revised. Fault diagnosis

techniques are indeed required for BMS [362]. These algorithms identify defects early and provide suitable and quick control measures for the public and battery [363]. **Figure 4.11** depicts the BMS's fault diagnostic method.

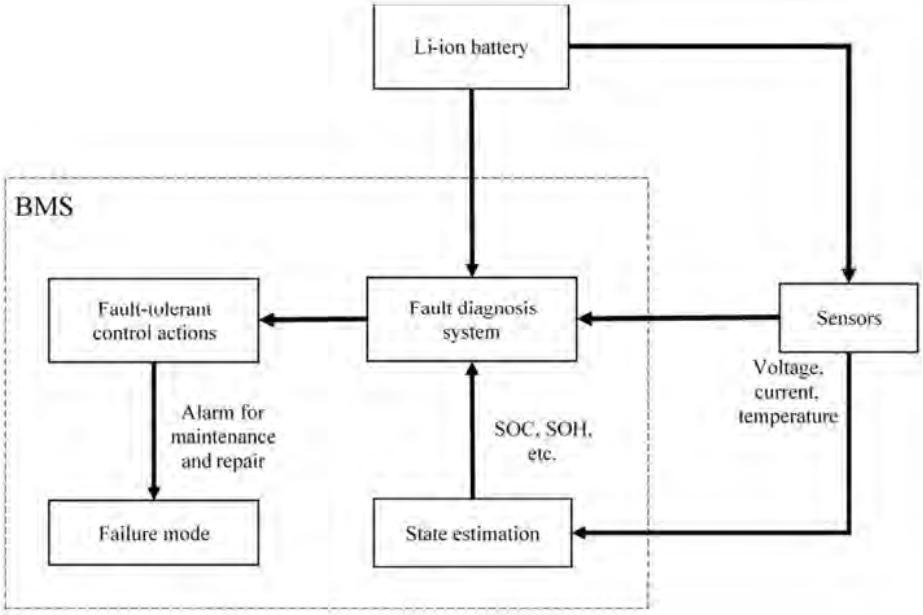

Figure 4.11. Illustration of fault diagnosis in BMS [364].

The BMS is important in failure analysis in the system of the battery since it contains various diagnostic modules and algorithms. It analyzes the system of the battery using sensors and condition estimation, as well as modeling or data processing to find any anomalies while battery system is operating. It is tough to do this activity properly due to the numerous internal and exterior flaws [270]. To effectively detect and identify a particular issue and provide the appropriate control action, many faults diagnostic methods must function in combination. The defect diagnosis algorithms in the BMS, on the other hand, have limited computational time and space. On account of huge quantity of cells in some systems, these fault diagnosis algorithms must be computationally efficient while preserving accuracy and dependability [365].

As previously stated, fault identification is a crucial function of the BMS. Fault identification, isolation, and estimate are all part of fault diagnosis. In diverse sectors, there are several defect diagnostic methods. Because errors in different usage of LIBs might been inner and linked, typical procedures used in other sectors are inapplicable. Fault diagnosis methods in LIBs are classified to 2 different models: model-based and non-model-based. **Figure 4.12** depicts the classification of fault diagnosis algorithms [366].

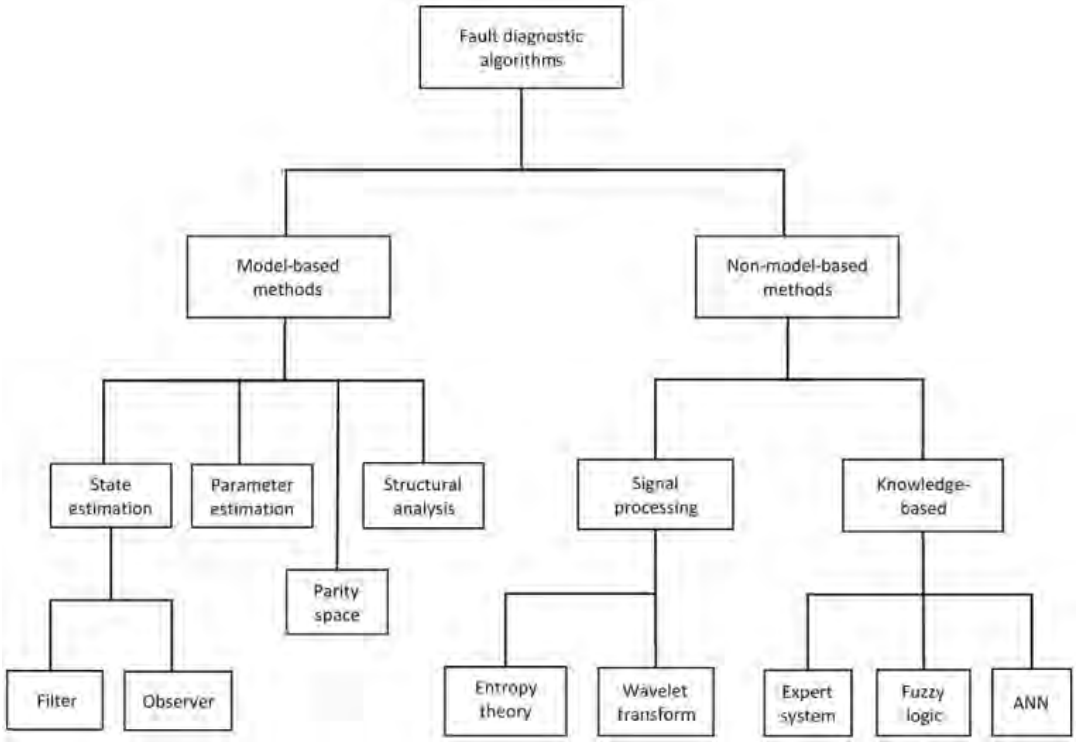

Figure 4.12. Fault diagnosis classification on LIBS [364].

In conclusion, while the fault diagnosis algorithms mentioned have significantly enhanced Li-ion battery safety, they still have limited practical uses. **Table 4.2** provides an overview of all the algorithms that have been studied. Model-based approaches can identify and localize faults in real time but need excellent computational efficiency.

Every one of these defect diagnosis approaches confronts several obstacles. First, because several defects have similar symptoms on the battery, correctly isolating each issue to give suitable remedies is challenging. Current solutions frequently imply that all the other parts of the system usually perform to minimize the requirement to isolate and identify observed defects. Following successful problem detection, further research shall focus on the design of fault detection methods. Because of a lack of knowledge of fault behavior, determining appropriate fault criteria for early and precise detection is another problematic issue. Moreover, building fault simulation software requires more excellent knowledge of battery failure behavior, as generating an accurate physical breakdown may be impracticable, expensive, and dangerous. As a result, further research on failure behavior must be undertaken using well-designed trials to obtain information for simulation and modeling purposes. Finally, the computing capabilities of the BMS must be increased and as a result diagnostic presicion would be more efficient. A

possible way to accomplished this is through th improvement of upcoming equipment to battery management systems, including cloud systems for battery state monitoring [364].

Table 4.2. A list of defect diagnosis algorithms for lithium-ion (Li-ion) batteries [364].

Type of Algorithm	Characterization	Algorithms
State Estimation	Via filters or spectators, the system state is predicted from a model. The residuals between predicted and calculated values reveal a defect.	Particle filter
		Kalman filter
		Luenberger observer
		Lyapunov-analysis-based nonlinear observer
		Partial-di fferential- equation-based observer
		Proportional integral observer
		Sliding mode observer
Parameter Calculation	Filter methods are used to calculate the model parameter from the data. The variation in the predicted model parameter identifies a flaw.	Recursive least squares
Parity space	A problem is discovered by producing residuals from the model's input/output relation and the measures.	Non-linear parity equations
Construction analysis	Structurally over-determined section of the system type is evaluated for discovering and seperating different failures.	Construction analysis
Sign processing	Sig are analyzed and converted to failure parameters like entropy or correlation coefficient. Abnormalities in these fault metrics indicate the presence of a fault.	Wavelet transform
		Correlation coefficient
		Shannon entropy
		Sensor topology
Knowledge-based	These algorithms apply the information gained from system inspections or data to develop guidelines or train data to identify a defect.	Rule based
		Blurry logic
		Differet forests analyzer
		Neural network

CHAPTER 5

Recycling of LIBs

5.1 Introduction

The need for lithium-ion batteries (LIBs) with better energy storage capacity, faster-charging abilities, and increased cycle life has increased due to advancements in electric vehicles (EVs), portable electronic gadgets, and renewable grid energy storage systems [3,367-369]. The global lithium-ion battery industry is predicted to reach $95 billion by 2025, with a compound annual growth rate (CAGR) of nearly 16%, which is estimated to result in the production of over 11 million metric tons of wasted LIBs by 2030 [370]. It is expected that by 2025, there will be 464000 tons of spent or discarded LIBs, up from 10 700 tons in 2012. Less than 6% of discarded LIBs are presently recycled worldwide, most of which are disposed of in landfills. This raises serious environmental worries since the spent LIBs have toxic metals (such as Co, Mn, and Ni) and combustible electrolytes that, when exposed to water, can generate hazardous gases [132,371,372]. These stockpiles of used LIBs also serve as valuable secondary resources for essential metals (such as lithium, manganese, cobalt, and nickel), whose global supply is at risk due to the rising demand for new LIBs. It's interesting to note that the raw materials used to make LIBs can only be mined and found in certain parts of the planet. For instance, China produces 70% of the world's graphite, Australia and Chile create 80% of the world's lithium, and the Republic of Congo generates around 60% of the world's cobalt [373]. However, it is possible to recover these essential components from used LIBs, preventing the exhaustion of scarce resources and lessening the supply chain's reliance on conventional mining. Much research has been done on these recycling methods, and as a result, some have been improved yearly. Various techniques of metal extraction and recycling are discussed in **Table 5.1**, including pyrometallurgy, hydrometallurgy, and direct recycling, each with advantages and disadvantages [374]. Promoting the circular economy approach that focuses on creating sustainable LIBs industries could be done by recycling discarded LIBs materials. It would collect and reuse valuable metals and reduce or eliminate potential environmental issues.

Table 5.1. Advantages and disadvantages of different recycling methods.

Recycling Method	Advantages	Disadvantages	Refs
Pyrometallurgy	Suitable for all battery configurations and kinds No further mechanical processing is required after sorting. High metals recovery (e.g., Ni, Co and Cu)	Li, Al, and LFP batteries cannot be recycled or treated. Gas cleaning is necessary to prevent harmful air emissions. Capital and energy intensive	[375] [376]
Hydrometallurgy	Suitable for use with any battery chemistry Flexible in recovery methods to focus on specific metals. High purity and recovery rates can be attained. Capital and energy efficient	Battery cells must be crushed (safety concerns) Acid treatment-related defects in the cathode structure. A large amount of processing efficiency must be handled, recycled, or disposed of. For lithium iron phosphate (LPF) batteries, not cost-effective There is a need for complicated mechanical treatments and separations.	[375] [377]
Direct recycling	Almost all battery components, including anode, electrolyte, and foils, can be recovered. Suitable for LFP batteries Energy efficient Practical for recycling manufacturing waste	When recovered material is introduced to the market, it might not function as well as virgin material or become outdated. Combining cathode materials might make recycled goods less valuable. Regeneration processes yet to be developed. Not called up to industrial level	[375] [378]

5.1.1 Pretreatment process

There are no established pretreatment method categories, as was noted in the Method section. In former times, four types of the mechanical devide, mechanochemical procedure, heat treating, and dissolution procedure were commonly employed [379-381], a more diverse categorization has been used recently. Yao et al. (2018) [382], for instance, separated pretreatment procedure within three phases: discharge, disassembly, and the disassociation of the active cathodic components. The pretreatment procedure was categorized by Zhang et al. (2018c) [383] identifying six distinct categories of physical pretreatment processes: disassembly and classification, crush, sieving, separation, and mechanochemical treating. Different words, including disassembly, stabilization, and passivation, were used by Harper et al. (2019) [384]. The lithium metal produced by overcharging batteries frequently bursts during recycling due to radical oxidation when subjected to mechanical stress from air exposure. LIBs typically have structures that are both complicated and dense hence their efficiency in direct pyrometallurgy or

hydrometallurgy will be low. So, before recovering the valuable metals from the waste, retreatment is first required [384].

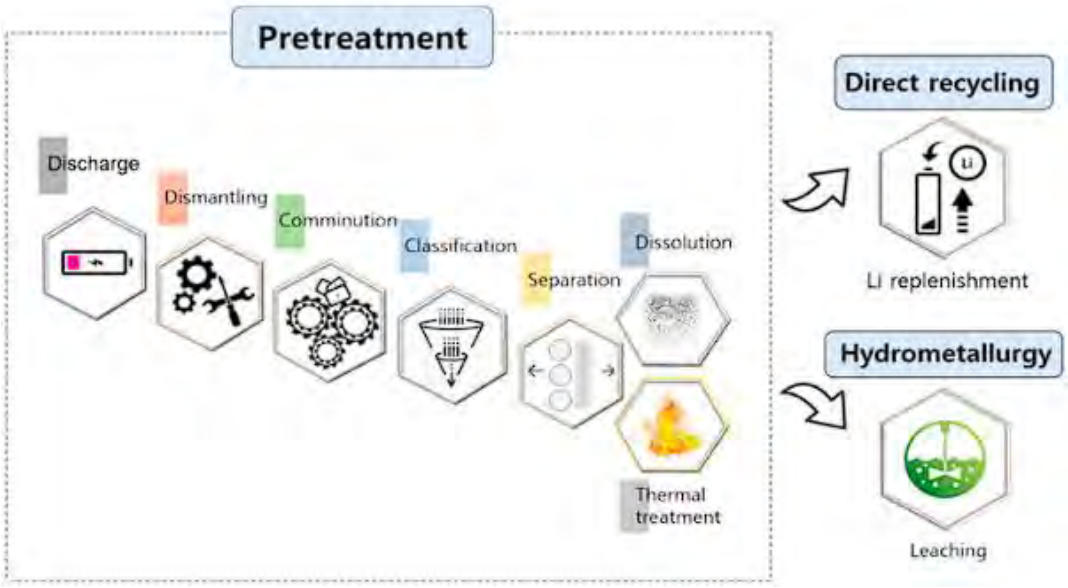

Figure 5.1. The parameters and ordering of the pretreatment steps in the LIB recycling process [385].

As a result, we define the first phase of each recycling scheme as follows, and the pretreatment procedures parameters were set in accordance with that definition.

- Pyrometallurgical process: a phase in which thermal treatment diminishes the active components of the electrode.
- Leaching is carried out during a step of the hydrometallurgical process.
- Direct recycling is a phase in which thermal treatment replenishes Li.

The majority of pretreatment techniques are depicted in **Figure 5.1**; there is a clear distinction exists betwixt the pretreatment step and the hydrometallurgical or direct recycling procedure since the pyrometallurgical process does not require pretreatment. Occasionally, it was possible to omit a stage in the preliminary procedure or to select one option in preference to another to achieve a particular objective. For instance, to get rid of a PVDF binder, we may use either solvent dissolving, thermal treatment, or both [385].

5.1.2 Discharging

When the spent LIBs are disassembled, the anodic and cathodic electrodes' vestigial power come easy into touch with one another and result in a short-circuit current flow [386,387]. This current produces Joule heat and sets the explosive and volatile on-fire solvent in the electrolyte, which causes the batteries to swell. Therefore, a discharging pre-treatment process was required before removing the battery housing to reduce the risk of self-ignition or a short circuit. Following a rolling press machine being implemented to create a short-circuit betwixt the two electrodes, the used LIBs based on Lithium cobalt oxide were immediately submerged in distilled water for a day to discharge [388]. **Figure 5.2** demonstrate the correlation between the discharge time in a Li-ion battery and the discharge efficiency and the effect of NaCl solution concentration [389].

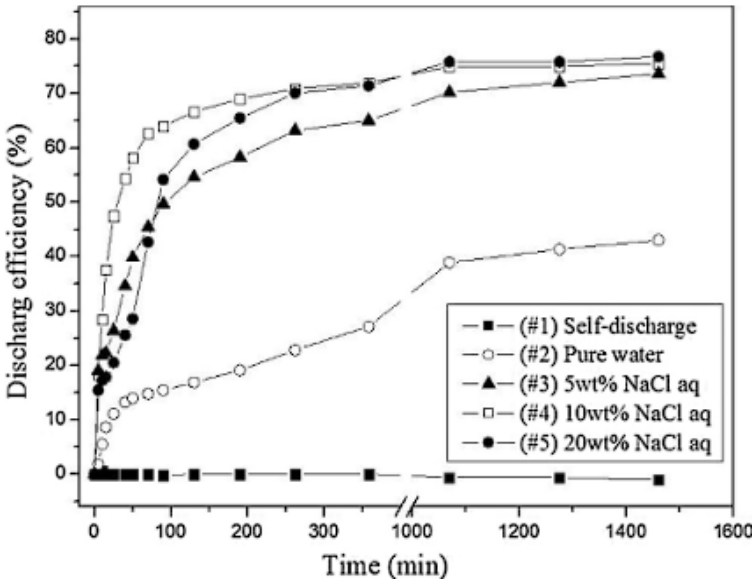

Figure 5.2. Discharge efficiency through time [389].

Used Lithium Ion Batteries consisting of Lithium-Nickel-Manganese-Cobalt-Oxide were disposed of using distilled water as the discharge solution. [390]. A battery cell could be completely discharged under a 70-min discharge condition, and the residual voltage being monitored during the discharging period started to drop significantly within 10 min. NaCl was added to water in hopes that the LIBs-based Lithium cobalt oxide would discharge more quickly [391-393]. The influence of the salt content on the discharge duration was examined using solutions of 1 wt.%, 5 wt.%, and 10 wt.% NaCl. The cell voltage in the 10 wt.% NaCl solution fell steadily for the first six minutes, then sharply after seven minutes, finally stabilizing at 0.5 V after ten minutes. After 7 minutes, the cell case started to leak, contaminating the electrodes inside with

salt solution and causing a rapid voltage fall. Compared to LIB cells, they were wholly depleted to 0.5 V in a solution of 1 wt.% diluted NaCl over a reasonably lengthy period—roughly 70 min—without any cell casing leakage. An examination was conducted to assess discharging efficiency under self-discharge settings and solutions with various NaCl concentrations, including 0, 5, 10, and 20 wt.% [389]. The Lithium-ion used batteries were discharged at 20 °C for 24 hours, and the solutions for the discharge were left to stand for another 24 hours, during which time layers of concentrated liquid and supernatant formed. The highest discharging efficiency was observed with the 10 wt.% NaCl solution, as illustrated in **Figure 5.3** [394].

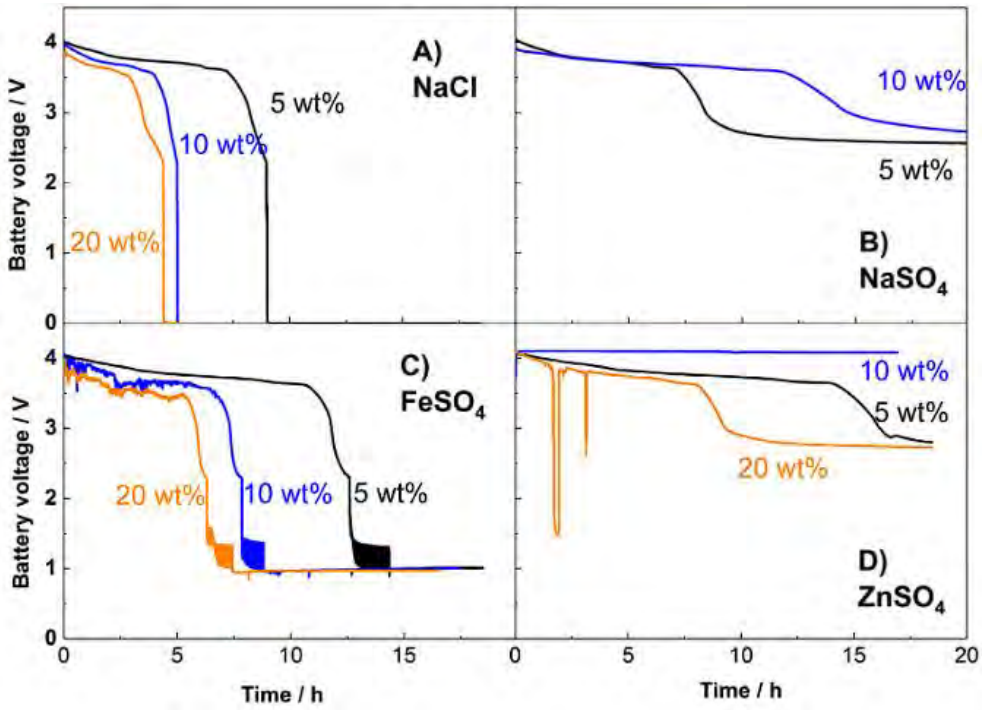

Figure 5.3. LIB discharging curves for various concentrations of in aqueous solutions (A)NaCl, (B) $NaSO_4$, (C) $FeSO_4$, and (D) $ZnSO_4$ [394].

The supernate and concentrated liquids contained high levels of sodium, aluminum, and iron, moderate amounts of cobalt, lithium, copper, calcium, and zinc, and low amounts of manganese, chromium, tin, zinc, barium, potassium, magnesium, and vanadium, respectively. Overall, the 10 wt.% NaCl solution appeared to provide the best discharge conditions, which enabled the supernatant to be reused and essential materials (Cobaltium and Lithium) extracted from the concentrated liquid.

Analysis was done on the LIBs discharging behaviors in various electrolyte solutions, with either no movement or stirring, and with sacrificial metal or not [394]. A LIB sample was discharged ex-situ using Pt wires attached to the battery poles and dipped into the electrolyte solutions on the other end. By examining **Figure 5.3**, it was observed that the LIBs voltage varied depending on the type of stationary solution used, such as NaCl, $NaSO_4$, $FeSO_4$, and $ZnSO_4$. The LIB discharge found NaCl to be the most efficient electrolyte, and discharge time decreased as salt concentration increased. The utilization of NaCl caused the release of chlorine gas, utilize of sulfate salts resulted in the formation of precipitation of metal on the Platinum wires, hindering the discharge process. In addition, corrosion of battery terminals is likely to be the biggest issue with discharging LIBs, as it can lead to partial discharging or seepage of the internal battery parts [395].

The data shown in **Figure 5.4** suggests that the rate of residual electricity (Re) to potassium chloride and sodium chloride solutions displays the most rapid decline. Additionally, organic electrolyte leakage and bimetallic corrosion of the iron shells were also noted. Moreover, with only slight levels of organics present, $NaNO_3$ and $MgSO_4$ solutions had similar levels of iron corrosion as the chloride-involving solutions [395].

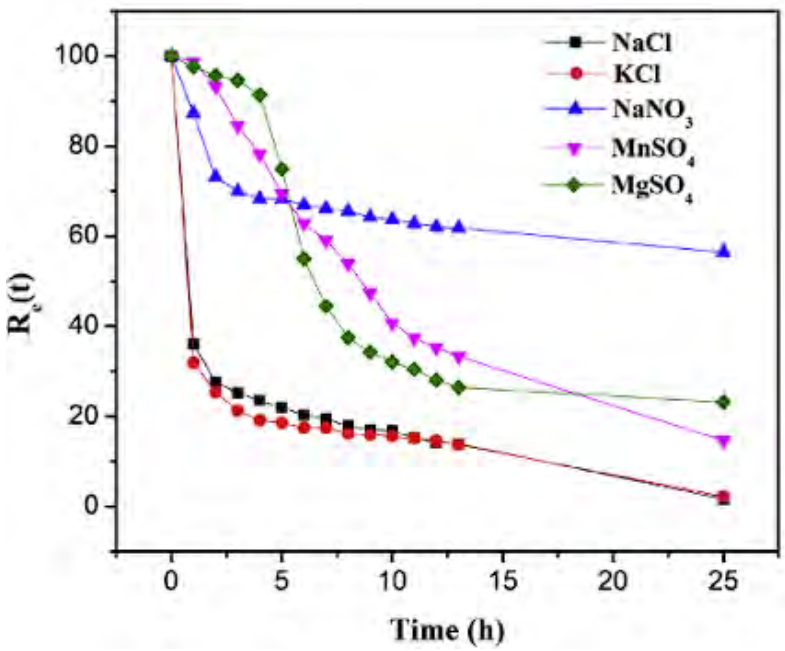

Figure 5.4. Residual Electricity Remaining in Solutions of Sodium Chloride(NaCl), Potassium Chloride(KCl), Sdium Nitrate($NaNO_3$), Manganese Sulfate($MnSO_4$),Magnesium Sulfate($MgSO_4$) [395]

$MnSO_4$ was demonstrated as the most advantageous discharging solution regarding its ability to inhibit bimetallic corrosion and limit organic electrolyte seepage. However, when setting the cut-off protective voltage to 1 Volt, the results of this study indicate that the efficacy of $FeSO_4$ is equal to NaCl, although the discharging efficiency of NaCl is higher than that of the other two solutions. (**Figure 5.5**) [396].

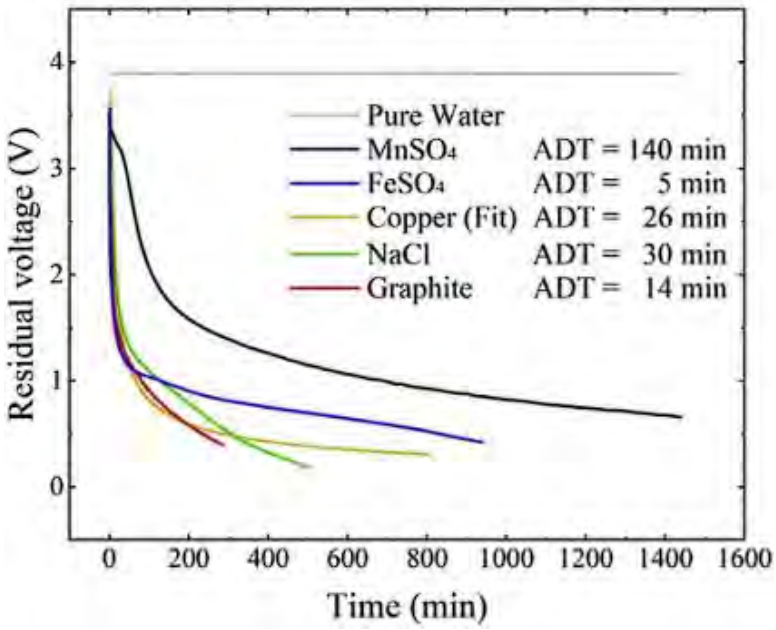

Figure 5.5. Demonstrates both chemical and physical discharge curves approaches, in which the control group was pure water, 0.8 mol/L of NaCl, 0.4 mol/L of $MnSO_4$, and 0.8 mol/L of $FeSO_4$ copper powder, graphite powder, and solution [396].

The physical discharging media, such as graphite dust and copper, disqualified for suitable large-scale discharging techniques due to linkage problem issues, readily oxidizing metallic surface, and risk of detonation from graphite dust. Hence, FeSO4 has been proposed as the most ecologically responsible solution for discharging due to the relatively small concentrations of components found at the supernate and the sediment components of the lithium-ion batteries.

5.1.3 Disassembly

In order to address safety concerns, the individual spent cells are often disassembled or dismantled manually using knives and saws [383]. The dismantling of the used LIBs allowed for investigation of the volatile organic compound emissions [389]. Dimethyl carbonate and tert-amylbenzene were found to be the two main organic vapor components that came from the

broken battery cells. A minimum ventilation pump flow rate was recommended to confirm the tolerated dimethyl carbonate concentrations. An automatic disassembly approach known as Z-folded electrode-separator elements was proposed to recycle lithium-ion batteries with the technique of pouch-type [397]. The proposed electrode careful separation of electrode materials extracted the cathode and the anode layers without applying destructive forces. Using unique toolsets to automatically stretch and feed the Z-folded separators, resulting in the removal of the cathode and anode layers fastened to the opposite sides, is an effective method.

5.1.4 Mechanical treatment

To release electrode elements from the disassembled Lithium-ion batteries, crushing and grinding are necessary. The importance of the comminution phase in the hydrometallurgy recycling technique cannot be overstated. The first large-scale battery recycling facility uses the hydrometallurgical Batenus method to shred various battery types in a gas-tight unit [398]. The Recupyl process includes two crushing processes [399], both of which take place in an inert atmosphere. The initial crushing is completed with a low-speed rotary mill, and a high-speed impact mill is used for the second crushing. Recycle of nickel metal hydride, Lithium-ion, and basically, Lithium batteries were accomplished simultaneously through two-blade rotors and hammer-crushing processes [400], where in the first case, no sieving control was used; in the second, a 5 mm sieve was employed. A comparison was made between double smashing using a twin-rotor crusher and crushing with a twin-rotor followed by hammer crushing, and the quantity of retrieved electrode dust was used as a benchmark. The quantity of electrode powder recovered was maximized using hammer crushing and a two-blade rotor crusher.

The recycling procedure of the used Lithium-ion batteries is founded on Lithium Cobalt Oxide cathode compared to wet and dry crushing methods [401]. According to **Figure 5.6**, the wet grinding apparatus was a blade grinder aquatic. The particles in the crusher's input formed slurry when water was added, which transported the shattered particulates passing inside a sieving plate. The dry crushed was completed with a collaborative two-step procedure. Before crushing in the impactor crusher, the used lithium-ion batteries at the beginning were broked into smaller fragments with a shredder crusher. The wet crush procedure caused the components of the used Lithium-ion batteries to be broked down into thinner pieces because of the cleansing ability of water, resulting in a more complex mixture of the final products with some of it being lost.

In contrast, spent LIBs selective crushing properties were fully utilized by the dry crushing approach, allowing the Lithium Cobalt Oxide and graphite electrode elements, released from the Aluminum and Copper sheets without over-crushing the other wasted LIB elements. The same authors used the dry crushed technique to chemically and mineralogically characterize the spent LIBs to provide fundamental knowledge about the efficient mechanical crusher and separation in this recycle procedure [402]. After dry sieving, the metal shell was broken by shear crushing, exposing the electrode elements, and the crushing by the impact was capable to crush the materials selectively. In hydrometallurgically recycled methods, a planetary ball mill is frequently employed to increase the leaching efficiencies of precious materials [393,403,404]. A new approach to extracting Lithium and Cobalt from used Lithium-ion Batteries was suggested involving a procedure using a planetary ball mill through a combination of mechanical and chemical means [405]. In order to gain a better understanding of the mechanochemical process and its effects, only pure Lithium-Cobalt-Oxide dust was utilized in the experiment to get rid of the interference of other elements. The experimental parameters comprised the Iron mass ratio used as a grinding aid to Lithium-Cobalt-Oxide, the speed of rotation, the mechanochemical milling period, and their influence on Lithium and Cobalt removing was studied.

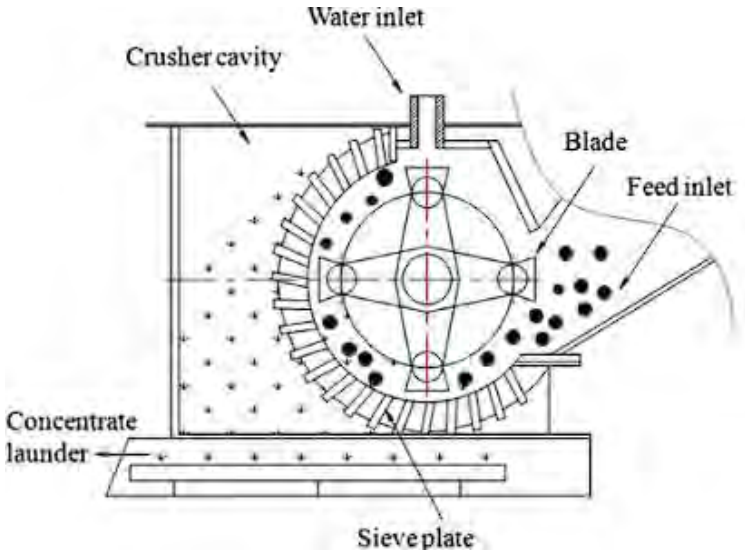

Figure 5.6. Sketch of wet impact crusher [401].

These variables had a positive impact on the drawing out of cobalt but negative impacts on lithium leach. The Lithium-ion batteries that utilized four other cathode types (Lithium-Cobalt-Oxide, Lithium-Ferro-Phosphate, Lithium-Manganese-Oxide, Alloy cathode) underwent a pretreatment procedure including mechanical comminution and a size-based sorting [406,407].

A continuous flow of Lithium-ion battery cells was mechanically cut into bits smaller than 7.5 mm using a commercial granulator. The authors argued that their suggested pretreatment method would use little energy and just a limited number of tools, such as a shredder, a machine for vibration, and sorting sieves. To reach a size lower than 10 mm, a one-shaft shredder with a shear-kind cutting facility was constructed in a specific way [408]. With the presence of water, the spent LIBs, who's cathodes primarily carry Cobalt and Manganese, are placed inside the shredder before being floated and sieved. Water operated as a cleaning agent and a temperature controller during the wet shredding, considering that it was performed at a temperature of 30 °C. Plastic-containing shredder output slurry floated on the water and was manually removed, while other components, like the electrode materials, were sieved out to separate them.

In the LithoRec process intended to recycle the NMC-based LIBs, the impact of a secondary crushing process on the output of the black material was examined [385]. A procedure of a two-stage crush consisted of the initial crush step, which used a grinder consisting of a six-plate rotor that had been adopted, and the next stage was a mild comminuting, which used a grinder with a 10 mm discharging screen. At the start of the crushing process, the volatile elements, consisting of the dissolvent of electrolytes and carbon dioxide and the necessary materials from the lithium-ion batteries, were released into the air. **Figure 5.7** compares the output of the black matter, including or not a secondary crush stage, which was done during the initial crush stage afterward and followed by air classification. The secondary crush stage raised the performance of the black matter from 60% to 75%, with no inclusion of the contamination from the Copper and Aluminum current-collectors [409].

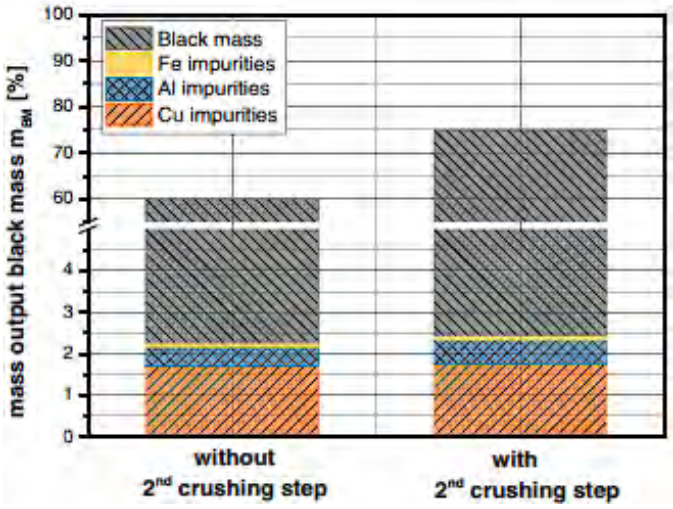

Figure 5.7. Black mass and impurity yield, including or not a second crush stage [409].

A process of grinding and flotation is suggested for extracting and regaining Lithium-Cobalt-Oxide and graphite from used Lithium-ion batteries [410]. First, an impact crusher was used to reduce the size of the cathode and anode strips to 0.074 mm. Steel balls were used to process the blended electrode dust, with shredding times ranging from 2.5 to 30 minutes. A significant purity and extraction efficiency level for Lithium-Cobalt-Oxide and graphite were attained using the ideal conditions of 5 minutes of grinding. According to **Figure 5.8**, the lamellar graphite structure slides, flakes, and exposes a significant number of new hydrophobic surfaces beneath the horizontal shear stress generated by the grinding media. However, the organic membrane covering the LCO particles must be partially replaced to restore the original hydrophilic surfaces.

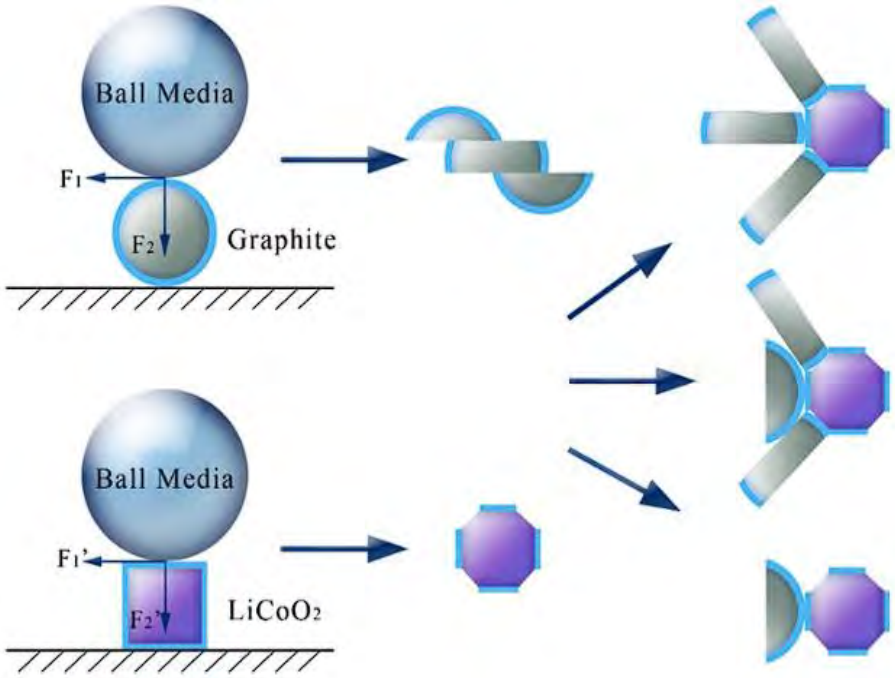

Figure 5.8. A mechanism for desiccation corresponding to mechanical abrasion [410].

The perpendicular rolling strain caused the Lithium-Cobalt-Oxide and graphite to adhere, which became more severe with time. Even though some of the Lithium-Cobalt-Oxides condense may have adhered to the graphite during the 5-minute grinding procedure, thereby reducing the recovering rate float, the considerable aqua-ability disparity still allowed for a satisfactory floating concentrate rate. An investigation was conducted into cryogenic grinding to recover from the negative electrode elements from used lithium-ion battery cells consisting of Lithium-Cobalt-Oxide [411]. The cryogenic grinding tools allowed at a low-temperature milling down to 77K (-196.15 ^{o}C) and was made up of an abrasive reservoir and a reservoir of LN_2. It was utilized for an impact

abrasive machine at a significant frequency with a brief operating period. Operating at lower temperatures would enable the targeted grinding of the negative electrode, which would result in the improved peel-off of the cathode materials, as the glass transition heat of Polyvinylidene fluoride (PVDF) is roughly 235K (-38.15 ºC), and the mechanical toughness of the Aluminum current gatherer upgraded at lower temperatures. When pre-treatment is done in cold conditions, the optimal results are achieved at 77K (-196.15 ºC) for 5 min and cryogenic grinding for 30 s, the peel-off efficiency of the cathode materials was increased from 25.03 to 87.29%. In the meantime, LCO and graphite were separated using froth flotation in conjunction with cryogenic grinding [412]. A one-ball mill was chilled using LN_2 for smashing the electrode elements.

5.1.5 Classification

Numerous pertinent investigative endeavors were developed categorization methods following Pulverization since the BATENUS process (a primary process for the hydrometallurgical reclamation of metals from secondary raw materials) described using a sieve for the button cells [398]. LCO-based cell phone batteries were deconstructed, with the operating of a rapid grinder and categorized in extent of 1–50 mm [413,414]. Three different-size sieves (106, 200, and 850 mm) were used to separate the results products of the crushing process from the used Lithium-ion batteries, which contain Lithium-Cobalt-Oxide [415]. Lithium-Cobalt-Oxide atoms and carbon were the small results of an 850 mm sieve, whereas the oversized outcomes were the plastic wrapping, steel sheath, Aluminum foil, Copper foil, and dividers. Similar to this, there are three diverse magnitude (8, 8/16, and 16 the mesh chosen was optimal for subsequent reductive leaching) were used to separate the pulverized wasted lithium-ion batteries that contained lithium cobalt oxide [416]. The LCO-containing ground products from the spent LIBs were sieved to 0.075 mm, and the oversize materials were again ground up and added to the undersized portion [417]. Vibro sieving was used to separate the pulverized dust from the used Lithium-ion batteries based on Lithium-Cobalt-Oxide make use of six different sieves with varying cut-offs (2 mm, 1 mm, 0.5 mm, 0.25 mm, 0.2 mm, and 0.125 mm) [418]. Except for Copper and Aluminium, the elements were found to be more concentrated in the fractions with a particle diameter larger than 1 mm and contained 67% of Aluminium and 79% of Copper. All the elements were primarily to be more concentrated in the fractions with a particle diameter smaller than 1 mm, which comprised 82% of Lithium, 81% of Cobalt, 88% of Manganese, and 62% of Nickel. Additionally, a succession with sieves with apertures measuring 0.5, 2, and 5 mm were used to screen the grinding process results created using a shear

crusher [391]. The impact of the size of the screening aperture was looked into using the pulverized elements taken from the used lithium-ion batteries [419]. There were no electrode elements in the biggest portions, and the 12-mm aperture screen performed better than the 2, 4, and 8-mm screens. Utilization of a 12-mm screening aperture, CO made up a bigger portion of the underflow and contained impurities in smaller amounts, as illustrated in **Figure 5.9**.

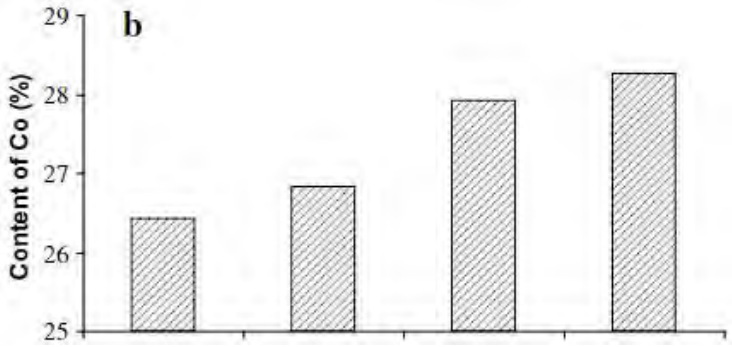

Figure 5.9. The effect of the screen aperture size on Co [419].

The material of the three size divisions allocated (Size fraction/mm: 2, -2 + 0.25, and 0.25) were compared in the recycling procedure of wasted Lithium-ion batteries with a Lithium-Cobalt-Oxide negative electrode [401]. The wet crush procedure created 27.57% of the material over 2-mm, 16.21% 2-0.25 mm, and 56.22% under 0.25-mm. As opposed to the wet crushing approach, which generated a modest performance in the medium-size fraction, the dry pulverization achieved yields of 21.28% over 2-mm, 30.46% 2-0.25 mm, and 48.26% under 0.25-mm. The procedure of the dried sieve comes after the dried crushed process, which resulted in eight different sample classes of varying sizes (Size fraction/mm, +2, -2+1, -1+0,5, -1.5+0,25, -0,25+0,1, -0,1+0,075, -0,075+0,045, and 0.045 mm) [383].

Al and Cu both had recovery rates of 94.14% on rough-size fractions over 0.25-mm. Instead, Cobalt was concentrated in the small-size ratios under 0.25-mm, leading to overall regaining ratios of 94.39%. In general, the pulverized remnants of the used Lithium-ion batteries could be divided into three fractions with sizes of +2, -2+0.25, and 0.25-mm, fractions, primarily made from Aluminium, Copper, and Cobalt and Graphite, respectively. The same team thought similar categorized criteria after pulverized LCO-based Lithium-ios batteries [420]. Five size fractions (+1.4, -1.4+0.71, -0.71+0.5, -0.5+0.2, and 0.2mm) were used in a sifting procedure.

The Aluminum and Copper foil concentration was predominantly over 1.4-mm, while the electrode elements were primarily under 0.2-mm.Using screening tests, it was determined how the

pyrolysis heat influenced the magnitude distribution of the pulverized products from the discarded Lithium-ion batteries that consist of LCO and graphite. [421]. The magnitude distribution of the crushed items, following sequential crushing, with pulverisation and pyrolysis in a nitrogen atmosphere at various temperatures is shown in **Figure 5.10**.

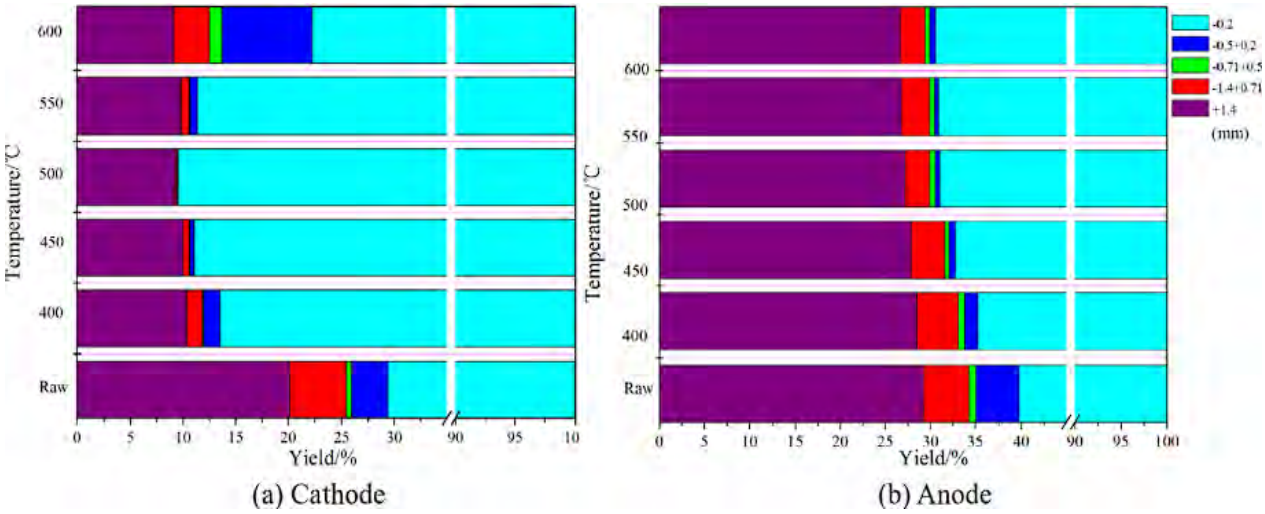

Fig 5.10. Size magnitude of products from crushing at various pyrolysis temperatures: (a) Cathode, (b) Anode [421].

Large metal cases and separator components mainly concentrate into parts of 2-mm and over, including Aluminium/Copper foils and dividers with fiber-like forms. Particles with a diameter of 0.2 millimetres were collected as a concentrated element for electrodes.

The greatest concentration of the 0.2-mm size fraction in the pyrolytic cathode led to the conclusion that 500 °C was the optimum pyrolysis temperature. It was shown that the deliverance of the electrode elements and the reduction of molecule conglomeration could benefit from pyrolysis. To determine the distribution of the crushing outcomes of the wasted Lithium-ion batteries based on Lithium-Cobalt-Oxide and a small amount of Nickel and Manganese was determined by the exact size requirement, and it was observed that 500 °C pyrolysis temperature resulting in the elevated deliverance effectiveness [422].

5.1.6 Separation

Once the Lithium-ion batteries fragmentation products have been classified based on molecule dimension, further refinement of the separation procedure is undertaken using magnetic, eddy current, electrostatic, gravity, and froth flotation methods. In the LIB recycling process, removing the components' containing iron has frequently been accomplished by using

magnetic separation. After vibration sieving, the anode, the steel cases, and the plastic packaging were separated from the cathode, which included the Lithium-Cobalt-Oxide active elements and the Aluminum current collector [415]. A rare earth magnet was passed over the elements to perform a magnetic division method which allowed the steel shells from the used lithium-ion batteries, mostly made of the Lithium-Cobalt-Oxide cathode, to be taken away [9]. Hand removal was required to remove steel components that held the non-ferrous appurtenances. During the Recupyl procedure at the industry scale, a high induction magnetic separator is employed to unpick the steel elements into distinct fractions effectively [399].

A sample eddy current separation device operating to recycle lithium-ferro-phosphate based (LFP) Lithium-ion batteries is shown in **Figure 5.11**. Eddy current separation permits the separation of electrical conductors from non-conductors or marginally conductive materials [423]. The Al and Cu foils are divided to a maximum particle proportion of 1.72 in the particle size scope of 2–20 mm due to their high electrical conductance and ability to produce a powerful vortex flow in an alternating magnetic field. For the eddy current separation, the authors developed models for the force and kinematics of the various elements in the Lithium-ferro-phosphate based Lithium-ion batteries. The pulverized remnants, which comprised ferrous metals, non-ferrous metals, and non-metals, were separated from the blend of nickel metal hydride, Lithium-ion, and primary lithium batteries utilizing an eddy current separator with a movable separator [400]. In the wasted LCO-based LIBs, the eddy current splitting offered a more effective division of Copper and Aluminum in the electromagnetic fraction, and the non-electromagnetic fraction had a more effective division of Cobalt and Lithium [424].

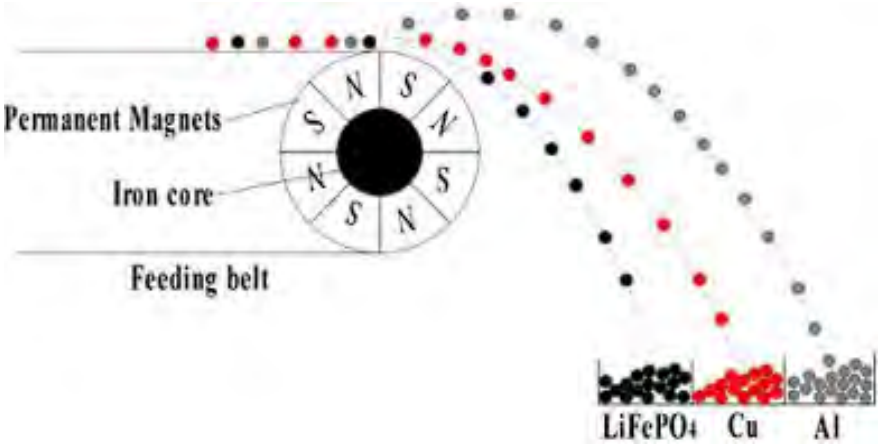

Figure 5.11. Eddy current separation utilized for the recycling of the $LiFePO_4$ based LIBs [423].

The divide membrane and metal case in the used Lithium-Cobalt-Oxide based Lithium-ion batteries were removed using the eddy current separation technique and pneumatic and magnetic separation techniques [422]. The forces acting on the charged or polarized particles in an electric field are used to create the electrostatic splitting influenced by the variations in the electrical characteristics of the elements. The elements were acquired after grinding, sifting, and drying procedures were separated using a roll-type electrostatic separation technique, and its schematic representation is given in **Figure 5.12** [425,426].

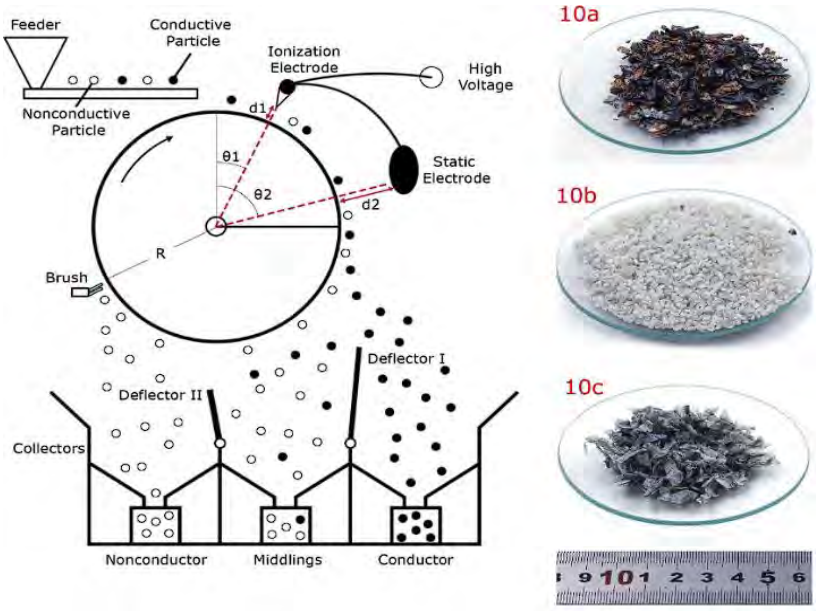

Figure 5.12. Schematic diagram of an electrostatic separator and the resulting products; 10a: Conductor, 10b: Middling's, 10c: Non-conductor [426].

The two primary parts of the electrostatic separator are ionization and static electrodes. The non-conductive materials were pinned to the roll by the ionization electrode, which then used a static brush to gather them at the roll's end. The middlings gathered as weightier particles than their pinning action, while the static electrode drew in the conductive materials. In the electrostatic splitting of the pulverized remnants from Lithium-Cobalt-Oxide based LIBs, the ideal the operational conditions achieved, comprised of the electrode voltage and the roll rotation speed [425]. The ideal working parameters were:

- 20 rpm roll rotation speed.
- 25 kV electrode voltage.
- 6 cm electrostatic electrode distance.

- 0 deflector inclination angle.

Even though the three separate LIB models had different compositions, a purity of more than 95 percent was obtained. Similarly, for the recycling of the Lithium-ion batteries based on Lithium-Cobalt-Oxide, attrition products > 38 mm were separated using a roll-type electrostatic separator after being scrubbed with silica sand media [427]. The following three fractions were created from the attrition products. The polymeric splitter and thin silica sand were gathered in the roll depicted in **Figure 5.12**. The electrode voltage was altered so that the large silica sand particles would not be held back by the polymeric separator like before but instead be gathered as middlings. The conductive Aluminum and Copper current collectors were also placed on the receptacle's right part. Using trial and error, the ideal operating conditions were modified based on those mentioned by Silveira et al. (2017) [425]. In a one-pass electrostatic separation, the middlings still carries a sizable quantity of conductor elements, whereas the container that holds the conductive material portion holds just Aluminum and Copper foils.

In order to extract LCO from the aluminum foil, the pulverized elements from the wasted Lithium-ion batteries were submitted in an ultrasonic cleaning tank with agitation [410]. Three different treatments, agitation, ultrasonication, and using both, contrast with separating the electrode materials. Although both agitation and ultrasonication failed to successfully remove the electrode elements from the aluminum foil, their combined use resulted in significant extraction of the electrode elements. The authors contended that the cavitation action of the ultrasonic process, which produced increased pressure, would help break down insoluble chemicals and disperse them in the water, making it more environmentally beneficial compared to other treatments, such as the use of organic solvents.

After shredding the inactivated cells from the Lithium-ion batteries remnants based on Lithium-Cobalt-Oxide, air separation was carried out in a zigzag classifier [428]. Two-phase comminution operations followed by an air-classification mechanical separation process were developed; Its procedure flow chart is illustrated in **Figure 5.13** [409]. During the initial crushing and drying phases, the precious elements from the Lithium-ion batteries and the gaseous components were released, and the number of their volatile components reduced the mass of the Lithium-ion batteries fragments. The first air categorization retrieved heavier components, including steel screws, electric cables, and casing materials.

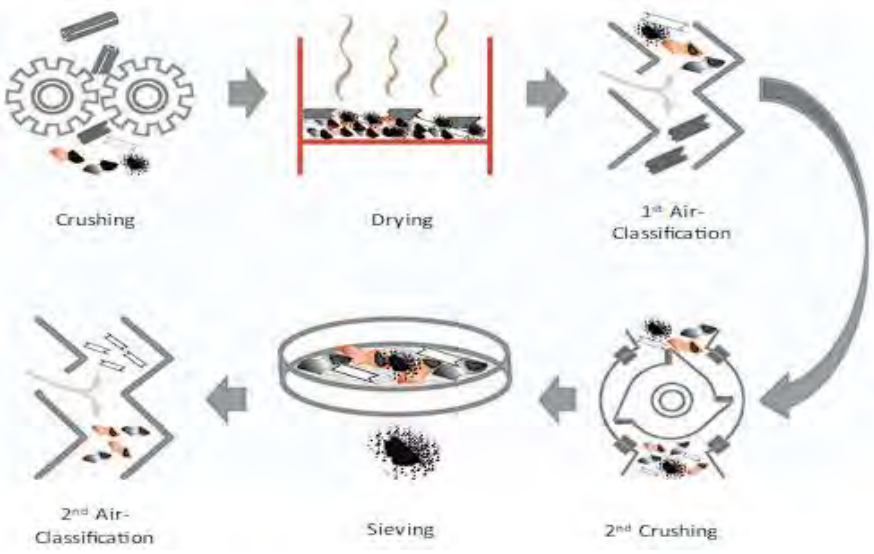

Figure 5.13. Process steps of the investigated recycling process with varied 2nd crushing [409].

A cascade of crossflow sieving was used to enable the splitting of elements with similar magnitudes of a particle but different densities via zigzag sieving. Without including contaminants from the Cu and Al current collectors, the second pulverization raised black matter output from 60% to 75%. The useless separators were removed from the shards of the current collector foil during the second air categorisation using one zigzag sieve. The proposed technique could split the weighty elements of the Lithium-ion batteries from the initial air categorization, the black matter from the sifting, and a foil fraction from the second air-categorization.

In recycling the LCO-based LIBs, various separation techniques that depend on the crushed products' particle size were suggested [9]. There are three size-based separation techniques. Al and the separator were the principal components of fractions over 2 mm, which the airflow easily separated. The crushed goods in fractions between 2 and 0.5 mm were composed of conductive components, such as metal foils and insulating materials. These fractions had a large concentration of Aluminum and Copper suitable for electrostatic separation. Due to Lithium-Cobalt-Oxide and graphite being dominant in particles under 0.25 mm, an additional grinding procedure was utilized for fractions between -0.5 mm and 0.075 mm. After taking out the binder from the cathode and anode, the float method would be the most suitable for splitting Lithium-Cobalt-Oxide and graphite into -0.075 mm pieces since Lithium-Cobalt-Oxide is water-attracting and graphite is water-repellent.

5.1.7 Dissolution

After the classification step and separation stage, some freed active elements are still linked to the current collectors, while the binders keep other separated active materials together. As a result, the appropriate solvents are frequently used to dissolve the binders or the aluminum foils.

Lithium-Cobalt-Oxide and graphite layers on the current collectors were separated using N-methyl pyrrolidone (NMP) at about 100 °C for one hour [424]. NMP has an elevated boiling temperature, around 200 °C, and is an excellent solvent for PVDF (solubility: 200 g/kg of solvent). Films were successfully separated from current collectors using the NMP procedure, and Copper and Aluminium in the metallic state were recovered by filtering them out of the N-methyl pyrrolidone (NMP) substance. N, N-Dimethylacetamide (DMAc), with its 10% solubility of Polyvinylidene fluoride (PVDF), was chosen over NMP for the splitting of the Lithium-Cobalt-Oxide, negative electrode elements from the Aluminium foil due to its economic advantage. DMAC can be evaporated at 120 °C for 12 hours since it has a boiling point of 165 °C. The Lithium-Nickel-Manganese-Cobalt-Oxide (NMC) and Lithium-Cobalt-Oxide (LCO) negative electrode elements were separated from the aluminum foil with the use of N, N-dimethylformamide (DMF) [429-432]. The cathode scrap materials were immersed in DMF or a DMF and ethanol mixture at 70 °C.

A range of solvents and NMP were used to separate the active cathode elements from the aluminum foil during an ultrasonic process [433-435]. The dissolution rates in aqua, acetone, dichloromethane, carbon tetrachloride, and NMP were evaluated using ultrasonication. The ultrasonication state was used to compare dissolution percentages, which are calculated by taking the rate of the differences betwixt the aggregate weight of the cathode elements and the Aluminium foil weight and dividing it by the total weight of the cathode materials in water, acetone, dichloromethane, carbon tetrachloride, and n-methyl-2-pyrrolidone (NMP) [428]. While the amounts of the other solvents were between 15% - 18% and remained stable with the amount of time and temperature monitored with ultrasonic technology increased, the dissolving rate in NMP was 99%. Compared to the current NMP dissolution settings, such as 100 °C for one hour, the researchers claimed that the suggested room temperature and the treating brief duration of the proposed ultrasonication conditions would be more environmentally friendly [429].

5.1.8 Thermal treatment

Thermal processing can be used to remove the binders that hold the active elements, and the carbon conductors are connected to the current collectors. A two-step thermal treatment and calcination procedure was used to separate the electrode elements from the current collectors and remove the carbon and binders [413]. The vibrating screening was used to separate the electrode materials from the Al current collectors after the electrode materials containing Li, and Co underwent a two-step heat treatment in a furnace at 300–500 °C for 1 hour. Next, the carbon and binders were burned off at a temperature between 500 and 900 °C for 0.5 -2 hours to obtain the LCO cathode active materials. The Lithium-Cobalt-Oxide was first taken away from aluminum foil. At the same time, Polyvinylidene fluoride (PVDF) and the carbon dust found in the cathode elements were destroyed through high-temperature calcination [436]. The dried powder was heated for a total of 5 hours at 600 °C after being heated for 2 hours at 450 °C in the air. Like Lee and Rhee (2002), the Lithium-Cobalt-Oxide negative-electrode elements were divided utilizing a thermal process of the wasted Lithium-ion batteries in two steps [413,437,438].

Burning the binders and organic additives occurred during the first heat process stage, which lasted an hour at 150–500 °C. For the second thermal treatment, carbon and the remaining unburned organics were removed for one hour at 700–900 °C. The thermal pretreatment was carried out to remove carbon and PVDF from the negative-electrode active elements after 24 hours of drying at 60 °C [403,439-441]. In a muffle furnace, the cathode active components from the used batteries were calcined at 700 °C for five hours before being cooled to room temperature.

The merged retrieval of Cobalt and Lithium from the used Lithium-ion batteries used vacuum pyrolysis [442]. To prevent air pollution and reduce cathode waste elements from the $LiPF_6$ electrolyte, the negative-electrode elements were placed in a vacuum furnace without breaking down. Under a test environment of 600 °C, a vacuum evaporation period of 30 minutes, and a residual gas pressure of 1 kPa, the Lithium-Cobalt-Oxide and Cobalt (II)-Oxide cathode dust detached entirely from the aluminum foils. The results of the vacuum pyrolysis of the cathode materials demonstrated this. The investigation into the vacuum pyrolysis temperature specifically covered between 450 - 700 °C, and the findings of the tests are shown in **Figure 5.14**. The graphs in **Figures 5.14a** and **c-f** show that the separation efficiency steadily increased as the pyrolysis temperature varied from 500 to 600 °C compared to the cathode before the vacuum pyrolysis. The aluminum foils were brittle above 600 °C, making separating the active cathode components

challenging. For comparison, the pyrolysis experiment was conducted at 600°C and low atmospheric pressure. As seen in **Figure 5.14h**, some of the cathode active materials were able to separate from the aluminum foils. Still, the cathode was bent and breakable, making it susceptible to oxidation at high temperatures. Sun and Qiu (2011) [442] for the simultaneous recovery of cobalt and lithium from used lithium-ion batteries, a unique process comprising vacuum pyrolysis and hydrometallurgical methods devised. The organic solvents and binders were removed from the discharged batteries by heating them to 600 °C in a vacuum for three hours [392].

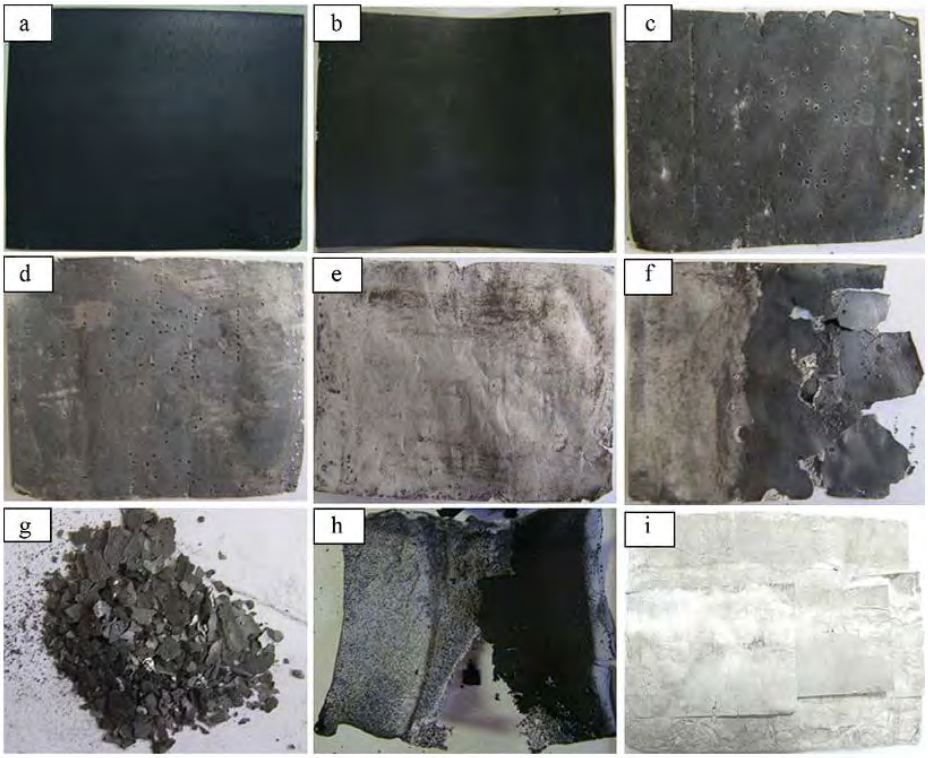

Figure 5.14. Images of the cathode electrode following various treatment: (a) cathode electrode after battery dismantling and cutting, Aluminum foil after vacuum pyrolysis (b) at 450 ◦ C, (c) at 500 ◦ C, (d) at 550 ◦ C, (e) at 600 ◦ C, (f) at 650 ◦ C, (g) at 700 ◦ C, (h) aluminum foil after heating in normal pressure at 600 ◦ C, (i) aluminum foils after acid washing [442].

A study reported that the electrical and chemical performance of the active elements retrieved from the recycled cathode of the lithium-ion battery is analyzed in the direct recycling technique was affected by thermal processing temperatures (400, 500, and 600 °C) [477]. The thermal disintegration reaction with nitrogen as the gas flow was used to separate active components from the aluminum foil and the binders made up of sodium carboxymethyl cellulose and styrene butadiene rubber. A similar strategy was adopted to recover Lithium-Ferro-

phosphate (LFP) from lithium-ion batteries containing the Polyvinylidene fluoride (PVDF) binder [443].

5.2 Pyrometallurgical Process

In this pyrometallurgical process (**Figure 5.15**), Li, Al, Si, Ca, and Fe are generated as slag, while metal species, including Co, Ni, and Cu, are recovered from LIBs in the form of alloys. Particularly for small-sized batteries, the batteries are mechanically processed initially, such as when the battery pack is disassembled, and then processed immediately in a high-temperature smelting furnace without the need to separate the cathode or anode layers. Two separate heat treatment procedures are applied to this treatment. In the first step, batteries are subjected to low-temperature treatment (150–500 °C), where electrolytes and organic solvents are gradually removed. The batteries are then subjected to a high-temperature treatment (1400-1700 °C) to produce Co, Ni, and Cu alloys as well as slag (Li_2O or Li_2CO_3) [373,444,445].

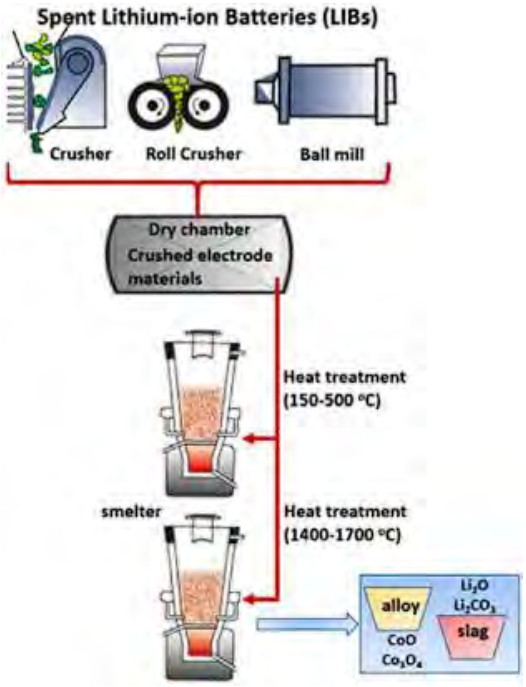

Fig 5.15. Pyrometallurgical process of spent LIBs [445].

This method is efficient for recovering Co and Ni; if we want to recover Li, a hydrometallurgy process should occur. Today, a few businesses, including Sony, Umicore, Accuracy, and Inmetco [446], have used the thermal method to generate alloys and slag for hydrometallurgical processing.

5.3 Hydrometallurgical Process

Due to their high Co, Ni, and Li recovery rates (>98%), low energy requirements, higher selectivity, common contaminants, and generally low cost at low production volumes, hydrometallurgical processes have attracted significant attention in research and development from academic institutions and industry [382].

Many researchers could extract high-purity cobalt from LIBs using low-cost, straightforward methods once the acid leaching and solvent extraction processes opened their eyes to the possibility. The hydrometallurgical process involves four distinct steps:

- acid leaching
- chemical precipitation
- solvent extraction
- electrochemical separation

The hydrometallurgy recycling process is separated into three stages: the pretreatment, the leaching, and the metal recovery. In the first stage, we opened and pretreated the batteries to isolate the electrode materials. Next, plastic and metal coatings need to be stripped off the batteries. Then we separate the cathodic material from the aluminum sheet when the batteries are opened. Afterward, we use organic or inorganic acids, bases, or bacteria at the leaching step to take the cathodic material and compel the metal ions into solution. In the final step, we recover the metal from the leached solution with the methods of chemical precipitation or electrochemical deposition, or solvent extraction. Anions that could form precipitates with metal ions in solution are used in chemical precipitation. Electrochemical distraction separates metals from solution through the difference in their electrode potential. Solvent extraction is a widely implemented method that uses solvents to selectively extract metal ions [428,447,448].

5.4 Direct recycling process

This recycling process is a non-destructive approach where we recover the active materials of lithium-ion batteries directly after the pretreatment process. Lithium-ion batteries are separated with physical methods like magnetic separation and thermal processing without affecting the original compound structure. In the next step, the recovered active materials are repaired with re-lithiation or hydrothermal process to restore surface and bulk defects. Direct recycling is still challenging due to the variety of functional materials inside the batteries, but reducing energy consumption, greenhouse gases, and Sulfur Oxide emissions is an up-and-

coming method for a sustainable future [447,449,450]. A schematic illustration of direct recycling is illustrated in **Figure 5.16** [378].

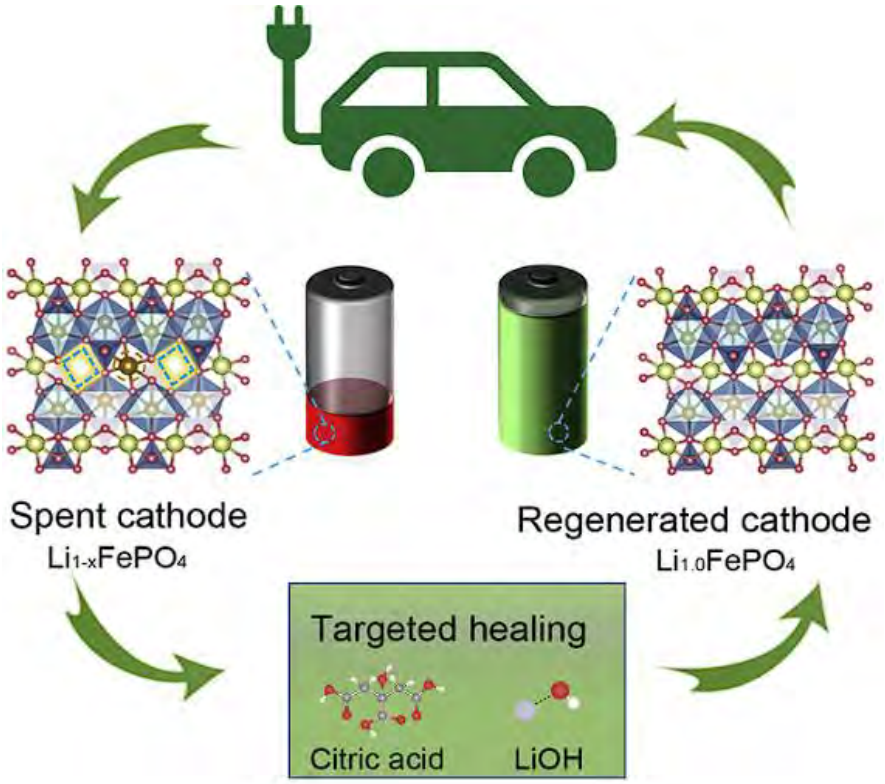

Figure 5.16. The composition, structure, and electrochemical performance of used $LiFePO_4$ cathodes with diverse degradation conditions can be entirely recovered to the same levels as those of the pristine materials using a paradigm-shifting lithium-ion battery recycling approach based on defect-targeted healing [378].

CHAPTER 6

Future Materials for LIBs

6.1 Introduction

LIBs offer much better energy and power densities than traditional batteries, hastening the adoption of fixed and portable energy storage devices and electric mobility in particular. Aside from the practical consequences such as current peak compensation and emission-free automobiles, LIBs place additional strain on natural resources, necessitating an effective and sustainable waste disposal strategy. Furthermore, they contain certain critical raw materials, as defined by the European Commission, in terms of dependability and sustainability, such as Co, L [451], natural graphite, and poisonous and hazardous compounds. Co is expected to be reduced or replaced in terms of mass share in cathode coatings, although Li and natural graphite will remain significant ingredients [451,452].Furthermore, cathode materials' essential qualities, problems, and potential for developing improved LIBs have been examined [453].

6.2 Cathodes

While anode compounds were developed with greater electrochemistry properties, researchers started paying attention in the development of cathode compounds as well. They focused more to voltage and capacity to achieve balance to the system with identical electrode capacities. Electrochemical properties , price and efficiency are crucial for the huge applications in modern industries [453].

6.2.1 Spinel

Promised applications for great Lithium-ion batteries are LiMn2O4 and $LiMn_{1.5}Ni_{0.5}O_2$. They are more eco-friendly, have low cost, have cubic spinel construction with space symmetry of Fd3m, and host construction for three-dimensional lithium diffusion paths [454,455]. Although these electrode materials have excellent electrochemical properties, they have a reduced capacity of 150 $mAhg^{-1}$ when operating at three volts or more. This phenomenon happens because there is a variation in the phase from spinel to salt resulting in additional lithiation [456]. Furthermore, Mn decomposition by disproportional and Jahn-Teller distortion

via active Mn3+ ions resulted in the permanent transformation of the shape from spinel to tetragonal. As a result, the limitations of spinel $LiMn_2O_4$ are increased [457,458]. $LiMn_2O_4$ could be more efficient if extensive running times without plug-ins are required. As a result, many methods to inhibit Mn dissolution and limit capacity fading have been documented. Some of them were doped of $LiMn_2O_4$, with other chemical elements such as titanium and nickel, etc., to increase electrochemical performance and to reduce the generation of Jahn-Teller effect Mn^{3+} ions[459].

6.2.2 Polyanions

Polyanions are a novel family of cathode chemicals that researchers have sought to produce. Their formula is $(XO_4)^{3-}$ they often have lattice type, raised firmness, and cathode material's redox potential [460]. $LiMPO_4$ is an interesting electrode material for high-rated lithium-ion batteries because of various inherent advantages, for instance, cost-effectiveness, low-toxicity, plentiful availability, minimal capacity fading, and high specific capacity [461]. Importantly, Padhi et al. discovered that $LiMPO_4$ had a reasonably constant discharge potential of roughly 3.4 volts, 170 $mAhg^{-1}$ capacity, excellent heat, and electrochemical firmness [462].

6.2.3 Textile cathodes

Even though currently on the market, LIBs have outstanding electrochemical performance, are eco-friendly, but they aren't viable. Developing Lithium-ion batteries with textile cathodes is desirable but problematic as well [463,464]. Zhu et al. created V_2O_5 empty multi-shelled (HoMSs)/Ni-cotton flexible three-dimensional textile-based electrodes to investigate a more excellent quality Lithium-ion battery for the current uses [463]. Three-dimensional textile cathodes are efficient and reliable because of long cyclic firmness, high-rate ability, good mechanical pliability, and the strong connection between V_2O_5 HoMSs and Ni-cotton [465].

6.2.4 Fluorine and chlorine compounds

Lately, they have been used as positive electrodes because of their theoretical specific and volumetric capacity. A significant disadvantage is that they have low conductivity, broad voltage limitations, adverse side reactions, and dissolution of active metals. Because of the vast band gap caused by the acquired high ionic character of the metal-halogen interaction, FeF_3 and

FeF_2 have low electrical conductivity, like metal chlorides [466]. However, these types of cathode materials like FeF_2 and BiF_3discovered catalyzed the cyclic carbonates at high electromotive force, and as a result, the cyclic stability is reduced [467,468].

6.2.5 Selenium and tellurium-based cathodes

They have recently gained popularity as electrodes for LIBs because they have better specific conductance than Sbased materials and greater capacity. Furthermore, they outperformed S-based compounds regarding rate capability and active material utilization. However, Se-based cathode materials have major drawbacks like decreased cyclic firmness, coulombic effectiveness, and increased capacity decay ratio [466]. Till now, there has been no report about the dissolution of polytellurides. Aside from these constraints, elements Se and Te showed significant volume increase. Also, they have significantly decreased liquefaction points, and as a result, the increase in their efficiency can happen because their processing is possible. Unfortunately, tellurium is rarely used in LIBs applications because its prices are high [469-472].

6.2.6 Sulfur and lithium sulfide

They are used as electrode compounds for Lithium-ion batteries as well because they have high theoretical volume, cost-effective, and Earth has widespread sources. Unfortunately, these materials must tolerate good specific conductance, polysulfide in the electrolyte, not good potential, vast volume growth, and low vaporization point [473]. As a result, electrical contact was lost in conventional carbon composite electrodes. To counteract these problems, it can be encapsulated into a hollow structure [474]. For instance, polyvinyl pyrrolidone, carbon, and TiO2 have been encapsulated with S using infiltration and chemical precipitation techniques [475-477].

6.2.7 Iodine-based compounds

These materials have been used in many applications, cooperating with LiI solid electrolytes achieving even higher electrochemical performance [478]. Iodine ions are becoming more attractive in lithium-ion batteries due to their excellent solubility in organic solvents. Furthermore, due to its low melting point (113 ^{o}C), active iodine entered the pores of the carbon.

As a result, this composite could have even more outstanding performance, such as better cyclic firmness and more significant potential [478-480].

6.2.8 Organic cathodes

Researchers have created sustainable cathode materials to hunt for even more efficient Lithium-ion batteries. In general, a great percentage of the materials used were inorganic, and they have some restrictions such as the actual amount of energy to be produced, not being environmentally friendly, limited capacity, insufficient sources, non-sustainable, and expensive. Organic materials manage to beat these restrictions, and as a result, they are promising for highly efficient lithium-ion batteries [481-483]. Furthermore, their structures and redox characteristics may be adjusted by introducing relevant functional groups during synthesis [484,485]. Organic cathode materials are divided into conductive polymers, organosulfur compounds, carbonyl compounds, imine compounds, and radical compounds based on their structural variations [486-490].

6.3 Anodes

The composition and qualities of the anode material were explicitly indicated to be critical to total battery performance, for instance, carbon materials have strong electronic properties and electrochemical performance [491]. The capacity and performance of the battery are heavily influenced not only by the inherent properties of the anode material but also by its shape. As a result, the proper and adequate structural design used is far more significant than the material chosen. Many high-performance anode materials have been investigated as innovative materials for the next generation of LIBs. Alloy materials, conversion-type transition metal compounds, silicon-based compounds, and carbon-based compounds are among them.

Adaptation to metal oxides such as iron, cobalt, nickel, copper, and zinc offer appealing properties that have caused much attention as top possibilities for LIB anode materials. They are non-toxic, have a significant power density and theoretical specific capacity, are abundant in nature, and are manufactured at a reasonable cost [492].

6.3.1 Metal Chalcogenides

Chalcogenides have emerged as appealing anode materials with a tremendous theoretical capacity [493]. This is owing to their ability to store Li (and Na) ions via electrochemical

conversion [494]. To improve the cycling stability and rate performance of chalcogenides (particularly cobalt sulfide), which are hampered by significant changes in the mass parameters of the material throughout charging/discharging, extremely conductive and stable materials such as polyaniline and graphene are applied as surface coatings on the sulfides [495,496].

6.3.2 Metal Oxalates

Metal oxalates are one of the most promising novel anodes to emerge in recent years, capturing the interest of experts. Because of the extraordinary development made by researchers in their electrochemical characteristics, they stand to be a far superior substitute for graphite as anode materials in future lithium-ion battery manufacturers. Zinc oxalates (ZnC_2O_4), cobalt oxalates (CoC_2O_4), manganese oxalates (MnC_2O_4), nickel oxalates (NiC_2O_4), and iron oxalates are examples of such chemicals (FeC_2O_4). However, these compounds have significant volume expansions during li-ion insertion/extraction, resulting in poor cycling performance. According to studies, changes in particle size, structure, and morphology of the materials will go a long way toward resolving this difficulty [492].

6.3.3 Metal carbides and nitrides (MXenes)

MXenes are highly prized materials due to their excellent chemical and thermal stability, outstanding mechanical qualities, metallic conductivities, high adsorption capacity due to their 2D structure, and unique topological features, which lead to their usage in a wide range of applications [497].

Transition metal compounds in the MXene family include titanium carbide ($Ti_3C_2T_x$) Mxene and selenides like CoSe, $FeSe_2$, and $NiSe_2$. $Ti_3C_2T_x$ has become a novel anode material for LIBs due to its high electrical conductivity, excellent chemical stability, and low lithium-ion diffusion impedance [498]. However, its commercialization is limited due to its low intrinsic capacity and restacking properties.

To address these disadvantages, high theoretical capacity transition metal oxides (such as Fe_3O_4) have been effectively incorporated into the layers of $Ti_3C_2T_x$ to generate hybrids with higher capacity for li-ion storage. The number of layers in the $Ti_3C_2T_x$ can be lowered to improve its electrochemical performance further, as it has been observed that the higher the number of layers present, the greater the possibility of some active layers in the internal surface

of the $Ti_3C_2T_x$ being neglected from Fe_3O_4 loading due to the multi-leveled nature of the $Ti_3C_2T_x$ MXenes [499,500].

6.3.4 Aluminum niobates

Aluminum niobates have emerged as a superior anode material for LIBs compared to typical titanium niobates ($TiNb_2O_7$ and $Ti_2Nb_{10}O_{29}$). Despite their appealingly large theoretical capacity and remarkable electrochemical characteristics, this is because titanium niobates have poor charge conductivity due to their low-rate capability [501-504].

6.3.5 Metal phosphides

Tin, cobalt, copper, nickel, and iron phosphides, as well as their corresponding composites, are important phosphides in this group. Transition metal phosphides have piqued the interest of researchers as excellent anode materials for lithium-ion batteries due to their metallic properties, higher thermal stability, extraordinary specific capacity, and safe operational potential [505,506]. Nonetheless, the phosphides' electrochemical performance is severely limited by their low intrinsic electrical conductivity and breaking of the active materials induced by massive phosphorus volume changes during the charging/discharging process [498]. According to studies, these disadvantages can be mitigated by reducing the particle sizes of metal phosphides to nano-sized structures [507].

6.3.6 Binary metal oxides

Binary transition metal oxides have received much interest as prospective anode materials for lithium-ion batteries because of their significant theoretical specific capacity, increased rate performance, and exceptional cycle stability. Binary transition metal oxides often outperform single transition metal oxides (such as Fe_2O_3, Co_3O_4, and Mn_3O_4) in electrochemical performance due to the synergistic impact of several metal components [508,509]. When compared to Fe or Co-based oxides, $ZnMn_2O_4$ has several benefits, including environmental friendliness, low cost, and a significantly lower operating voltage [510]. The anode material can provide a better energy density with a lower charge voltage. As a result, $ZnMn_2O_4$ has been recommended as a suitable anode alternative to graphite for LIBs. LIBs have been studied utilizing $ZnMn_2O_4$ nanomaterials as anodes in various morphologies, including nanoflakes, nanowires, nanoparticles, and nanoflowers [511].

6.4 Electrolytes

Any electrochemical device would be complete with an electrolyte. Electrode chemistries' evolution was intimately related to the development of electrolytes in lithium-ion batteries. As new battery chemistries develop, electrolyte compositions will continue to evolve, however, some current and prospects for electrolytes will be discussed [512].

6.4.1 Aqueous liquid electrolytes

Water is primarily used as an excellent solution solvent in aqueous secondary batteries, which may alleviate safety issues in the manufacturing and production processes while reducing resource consumption and production costs [513]. Based on the considerations above, aqueous secondary batteries have lately attracted extensive interest and their advantages are [514-516]:

1. Inexpensive, easy availability, solvent water is significantly cheaper than nonaqueous electrolyte,
2. Greater ionic conductivity than organic liquid electrolytes,
3. Cannot explode due to the electrolyte's flammability,
4. Not affected by overcharge.
5. Minimal functional demands from the surrounding, lowering manufacturing expenses.
6. Diaphragm needs are significantly decreased.
7. Ecologically friendly [513,517,518].

Even though research on aqueous electrolytes has been brisk due to the benefits listed above, inevitable drawbacks are impeding progress, most notably:

1. The potential window is limmited owing to H_2O electrolysis.
2. Side reactions can result before metal ion interference and separation due to p+ action.
3. The battery's lifespan is reduced because the cathode and anode materials cannot be protected due to their structure.

As an increased energy storage device, aqueous-based batteries may successfully handle resource cost and safety constraints. However, the existing small electrochemical window remains an important disadvantage, so it cannot be used as an alternative source. Constructing a steady, solid electrolyte interface coating with an electrode-electrolyte interface broadens the potential window. Developing a breakthrough in electrolyte preparation should be considered to expand the potential window [519-521].

6.4.2 Liquid electrolytes

Non-liquid batteries still occupy the existing electrochemical energy storage business with excellent stability, great energy density, and energy efficiency, among others. As a result, the organic liquid electrolyte has the upper hand [521-523]. The general criteria for multivalent metal battery liquid electrolytes include a greater amount of migrate ions, heat resistance, chemical firmness, and a broader potential window [524,525]. The metal ion transport is accomplished with the help of the liquid electrolyte. During the discharge process, ions dissolve into the electrolyte then they are injected to the cathode with the use of a layer or path. Ions are removed during the charging process and deposited on the cathode layer relating to the anode electrode. Then the rechargeable metal secondary battery is created after repeated charging and discharging operations. It can be observed that the liquid electrolyte's duty in metal batteries is to allow ion transfer to prevent immediate touch with the two electrodes; a separator is also necessary. In summary, aqueous-based batteries may successfully handle resource cost and safety constraints as an increased energy storage device [526].

6.4.3 Solid-state electrolytes

Usually, solid-state electrolytes are made up of solely metal salts and electrolyte matrices. The following are the overall criteria for solid electrolytes for multivalent metal batteries:

1. Strong ionic conductance
2. Perfect electrochemical firmness
3. Great SEI contact to electrodes and electroylte
4. Good corrosion resistance
5. Enough robustness
6. Secure
7. Inexpensive [527,528].

6.4.4 Gel electrolytes

In terms of shape, they are categorized as quasi-solid electrolytes, and their ion transfer mechanism, free solvent, and efficiency differ significantly from the solid electrolytes. Polymers are now used as monomers to manufacture gel electrolytes [529]. High-particle polymers are inflated with low particles to create a network formation under the influence of initiator crosslinking chemicals [530]. After that, a polymer gel is created by the expansion of the

solution in which it will not possess solid electrolytes' fluidity. As a result, the gel electrolyte possesses solid qualities such as structure, strength, elasticity, and so on, and liquid properties like ion mobility and ion conductivity [531]. There are two types of gel electrolyte synthesis methods: natural and electrochemical. The former refers to the network structure generated by the involvement or not complete polymer principal chains crystallization, a network structure formed by heat or photopolymerization of covalent connections between polymer leading chains. The chemical crosslinked gel polymer electrolyte has a predetermined amount of crosslinking sites, which do not vary with environmental conditions that change, but the generation of crystals does not happen [532].

6.4.5 Composite solid electrolytes (CSEs)

Battery specifications for CSEs:

- Outstanding thermal firmness
- Excellent electrochemical firmness
- Increased ionic stability
- Enhanced battery specific condustance
- Increased voltage affinity
- Battery density
- Thereby suppressing dendritic formation
- Improved safety performance

Previous research addressed the issue of polymer with poor mechanical strength and ionic conductivity by incorporating inorganic ceramic particles into the solid electrolytes' dielectric polymer. Electrochemical action and inertness are two categories of inorganic molecules with an increased specific layer area. The reverse lack of oxygen from cell relates to inert compounds whose inorganic fillers, such as SiO2 and Al2O3, cannot transport ions [533].

On the other hand, the touch of electrolytes and electrodes has traditionally been a fundamental impediment to the development of ISEs. Including a minimal amount of polymer ingredients reduce the resistance of the area where they are linked, and the chemical unreliability is eliminated. Plenty of molecules that match various polymers increase cell efficiency differently. As a result, selecting fine inorganic particles, in conjunction with polymer characteristics, is a critical step in preparing high-performance CSEs [534].

6.4.6 Inorganic solid electrolytes (ISEs)

Their characteristics are as follows:

- great thermal firmness
- strong electrochemical firmness
- ability to boost battery energy density
- effectively inhibit dendrite formation [249].

Based on their crystalline condition, inorganic solid electrolytes are classified as crystalline ISEs or glassy ISEs [535]. The former is a shapeless material shaped by liquefying and extinguishing a forerunner, primarily an oxide or sulfide crystal electrolyte. Ions diffuse into the whole material following activation at specific places in the ion conduction technique of glassy inorganic solid electrolyte. Unfortunately, since the inorganic solid electrolyte has a metastable structure when the material crystallizes, the ion-specific condensate drops dramatically.

In comparison, there have been more studies on crystalline ISEs with excellent thermal firmness, such as NASICON, LISICON, garnet, and perovskite. This type of electrolyte's ion conduction mechanism is primarily defined by the presence of gaps in the crystal lattice that serve as ion transport channels [536,537]. Even though the mechanical characteristics are outstanding, interface resistance has changed to a significant barrier; as a result, the primary solution method is to modify the interface.

Furthermore, it is envisaged that an intentionally built SEI layer will effectively inhibit the interface interaction to establish a great contact area. Solely inorganic solid electrolytes have a tough time accounting for the many signs of solid-state batteries. The only method to use solid electrolytes is via a polymer-inorganic composite solid electrolyte [538].

6.4.7 Ionic liquid electrolytes

Their main characteristics are:

1. Strong specific conductance
2. Decreased steam pressure
3. Broad fluid area
4. Good firmness
5. Nonflammable
6. Eco-friendly, and it can be recycled easily [539,540].

It is also a designer solvent since it is feasible to mix various positively and negatively charged ions, and as a result, it can build ionic fluids for specific applications [541]. Nonflammability is predicted to address the safety issue of electrolyte flammability in organic systems [542]. However, ionic liquid features, for instance, resistance to flow, will reduce the spreading habit of ions in the electrolyte, results in a low-quality interface affinity. Much research has related ionic liquids to other electrolytes in recent years. Ionic liquids, in particular, relate to ionic-specific conductance flaws induced by polymer SEI difficulties in polymer solid electrolytes [543]. For example, when paired with inorganic solid electrolytes, the issue of Sei electrode affinity can be managed efficiently. Ionic liquids are applied in gel electrolytes as well [544]. Yu [545]proposed an organic-inorganic dual network structure solved ionic liquid gel electrolyte SIGE. The electrolyte combines the benefits of a solvated ionic liquid with an organic-inorganic double network framework structure. The double network structure offers the electrolyte outstanding mechanical characteristics, and the solvated ionic liquid has high thermal stability, reduced ignitability, and an incredible lithium-ion migration number. They all serve as models for developing high-performance ionic liquid gel electrolytes. In the future, a key role in creating even more efficient electrolytes will be achieved by ionic liquid electrolytes [545].

6.4.8 Solid polymer electrolytes (SPEs)

The need for them has increased ionic-specific conductance, great-voltage affinity, and improved safety performance. The solid polymer electrolyte (SPE) comprises a polymer matrix and a metal salt. Li ions prefer to migrate from one point to another when subjected to an electric field. As a result, ion hopping occurs mainly in the polymer's non-oriented area, also known as the amorphous region. Among the polymer matrices are:

- poly alkenyl (PVDF),
- PAN
- PMMA,
- polyvinyl
- polycarbonate
- (PEC), poly (trimethylene carbonate) (PTMC) and poly (vinylene carbonate)
- PVCA
- poly (propylene carbonate) (PPC)).
- Polysiloxane basis [527,528].

6.4.9 Summary of different types of electrolytes

Table 6.1. Summary of electrolytes depending on their performance [546].

Type	Performance				
	State	Conductivity	Temperature Adaptability	Safety	Price
Aqueous liquid electrolytes	Liquid	Competitive High	Normal	Great	Cheap
Gel electrolytes	Quasi-solid state	Competitive High	Great	Normal	Competitive High
Solid polymer electrolytes	Solid	Low	Normal	Great	Competitive High
Inorganic polymer electrolytes	Solid	Low	Normal	Great	Competitive High
Organic liquid electrolytes	Liquid	High	Not good	Not good	Competitive high
Ionic liquid electrolytes	Liquid	Low	Normal	Great	Competitive Low

6.5 Separators

As already mentioned, separators are a crucial component for the pure operation of LIBs. A few alternative materials for new types of separators are presented [547]:

Polyamide separators

Polyamide is a polymer made up of repeated units of amide bonds. It has strong solvent resistance and moderately high chemical and thermal stability. When dried, it also provides excellent insulation. These characteristics make it an effective LIB separator. Furthermore, due to its polarity groups, polyamide has a stronger attraction for lithium-ion electrolytes as an alternative polymer material for polyolefin. For better performance as a separator in lithium-ion batteries, researchers alter polyamide materials or mix them with other materials [548]. For example, Saleh and colleagues use in situ interfacial polymerization to incorporate alumina nanoparticles into a polyamide (PA) nanocomposite membrane. These nanoparticles in the membrane contribute to improved permeate flow and salt rejection and improve the material's hydrophilicity [549].

Furthermore, polyamide materials are frequently utilized in combination with other materials to create a single-ion electrolyte membrane as a LIB separator. Sun [550] created a polyamide single-ion electrolyte membrane. It is a high molecular weight gel single-ion

polyamide polymer electrolyte membrane (LiPA) with bis(sulfonyl)imide incorporation generated by a polycondensation procedure. The H^+ ions were then swapped for Li^+ ions. As a single-ion polymer electrolyte membrane, all bis(sulfonyl)imide anions have been resisted in the polymer chains, allowing the number of transported Li+ ions to climb to 0.88.

Furthermore, the novel material provides smooth pathways for Li^+ transfer. They also discovered that when mixed with other materials, polyamide might assist in improving the resilience of separators at high temperatures [549,551]. Li et al. [551] described a unique electrospun single-ion conducting polymer electrolyte (SIPE) made of nanoscale mixed poly (vinylidene fluoride-co-hexafluoropropylene) (PVDF-HFP) and lithium poly (4,4′-diamino diphenyl sulfone, bis (4-carbonyl benzene sulfonyl)) (LiPSI). With superior thermal stability, electrolyte wettability, and increased porosity, the material performs significantly better as a separator in LIB than polyolefin materials. While using SIPE, Li/$LiFePO_4$ battery cells demonstrate high-rate capacity and outstanding electrochemical stability over 1000 cycles. It is an excellent material for a separator in great-energy-density LIB [552].

Polybenzoxazole separators

Thermally rearranged poly(benzoxazole-co-imide) (TR-PBO) electrospun membrane is a novel separator for high power density LIB developed lately by scientists. It features a high distribution of nanoporous cavities and exceptional permeability and selectivity. It also has high thermal stability, chemical resistance, and processability. These characteristics make it an excellent material for lithium-ion battery separators [553].

TR-PBO materials were initially produced by M.J. Lee and his colleagues in 2015. All of the samples outperformed commercial separators regarding cycling stability and cycle retention. They enhanced the material the next year [553]. The clean membranes were covered with spherically shaped hydroxyl copolyimide 1 and sea-squirt-shaped nanoparticles. They are then heat treated to form TR-PBO1 and TR-PBO4 nanocomposite membranes. These membranes demonstrated excellent electrolyte wettability, superior pore size distribution, and thermal stability. Furthermore, both membranes outperformed the Celgard membrane in terms of cycle retention. These benefits show that TR-PBO membranes are excellent options for high-power-density LIB separators [554].

Multi-layer separators

With the rising of LIB's efficiency, a base material can no longer provide the high performance required as cell separators. As a result, researchers have been investigating composite

materials, with multi-layer materials becoming increasingly common. Benefits from various materials might be incorporated by building multi-layer separators. Electro-spinning is a popular method for creating multi-layer materials. Electrostatic spinning is a unique fiber production technology. This procedure will inject a polymer solution or melt in a high electric field [555].

A PVDF-HFP/PI bicomponent electrospun separator with a cross-linked structure for LIB was successfully created by Cai and his colleague. This material combines the remarkable properties of PVDF-HFP and PI and boosts mechanical strength by maintaining a high porosity level. Furthermore, the composite material exhibits excellent thermal dimensional stability (up to 200°C), good ionic conductivity (1.78 x 10^{-3} S/cm), high electrolyte uptake (483.5%), a wide electrochemical stability window (up to 4.94 V vs. Li^+/Li), self-extinguishment, and a favorable interface structure, among other outstanding properties. Furthermore, lithium-ion batteries using this separator type have good discharge capacity at 45°C under varied C-rates. All the benefits listed above demonstrate that the composite material may be used as a cell separator. It was reported that a tri-layered SiO_2@PI/m-PE/SiO_2@PI nanofiber composite membrane was developed [556].

This tri-layered hybrid separator combines the core layer's thermal runaway and thermal stability at high temperatures with the thermal shut-down function at low temperatures. Because of the mechanical stability the sheath layers provide, it is a suitable separator for lithium-ion batteries. Multi-layer materials will occasionally be doped with additional compounds to improve performance. Wang and her team changed the PVDF-CTFE compound, which might assist in increasing the composite material's strength. Moreover, the redesigned PVDF-CTFE membrane demonstrated synergistic solid properties. This material has the advantages of flame resistance, higher thermal stability, excellent wettability, solid ionic conductivity, and decreased interfacial resistance [557].

Another novel of LIB separators

Apart from the three types of novel separators, various additional advanced materials, such as non-oxide inorganic compounds, γ-Li_3PO_4 oxides, garnet-type oxides, NASICON-type oxides, perovskite-type oxides, single crystalline silicon, and the like, have a high potential for processing into LIB separators [558]. Scientists are not only finding new materials for separators but also developing theoretical and physical models to continue the analytical work on separators to identify better materials theoretically.

Separators with improved performance are required as the LIB technology evolves. The current separators continue to face several challenges. An excellent separator should feature exceptional water solubility, thermal stability, mechanical properties, good ionic conductivity, and considerable tortuosity to avoid dendritic lithium development. It should also be as thin as feasible. However, it is tough to accomplish all of these features at the same time, thus, it is critical to control them and focus on particular properties specific to distinct lithium-ion batteries. In general, significant effort must be made to develop improved separators for the safety and efficiency of lithium-ion batteries [559].

6.6 Projections of future lithium

Lithium is used in many applications due to its small weight, high reactivity, and low thermal expansion coefficient [560]. The electrochemical potential of lithium is one of the highest because lithium is a lightweight metal; it offers significant energy and power density [561]. As a result, in the future, LIBs are expected to dominate the energy reserve systems [562]. **Figure 6.1** depicts the different applications of lithium.

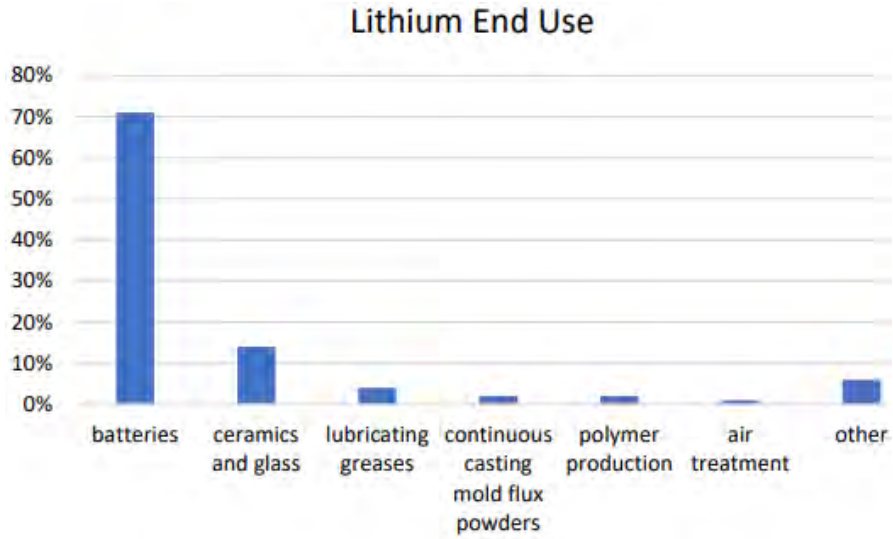

Figure 6.1. Uses of Lithium [563].

LIBs have turned into one of the biggest demand for 2015, in the category of batteries that are able to be recharged, especially these for vehicles. They dominate lithium utilization, especially for vehicles. According to Miao et al., LIBs will contribute in the most of battery industry over the following years at a rapidly expanding rate [564].

6.6.1 Geological Overview

Brine, metals, and saltwater are the three primary forms of lithium deposits. The majority of lithium sources are located in alloys and brine. One hundred twenty lithium-containing mines currently investigated have significant amounts [565]. Pegmatites are lithium-containing minerals, including spodumene, petalite, lepidolite, and eucryptite. Brine is the world's largest and most inexpensive source of lithium. They are primarily found in South America, notably in Chile's Salar de Atacama [565]. Oceans are expected to have around 44.8 bn Tn of lithium that can be extracted [566]. Nevertheless, it has to be examined even better if it's efficient to take out depending on the required initial cost [567].

Some problem that can occur is that the increased amounts of Mg in reserves impede lithium uprooting inner seawater due to the exact proportions of the two metals [567]. Li reserves in formed stones aren't the cheapest viable way of getting them due to the minimal cost of extracting the Li accessible in brine [568].

Lithium is manufactured in various forms, including lithium carbonate, chloride, and hydroxide [569]. However, lithium-ion batteries are often made with lithium carbonate ($LiCO_3$). According to the US Geological Survey, the US, Chile, and Argentina extract lithium from brine, whereas Australia generates lithium from mineral-based sources. Lithium is produced in China using a mix of brine and minerals [570].

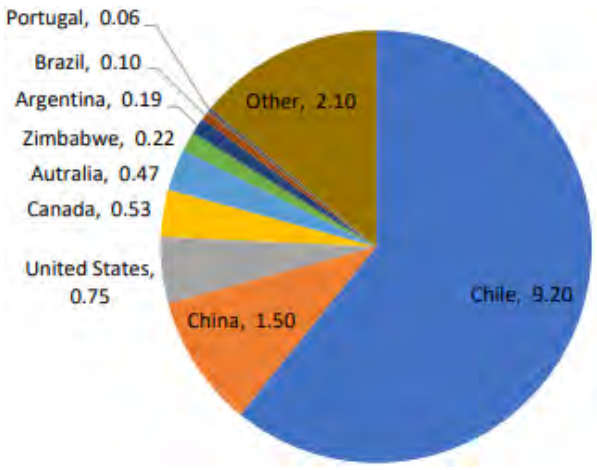

Figure 6.2 Lithium reserves [563].

It is worth noting that the distribution of lithium is much less regionally diversified than that of oil. **Figures 6.2** and **6.3** depict the regional distribution of lithium resources and reserves [563].

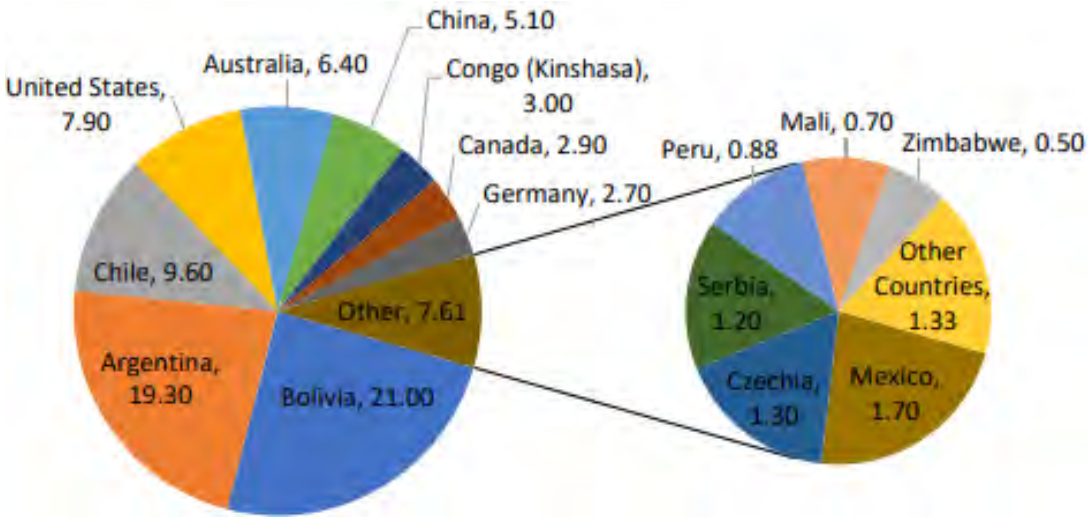

Figure 6.3. Lithium resources [563].

6.6.2 Recycling

The problem of end-of-life battery disposal is a severe worry concerning the sustainability of electric cars, especially as electric vehicles gain market penetration. Recycling is a possible source of lithium supply. Currently, only a tiny amount of lithium gets recycled [571]. Nonetheless, lithium's estimated price is relatively low compared to the average battery cost. According to Kushnir and Sandén, raw lithium contributes around 1-2% of the entire cost of an electric car battery [572].

In addition, the enormous amount of batteries is not recycled, although Li is a recyclable material, because getting new lithium is still the cheapest option. As a result, when lithium from brine is generated at considerably lower prices, buying recycled Li would mean reduced profits for industry makers [573]. Industries paid attention to recycling Co and Ni because getting Li from batteries is more expensive. Lithium and manganese should be utilized more. However, with the rising appeal for Li, especially in vehicle industries, reuse is projected to be crucial in predicting lithium's future viability for PEV battery manufacture. Lithium battery recycling will become increasingly important as the need for Li-ion batteries rises in the following decade. Huge volumes of electric car batteries lives will be expired in the coming years, making recycling economically possible. Closed-loop recycling will be required in the medium to long term to eliminate price volatility and potential supply interruptions. As a result, new ideas of reusing Li are vital for the following years [568,574-576].

Significant challenges for lithium recycling are price-related since battery recycling plants must reclaim secondary lithium equivalent to freshly manufactured Li. Consequently, facilities for reusing Li specialized for car batteries have not been developed. Nevertheless, there is a considerable opportunity for lithium recovery from wasted batteries [577]. Rosendahl and Rubiano contend that without lithium recycling and growing costs, lithium shortage will become more apparent [577]. While recycling end-of-life batteries is undesirable due to significant material and energy losses, a recycling solution is adapting old batteries for new use has evolved because batteries may no longer be appropriate for vehicle usage after a 20% capacity loss, its more attractive to utilize them for storage systems [578].

6.6.3 Future Supply

Forecasts of Li deposits and reserves vary significantly among research, and worries regarding lithium production rates being able to satisfy rising demand still need to be well addressed [558]. It needs to be more predictable about raw material supply. Finding new resources is an essential factor that will impact lithium supplies. As previously stated, new lithium resources and reserves will likely be discovered. Upcoming manufacturing and accessible forecasts differ significantly, from sixteen thousand to one hundred ten thousand tons for 2020 output to two with twenty million tons of accessible Li till 2100 [569]. In 2020, worldwide lithium output was eighty two thousand tons [569]. This amount is expected to rise as the cost of lithium rises. Yaksic and Tilton, for example, calculate that twenty-two millions tons of Li can be accessible if the price ranges from $1.40 to $2. That amount rose more than a hundred percent in case the price of lithium carbonate fell between $7 and $10 per pound, allowing lithium to be harvested from seawater [565].

6.6.4 Demand Forecast for Lithium

Because of the uncertainties around cell size and Li efficiency, several possibilities for world lithium demand exist. Furthermore, the rate of customer acceptance will impact demand [579]. Currently, lithium is anticipated to have a great variety of cell sizes and component power. Since PEVs battery sizes are not specified, manufacturers can make various PEVs with varying weights and AER. The limited range of PEVs is a crucial source of worry. Most buyers desire PEVs, particularly battery electric cars, to have the same range as a traditional fueled vehicle (300 miles). As a result, car manufacturers will likely prioritize expanding vehicle range over lowering the

material intensity. This indicates that if it becomes cost viable, the size of PEV batteries and the need for lithium will grow in the future years [569].

6.6.5 Future Demand

Several research's examined possibilities for subsequent x lithium demand by various technologies. They vary from highly optimistic to unfortunate situations. However, there are several unknowns when doing a forecast about Li. According to one study, lithium consumption can reach six hundred thousand by 2050. According to another analysis, which believes that upcoming Li could be led from the development of Li cells used in cars, Li can reach four hundred thousand tons per year by 2050. The study concludes that, in the best case, lithium supplies cannot support 100% adoption of electric cars. Likewise, Maxwell and Mora predict a demand of over 500,000 tons per year by 2025 and over 1,500,000 tons per year by 2037 [580-582]. According to **Figure 6.4**, the lithium consumption for electric vehicles is getting increased year over year.

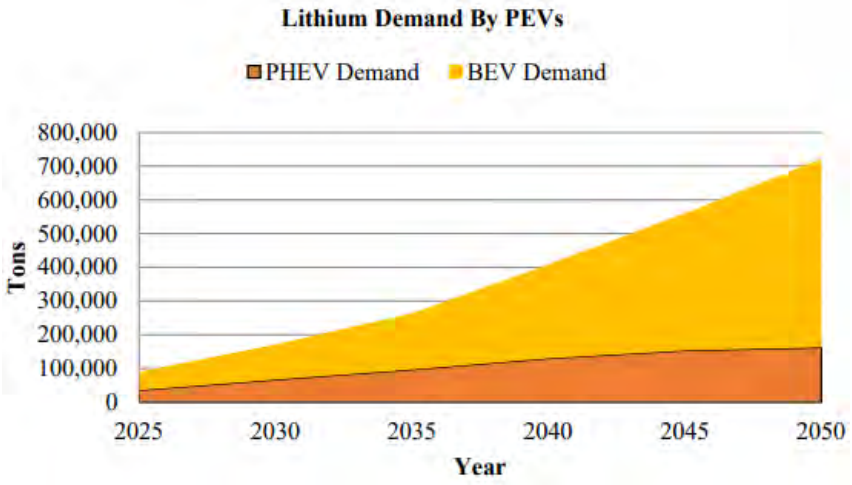

Figure 6.4. Future projections for the demand of lithium PEV [563].

This amount is far higher than the present production capacity of 82,000 tons and will necessitate a significant increase in current production capacity [569]. Based on the International Energy Agency, worldwide lithium output is expected to be around 300 kt in 2030 and 600 kt in 2050, assuming an environmental sustainability scenario [583]. This figure also raises questions regarding the supply of lithium for future PEVs. If yearly car sales continue at the same rate as in 2050, the US Geological Survey's currently recognized reserves of approximately 21 million tons will be deleted. Nevertheless, recycling will be essential at this stage in order to provide

secondary lithium. If consumed lithium is recycled in high quantities, the overall lithium accessible during this period can be much higher. PEV batteries are expected to last roughly ten years. Thus, the number of PEV batteries suitable for recycling might be significant by 2030. It will also be critical to identify fresh reserves [571] .

CHAPTER 7

CONCLUSIONS

In recent years, electrochemical devices have improved dramatically. This is because new materials, for instance, electrodes, have increased the performance toward required targets. However, due to the high demand, understanding these technologies, like lithium-ion batteries in failures and recycling, should be improved. Our number one priority is an eco-friendly planet and maximizing safety operations. As a result, the conclusions from this review are:

1. The primary source of energy production globally, accounting for approximately 80% of the worldwide energy supply, is fossil fuels. However, reliance on fossil fuels has decreased throughout time, with increased emphasis placed on employing cleaner technologies such as hydro power, renewable energy, biomass, waste, and, most critically, fuel cells. Fuel cells are simple devices. Their primary role is transforming chemical energy into electrical energy, caused by their excellent energy conversion efficiency and low energy loss as heat.
2. A lithium-ion battery looks to possess a premier market presence, and it took nearly a decade to achieve this leading position. Efforts have been undertaken to minimize the usage of harmful heavy metals, prevent environmental dangers, and increase material cost-effectiveness. Many studies have been conducted on the cathode, anode, and electrolyte, as well as the simplification of the production process. Advanced materials and technological breakthroughs are projected to aid in realizing the objective of huge batteries to power many applications like electric vehicles, as well as the production of a range of compact batteries for the future millennium.
3. The most significant barrier to using LIBs in a wide range of applications like EVs and systems for energy storage is still safety. The primary heat sources producing thermal runaway are thermal energy generated from internal short circuits and chemical interactions between battery components. The degradation of electrolytes and interactions between active materials, particularly intercalated lithium and solvents, can produce

flammable gases such as H_2, CO, and hydrocarbons. When combustible gases and solvent vapors combine with oxygen, they can ignite and cause a fire.

4. The growth of dendrites on the anode's surface affects not only the declining performance of the battery but also the safety concern. However, dendrite development is a continual process that will unavoidably increase with increasing current density and cycle life. As a result, understanding how to control the creation and proliferation of homogeneous dendrites is critical. It should be noted that dendritic control allows for dendrite development, but steps are made to smooth it out. Finally, three primary ways for regulating metal growth are presented: A) Suppression, B) regulation, and C) elimination are the three options. The substrate and metal atom interface energy are crucial in these reactions.
5. Scientists have been paying close attention to the safety of Li-ion battery technology. Internal and external battery problems can impede battery performance and result in various potentially hazardous outcomes, such as fires or explosions. The fault diagnostic feature of the BMS is responsible for identifying problems early and delivering control measures to minimize fault impacts. As a result, in recent years, Li-ion battery defect detection techniques have been extensively developed.
6. The battery's lifespan can be prolonged by improving the programs of the battery management system (BMS); thus, the system will maintain low temperatures.
7. Copper, Nickel, and Cobalt are the most usually recovered materials, equal to the most valued materials. So, the goal is to reduce the extraction of these materials and increase the efficiency of the recycling process.
8. Because it is quick and easy to scale up, the pyrometallurgy technique is the most often used method in the industry. However, the disadvantage is that the energy consumption is substantial, and lithium is frequently lost in the slag. Off-gas and dust treatment require more processing stages, and as a consequence, the science around LIB should include topics about lowering energy use and recycling lithium effectively.
9. The metal extraction process is critical to recovery, with hydrometallurgy and pyrometallurgy being the most often used procedures. However, these processes have several environmental challenges that need to be addressed, such as waste of water, residue, and exhaust gas, all of which are hazardous to the environment and human

health. As a result, secondary pollution reduction or avoidance is a crucial challenge for recycling. Because of the complex metal components of wasted LIBs, the recovery procedure is challenging. After the metal extraction process, the metal components are complex, and their separation and recovery form need a combination of chemical precipitation and solvent extraction. In the direct synthesis of cathode materials, the performance of the materials as the cost of recycling should be examined.

REFERENCES

1. Piccolino, M. The bicentennial of the Voltaic battery (1800-2000): the artificial electric organ. *Trends Neurosci* **2000**, *23*, 147-151.
2. Fuelsave-global. Is the 'Babylon Battery' the World's First Electrochemical Battery? Available online: https://fuelsave-global.com/is-the-babylon-battery-the-worlds-first-electrochemical-battery/.
3. Li, M.; Lu, J.; Chen, Z.; Amine, K. 30 Years of Lithium-Ion Batteries. *Advanced Materials* **2018**, *30*, 1800561.
4. Wang, Z.; Shi, C.; Li, Q.; Wang, G. Impact of heavy industrialization on the carbon emissions: An empirical study of China. *Energy Procedia* **2011**, *5*, 2610-2616.
5. Council, W.E. World energy focus annual 2017: The energy transition. How innovation is driving change: https://www.worldenergy.org/assets/downloads/WEF-WEC_Annual_2017_Web_LowRes.pdf.
6. Kwade, A.; Diekmann, J. Recycling of lithium-ion batteries. *The LithoRec Way, Switzerland: Springler International Publishing AG* **2018**.
7. Yun, L.; Linh, D.; Shui, L.; Peng, X.; Garg, A.; Le, M.L.P.; Asghari, S.; Sandoval, J. Metallurgical and mechanical methods for recycling of lithium-ion battery pack for electric vehicles. *Resources, Conservation and Recycling* **2018**, *136*, 198-208.
8. Georgi-Maschler, T.; Friedrich, B.; Weyhe, R.; Heegn, H.; Rutz, M.P. Development of a recycling process for Li-ion batteries. *Journal of Power Sources* **2012**, *207*, 173-182.
9. Gratz, E.; Sa, Q.; Apelian, D.; Wang, Y. A closed loop process for recycling spent lithium ion batteries. *Journal of Power Sources* **2014**, *262*, 255–262.
10. Gaines, L. The future of automotive lithium-ion battery recycling: Charting a sustainable course. *Sustainable Materials and Technologies* **2014**, *1*, 2-7.
11. Heelan, J.; Gratz, E.; Zheng, Z.; Wang, Q.; Chen, M.; Apelian, D.; Wang, Y. Current and Prospective Li-Ion Battery Recycling and Recovery Processes. *JOM* **2016**, *68*, 2632-2638.
12. Ekberg, C.; Petranikova, M. Chapter 7 - Lithium Batteries Recycling. In *Lithium Process Chemistry*, Chagnes, A., Światowska, J., Eds.; Elsevier: Amsterdam, 2015; pp. 233-267.
13. European Parliament, C.o.t.E.U. DIRECTIVE 2006/66/EC OF THE EUROPEAN PARLIAMENT AND OF THE COUNCIL of 6/9/2006 on batteries and accumulators and waste batteries and accumulators and repealing Directive 91/157/EEC: https://eur-lex.europa.eu/legal-content/EN/ALL/?uri=CELEX%3A32006L0066.
14. Dincer, I. Energy and environmental impacts: present and future perspectives. *Energy sources* **1998**, *20*, 427-453.
15. Agency, E.U.S.E.P. About the U.S. Electricity System and its Impact on the Environment: https://www.epa.gov/energy/about-us-electricity-system-and-its-impact-environment.
16. Nazir, M.S.; Qi, W. Impact of symmetrical short-circuit fault on doubly-fed induction generator controller. *International Journal of Electronics* **2020**, *107*, 2028-2043.
17. Nazir, M.S.; Wang, Y.; Mahdi, A.J.; Sun, X.; Zhang, C.; Abdalla, A.N. Improving the performance of doubly fed induction generator using fault tolerant control—a hierarchical approach. *Applied Sciences* **2020**, *10*, 924.
18. Khafaie, M.A.; Sayyah, M.; Rahim, F. Extreme pollution, climate change, and depression. *Environmental Science and Pollution Research* **2019**, *26*, 22103-22105.
19. Bilgili, F.; Ulucak, R.; Koçak, E.; İlkay, S.Ç. Does globalization matter for environmental sustainability? Empirical investigation for Turkey by Markov regime switching models. *Environmental Science and Pollution Research* **2020**, *27*, 1087-1100.
20. Bilgili, F.; Kuşkaya, S.; Ünlü, F.; Gençoğlu, P. Does waste energy usage mitigate the CO2 emissions? A time-frequency domain analysis. *Environmental Science and Pollution Research* **2020**, *27*, 5056-5073.

21. Nazir, M.S.; Ali, Z.M.; Bilal, M.; Sohail, H.M.; Iqbal, H.M. Environmental impacts and risk factors of renewable energy paradigm—a review. *Environmental Science and Pollution Research* **2020**, *27*, 33516-33526.
22. Godwill Azeh, E.; Paschaline Udoka, F.; Friday Nweke, N.; Marian, N.U. Mechanism and Health Effects of Heavy Metal Toxicity in Humans. In *Poisoning in the Modern World*, Ozgur, K., Banu, A., Eds.; IntechOpen: Rijeka, 2019; p. Ch. 5.
23. Hamilton, C. Battery Raw Materials –The Fundamentals: https://iea.blob.core.windows.net/assets/imports/events/71/Session3ColinHamiltonBMO.pdf.
24. Song, X.; Hu, S.; Chen, D.; Zhu, B. Estimation of waste battery generation and analysis of the waste battery recycling system in China. *Journal of Industrial Ecology* **2017**, *21*, 57-69.
25. Gu, F.; Guo, J.; Yao, X.; Summers, P.A.; Widijatmoko, S.D.; Hall, P. An investigation of the current status of recycling spent lithium-ion batteries from consumer electronics in China. *Journal of cleaner production* **2017**, *161*, 765-780.
26. Marques, P.; Garcia, R.; Kulay, L.; Freire, F. Comparative life cycle assessment of lithium-ion batteries for electric vehicles addressing capacity fade. *Journal of Cleaner Production* **2019**, *229*, 787-794.
27. Parliament, E.; Union, D.-G.f.I.P.o.t. *Battery-powered electric vehicles : market development and lifecycle emissions : research for TRAN Committee*; European Parliament: 2018.
28. Chagnes, A.; Pospiech, B. A brief review on hydrometallurgical technologies for recycling spent lithium-ion batteries. *Journal of Chemical Technology & Biotechnology* **2013**, *88*, 1191-1199.
29. Zhao, S.; You, F. Comparative life-cycle assessment of Li-ion batteries through process-based and integrated hybrid approaches. *ACS Sustainable Chemistry & Engineering* **2019**, *7*, 5082-5094.
30. Sun, X.; Hao, H.; Zhao, F.; Liu, Z. Tracing global lithium flow: A trade-linked material flow analysis. *Resources, Conservation and Recycling* **2017**, *124*, 50-61.
31. Oliveira, L.; Messagie, M.; Rangaraju, S.; Sanfelix, J.; Rivas, M.H.; Van Mierlo, J. Key issues of lithium-ion batteries–from resource depletion to environmental performance indicators. *Journal of Cleaner Production* **2015**, *108*, 354-362.
32. Dewulf, J.; Van der Vorst, G.; Denturck, K.; Van Langenhove, H.; Ghyoot, W.; Tytgat, J.; Vandeputte, K. Recycling rechargeable lithium ion batteries: Critical analysis of natural resource savings. *Resources, Conservation and Recycling* **2010**, *54*, 229-234.
33. Wang, C.; Chen, B.; Yu, Y.; Wang, Y.; Zhang, W. Carbon footprint analysis of lithium ion secondary battery industry: two case studies from China. *Journal of Cleaner Production* **2017**, *163*, 241-251.
34. Unterreiner, L.; Jülch, V.; Reith, S. Recycling of battery technologies–ecological impact analysis using Life Cycle Assessment (LCA). *Energy Procedia* **2016**, *99*, 229-234.
35. Zackrisson, M.; Avellán, L.; Orlenius, J. Life cycle assessment of lithium-ion batteries for plug-in hybrid electric vehicles–Critical issues. *Journal of Cleaner Production* **2010**, *18*, 1519-1529.
36. Costa, C.M.; Barbosa, J.C.; Gonçalves, R.; Castro, H.; Del Campo, F.; Lanceros-Méndez, S. Recycling and environmental issues of lithium-ion batteries: Advances, challenges and opportunities. *Energy Storage Materials* **2021**, *37*, 433-465.
37. Zackrisson, M.; Fransson, K.; Hildenbrand, J.; Lampic, G.; O'Dwyer, C. Life cycle assessment of lithium-air battery cells. *Journal of Cleaner Production* **2016**, *135*, 299-311.
38. Wanger, T.C. The Lithium future—resources, recycling, and the environment. *Conservation Letters* **2011**, *4*, 202-206.
39. Dunn, J.B.; Gaines, L.; Sullivan, J.; Wang, M.Q. Impact of recycling on cradle-to-gate energy consumption and greenhouse gas emissions of automotive lithium-ion batteries. *Environmental science & technology* **2012**, *46*, 12704-12710.

40. Nguyen, V.T.; Lee, J.-c.; Jeong, J.; Kim, B.-S.; Pandey, B. Selective recovery of cobalt, nickel and lithium from sulfate leachate of cathode scrap of Li-ion batteries using liquid-liquid extraction. *Metals and Materials International* **2014**, *20*, 357-365.
41. Lisbona, D.; Snee, T. A review of hazards associated with primary lithium and lithium-ion batteries. *Process safety and environmental protection* **2011**, *89*, 434-442.
42. Bozich, J.; Hang, M.; Hamers, R.; Klaper, R. Core chemistry influences the toxicity of multicomponent metal oxide nanomaterials, lithium nickel manganese cobalt oxide, and lithium cobalt oxide to Daphnia magna. *Environmental toxicology and chemistry* **2017**, *36*, 2493-2502.
43. Siwal, S.S.; Zhang, Q.; Devi, N.; Thakur, V.K. Carbon-based polymer nanocomposite for high-performance energy storage applications. *Polymers* **2020**, *12*, 505.
44. Gorbova, E.; Maragou, V.; Medvedev, D.; Demin, A.; Tsiakaras, P. Influence of sintering additives of transition metals on the properties of gadolinium-doped barium cerate. *Solid State Ionics* **2008**, *179*, 887-890.
45. Walsh, F.C. A first course in electrochemical engineering. **1993**.
46. Davis, T.; Genders, J.; Pletcher, D. A First Course in Ion Permeable Membranes, the Electrochemical Consultancy. *Hants, England* **1997**.
47. Fujishima, A.; Honda, K. Electrochemical photolysis of water at a semiconductor electrode. *nature* **1972**, *238*, 37-38.
48. Pletcher, D. A first course in electrode processes, The Electrochemical Consultancy. *Hampshire* **1991**.
49. Reddy, T.B. *Handbook of Batteries*, third ed.; McGraw-Hill: 2002.
50. Kurzweil, P. Gaston Planté and his invention of the lead–acid battery—The genesis of the first practical rechargeable battery. *Journal of Power Sources* **2010**, *195*, 4424-4434.
51. Howard, P.L.; Vinal, G.W. *Battery additives*; US Government Printing Office: 1951; Volume 504.
52. Whittingham, M.S. Electrical energy storage and intercalation chemistry. *Science* **1976**, *192*, 1126-1127.
53. Chan, C.K.; Peng, H.; Liu, G.; McIlwrath, K.; Zhang, X.F.; Huggins, R.A.; Cui, Y. High-performance lithium battery anodes using silicon nanowires. *Nature nanotechnology* **2008**, *3*, 31-35.
54. Culter, T. A design guide for rechargeable zinc-air battery technology. In Proceedings of the southcon/96 conference record, 1996; pp. 616-621.
55. Li, Y.; Dai, H. Recent advances in zinc–air batteries. *Chemical Society Reviews* **2014**, *43*, 5257-5275.
56. Hiroko Kaneko; Akira Negishi; Ken NozakiKanji Sato; Nakajima, M. Redox battery. 1994.
57. Saad, A.; Gao, Y.; Ramiere, A.; Chu, T.; Yasin, G.; Wu, Y.; Ibraheem, S.; Wang, M.; Guo, H.; Tsiakaras, P. Understanding the Surface Reconstruction on Ternary WxCoBx for Water Oxidation and Zinc–Air Battery Applications. *Small* **2022**, *18*, 2201067.
58. Najam, T.; Shah, S.S.A.; Ibraheem, S.; Cai, X.; Hussain, E.; Suleman, S.; Javed, M.S.; Tsiakaras, P. Single-atom catalysis for zinc-air/O2 batteries, water electrolyzers and fuel cells applications. *Energy Storage Materials* **2022**, *45*, 504-540.
59. Lyu, D.; Yao, S.; Ali, A.; Tian, Z.Q.; Tsiakaras, P.; Shen, P.K. N, S Codoped Carbon Matrix-Encapsulated Co9S8 Nanoparticles as a Highly Efficient and Durable Bifunctional Oxygen Redox Electrocatalyst for Rechargeable Zn–Air Batteries. *Advanced Energy Materials* **2021**, *11*, 2101249.
60. Shah, S.S.A.; Najam, T.; Brouzgou, A.; Tsiakaras, P. Alkaline Oxygen Electrocatalysis for Fuel Cells and Metal–Air Batteries. In *Encyclopedia of Electrochemistry*; 2023; pp. 1-28.
61. Vayenas, C.; Bebelis, S.; Yentekakis, I.; Tsiakaras, P.; Karasali, H. Non-faradaic electrochemical modification of catalytic activity reversible promotion of platinum metals catalysts. *Platinum Met. Rev* **1990**, *34*, 122-130.

62. Oshima, T.; Kajita, M.; Okuno, A. Development of sodium-sulfur batteries. *International Journal of Applied Ceramic Technology* **2004**, *1*, 269-276.
63. Kalyakin, A.; Fadeyev, G.; Demin, A.; Gorbova, E.; Brouzgou, A.; Volkov, A.; Tsiakaras, P. Application of Solid oxide proton-conducting electrolytes for amperometric analysis of hydrogen in H2+ N2+ H2O gas mixtures. *Electrochimica Acta* **2014**, *141*, 120-125.
64. Fadeyev, G.; Kalakin, A.; Demin, A.; Volkov, A.; Brouzgou, A.; Tsiakaras, P. Electrodes for solid electrolyte sensors for the measurement of CO and H2 content in air. *International Journal of Hydrogen Energy* **2013**, *38*, 13484-13490.
65. Gorbova, E.; Tzorbatzoglou, F.; Molochas, C.; Chloros, D.; Demin, A.; Tsiakaras, P. Fundamentals and principles of solid-state electrochemical sensors for high temperature gas detection. *Catalysts* **2022**, *12*, 1.
66. Demin, A.; Gorbova, E.; Brouzgou, A.; Volkov, A.; Tsiakaras, P. Sensors based on solid oxide electrolytes. In *Solid Oxide-Based Electrochemical Devices*; Elsevier: 2020; pp. 167-215.
67. Kalyakin, A.; Volkov, A.; Lyagaeva, J.; Medvedev, D.; Demin, A.; Tsiakaras, P. Combined amperometric and potentiometric hydrogen sensors based on BaCe0.7Zr0.1Y0.2O3−δ proton-conducting ceramic. *Sensors and Actuators B: Chemical* **2016**, *231*, 175-182.
68. Volkov, A.; Gorbova, E.; Vylkov, A.; Medvedev, D.; Demin, A.; Tsiakaras, P. Design and applications of potentiometric sensors based on proton-conducting ceramic materials. A brief review. *Sensors and Actuators B: Chemical* **2017**, *244*, 1004-1015.
69. Fadeyev, G.; Kalyakin, A.; Gorbova, E.; Brouzgou, A.; Demin, A.; Volkov, A.; Tsiakaras, P. A simple and low-cost amperometric sensor for measuring H2, CO, and CH4. *Sensors and Actuators B: Chemical* **2015**, *221*, 879-883.
70. Dunyushkina, L.A.; Pankratov, A.A.; Gorelov, V.P.; Brouzgou, A.; Tsiakaras, P. Deposition and Characterization of Y-doped CaZrO_3 Electrolyte Film on a Porous SrTi_0__8Fe_0__2O_3_-_δ Substrate. *Electrochimica Acta* **2016**, 39-46.
71. Kalyakin, A.; Demin, A.; Gorbova, E.; Volkov, A.; Tsiakaras, P. Combined amperometric-potentiometric oxygen sensor. *Sensors and Actuators B: Chemical* **2020**, *313*, 127999.
72. Kalyakin, A.; Volkov, A.; Demin, A.; Gorbova, E.; Tsiakaras, P. Determination of nitrous oxide concentration using a solid-electrolyte amperometric sensor. *Sensors and Actuators B: Chemical* **2019**, *297*, 126750.
73. Kalyakin, A.; Lyagaeva, J.; Medvedev, D.; Volkov, A.; Demin, A.; Tsiakaras, P. Characterization of proton-conducting electrolyte based on La0.9Sr0.1YO3–δ and its application in a hydrogen amperometric sensor. *Sensors and Actuators B: Chemical* **2016**, *225*, 446-452.
74. Balkourani, G.; Damartzis, T.; Brouzgou, A.; Tsiakaras, P. Cost Effective Synthesis of Graphene Nanomaterials for Non-Enzymatic Electrochemical Sensors for Glucose: A Comprehensive Review. *Sensors* **2022**, *22*, 355.
75. Brouzgou, A.; Gorbova, E.; Wang, Y.; Jing, S.; Seretis, A.; Liang, Z.; Tsiakaras, P. Nitrogen-doped 3D hierarchical ordered mesoporous carbon supported palladium electrocatalyst for the simultaneous detection of ascorbic acid, dopamine, and glucose. *Ionics* **2019**, *25*, 6061-6070.
76. Balkourani, G.; Brouzgou, A.; Archonti, M.; Papandrianos, N.; Song, S.; Tsiakaras, P. Emerging materials for the electrochemical detection of COVID-19. *J Electroanal Chem (Lausanne)* **2021**, *893*, 115289.
77. Balkourani, G.; Brouzgou, A.; Vecchio, C.L.; Aricò, A.S.; Baglio, V.; Tsiakaras, P. Selective electro-oxidation of dopamine on Co or Fe supported onto N-doped ketjenblack. *Electrochimica Acta* **2022**, *409*, 139943.
78. Gorbova, E.; Balkourani, G.; Molochas, C.; Sidiropoulos, D.; Brouzgou, A.; Demin, A.; Tsiakaras, P. Brief Review on High-Temperature Electrochemical Hydrogen Sensors. *Catalysts* **2022**, *12*, 1647.

79. Goula, M.A.; Kontou, S.K.; Tsiakaras, P.E. Hydrogen production by ethanol steam reforming over a commercial Pd/γ-Al2O3 catalyst. *Applied Catalysis B: Environmental* **2004**, *49*, 135-144.
80. Pauling, L. *General chemistry*; Courier Corporation: 1988.
81. Zhang, B.; Shan, J.; Wang, W.; Tsiakaras, P.; Li, Y. Oxygen Vacancy and Core–Shell Heterojunction Engineering of Anemone-Like CoP@CoOOH Bifunctional Electrocatalyst for Efficient Overall Water Splitting. *Small* **2022**, *18*, 2106012.
82. Long, G.-f.; Wan, K.; Liu, M.-y.; Liang, Z.-x.; Piao, J.-h.; Tsiakaras, P. Active sites and mechanism on nitrogen-doped carbon catalyst for hydrogen evolution reaction. *Journal of Catalysis* **2017**, *348*, 151-159.
83. Xu, P.; Qiu, L.; Wei, L.; Liu, Y.; Yuan, D.; Wang, Y.; Tsiakaras, P. Efficient overall water splitting over Mn doped Ni2P microflowers grown on nickel foam. *Catalysis Today* **2020**, *355*, 815-821.
84. Zhang, L.; Lu, J.; Yin, S.; Luo, L.; Jing, S.; Brouzgou, A.; Chen, J.; Shen, P.K.; Tsiakaras, P. One-pot synthesized boron-doped RhFe alloy with enhanced catalytic performance for hydrogen evolution reaction. *Applied Catalysis B: Environmental* **2018**, *230*, 58-64.
85. Yu, C.; Xu, F.; Luo, L.; Abbo, H.S.; Titinchi, S.J.J.; Shen, P.K.; Tsiakaras, P.; Yin, S. Bimetallic Ni–Co phosphide nanosheets self-supported on nickel foam as high-performance electrocatalyst for hydrogen evolution reaction. *Electrochimica Acta* **2019**, *317*, 191-198.
86. Lu, J.; Tang, Z.; Luo, L.; Yin, S.; Kang Shen, P.; Tsiakaras, P. Worm-like S-doped RhNi alloys as highly efficient electrocatalysts for hydrogen evolution reaction. *Applied Catalysis B: Environmental* **2019**, *255*, 117737.
87. Jing, S.; Wang, D.; Yin, S.; Lu, J.; Shen, P.K.; Tsiakaras, P. P-doped CNTs encapsulated nickel hybrids with flower-like structure as efficient catalysts for hydrogen evolution reaction. *Electrochimica Acta* **2019**, *298*, 142-149.
88. Yan, L.; Zhang, B.; Zhu, J.; Li, Y.; Tsiakaras, P.; Kang Shen, P. Electronic modulation of cobalt phosphide nanosheet arrays via copper doping for highly efficient neutral-pH overall water splitting. *Applied Catalysis B: Environmental* **2020**, *265*, 118555.
89. Bagotsky, V.S. *Fuel Cells: Problems and Solutions*; wiley: 2012.
90. Saad, A.; Gao, Y.; Owusu, K.A.; Liu, W.; Wu, Y.; Ramiere, A.; Guo, H.; Tsiakaras, P.; Cai, X. Ternary Mo2NiB2 as a Superior Bifunctional Electrocatalyst for Overall Water Splitting. *Small* **2022**, *18*, 2104303.
91. Zittel, W.; Wurster, R. Chapter 3: Production of Hydrogen. Part 4: Production from electricity by means of electrolysis. *HyWeb: Knowledge-Hydrogen in the Energy Sector* **1996**, 07-08.
92. Long, B.; Yang, H.; Li, M.; Balogun, M.-S.; Mai, W.; Ouyang, G.; Tong, Y.; Tsiakaras, P.; Song, S. Interface charges redistribution enhanced monolithic etched copper foam-based Cu2O layer/TiO2 nanodots heterojunction with high hydrogen evolution electrocatalytic activity. *Applied Catalysis B: Environmental* **2019**, *243*, 365-372.
93. Shah, S.S.A.; Khan, N.A.; Imran, M.; Rashid, M.; Tufail, M.K.; Rehman, A.u.; Balkourani, G.; Sohail, M.; Najam, T.; Tsiakaras, P. Recent Advances in Transition Metal Tellurides (TMTs) and Phosphides (TMPs) for Hydrogen Evolution Electrocatalysis. *Membranes* **2023**, *13*, 113.
94. Wang, K.; Wang, Y.; Liang, Z.; Liang, Y.; Wu, D.; Song, S.; Tsiakaras, P. Ordered mesoporous tungsten carbide/carbon composites promoted Pt catalyst with high activity and stability for methanol electrooxidation. *Applied Catalysis B: Environmental* **2014**, *147*, 518-525.
95. Chouhan, N.; Liu, R.-S. Electrochemical Technologies for Energy Storage and Conversion. 2011; pp. 23-44.
96. Yu, C.; Lu, J.; Luo, L.; Xu, F.; Shen, P.K.; Tsiakaras, P.; Yin, S. Bifunctional catalysts for overall water splitting: CoNi oxyhydroxide nanosheets electrodeposited on titanium sheets. *Electrochimica Acta* **2019**, *301*, 449-457.

97. Thaminimulla, C.; Takata, T.; Hara, M.; Kondo, J.; Domen, K. Effect of chromium addition for photocatalytic overall water splitting on Ni–K2La2Ti3O10. *Journal of Catalysis* **2000**, *196*, 362-365.
98. Bockris, J.M.; Reddy, A.K. *Electrodics in Chemistry, Engineering, Biology, and Environmental Science*, 2nd ed.; Kluwer Academic Publishers: 2004; Volume 2B.
99. Li, R. Latest progress in hydrogen production from solar water splitting via photocatalysis, photoelectrochemical, and photovoltaic-photoelectrochemical solutions. *Chinese Journal of Catalysis* **2017**, *38*, 5-12.
100. Williams, M.C. Status and promise of fuel cell technology. *Fuel Cells* **2001**, *1*, 87-91.
101. Tsiakaras, P.; Vayenas, C.G. Oxidative Coupling of CH4 on Ag Catalyst-Electrodes Deposited on ZrO2 (8 mol% Y2O3). *Journal of Catalysis* **1993**, *144*, 333-347.
102. Tsiakaras, P.; Athanasiou, C.; Marnellos, G.; Stoukides, M.; ten Elshof, J.E.; Bouwmeester, H.J. Methane activation on a La0. 6Sr0. 4Co0. 8Fe0. 2O3 perovskite: Catalytic and electrocatalytic results. *Applied catalysis A: general* **1998**, *169*, 249-261.
103. Tan, A.-d.; Wang, Y.-f.; Fu, Z.-y.; Tsiakaras, P.; Liang, Z.-x. Highly effective oxygen reduction reaction electrocatalysis: Nitrogen-doped hierarchically mesoporous carbon derived from interpenetrated nonporous metal-organic frameworks. *Applied Catalysis B: Environmental* **2017**, *218*, 260-266.
104. Benz, J.; Ortiz, B.; Roth, W.; Sauer, D.; Steinhüser, A. Fuel cells in photovoltaic hybrid systems for stand-alone power supplies. In Proceedings of the 2nd European PV-Hybrid and Mini-Grid Conference, 2003; pp. 232-239.
105. Song, S.; Maragou, V.; Tsiakaras, P. How far are direct alcohol fuel cells from our energy future? **2007**.
106. Merle, G.; Wessling, M.; Nijmeijer, K. Anion exchange membranes for alkaline fuel cells: A review. *Journal of Membrane Science* **2011**, *377*, 1-35.
107. Yu, P.T.; Gu, W.; Zhang, J.; Makharia, R.; Wagner, F.T.; Gasteiger, H.A. Carbon-support requirements for highly durable fuel cell operation. In *Polymer electrolyte fuel cell durability*; Springer: 2009; pp. 29-53.
108. Andreadis, G.; Podias, A.; Tsiakaras, P. The effect of the parasitic current on the direct ethanol PEM fuel cell operation. *Journal of Power Sources* **2008**, *181*, 214-227.
109. Shah, S.S.A.; Najam, T.; Javed, M.S.; Rahman, M.M.; Tsiakaras, P. Novel Mn-/Co-N_x Moieties Captured in N-Doped Carbon Nanotubes for Enhanced Oxygen Reduction Activity and Stability in Acidic and Alkaline Media. **2021**.
110. Ye, Y.-S.; Rick, J.; Hwang, B.-J. Water Soluble Polymers as Proton Exchange Membranes for Fuel Cells. *Polymers* **2012**, *4*, 913-963.
111. Odeh, A.; Osifo, P.; Noemagus, H. Chitosan: a low cost material for the production of membrane for use in PEMFC-A review. *Energy sources, part A: recovery, utilization, and environmental effects* **2013**, *35*, 152-163.
112. Hoogers, G. *Fuel cell technology handbook*; CRC press: 2002.
113. Wang, K.; Chen, H.; Zhang, X.; Tong, Y.; Song, S.; Tsiakaras, P.; Wang, Y. Iron oxide@graphitic carbon core-shell nanoparticles embedded in ordered mesoporous N-doped carbon matrix as an efficient cathode catalyst for PEMFC. *Applied Catalysis B: Environmental* **2020**, *264*, 118468.
114. Wang, Y.; He, C.; Brouzgou, A.; Liang, Y.; Fu, R.; Wu, D.; Tsiakaras, P.; Song, S. A facile soft-template synthesis of ordered mesoporous carbon/tungsten carbide composites with high surface area for methanol electrooxidation. *Journal of power sources* **2012**, *200*, 8-13.
115. Dohle, H.; Mergel, J.; Stolten, D. Heat and power management of a direct-methanol-fuel-cell (DMFC) system. *Journal of Power Sources* **2002**, *111*, 268-282.

116. Dillon, R.; Srinivasan, S.; Arico, A.; Antonucci, V. International activities in DMFC R&D: status of technologies and potential applications. *Journal of Power Sources* **2004**, *127*, 112-126.
117. Ren, X.; Zelenay, P.; Thomas, S.; Davey, J.; Gottesfeld, S. Recent advances in direct methanol fuel cells at Los Alamos National Laboratory. *Journal of Power Sources* **2000**, *86*, 111-116.
118. Kreuer, K. On the development of proton conducting polymer membranes for hydrogen and methanol fuel cells. *Journal of membrane science* **2001**, *185*, 29-39.
119. Brouzgou, A.; Song, S.; Tsiakaras, P. Carbon-supported PdSn and Pd3Sn2 anodes for glucose electrooxidation in alkaline media. *Applied Catalysis B: Environmental* **2014**, *158*, 209-216.
120. Cutlip, M.; Yang, S.; Stonehart, P. Simulation and optimization of porous gas-diffusion electrodes used in hydrogen oxygen phosphoric acid fuel cells—II development of a detailed anode model. *Electrochimica acta* **1991**, *36*, 547-553.
121. Shim, J.-C.; Rim, H.-R.; Yoo, D.-Y.; Park, J.-I.; Kim, J.-W.; Lee, J.-S. Development of electrode structure via loading Pt catalysts on PTFE/C powder by colloidal method in PAFC. *Journal of Industrial and Engineering Chemistry* **2000**, *6*, 79-84.
122. Bischoff, M. Molten carbonate fuel cells: A high temperature fuel cell on the edge to commercialization. *Journal of Power Sources* **2006**, *160*, 842-845.
123. Amorelli, A.; Wilkinson, M.; Bedont, P.; Capobianco, P.; Marcenaro, B.; Parodi, F.; Torazza, A. An experimental investigation into the use of molten carbonate fuel cells to capture CO2 from gas turbine exhaust gases. In Proceedings of the Greenhouse Gas Control Technologies-6th International Conference, 2003; pp. 1325-1330.
124. Li, X. *Principles of fuel cells*; CRC press: 2005.
125. Medvedev, D.A.; Maragou, V.; Pikalova, E.Y.; Demin, A.K.; Tsiakaras, P. Novel composite solid state electrolytes on the base of BaCeO3 and CeO2 for intermediate temperature electrochemical devices. *Journal of Power Sources* **2013**, *221*, 217-227.
126. Coutelieris, F.A.; Douvartzides, S.; Tsiakaras, P. The importance of the fuel choice on the efficiency of a solid oxide fuel cell system. *Journal of Power Sources* **2003**, *123*, 200-205.
127. Matelli, J.A.; Bazzo, E. A methodology for thermodynamic simulation of high temperature, internal reforming fuel cell systems. *Journal of Power Sources* **2005**, *142*, 160-168.
128. Song, S.-J.; Moon, J.-H.; Lee, T.H.; Dorris, S.E.; Balachandran, U.; Systems, E.; Univ., C.N. Thickness dependence of hydrogen permeability for Ni-BaCe{sub 0.8}Y{sub 0.2}O{sub 3-{delta}}. *Solid State Ionics* **2008**, *179*, Medium: X; Size: 1854-1857.
129. Lagaeva, J.; Medvedev, D.; Demin, A.; Tsiakaras, P. Insights on thermal and transport features of BaCe0.8−xZrxY0.2O3−δ proton-conducting materials. *Journal of Power Sources* **2015**, *278*, 436-444.
130. Lu, J.; Wu, T.; Amine, K. State-of-the-art characterization techniques for advanced lithium-ion batteries. *Nature Energy* **2017**, *2*, 1-13.
131. Deng, D.; Kim, M.G.; Lee, J.Y.; Cho, J. Green energy storage materials: Nanostructured TiO 2 and Sn-based anodes for lithium-ion batteries. *Energy & Environmental Science* **2009**, *2*, 818-837.
132. Tarascon, J.M.; Armand, M. Issues and challenges facing rechargeable lithium batteries. *Nature* **2001**, *414*, 359-367.
133. Bloomberg. Electric Vehicle Outlook 2017: https://data.bloomberglp.com/bnef/sites/14/2017/07/BNEF_EVO_2017_ExecutiveSummary.pdf
134. Deng, D. Li-ion batteries: basics, progress, and challenges. *Energy Science & Engineering* **2015**, *3*, 385-418.
135. Nitta, N.; Wu, F.; Lee, J.T.; Yushin, G. Li-ion battery materials: present and future. *Materials today* **2015**, *18*, 252-264.
136. LeVine, S. THE GREAT BATTERY RACE. *Foreign Policy* **2010**, 88-95.

137. Besenhard, J.; Fritz, H. Cathodic reduction of graphite in organic solutions of alkali and NR4+ salts. *Journal of Electroanalytical Chemistry - J ELECTROANAL CHEM* **1974**, *53*, 329-333.
138. Besenhard, J. The electrochemical preparation and properties of ionic alkali metal-and NR4-graphite intercalation compounds in organic electrolytes. *Carbon* **1976**, *14*, 111-115.
139. Schöllhorn, R.; Kuhlmann, R.; Besenhard, J. Topotactic redox reactions and ion exchange of layered MoO3 bronzes. *Materials Research Bulletin* **1976**, *11*, 83-90.
140. Besenhard, J.; Schöllhorn, R. The discharge reaction mechanism of the MoO3 electrode in organic electrolytes. *Journal of Power Sources* **1976**, *1*, 267-276.
141. Besenhard, J.; Eichinger, G. High energy density lithium cells: Part I. Electrolytes and anodes. *Journal of Electroanalytical Chemistry and Interfacial Electrochemistry* **1976**, *68*, 1-18.
142. Eichinger, G.; Besenhard, J. High energy density lithium cells: Part II. Cathodes and complete cells. *Journal of Electroanalytical Chemistry and Interfacial Electrochemistry* **1976**, *72*, 1-31.
143. Godshall, N.A.; Raistrick, I.; Huggins, R. Thermodynamic investigations of ternary lithium-transition metal-oxygen cathode materials. *Materials Research Bulletin* **1980**, *15*, 561-570.
144. Mizushima, K.; Jones, P.; Wiseman, P.; Goodenough, J.B. LixCoO2 (0< x<-1): A new cathode material for batteries of high energy density. *Materials Research Bulletin* **1980**, *15*, 783-789.
145. Yazami, R.; Touzain, P. A reversible graphite-lithium negative electrode for electrochemical generators. *Journal of Power Sources* **1983**, *9*, 365-371.
146. Ian D. Raistrick, N.A.G., Robert A. Huggins. Ternary compound electrode for lithium cells. 1982.
147. Thackeray, M.; David, W.; Bruce, P.; Goodenough, J. Lithium insertion into manganese spinels. *Materials research bulletin* **1983**, *18*, 461-472.
148. A. Yoshino, K.S., T. Nakajima Secondary battery. 1987.
149. M. Wakihara, O.Y. *Lithium ion batteries : fundamentals and performance*; Wiley-VCH ; Kodansha Ltd.: 1998.
150. Padhi, A.; Nanjundaswamy, K.; Goodenough, J. LiFePO4: a novel cathode material for rechargeable batteries. In Proceedings of the Electrochemical Society Meeting Abstracts, 1996; p. 73.
151. Market Share Data, Industry Trends, Market Analysis, and Project Tracking by World Region, Technology, Application, and Market Segment. **2017:** https://www.prnewswire.com/news-releases/energy-storage-tracker-3q14--global-energy-storage-installations-market-share-data-industry-trends-market-analysis-and-project-tracking-by-world-region-technology-application-and-market-segment-278570681.html .
152. Bhatt, M.D.; O'Dwyer, C. Recent progress in theoretical and computational investigations of Li-ion battery materials and electrolytes. *Physical Chemistry Chemical Physics* **2015**, *17*, 4799-4844.
153. SPANGENBERGER, J. INTRODUCTION TO LITHIUM ION BATTERIES. Available online: https://www.epa.gov/sites/default/files/2018-03/documents/spanenberger_epa_webinar_-_3-22-18_-_argonne.pdf.
154. Osiak, M.; Geaney, H.; Armstrong, E.; O'Dwyer, C. Structuring materials for lithium-ion batteries: advancements in nanomaterial structure, composition, and defined assembly on cell performance. *Journal of Materials Chemistry A* **2014**, *2*, 9433-9460.
155. Hammouche, A.; Karden, E.; De Doncker, R.W. Monitoring state-of-charge of Ni–MH and Ni–Cd batteries using impedance spectroscopy. *Journal of Power Sources* **2004**, *127*, 105-111.
156. Baughman, R.H.; Zakhidov, A.A.; De Heer, W.A. Carbon nanotubes--the route toward applications. *science* **2002**, *297*, 787-792.
157. Che, G.; Lakshmi, B.B.; Fisher, E.R.; Martin, C.R. Carbon nanotubule membranes for electrochemical energy storage and production. *Nature* **1998**, *393*, 346-349.
158. Scarselli, M.; Castrucci, P.; De Crescenzi, M. Electronic and optoelectronic nano-devices based on carbon nanotubes. *Journal of Physics: Condensed Matter* **2012**, *24*, 313202.

159. Qi, W.; Shapter, J.G.; Wu, Q.; Yin, T.; Gao, G.; Cui, D. Nanostructured anode materials for lithium-ion batteries: principle, recent progress and future perspectives. *Journal of Materials Chemistry A* **2017**, *5*, 19521-19540.
160. Kim, Y.; Song, W.; Lee, S.; Jeon, C.; Jung, W.; Kim, M.; Park, C.-Y. Low-temperature synthesis of graphene on nickel foil by microwave plasma chemical vapor deposition. *Applied physics letters* **2011**, *98*, 263106.
161. Urban, A.; Seo, D.-H.; Ceder, G. Computational understanding of Li-ion batteries. *npj Computational Materials* **2016**, *2*, 1-13.
162. Croy, J.R.; Balasubramanian, M.; Gallagher, K.G.; Burrell, A.K. Review of the US Department of Energy's "deep dive" effort to understand voltage fade in Li-and Mn-rich cathodes. *Accounts of chemical research* **2015**, *48*, 2813-2821.
163. Wang, Y.; Cao, G. Developments in nanostructured cathode materials for high-performance lithium-ion batteries. *Advanced materials* **2008**, *20*, 2251-2269.
164. Ji, L.; Lin, Z.; Alcoutlabi, M.; Zhang, X. Recent developments in nanostructured anode materials for rechargeable lithium-ion batteries. *Energy & Environmental Science* **2011**, *4*, 2682-2699.
165. Yang, Y.; McDowell, M.T.; Jackson, A.; Cha, J.J.; Hong, S.S.; Cui, Y. New nanostructured Li2S/silicon rechargeable battery with high specific energy. *Nano letters* **2010**, *10*, 1486-1491.
166. Rui, X.; Yan, Q.; Skyllas-Kazacos, M.; Lim, T.M. Li3V2 (PO4) 3 cathode materials for lithium-ion batteries: a review. *Journal of Power Sources* **2014**, *258*, 19-38.
167. Guan, P.; Zhou, L.; Yu, Z.; Sun, Y.; Liu, Y.; Wu, F.; Jiang, Y.; Chu, D. Recent progress of surface coating on cathode materials for high-performance lithium-ion batteries. *Journal of Energy Chemistry* **2020**, *43*, 220-235.
168. Islam, M.S.; Fisher, C.A. Lithium and sodium battery cathode materials: computational insights into voltage, diffusion and nanostructural properties. *Chemical Society Reviews* **2014**, *43*, 185-204.
169. Lagadec, M.F.; Zahn, R.; Wood, V. Characterization and performance evaluation of lithium-ion battery separators. *Nature Energy* **2019**, *4*, 16-25.
170. Li, Y.; Li, Q.; Tan, Z. A review of electrospun nanofiber-based separators for rechargeable lithium-ion batteries. *Journal of Power Sources* **2019**, *443*, 227262.
171. Liu, Z.; Jiang, Y.; Hu, Q.; Guo, S.; Yu, L.; Li, Q.; Liu, Q.; Hu, X. Safer Lithium-Ion Batteries from the Separator Aspect: Development and Future Perspectives. *ENERGY & ENVIRONMENTAL MATERIALS* **2021**, *4*, 336-362.
172. Arora, P.; Zhang, Z. Battery separators. *Chemical reviews* **2004**, *104*, 4419-4462.
173. Costa, C.; Lizundia, E.; Lanceros-Méndez, S. Polymers for advanced lithium-ion batteries: State of the art and future needs on polymers for the different battery components. *Progress in Energy and Combustion Science* **2020**, *79*, 100846.
174. Lee, H.; Yanilmaz, M.; Toprakci, O.; Fu, K.; Zhang, X. A review of recent developments in membrane separators for rechargeable lithium-ion batteries. *Energy & Environmental Science* **2014**, *7*, 3857-3886.
175. Yuan, M.; Liu, K. Rational design on separators and liquid electrolytes for safer lithium-ion batteries. *Journal of Energy Chemistry* **2020**, *43*, 58-70.
176. Waqas, M.; Ali, S.; Feng, C.; Chen, D.; Han, J.; He, W. Recent development in separators for high-temperature lithium-ion batteries. *Small* **2019**, *15*, 1901689.
177. Guo, J.; Wang, C. Nanostructured metal oxides for Li-Ion batteries. In *Functional Metal Oxide Nanostructures*; Springer: 2012; pp. 337-363.
178. Xu, K. Nonaqueous liquid electrolytes for lithium-based rechargeable batteries. *Chemical reviews* **2004**, *104*, 4303-4418.

179. B . Yebka , J.R.C., L. G. Estes, J. A. Holung, T. Humphrey , T. L. Wong. Venting mechanism for battery cell US patent 8 263 242 B@. **2012**.
180. S. T. Mayer, J.C.W. Overcharge protection battery vent. 1998.
181. Kong, L.; Li, C.; Jiang, J.; Pecht, M.G. Li-ion battery fire hazards and safety strategies. *Energies* **2018**, *11*, 2191.
182. Swart, J.; Arora, A.; Megerle, M.; Nilsson, S. Methods for measuring the mechanical safety vent pressure of lithium ion battery cells. In Proceedings of the 2006 IEEE Symposium on Product Safety Engineering, 2006; pp. 1-4.
183. Yao, X.-Y.; Kong, L.; Pecht, M.G. Reliability of cylindrical li-ion battery safety vents. *IEEE Access* **2020**, *8*, 101859-101866.
184. Yebka, B.; Holung, J.A.; Wong, T.-L.; Seethaler, K.S. Double acting venting mechanism for battery cells. **2011**.
185. Cheon, S.-E.; Kim, J.-K.; Yoon, H.-W.; Yoo, S.-Y. Rechargeable battery with gas release safety vent. **2010**.
186. LePort, F.; Kohn, S.I.; King, O.A.; Prilutsky, A. Battery cap assembly with high efficiency vent. **2016**.
187. Mousavi, M.; Hoque, S.; Rahnamayan, S.; Dincer, I.; Naterer, G.F. Optimal design of an air-cooling system for a Li-Ion battery pack in Electric Vehicles with a genetic algorithm. In Proceedings of the 2011 IEEE Congress of Evolutionary Computation (CEC), 2011; pp. 1848-1855.
188. Yano, A.; Shikano, M.; Ueda, A.; Sakaebe, H.; Ogumi, Z. LiCoO2 degradation behavior in the high-voltage phase transition region and improved reversibility with surface coating. *Journal of The Electrochemical Society* **2016**, *164*, A6116.
189. Zhang, C.; Shen, L.; Li, H.; Ping, N.; Zhang, X. Enhanced electrochemical properties of MgF2 and C co-coated Li3V2 (PO4) 3 composite for Li-ion batteries. *Journal of Electroanalytical Chemistry* **2016**, *762*, 1-6.
190. Zuo, D.; Tian, G.; Li, X.; Chen, D.; Shu, K. Recent progress in surface coating of cathode materials for lithium ion secondary batteries. *Journal of Alloys and Compounds* **2017**, *706*, 24-40.
191. Julien, C.M.; Mauger, A. NCA, NCM811, and the route to Ni-richer lithium-ion batteries. *Energies* **2020**, *13*, 6363.
192. Wang, C.-C.; Lin, J.-W.; Yu, Y.-H.; Lai, K.-H.; Chiu, K.-F.; Kei, C.-C. Electrochemical and structural investigation on ultrathin ALD ZnO and TiO2 coated lithium-rich layered oxide cathodes. *ACS Sustainable Chemistry & Engineering* **2018**, *6*, 16941-16950.
193. Luo, W.; Liu, L.; Li, X.; Yu, J.; Fang, C. Templated assembly of LiNi0· 8Co0· 15Al0· 05O2/graphene nano composite with high rate capability and long-term cyclability for lithium ion battery. *Journal of Alloys and Compounds* **2019**, *810*, 151786.
194. Tian, L.; Liang, K.; Wen, X.; Shi, K.; Zheng, J. Enhanced cycling stability and rate capability of LiNi0. 80Co0. 15Al0. 05O2 cathode material by a facile coating method. *Journal of Electroanalytical Chemistry* **2018**, *812*, 22-27.
195. Xia, S.; Li, F.; Chen, F.; Guo, H. Preparation of FePO4 by liquid-phase method and modification on the surface of LiNi0. 80Co0. 15Al0. 05O2 cathode material. *Journal of Alloys and Compounds* **2018**, *731*, 428-436.
196. Xia, S.; Zhang, Y.; Dong, P.; Zhang, Y. Synthesis cathode material LiNi0. 80Co0. 15Al0. 05O2 with two step solid-state method under air stream. *The European Physical Journal-Applied Physics* **2014**, *65*.
197. Wu, N.; Wu, H.; Yuan, W.; Liu, S.; Liao, J.; Zhang, Y. Facile synthesis of one-dimensional LiNi 0.8 Co 0.15 Al 0.05 O 2 microrods as advanced cathode materials for lithium ion batteries. *Journal of Materials Chemistry A* **2015**, *3*, 13648-13652.

198. Xie, H.; Du, K.; Hu, G.; Duan, J.; Peng, Z.; Zhang, Z.; Cao, Y. Synthesis of LiNi 0.8 Co 0.15 Al 0.05 O 2 with 5-sulfosalicylic acid as a chelating agent and its electrochemical properties. *Journal of Materials Chemistry A* **2015**, *3*, 20236-20243.
199. Makimura, Y.; Sasaki, T.; Nonaka, T.; Nishimura, Y.F.; Uyama, T.; Okuda, C.; Itou, Y.; Takeuchi, Y. Factors affecting cycling life of LiNi 0.8 Co 0.15 Al 0.05 O 2 for lithium-ion batteries. *Journal of Materials Chemistry A* **2016**, *4*, 8350-8358.
200. Qiu, Z.; Zhang, Y.; Dong, P.; Xia, S.; Yao, Y. A facile method for synthesis of LiNi0. 8Co0. 15Al0. 05O2 cathode material. *Solid State Ionics* **2017**, *307*, 73-78.
201. Nie, Y.; Xiao, W.; Miao, C.; Fang, R.; Kou, Z.; Wang, D.; Xu, M.; Wang, C. Boosting the electrochemical performance of LiNi0. 8Co0. 15Al0. 05O2 cathode materials in-situ modified with Li1. 3Al0. 3Ti1. 7 (PO4) 3 fast ion conductor for lithium-ion batteries. *Electrochimica Acta* **2020**, *353*, 136477.
202. Nie, Y.; Xiao, W.; Miao, C.; Xu, M.; Wang, C. Effect of calcining oxygen pressure gradient on properties of LiNi0. 8Co0. 15Al0. 05O2 cathode materials for lithium ion batteries. *Electrochimica Acta* **2020**, *334*, 135654.
203. Yang, Z.; Li, Z.; Huang, Y.; Zhang, M.; Liu, C.; Zhang, D.; Cao, G. Artificial interface stabilized LiNi0. 80Co0. 15Al0. 05O2@ Polysiloxane cathode for stable cycling lithium-ion batteries. *Journal of Power Sources* **2020**, *471*, 228480.
204. Lim, S.N.; Ahn, W.; Yeon, S.-H.; Park, S.B. Enhanced elevated-temperature performance of Li (Ni0. 8Co0. 15Al0. 05) O2 electrodes coated with Li2O-2B2O3 glass. *Electrochimica Acta* **2014**, *136*, 1-9.
205. Srur-Lavi, O.; Miikkulainen, V.; Markovsky, B.; Grinblat, J.; Talianker, M.; Fleger, Y.; Cohen-Taguri, G.; Mor, A.; Tal-Yosef, Y.; Aurbach, D. Studies of the electrochemical behavior of LiNi0. 80Co0. 15Al0. 05O2 electrodes coated with LiAlO2. *Journal of The Electrochemical Society* **2017**, *164*, A3266.
206. Song, C.; Wang, W.; Peng, H.; Wang, Y.; Zhao, C.; Zhang, H.; Tang, Q.; Lv, J.; Du, X.; Dou, Y. Improving the electrochemical performance of LiNi0. 80Co0. 15Al0. 05O2 in lithium ion batteries by LiAlO2 surface modification. *Applied Sciences* **2018**, *8*, 378.
207. Xiong, F.; Chen, Z.; Huang, C.; Wang, T.; Zhang, W.; Yang, Z.; Chen, F. Near-equilibrium control of Li2TiO3 nanoscale layer coated on LiNi0. 8Co0. 1Mn0. 1O2 cathode materials for enhanced electrochemical performance. *Inorganic Chemistry* **2019**, *58*, 15498-15506.
208. Liu, P.; Xiao, L.; Chen, Y.; Chen, H. Highly enhanced electrochemical performances of LiNi0. 815Co0. 15Al0. 035O2 by coating via conductively LiTiO2 for lithium-ion batteries. *Ceramics International* **2019**, *45*, 18398-18405.
209. He, X.; Feng, Z.; Zhou, L.; Xu, X. A synchronously dual-conductive coating towards enhancing the electrochemical performance of LiNi0· 8Co0· 15Al0· 05O2 cathode material. *Journal of Alloys and Compounds* **2021**, *852*, 156966.
210. Kalluri, S.; Yoon, M.; Jo, M.; Liu, H.K.; Dou, S.X.; Cho, J.; Guo, Z. Feasibility of cathode surface coating technology for high-energy lithium-ion and beyond-lithium-ion batteries. *Advanced materials* **2017**, *29*, 1605807.
211. Kalluri, S.; Yoon, M.; Jo, M.; Park, S.; Myeong, S.; Kim, J.; Dou, S.X.; Guo, Z.; Cho, J. Surface Engineering Strategies of Layered LiCoO2 Cathode Material to Realize High-Energy and High-Voltage Li-Ion Cells. *Advanced energy materials* **2017**, *7*, 1601507.
212. Yang, X.; Shen, L.; Wu, B.; Zuo, Z.; Mu, D.; Wu, B.; Zhou, H. Improvement of the cycling performance of LiCoO2 with assistance of cross-linked PAN for lithium ion batteries. *Journal of Alloys and Compounds* **2015**, *639*, 458-464.
213. Kim, J.-M.; Park, J.-H.; Lee, C.K.; Lee, S.-Y. Multifunctional semi-interpenetrating polymer network-nanoencapsulated cathode materials for high-performance lithium-ion batteries. *Scientific reports* **2014**, *4*, 1-7.

214. Zhou, A.; Xu, J.; Dai, X.; Yang, B.; Lu, Y.; Wang, L.; Fan, C.; Li, J. Improved high-voltage and high-temperature electrochemical performances of LiCoO2 cathode by electrode sputter-coating with Li3PO4. *Journal of Power Sources* **2016**, *322*, 10-16.
215. Park, J.S.; Mane, A.U.; Elam, J.W.; Croy, J.R. Amorphous metal fluoride passivation coatings prepared by atomic layer deposition on LiCoO2 for Li-ion batteries. *Chemistry of Materials* **2015**, *27*, 1917-1920.
216. Zhao, J.; Wang, Z.; Wang, J.; Guo, H.; Li, X.; Gui, W.; Chen, N.; Yan, G. Anchoring K+ in Li+ sites of LiNi0. 8Co0. 15Al0. 05O2 cathode material to suppress its structural degradation during high-voltage cycling. *Energy technology* **2018**, *6*, 2358-2366.
217. Chen, T.; Wang, F.; Li, X.; Yan, X.; Wang, H.; Deng, B.; Xie, Z.; Qu, M. Dual functional MgHPO4 surface modifier used to repair deteriorated Ni-Rich LiNi0. 8Co0. 15Al0. 05O2 cathode material. *Applied surface science* **2019**, *465*, 863-870.
218. Yang, Z.; Xiang, W.; Wu, Z.; He, F.; Zhang, J.; Xiao, Y.; Zhong, B.; Guo, X. Effect of niobium doping on the structure and electrochemical performance of LiNi0. 5Co0. 2Mn0. 3O2 cathode materials for lithium ion batteries. *Ceramics International* **2017**, *43*, 3866-3872.
219. Jia, X.; Yan, M.; Zhou, Z.; Chen, X.; Yao, C.; Chen, D.; Chen, Y. Nd-doped LiNi0. 5Co0. 2Mn0. 3O2 as a cathode material for better rate capability in high voltage cycling of Li-ion batteries. *Electrochimica Acta* **2017**, *254*, 50-58.
220. Weigel, T.; Schipper, F.; Erickson, E.M.; Susai, F.A.; Markovsky, B.; Aurbach, D. Structural and electrochemical aspects of LiNi0. 8Co0. 1Mn0. 1O2 cathode materials doped by various cations. *ACS energy letters* **2019**, *4*, 508-516.
221. Chen, M.; Zhao, E.; Chen, D.; Wu, M.; Han, S.; Huang, Q.; Yang, L.; Xiao, X.; Hu, Z. Decreasing Li/Ni disorder and improving the electrochemical performances of Ni-rich LiNi0. 8Co0. 1Mn0. 1O2 by Ca doping. *Inorganic Chemistry* **2017**, *56*, 8355-8362.
222. Susai, F.A.; Kovacheva, D.; Chakraborty, A.; Kravchuk, T.; Ravikumar, R.; Talianker, M.; Grinblat, J.; Burstein, L.; Kauffmann, Y.; Major, D.T. Improving performance of LiNi0. 8Co0. 1Mn0. 1O2 cathode materials for lithium-ion batteries by doping with molybdenum-ions: theoretical and experimental studies. *ACS applied energy materials* **2019**, *2*, 4521-4534.
223. Chen, H.; Hu, Q.; Huang, Z.; He, Z.; Wang, Z.; Guo, H.; Li, X. Synthesis and electrochemical study of Zr-doped Li [Li0. 2Mn0. 54Ni0. 13Co0. 13] O2 as cathode material for Li-ion battery. *Ceramics International* **2016**, *42*, 263-269.
224. Du, F.; Chen, R.; Zhuang, Y.; Zhu, L.; Cao, H.; Dai, H.; Adkins, J.; Zhou, Q.; Zheng, J. Effect of substitution of cobalt with iron on electrochemical behavior and solid electrolyte interface of LiNi0. 8Co0. 15Al0. 05O2. *Applied Surface Science* **2019**, *484*, 374-382.
225. Xi, Z.; Wang, Z.; Peng, W.; Guo, H.; Wang, J. Effect of copper and iron substitution on the structures and electrochemical properties of LiNi0. 8Co0. 15Al0. 05O2 cathode materials. *Energy Science & Engineering* **2020**, *8*, 1868-1879.
226. Liu, D.; Liu, S.; Zhang, C.; You, L.; Huang, T.; Yu, A. Revealing the Effect of Ti Doping on Significantly Enhancing Cyclic Performance at a High Cutoff Voltage for Ni-Rich LiNi0.8Co0.15Al0.05O2 Cathode. *ACS Sustainable Chemistry & Engineering* **2019**, *7*, 10661-10669.
227. Du, F.; Zhou, Q.; Cao, H.; Dai, H.; Hu, D.; Sun, P.; Adkins, J.; Zheng, J. Confined growth of primary grains towards stabilizing integrated structure of Ni-rich materials. *Journal of Power Sources* **2020**, *478*, 228737.
228. Huang, Y.; Liu, X.; Yu, R.; Cao, S.; Pei, Y.; Luo, Z.; Zhao, Q.; Chang, B.; Wang, Y.; Wang, X. Tellurium surface doping to enhance the structural stability and electrochemical performance of layered Ni-rich cathodes. *ACS applied materials & interfaces* **2019**, *11*, 40022-40033.

229. Xie, H.; Du, K.; Hu, G.; Peng, Z.; Cao, Y. The role of sodium in LiNi0. 8Co0. 15Al0. 05O2 cathode material and its electrochemical behaviors. *The Journal of Physical Chemistry C* **2016**, *120*, 3235-3241.
230. Natarajan, S.; Moodakare, S.B.; Haridoss, P.; Gopalan, R. Concentration gradient-driven aluminum diffusion in a single-step coprecipitation of a compositionally graded precursor for LiNi0. 8Co0. 135Al0. 065O2 with mitigated irreversibility of H2↔ H3 phase transition. *ACS applied materials & interfaces* **2020**, *12*, 34959-34970.
231. Liang, M.; Sun, Y.; Song, D.; Shi, X.; Han, Y.; Zhang, H.; Zhang, L. Superior electrochemical performance of quasi-concentration-gradient LiNi0. 8Co0. 15Al0. 05O2 cathode material synthesized with multi-shell precursor and new aluminum source. *Electrochimica acta* **2019**, *300*, 426-436.
232. He, T.; Lu, Y.; Su, Y.; Bao, L.; Tan, J.; Chen, L.; Zhang, Q.; Li, W.; Chen, S.; Wu, F. Sufficient utilization of zirconium ions to improve the structure and surface properties of nickel-rich cathode materials for lithium-ion batteries. *ChemSusChem* **2018**, *11*, 1639-1648.
233. Zhang, D.; Liu, Y.; Wu, L.; Feng, L.; Jin, S.; Zhang, R.; Jin, M. Effect of Ti ion doping on electrochemical performance of Ni-rich LiNi0. 8Co0. 1Mn0. 1O2 cathode material. *Electrochimica Acta* **2019**, *328*, 135086.
234. Jiang, Y.; Bi, Y.; Liu, M.; Peng, Z.; Huai, L.; Dong, P.; Duan, J.; Chen, Z.; Li, X.; Wang, D. Improved stability of Ni-rich cathode by the substitutive cations with stronger bonds. *Electrochimica Acta* **2018**, *268*, 41-48.
235. Do, S.J.; Santhoshkumar, P.; Kang, S.H.; Prasanna, K.; Jo, Y.N.; Lee, C.W. Al-doped Li [Ni0. 78Co0. 1Mn0. 1Al0. 02] O2 for high performance of lithium ion batteries. *Ceramics International* **2019**, *45*, 6972-6977.
236. Kim, U.-H.; Myung, S.-T.; Yoon, C.S.; Sun, Y.-K. Extending the battery life using an Al-doped Li [Ni0. 76Co0. 09Mn0. 15] O2 cathode with concentration gradients for lithium ion batteries. *ACS Energy Letters* **2017**, *2*, 1848-1854.
237. Hou, P.; Li, F.; Sun, Y.; Pan, M.; Wang, X.; Shao, M.; Xu, X. Improving Li+ kinetics and structural stability of nickel-rich layered cathodes by heterogeneous inactive-Al3+ doping. *ACS Sustainable Chemistry & Engineering* **2018**, *6*, 5653-5661.
238. Yuan, A.; Tang, H.; Liu, L.; Ying, J.; Tan, L.; Tan, L.; Sun, R. High performance of phosphorus and fluorine co-doped LiNi0. 8Co0. 1Mn0. 1O2 as a cathode material for lithium ion batteries. *Journal of Alloys and Compounds* **2020**, *844*, 156210.
239. Zhang, M.; Zhao, H.; Tan, M.; Liu, J.; Hu, Y.; Liu, S.; Shu, X.; Li, H.; Ran, Q.; Cai, J. Yttrium modified Ni-rich LiNi0. 8Co0. 1Mn0. 1O2 with enhanced electrochemical performance as high energy density cathode material at 4.5 V high voltage. *Journal of Alloys and Compounds* **2019**, *774*, 82-92.
240. Wu, F.; Li, Q.; Chen, L.; Zhang, Q.; Wang, Z.; Lu, Y.; Bao, L.; Chen, S.; Su, Y. Improving the structure stability of LiNi0. 8Co0. 1Mn0. 1O2 by surface perovskite-like La2Ni0. 5Li0. 5O4 self-assembling and subsurface La3+ doping. *ACS Applied Materials & Interfaces* **2019**, *11*, 36751-36762.
241. Yang, J.; Xia, Y. Enhancement on the cycling stability of the layered Ni-rich oxide cathode by in-situ fabricating nano-thickness cation-mixing layers. *Journal of The Electrochemical Society* **2016**, *163*, A2665.
242. Wang, Z.; Zhong, H.; Song, G. Enhancing high-voltage performance of LiNi0. 8Co0. 1Mn0. 1O2 by coating with NASICON fast ionic conductor Li1. 5Al0. 5Zr1. 5 (PO4) 3. *Journal of Alloys and Compounds* **2020**, *849*, 156467.
243. Cao, Y.; Qi, X.; Hu, K.; Wang, Y.; Gan, Z.; Li, Y.; Hu, G.; Peng, Z.; Du, K. Conductive polymers encapsulation to enhance electrochemical performance of Ni-rich cathode materials for Li-ion batteries. *ACS applied materials & interfaces* **2018**, *10*, 18270-18280.

244. Xu, G.-L.; Liu, Q.; Lau, K.K.; Liu, Y.; Liu, X.; Gao, H.; Zhou, X.; Zhuang, M.; Ren, Y.; Li, J. Building ultraconformal protective layers on both secondary and primary particles of layered lithium transition metal oxide cathodes. *Nature Energy* **2019**, *4*, 484-494.
245. Jerng, S.E.; Chang, B.; Shin, H.; Kim, H.; Lee, T.; Char, K.; Choi, J.W. Pyrazine-linked 2D covalent organic frameworks as coating material for high-nickel layered oxide cathodes in lithium-ion batteries. *ACS applied materials & interfaces* **2020**, *12*, 10597-10606.
246. Zha, G.; Luo, Y.; Hu, N.; Ouyang, C.; Hou, H. Surface modification of the LiNi0. 8Co0. 1Mn0. 1O2 cathode material by coating with FePO4 with a yolk–shell structure for improved electrochemical performance. *ACS Applied Materials & Interfaces* **2020**, *12*, 36046-36053.
247. Xie, J.; Sendek, A.D.; Cubuk, E.D.; Zhang, X.; Lu, Z.; Gong, Y.; Wu, T.; Shi, F.; Liu, W.; Reed, E.J. Atomic layer deposition of stable LiAlF4 lithium ion conductive interfacial layer for stable cathode cycling. *Acs Nano* **2017**, *11*, 7019-7027.
248. Jiang, H.; Li, J.; Lei, Y.; Chen, Y.; Lai, C.; Shi, L.; Peng, C. Stabling LiNi0. 8Co0. 1Mn0. 1O2 by PVP-assisted LiF-LaF3 layer for lithium ion batteries with improved electrochemical properties at high cut-off voltage. *Journal of the Taiwan Institute of Chemical Engineers* **2020**, *114*, 331-340.
249. Liang, L.; Sun, X.; Zhang, J.; Sun, J.; Hou, L.; Liu, Y.; Yuan, C. Sur-/interfacial regulation in all-solid-state rechargeable Li-ion batteries based on inorganic solid-state electrolytes: advances and perspectives. *Materials Horizons* **2019**, *6*, 871-910.
250. Li, Y.-C.; Zhao, W.-M.; Xiang, W.; Wu, Z.-G.; Yang, Z.-G.; Xu, C.-L.; Xu, Y.-D.; Wang, E.-H.; Wu, C.-J.; Guo, X.-D. Promoting the electrochemical performance of LiNi0.8Co0.1Mn0.1O2 cathode via LaAlO3 coating. *Journal of Alloys and Compounds* **2018**, *766*, 546-555.
251. Tong, H.; Dong, P.; Zhang, J.; Zheng, J.; Yu, W.; Wei, K.; Zhang, B.; Liu, Z.; Chu, D. Cathode material LiNi0. 8Co0. 1Mn0. 1O2/LaPO4 with high electrochemical performance for lithium-ion batteries. *Journal of Alloys and Compounds* **2018**, *764*, 44-50.
252. Peng, Z.; Li, T.; Zhang, Z.; Du, K.; Hu, G.; Cao, Y. Surface architecture decoration on enhancing properties of LiNi0· 8Co0· 1Mn0· 1O2 with building bi-phase Li3PO4 and AlPO4 by Al (H2PO4) 3 treatment. *Electrochimica Acta* **2020**, *338*, 135870.
253. Chen, X.; Tang, Y.; Fan, C.; Han, S. A highly stabilized single crystalline nickel-rich LiNi0. 8Co0. 1Mn0. 1O2 cathode through a novel surface spinel-phase modification. *Electrochimica Acta* **2020**, *341*, 136075.
254. Gan, Z.; Hu, G.; Peng, Z.; Cao, Y.; Tong, H.; Du, K. Surface modification of LiNi0. 8Co0. 1Mn0. 1O2 by WO3 as a cathode material for LIB. *Applied surface science* **2019**, *481*, 1228-1238.
255. Zhao, E.; Chen, M.; Hu, Z.; Chen, D.; Yang, L.; Xiao, X. Improved cycle stability of high-capacity Ni-rich LiNi0. 8Mn0. 1Co0. 1O2 at high cut-off voltage by Li2SiO3 coating. *Journal of Power Sources* **2017**, *343*, 345-353.
256. Lu, J.; Peng, Q.; Wang, W.; Nan, C.; Li, L.; Li, Y. Nanoscale coating of LiMO2 (M= Ni, Co, Mn) nanobelts with Li+-conductive Li2TiO3: toward better rate capabilities for Li-ion batteries. *Journal of the American Chemical Society* **2013**, *135*, 1649-1652.
257. Huang, J.; Fang, X.; Wu, Y.; Zhou, L.; Wang, Y.; Jin, Y.; Dang, W.; Wu, L.; Rong, Z.; Chen, X. Enhanced electrochemical performance of LiNi0. 8Co0. 1Mn0. 1O2 by surface modification with lithium-active MoO3. *Journal of Electroanalytical Chemistry* **2018**, *823*, 359-367.
258. Zhang, W.; Liang, L.; Zhao, F.; Liu, Y.; Hou, L.; Yuan, C. Ni-rich LiNi0· 8Co0· 1Mn0· 1O2 coated with Li-ion conductive Li3PO4 as competitive cathodes for high-energy-density lithium ion batteries. *Electrochimica Acta* **2020**, *340*, 135871.
259. Chen, S.; He, T.; Su, Y.; Lu, Y.; Bao, L.; Chen, L.; Zhang, Q.; Wang, J.; Chen, R.; Wu, F. Ni-rich LiNi0. 8Co0. 1Mn0. 1O2 oxide coated by dual-conductive layers as high performance cathode material for lithium-ion batteries. *ACS applied materials & interfaces* **2017**, *9*, 29732-29743.

260. Feng, Z.; Rajagopalan, R.; Sun, D.; Tang, Y.; Wang, H. In-situ formation of hybrid Li3PO4-AlPO4-Al (PO3) 3 coating layer on LiNi0. 8Co0. 1Mn0. 1O2 cathode with enhanced electrochemical properties for lithium-ion battery. *Chemical Engineering Journal* **2020**, *382*, 122959.
261. Liang, H.; Jia, L.; Chen, F.; Jing, S.; Tsiakaras, P. A novel efficient electrocatalyst for oxygen reduction and oxygen evolution reaction in Li-O2 batteries: Co/CoSe embedded N, Se co-doped carbon. *Applied Catalysis B: Environmental* **2022**, *317*, 121698.
262. Jing, S.; Gai, Z.; Li, M.; Tang, S.; Ji, S.; Liang, H.; Chen, F.; Yin, S.; Tsiakaras, P. Enhanced electrochemical performance of a Li-O2 battery using Co and N co-doped biochar cathode prepared in molten salt medium. *Electrochimica Acta* **2022**, *410*, 140002.
263. Liang, H.; Gong, X.; Jia, L.; Chen, F.; Rao, Z.; Jing, S.; Tsiakaras, P. Highly efficient Li-O2 batteries based on self-standing NiFeP@ NC/BC cathode derived from biochar supported Prussian blue analogues. *Journal of Electroanalytical Chemistry* **2020**, *867*, 114124.
264. Jing, S.; Ding, P.; Zhang, Y.; Liang, H.; Yin, S.; Tsiakaras, P. Lithium-sulfur battery cathodes made of porous biochar support CoFe@ NC metal nanoparticles derived from Prussian blue analogues. *Ionics* **2019**, *25*, 5297-5304.
265. Anuphappharadorn, S.; Sukchai, S.; Sirisamphanwong, C.; Ketjoy, N. Comparison the economic analysis of the battery between lithium-ion and lead-acid in PV stand-alone application. *Energy Procedia* **2014**, *56*, 352-358.
266. Wang, Q.; Ping, P.; Zhao, X.; Chu, G.; Sun, J.; Chen, C. Thermal runaway caused fire and explosion of lithium ion battery. *Journal of power sources* **2012**, *208*, 210-224.
267. Wu, C.; Zhu, C.; Ge, Y.; Zhao, Y. A review on fault mechanism and diagnosis approach for Li-ion batteries. *Journal of Nanomaterials* **2015**, *2015*.
268. Pharr, M.M. Diffusion, deformation, and damage in lithium-ion batteries and microelectronics. 2014.
269. Feng, X.; Sun, J.; Ouyang, M.; Wang, F.; He, X.; Lu, L.; Peng, H. Characterization of penetration induced thermal runaway propagation process within a large format lithium ion battery module. *Journal of Power Sources* **2015**, *275*, 261-273.
270. Lelie, M.; Braun, T.; Knips, M.; Nordmann, H.; Ringbeck, F.; Zappen, H.; Sauer, D.U. Battery Management System Hardware Concepts: An Overview. *Applied Sciences* **2018**, *8*, 534.
271. Liu, Y.; Xie, J. Failure study of commercial LiFePO4 cells in overcharge conditions using electrochemical impedance spectroscopy. *Journal of The Electrochemical Society* **2015**, *162*, A2208.
272. Ouyang, D.; Chen, M.; Liu, J.; Wei, R.; Weng, J.; Wang, J. Investigation of a commercial lithium-ion battery under overcharge/over-discharge failure conditions. *RSC advances* **2018**, *8*, 33414-33424.
273. Guo, R.; Lu, L.; Ouyang, M.; Feng, X. Mechanism of the entire overdischarge process and overdischarge-induced internal short circuit in lithium-ion batteries. *Scientific reports* **2016**, *6*, 1-9.
274. Fear, C.; Juarez-Robles, D.; Jeevarajan, J.A.; Mukherjee, P.P. Elucidating copper dissolution phenomenon in Li-ion cells under overdischarge extremes. *Journal of The Electrochemical Society* **2018**, *165*, A1639.
275. Doughty, D.H.; Roth, E.P. A general discussion of Li ion battery safety. *The Electrochemical Society Interface* **2012**, *21*, 37.
276. Wang, H.; Simunovic, S.; Maleki, H.; Howard, J.N.; Hallmark, J.A. Internal configuration of prismatic lithium-ion cells at the onset of mechanically induced short circuit. *Journal of Power Sources* **2016**, *306*, 424-430.
277. Abaza, A.; Ferrari, S.; Wong, H.K.; Lyness, C.; Moore, A.; Weaving, J.; Blanco-Martin, M.; Dashwood, R.; Bhagat, R. Experimental study of internal and external short circuits of commercial automotive pouch lithium-ion cells. *Journal of Energy Storage* **2018**, *16*, 211-217.

278. Mao, B.; Chen, H.; Cui, Z.; Wu, T.; Wang, Q. Failure mechanism of the lithium ion battery during nail penetration. *International Journal of Heat and Mass Transfer* **2018**, *122*, 1103-1115.
279. Lyu, D.; Ren, B.; Li, S. Failure modes and mechanisms for rechargeable Lithium-based batteries: a state-of-the-art review. *Acta Mechanica* **2019**, *230*, 701-727.
280. Steiger, J.; Kramer, D.; Mönig, R. Mechanisms of dendritic growth investigated by in situ light microscopy during electrodeposition and dissolution of lithium. *Journal of Power Sources* **2014**, *261*, 112-119.
281. Sano, H.; Kitta, M.; Matsumoto, H. Effect of charge transfer resistance on morphology of lithium electrodeposited in ionic liquid. *Journal of The Electrochemical Society* **2016**, *163*, D3076.
282. Tang, C.-Y.; Dillon, S.J. In situ scanning electron microscopy characterization of the mechanism for Li dendrite growth. *Journal of The Electrochemical Society* **2016**, *163*, A1660.
283. Hagopian, A.; Doublet, M.-L.; Filhol, J.-S. Thermodynamic origin of dendrite growth in metal anode batteries. *Energy & Environmental Science* **2020**, *13*, 5186-5197.
284. Stark, J.K.; Ding, Y.; Kohl, P.A. Nucleation of electrodeposited lithium metal: dendritic growth and the effect of co-deposited sodium. *Journal of The Electrochemical Society* **2013**, *160*, D337.
285. Liu, X.H.; Zhong, L.; Zhang, L.Q.; Kushima, A.; Mao, S.X.; Li, J.; Ye, Z.Z.; Sullivan, J.P.; Huang, J.Y. Lithium fiber growth on the anode in a nanowire lithium ion battery during charging. *Applied Physics Letters* **2011**, *98*, 183107.
286. Porthault, H.; Decaux, C. Electrodeposition of lithium metal thin films and its application in all-solid-state microbatteries. *Electrochimica Acta* **2016**, *194*, 330-337.
287. Aslam, M.K.; Niu, Y.; Hussain, T.; Tabassum, H.; Tang, W.; Xu, M.; Ahuja, R. How to avoid dendrite formation in metal batteries: innovative strategies for dendrite suppression. *Nano Energy* **2021**, *86*, 106142.
288. Kriston, A.; Pfrang, A.; Döring, H.; Fritsch, B.; Ruiz, V.; Adanouj, I.; Kosmidou, T.; Ungeheuer, J.; Boon-Brett, L. External short circuit performance of Graphite-LiNi1/3Co1/3Mn1/3O2 and Graphite-LiNi0. 8Co0. 15Al0. 05O2 cells at different external resistances. *Journal of Power Sources* **2017**, *361*, 170-181.
289. Rheinfeld, A.; Sturm, J.; Frank, A.; Kosch, S.; Erhard, S.V.; Jossen, A. Impact of cell size and format on external short circuit behavior of lithium-ion cells at varying cooling conditions: modeling and simulation. *Journal of The Electrochemical Society* **2019**, *167*, 013511.
290. Panda, S.; Sahu, B.K.; Mohanty, P.K. Design and performance analysis of PID controller for an automatic voltage regulator system using simplified particle swarm optimization. *Journal of the Franklin Institute* **2012**, *349*, 2609-2625.
291. Lystianingrum, V.; Hredzak, B.; Agelidis, V.G. Multiple model estimator based detection of abnormal cell overheating in a Li-ion battery string with minimum number of temperature sensors. *Journal of Power Sources* **2015**, *273*, 1171-1181.
292. Ruiz, V.; Pfrang, A.; Kriston, A.; Omar, N.; Van den Bossche, P.; Boon-Brett, L. A review of international abuse testing standards and regulations for lithium ion batteries in electric and hybrid electric vehicles. *Renewable and Sustainable Energy Reviews* **2018**, *81*, 1427-1452.
293. Larsson, F.; Andersson, P.; Blomqvist, P.; Mellander, B.-E. Toxic fluoride gas emissions from lithium-ion battery fires. *Scientific reports* **2017**, *7*, 1-13.
294. Ma, S.; Jiang, M.; Tao, P.; Song, C.; Wu, J.; Wang, J.; Deng, T.; Shang, W. Temperature effect and thermal impact in lithium-ion batteries: A review. *Progress in Natural Science: Materials International* **2018**, *28*, 653-666.
295. Wilke, S.; Schweitzer, B.; Khateeb, S.; Al-Hallaj, S. Preventing thermal runaway propagation in lithium ion battery packs using a phase change composite material: An experimental study. *Journal of Power Sources* **2017**, *340*, 51-59.

296. Galushkin, N.E.; Yazvinskaya, N.N.; Galushkin, D.N. Mechanism of Thermal Runaway in Lithium-Ion Cells. *Journal of The Electrochemical Society* **2018**, *165*, A1303.
297. Laidler, K.J. The development of the Arrhenius equation. *Journal of chemical Education* **1984**, *61*, 494.
298. Zhang, S.; Xu, K.; Jow, T. Low-temperature performance of Li-ion cells with a LiBF4-based electrolyte. *Journal of Solid State Electrochemistry* **2003**, *7*, 147-151.
299. Jaguemont, J.; Boulon, L.; Dubé, Y. A comprehensive review of lithium-ion batteries used in hybrid and electric vehicles at cold temperatures. *Applied Energy* **2016**, *164*, 99-114.
300. Jow, T.R.; Delp, S.A.; Allen, J.L.; Jones, J.-P.; Smart, M.C. Factors limiting Li+ charge transfer kinetics in Li-ion batteries. *Journal of the electrochemical society* **2018**, *165*, A361.
301. Nagasubramanian, G. Electrical characteristics of 18650 Li-ion cells at low temperatures. *Journal of applied electrochemistry* **2001**, *31*, 99-104.
302. Zhang, X.; Zhang, W.; Li, H.; Zhang, M. Review on state of charge estimation methods for li-ion batteries. *Transactions on Electrical and Electronic Materials* **2017**, *18*, 136-140.
303. Bugga, R.; Smart, M.; Whitacre, J.; West, W. Lithium ion batteries for space applications. In Proceedings of the 2007 IEEE Aerospace Conference, 2007; pp. 1-7.
304. Wang, H.; Zhang, H.; Cheng, Y.; Feng, K.; Li, X.; Zhang, H. All-NASICON LVP-LTP aqueous lithium ion battery with excellent stability and low-temperature performance. *Electrochimica Acta* **2018**, *278*, 279-289.
305. Li, Q.; Jiao, S.; Luo, L.; Ding, M.S.; Zheng, J.; Cartmell, S.S.; Wang, C.-M.; Xu, K.; Zhang, J.-G.; Xu, W. Wide-temperature electrolytes for lithium-ion batteries. *ACS applied materials & interfaces* **2017**, *9*, 18826-18835.
306. Kinoshita, S.-c.; Kotato, M.; Sakata, Y.; Ue, M.; Watanabe, Y.; Morimoto, H.; Tobishima, S.-i. Effects of cyclic carbonates as additives to γ-butyrolactone electrolytes for rechargeable lithium cells. *Journal of power sources* **2008**, *183*, 755-760.
307. Yang, B.; Zhang, H.; Yu, L.; Fan, W.; Huang, D. Lithium difluorophosphate as an additive to improve the low temperature performance of LiNi0.5Co0.2Mn0.3O2/graphite cells. *Electrochimica Acta* **2016**, *221*, 107-114.
308. Aris, A.M.; Shabani, B. An experimental study of a lithium ion cell operation at low temperature conditions. *Energy Procedia* **2017**, *110*, 128-135.
309. Gao, F.; Tang, Z. Kinetic behavior of LiFePO4/C cathode material for lithium-ion batteries. *Electrochimica Acta* **2008**, *53*, 5071-5075.
310. Zhang, S.; Xu, K.; Jow, T. The low temperature performance of Li-ion batteries. *Journal of Power Sources* **2003**, *115*, 137-140.
311. Rui, X.; Jin, Y.; Feng, X.; Zhang, L.; Chen, C. A comparative study on the low-temperature performance of LiFePO4/C and Li3V2 (PO4) 3/C cathodes for lithium-ion batteries. *Journal of Power Sources* **2011**, *196*, 2109-2114.
312. Petzl, M.; Danzer, M.A. Nondestructive detection, characterization, and quantification of lithium plating in commercial lithium-ion batteries. *Journal of Power Sources* **2014**, *254*, 80-87.
313. Petzl, M.; Kasper, M.; Danzer, M.A. Lithium plating in a commercial lithium-ion battery–A low-temperature aging study. *Journal of power sources* **2015**, *275*, 799-807.
314. Zinth, V.; Von Lüders, C.; Hofmann, M.; Hattendorff, J.; Buchberger, I.; Erhard, S.; Rebelo-Kornmeier, J.; Jossen, A.; Gilles, R. Lithium plating in lithium-ion batteries at sub-ambient temperatures investigated by in situ neutron diffraction. *Journal of Power Sources* **2014**, *271*, 152-159.
315. Gunawardhana, N.; Dimov, N.; Sasidharan, M.; Park, G.-J.; Nakamura, H.; Yoshio, M. Suppression of lithium deposition at sub-zero temperatures on graphite by surface modification. *Electrochemistry communications* **2011**, *13*, 1116-1118.

316. Liu, H.; Wei, Z.; He, W.; Zhao, J. Thermal issues about Li-ion batteries and recent progress in battery thermal management systems: A review. *Energy conversion and management* **2017**, *150*, 304-330.
317. Knazs, E. A Safer Way to Design Electric Vehicle Battery Packs. Available online: https://www.hbfuller.com/zh/asia-pacific/news-and-events/glue-talk-blog/2019/september/a-safer-way-to-design-electric-vehicle-battery-packs.
318. Xiao, M.; Choe, S.-Y. Theoretical and experimental analysis of heat generations of a pouch type LiMn2O4/carbon high power Li-polymer battery. *Journal of power sources* **2013**, *241*, 46-55.
319. Zhang, X. Thermal analysis of a cylindrical lithium-ion battery. *Electrochimica Acta* **2011**, *56*, 1246-1255.
320. Yang, H.; Prakash, J. Determination of the Reversible and Irreversible Heats of a LiNi0. 8Co0. 15Al0. 05 O 2/Natural Graphite Cell Using Electrochemical-Calorimetric Technique. *Journal of the Electrochemical Society* **2004**, *151*, A1222.
321. Lu, W.; Prakash, J. In situ measurements of heat generation in a Li/mesocarbon microbead half-cell. *Journal of the Electrochemical Society* **2003**, *150*, A262.
322. Robinson, J.B.; Shearing, P.R.; Brett, D.J. Thermal imaging of electrochemical power systems: a review. *Journal of Imaging* **2016**, *2*, 2.
323. Lai, Y.; Du, S.; Ai, L.; Ai, L.; Cheng, Y.; Tang, Y.; Jia, M. Insight into heat generation of lithium ion batteries based on the electrochemical-thermal model at high discharge rates. *International Journal of Hydrogen Energy* **2015**, *40*, 13039-13049.
324. Du, S.; Lai, Y.; Ai, L.; Ai, L.; Cheng, Y.; Tang, Y.; Jia, M. An investigation of irreversible heat generation in lithium ion batteries based on a thermo-electrochemical coupling method. *Applied Thermal Engineering* **2017**, *121*, 501-510.
325. Nyman, A.; Zavalis, T.G.; Elger, R.; Behm, M.; Lindbergh, G. Analysis of the polarization in a Li-ion battery cell by numerical simulations. *Journal of The Electrochemical Society* **2010**, *157*, A1236.
326. Yang, X.-G.; Zhang, G.; Wang, C.-Y. Computational design and refinement of self-heating lithium ion batteries. *Journal of Power Sources* **2016**, *328*, 203-211.
327. Yan, B.; Lim, C.; Yin, L.; Zhu, L. Simulation of heat generation in a reconstructed LiCoO2 cathode during galvanostatic discharge. *Electrochimica Acta* **2013**, *100*, 171-179.
328. Bernardi, D.; Pawlikowski, E.; Newman, J. A general energy balance for battery systems. *Journal of the electrochemical society* **1985**, *132*, 5.
329. Esmaeili, J.; Jannesari, H. Developing heat source term including heat generation at rest condition for Lithium-ion battery pack by up scaling information from cell scale. *Energy Conversion and Management* **2017**, *139*, 194-205.
330. Vishwakarma, V.; Jain, A. Measurement of in-plane thermal conductivity and heat capacity of separator in Li-ion cells using a transient DC heating method. *Journal of Power Sources* **2014**, *272*, 378-385.
331. Yang, Y.; Huang, X.; Cao, Z.; Chen, G. Thermally conductive separator with hierarchical nano/microstructures for improving thermal management of batteries. *Nano Energy* **2016**, *22*, 301-309.
332. Maleki, H.; Al Hallaj, S.; Selman, J.R.; Dinwiddie, R.B.; Wang, H. Thermal properties of lithium-ion battery and components. *Journal of the Electrochemical Society* **1999**, *146*, 947.
333. Zavalis, T.G.; Klett, M.; Kjell, M.H.; Behm, M.; Lindström, R.W.; Lindbergh, G. Aging in lithium-ion batteries: Model and experimental investigation of harvested LiFePO4 and mesocarbon microbead graphite electrodes. *Electrochimica Acta* **2013**, *110*, 335-348.
334. Ecker, M.; Nieto, N.; Käbitz, S.; Schmalstieg, J.; Blanke, H.; Warnecke, A.; Sauer, D.U. Calendar and cycle life study of Li (NiMnCo) O2-based 18650 lithium-ion batteries. *Journal of Power Sources* **2014**, *248*, 839-851.

335. Liu, Y.; Xie, K.; Pan, Y.; Li, Y.; Wang, H.; Lu, W.; Zheng, C. LiPON as a protective layer on graphite anode to extend the storage life of Li-ion battery at elevated temperature. *Ionics* **2018**, *24*, 723-734.
336. Gabrisch, H.; Ozawa, Y.; Yazami, R. Crystal structure studies of thermally aged LiCoO2 and LiMn2O4 cathodes. *Electrochimica Acta* **2006**, *52*, 1499-1506.
337. Bodenes, L.; Naturel, R.; Martinez, H.; Dedryvère, R.; Menetrier, M.; Croguennec, L.; Pérès, J.-P.; Tessier, C.; Fischer, F. Lithium secondary batteries working at very high temperature: Capacity fade and understanding of aging mechanisms. *Journal of Power Sources* **2013**, *236*, 265-275.
338. Waldmann, T.; Wilka, M.D.; Kasper, M.; Fleischhammer, M.; Wohlfahrt-Mehrens, M. Temperature dependent ageing mechanisms in Lithium-ion batteries – A Post-Mortem study. *Journal of Power Sources* **2014**, *262*, 129-135.
339. Handel, P.; Fauler, G.; Kapper, K.; Schmuck, M.; Stangl, C.; Fischer, R.; Uhlig, F.; Koller, S. Thermal aging of electrolytes used in lithium-ion batteries – An investigation of the impact of protic impurities and different housing materials. *Journal of Power Sources* **2014**, *267*, 255-259.
340. Leng, F.; Tan, C.M.; Pecht, M. Effect of Temperature on the Aging rate of Li Ion Battery Operating above Room Temperature. *Scientific Reports* **2015**, *5*, 12967.
341. Diao, W.; Xing, Y.; Saxena, S.; Pecht, M. Evaluation of Present Accelerated Temperature Testing and Modeling of Batteries. *Applied Sciences* **2018**, *8*, 1786.
342. Xu, B.; Shi, Y.; Kirschen, D.S.; Zhang, B. Optimal regulation response of batteries under cycle aging mechanisms. *2017 IEEE 56th Annual Conference on Decision and Control (CDC)* **2017**, 751-756.
343. Xu, J.; Deshpande, R.; Pan, J.; Cheng, Y.-T.; Battaglia, V. Electrode Side Reactions, Capacity Loss and Mechanical Degradation in Lithium-Ion Batteries. *Journal of The Electrochemical Society* **2015**, *162*, 2026-2035.
344. Kanevskii, L.S.; Dubasova, V.S. Degradation of lithium-ion batteries and how to fight it: A review. *Russian Journal of Electrochemistry* **2005**, *41*, 1-16.
345. Z. Liu, Q.A., G. Rizzoni, H. He. *Fault Detection and Isolation for Lithium-Ion Battery System Using Structural Analysis and Sequential Residual Generation. In Proceedings of the ASME 7th annual dynamic systems and control conference*; San Antonio, 2014; Volume TX.
346. Tran, M.-K.; Fowler, M. Sensor Fault Detection and Isolation for Degrading Lithium-Ion Batteries in Electric Vehicles Using Parameter Estimation with Recursive Least Squares. *Batteries* **2020**, *6*, 1.
347. Xiong, R.; Yu, Q.; Shen, W. Review on sensors fault diagnosis and fault-tolerant techniques for lithium ion batteries in electric vehicles. *2018 13th IEEE Conference on Industrial Electronics and Applications (ICIEA)* **2018**, 406-410.
348. Xiong, R.; Yu, Q.; Shen, W.; Lin, C.; Sun, F. A Sensor Fault Diagnosis Method for a Lithium-Ion Battery Pack in Electric Vehicles. *IEEE Transactions on Power Electronics* **2019**, *34*, 9709-9718.
349. Lee, C.-Y.; Lee, S.-J.; Tang, M.-S.; Chen, P.-C. In Situ Monitoring of Temperature inside Lithium-Ion Batteries by Flexible Micro Temperature Sensors. *Sensors* **2011**, *11*, 9942-9950.
350. Micro-Measurements -VPG. **(2021)**.
351. C. Zheng, Z.C., D. Huang. Fault diagnosis of voltage sensor and current sensor for lithium-ion battery pack using hybrid system modeling and unscented particle filter. *Energy* **(2020)**, *191*, 116504.
352. Liu, Z.; Ahmed, Q.; Zhang, J.; Rizzoni, G.; He, H. Structural analysis based sensors fault detection and isolation of cylindrical lithium-ion batteries in automotive applications. *Control Engineering Practice* **2016**, *52*, 46-58.
353. Xia, G.; Cao, L.; Bi, G. A review on battery thermal management in electric vehicle application. *Journal of Power Sources* **2017**, *367*, 90-105.
354. Ling, C. A Review of Lithium-Ion Battery Thermal Management System Strategies and the Evaluate Criteria. *International journal of electrochemical science* **2020**, *14*, 6077-6107.

355. Yao, L.; Wang, Z.; Ma, J. Fault detection of the connection of lithium-ion power batteries based on entropy for electric vehicles. *Journal of Power Sources* **2015**, *293*, 548-561.
356. Offer, G.; Yufit, V.; Howey, D.; Wu, B.; Brandon, N. Module design and fault diagnosis in electric vehicle batteries. *Journal of Power Sources* **2012**, *206*, 383-392.
357. Kang, T.; Park, S.; Lee, P.-Y.; Cho, I.-H.; Yoo, K.; Kim, J. Thermal Analysis of a Parallel-Configured Battery Pack (1S18P) Using 21700 Cells for a Battery-Powered Train. *Electronics* **2020**, *9*, 447.
358. Lee, S.; Kim, J. Power Capability Analysis of Lithium Battery and Supercapacitor by Pulse Duration. *Electronics* **2019**, *8*, 1395.
359. Gabbar, H.A.; Othman, A.M.; Abdussami, M.R. Review of Battery Management Systems (BMS) Development and Industrial Standards. *Technologies* **2021**, *9*, 28.
360. Kokkotis, P.I.; Psomopoulos, C.S.; Ioannidis, G.C.; Kaminaris, S.D. Small scale energy storage systems. A short review in their potential environmental impact. *Fresenius Environ. Bull* **2017**, *26*, 5658-5665.
361. Lelie, M.; Braun, T.; Knips, M.; Nordmann, H.; Ringbeck, F.; Zappen, H.; Sauer, D.U. Battery Management System Hardware Concepts: An Overview. *Applied Sciences* **2018**, *8*, 534.
362. Rahimi-Eichi, H.; Ojha, U.; Baronti, F.; Chow, M.-Y. Battery Management System: An Overview of Its Application in the Smart Grid and Electric Vehicles. *IEEE Industrial Electronics Magazine* **2013**, *7*, 4-16.
363. Lu, L.; Han, X.; Jianqiu, L.; Hua, J.; Ouyang, M. A review on the key issues for lithium-ion battery management in electric vehicles. *Journal of Power Sources* **2013**, *226*, 272–288.
364. Francesco Ferracuti; and, A.F.; Monteriù, A. *Algorithms for Fault Detection and Diagnosis*; Switzerland, 2021.
365. Alavi, S.M.M.; Samadi, M.F.; Saif, M. Diagnostics in Lithium-Ion Batteries: Challenging Issues and Recent Achievements. In *Integration of Practice-Oriented Knowledge Technology: Trends and Prospectives*, Fathi, M., Ed.; Springer Berlin Heidelberg: Berlin, Heidelberg, 2013; pp. 277-291.
366. Venkatasubramanian, V.; Rengaswamy, R.; Yin, K.; Kavuri, S.N. A review of process fault detection and diagnosis: Part I: Quantitative model-based methods. *Computers & Chemical Engineering* **2003**, *27*, 293-311.
367. Piątek, J.; Afyon, S.; Budnyak, T.M.; Budnyk, S.; Sipponen, M.H.; Slabon, A. Sustainable Li-Ion Batteries: Chemistry and Recycling. *Advanced Energy Materials* **2021**, *11*, 2003456.
368. Fan, E.; Li, L.; Wang, Z.; Lin, J.; Huang, Y.; Yao, Y.; Chen, R.; Wu, F. Sustainable Recycling Technology for Li-Ion Batteries and Beyond: Challenges and Future Prospects. *Chemical Reviews* **2020**, *120*, 7020-7063.
369. Lai, X.; Huang, Y.; Gu, H.; Deng, C.; Han, X.; Feng, X.; Zheng, Y. Turning waste into wealth: A systematic review on echelon utilization and material recycling of retired lithium-ion batteries. *Energy Storage Materials* **2021**, *40*, 96-123.
370. Zheng, X.; Zhu, Z.; Lin, X.; Zhang, Y.; He, Y.; Cao, H.; Sun, Z. A Mini-Review on Metal Recycling from Spent Lithium Ion Batteries. *Engineering* **2018**, *4*, 361-370.
371. Hayes, S.M.; McCullough, E.A. Critical minerals: A review of elemental trends in comprehensive criticality studies. *Resources Policy* **2018**, *59*, 192-199.
372. Yan, W.; Cao, H.; Zhang, Y.; Ning, P.; Song, Q.; Yang, J.; Sun, Z. Rethinking Chinese supply resilience of critical metals in lithium-ion batteries. *Journal of Cleaner Production* **2020**, *256*, 120719.
373. Chen, M.; Ma, X.; Chen, B.; Arsenault, R.; Karlson, P.; Simon, N.; Wang, Y. Recycling End-of-Life Electric Vehicle Lithium-Ion Batteries. *Joule* **2019**, *3*, 2622-2646.
374. Zhao, S.; He, W.; Li, G. Recycling Technology and Principle of Spent Lithium-Ion Battery. In *Recycling of Spent Lithium-Ion Batteries: Processing Methods and Environmental Impacts*, An, L., Ed.; Springer International Publishing: Cham, 2019; pp. 1-26.

375. Beaudet, A.; Larouche, F.; Amouzegar, K.; Bouchard, P.; Zaghib, K. Key Challenges and Opportunities for Recycling Electric Vehicle Battery Materials. *Sustainability* **2020**, *12*, 5837.
376. Larouche, F.; Tedjar, F.; Amouzegar, K.; Houlachi, G.; Bouchard, P.; Demopoulos, G.P.; Zaghib, K. Progress and Status of Hydrometallurgical and Direct Recycling of Li-Ion Batteries and Beyond. *Materials* **2020**, *13*, 801.
377. Mayyas, A.; Steward, D.; Mann, M. The case for recycling: Overview and challenges in the material supply chain for automotive li-ion batteries. *Sustainable Materials and Technologies* **2019**, *19*, e00087.
378. Xu, P.; Dai, Q.; Gao, H.; Liu, H.; Zhang, M.; Li, M.; Chen, Y.; An, K.; Meng, Y.S.; Liu, P.; et al. Efficient Direct Recycling of Lithium-Ion Battery Cathodes by Targeted Healing. *Joule* **2020**, *4*, 2609-2626.
379. Xu, J.; Thomas, H.R.; Francis, R.W.; Lum, K.R.; Wang, J.; Liang, B. A review of processes and technologies for the recycling of lithium-ion secondary batteries. *Journal of Power Sources* **2008**, *177*, 512-527.
380. Vanitha, M.; Balasubramanian, N. Waste minimization and recovery of valuable metals from spent lithium-ion batteries – a review. *Environmental Technology Reviews* **2013**, *2*, 101-115.
381. Ordoñez, J.; Gago, E.J.; Girard, A. Processes and technologies for the recycling and recovery of spent lithium-ion batteries. *Renewable and Sustainable Energy Reviews* **2016**, *60*, 195-205.
382. Yao, Y.; Zhu, M.; Zhao, Z.; Tong, B.; Fan, Y.; Hua, Z. Hydrometallurgical Processes for Recycling Spent Lithium-Ion Batteries: A Critical Review. *ACS Sustainable Chemistry & Engineering* **2018**, *6*, 13611-13627.
383. Zhang, X.; Li, L.; Fan, E.; Xue, Q.; Bian, Y.; Wu, F. Toward sustainable and systematic recycling of spent rechargeable batteries. *Chemical Society Reviews* **2018**, *47*.
384. Zeng, X.; Li, J.; Singh, N. Recycling of Spent Lithium-Ion Battery: A Critical Review. *Critical Reviews in Environmental Science and Technology* **2014**, *44*, 1129-1165.
385. Kim, S.; Bang, J.; Yoo, J.; Shin, Y.; Bae, J.; Jeong, J.; Kim, K.; Dong, P.; Kwon, K. A comprehensive review on the pretreatment process in lithium-ion battery recycling. *Journal of Cleaner Production* **2021**, *294*, 126329.
386. T. Tanii, S.T., S. Honmura, T. Kamimura, K. Sasaki, M. Yabuki, K. Nishida. Method for crushing cell. *US Patent 6*, 737.
387. Ku, H.; Jung, Y.; Jo, M.; Park, S.; Kim, S.; Yang, D.; Rhee, K.; An, E.M.; Sohn, J.; Kwon, K. Recycling of spent lithium-ion battery cathode materials by ammoniacal leaching. *J Hazard Mater* **2016**, *313*, 138-146.
388. Kang, J.; Sohn, J.-S.; Chang, H.; Senanayake, G.; Shin, S. Preparation of cobalt oxide from concentrated cathode material of spent lithium ion batteries by hydrometallurgical method. *Advanced Powder Technology - ADVANCED POWDER TECHNOL* **2010**, *21*, 175-179.
389. Li, J.; Wang, G.; Xu, Z. Generation and detection of metal ions and volatile organic compounds (VOCs) emissions from the pretreatment processes for recycling spent lithium-ion batteries. *Waste Management* **2016**, *52*, 221-227.
390. Kim, S.; Yang, D.; Rhee, K.; Sohn, J. Recycling process of spent battery modules in used hybrid electric vehicles using physical/chemical treatments. *Research on Chemical Intermediates* **2014**, *40*, 2447-2456.
391. Wang, J.; Chen, M.; Chen, H.; Luo, T.; Xu, Z. Leaching Study of Spent Li-ion Batteries. *Procedia Environmental Sciences* **2012**, *16*, 443-450.
392. Lu, M.; Zhang, H.; Wang, B.; Zheng, X.; Dai, C. The Re-Synthesis of LiCoO2 from Spent Lithium Ion Batteries Separated by Vacuum-Assisted Heat-Treating Method. 2013.

393. Li, L.; Ge, J.; Chen, R.; Wu, F.; Chen, S.; Zhang, X. Environmental friendly leaching reagent for cobalt and lithium recovery from spent lithium-ion batteries. *Waste Manag* **2010**, *30*, 2615-2621.
394. Ojanen, S.; Lundström, M.; Santasalo-Aarnio, A.; Serna-Guerrero, R. Challenging the concept of electrochemical discharge using salt solutions for lithium-ion batteries recycling. *Waste Management* **2018**, *76*, 242-249.
395. Xiao, J.; Guo, J.; Zhan, L.; Xu, Z. A cleaner approach to the discharge process of spent lithium ion batteries in different solutions. *Journal of Cleaner Production* **2020**, *255*, 120064.
396. Yao, L.P.; Zeng, Q.; Qi, T.; Li, J. An environmentally friendly discharge technology to pretreat spent lithium-ion batteries. *Journal of Cleaner Production* **2020**, *245*, 118820.
397. Li, L.; Zheng, P.; Yang, T.; Sturges, R.; Ellis, M.W.; Li, Z. Disassembly Automation for Recycling End-of-Life Lithium-Ion Pouch Cells. *JOM* **2019**, *71*, 4457-4464.
398. Fröhlich, S.; Sewing, D. The BATENUS process for recycling mixed battery waste. *Journal of Power Sources* **1995**, *57*, 27-30.
399. Pinegar, H.; Smith, Y.R. Recycling of End-of-Life Lithium Ion Batteries, Part I: Commercial Processes. *Journal of Sustainable Metallurgy* **2019**, *5*, 402 - 416.
400. Granata, G.; Pagnanelli, F.; Moscardini, E.; Takacova, Z.; Havlik, T.; Toro, L. Simultaneous recycling of nickel metal hydride, lithium ion and primary lithium batteries: Accomplishment of European Guidelines by optimizing mechanical pre-treatment and solvent extraction operations. *Journal of Power Sources* **2012**, *212*, 205-211.
401. Zhang, T.; He, Y.; Ge, L.; Fu, R.; Zhang, X.; Huang, Y. Characteristics of wet and dry crushing methods in the recycling process of spent lithium-ion batteries. *Journal of Power Sources* **2013**, *240*, 766-771.
402. Zhang, T.; He, Y.; Wang, F.; Ge, L.; Zhu, X.; Li, H. Chemical and process mineralogical characterizations of spent lithium-ion batteries: an approach by multi-analytical techniques. *Waste Manag* **2014**, *34*, 1051-1058.
403. Li, L.; Ge, J.; Wu, F.; Chen, R.; Chen, S.; Wu, B. Recovery of cobalt and lithium from spent lithium ion batteries using organic citric acid as leachant. *J Hazard Mater* **2010**, *176*, 288-293.
404. Li, L.; Dunn, J.B.; Zhang, X.X.; Gaines, L.; Chen, R.J.; Wu, F.; Amine, K. Recovery of metals from spent lithium-ion batteries with organic acids as leaching reagents and environmental assessment. *Journal of Power Sources* **2013**, *233*, 180-189.
405. Guan, J.; Li, Y.; Guo, Y.; Su, R.; Gao, G.; Song, H.; Yuan, H.; Liang, B.; Guo, Z. Mechanochemical Process Enhanced Cobalt and Lithium Recycling from Wasted Lithium-Ion Batteries. *ACS Sustainable Chemistry & Engineering* **2017**, *5*, 1026-1032.
406. Wang, X.; Gaustad, G.; Babbitt, C.W. Targeting high value metals in lithium-ion battery recycling via shredding and size-based separation. *Waste Manag* **2016**, *51*, 204-213.
407. Pagnanelli, F.; Moscardini, E.; Altimari, P.; Abo Atia, T.; Toro, L. Cobalt products from real waste fractions of end of life lithium ion batteries. *Waste Manag* **2016**, *51*, 214-221.
408. Barik, S.P.; Prabaharan, G.; Kumar, L. Leaching and separation of Co and Mn from electrode materials of spent lithium-ion batteries using hydrochloric acid: Laboratory and pilot scale study. *Journal of Cleaner Production* **2017**, *147*, 37-43.
409. Diekmann, J.; Hanisch, C.; Froböse, L.; Schälicke, G.; Loellhoeffel, T.; Fölster, A.-S.; Kwade, A. Ecological Recycling of Lithium-Ion Batteries from Electric Vehicles with Focus on Mechanical Processes. *Journal of The Electrochemical Society* **2017**, *164*, A6184.
410. Yu, J.; He, Y.; Ge, Z.; Li, H.; Xie, W.; Wang, S. A promising physical method for recovery of LiCoO2 and graphite from spent lithium-ion batteries: Grinding flotation. *Separation and Purification Technology* **2018**, *190*, 45-52.

411. Wang, H.; Liu, J.; Bai, X.; Wang, S.; Yang, D.; Fu, Y.; He, Y. Separation of the cathode materials from the Al foil in spent lithium-ion batteries by cryogenic grinding. *Waste Manag* **2019**, *91*, 89-98.
412. Liu, J.; Wang, H.; Hu, T.; Bai, X.; Wang, S.; Xie, W.; Hao, J.; He, Y. Recovery of LiCoO2 and graphite from spent lithium-ion batteries by cryogenic grinding and froth flotation. *Minerals Engineering* **2020**, *148*, 106223.
413. Lee, C.K.; Rhee, K.-I. Preparation of LiCoO2 from spent lithium-ion batteries. *Journal of Power Sources* **2002**, *109*, 17-21.
414. Chen, L.; Tang, X.; Zhang, Y.; Li, L.; Zeng, Z.; Zhang, Y. Process for the recovery of cobalt oxalate from spent lithium-ion batteries. *Hydrometallurgy* **2011**, *108*, 80-86.
415. Shin, S.M.; Kim, N.H.; Sohn, J.S.; Yang, D.H.; Kim, Y.H. Development of a metal recovery process from Li-ion battery wastes. *Hydrometallurgy* **2005**, *79*, 172-181.
416. Kang, J.; Senanayake, G.; Sohn, J.; Shin, S.M. Recovery of cobalt sulfate from spent lithium ion batteries by reductive leaching and solvent extraction with Cyanex 272. *Hydrometallurgy* **2010**, *100*, 168-171.
417. Zeng, G.; Deng, X.; Luo, S.; Luo, X.; Zou, J. A copper-catalyzed bioleaching process for enhancement of cobalt dissolution from spent lithium-ion batteries. *J Hazard Mater* **2012**, *199-200*, 164-169.
418. Granata, G.; Moscardini, E.; Pagnanelli, F.; Trabucco, F.; Toro, L. Product recovery from Li-ion battery wastes coming from an industrial pre-treatment plant: Lab scale tests and process simulations. *Journal of Power Sources* **2012**, *206*, 393-401.
419. Li, J.; Shi, P.; Wang, Z.; Chen, Y.; Chang, C.C. A combined recovery process of metals in spent lithium-ion batteries. *Chemosphere* **2009**, *77*, 1132-1136.
420. Zhang, G.; Du, Z.; He, Y.; Wang, H.; Xie, W.; Zhang, T. A Sustainable Process for the Recovery of Anode and Cathode Materials Derived from Spent Lithium-Ion Batteries. *Sustainability* **2019**, *11*, 2363.
421. Zhang, G.; He, Y.; Feng, Y.; Wang, H.; Zhang, T.; Xie, W.; Zhu, X. Enhancement in liberation of electrode materials derived from spent lithium-ion battery by pyrolysis. *Journal of Cleaner Production* **2018**, *199*, 62-68.
422. Zhang, G.; He, Y.; Wang, H.; Feng, Y.; Xie, W.; Zhu, X. Removal of Organics by Pyrolysis for Enhancing Liberation and Flotation Behavior of Electrode Materials Derived from Spent Lithium-Ion Batteries. *ACS Sustainable Chemistry & Engineering* **2020**, *8*, 2205-2214.
423. Bi, H.; Zhu, H.; Zu, L.; Bai, Y.; Gao, S.; Gao, Y. A new model of trajectory in eddy current separation for recovering spent lithium iron phosphate batteries. *Waste Management* **2019**, *100*, 1-9.
424. Marinos, D.; Mishra, B. An Approach to Processing of Lithium-Ion Batteries for the Zero-Waste Recovery of Materials. *Journal of Sustainable Metallurgy* **2015**, *1*, 263-274.
425. A.V.M. Silveira, M.P.S., E.H. Tanabe D.A. Bertuol. Recovery of valuable materials from spent lithium-ion batteries using electrostatic separation. *Int. J. Miner. Process.* **2017**, *169*, 91-98.
426. Widijatmoko, S.D.; Fu, G.; Wang, Z.; Hall, P. Recovering lithium cobalt oxide, aluminium, and copper from spent lithium-ion battery via attrition scrubbing. *Journal of Cleaner Production* **2020**, *260*, 120869.
427. Widijatmoko, S.D.; Gu, F.; Wang, Z.; Hall, P. Selective liberation in dry milled spent lithium-ion batteries. *Sustainable Materials and Technologies* **2020**, *23*, e00134.
428. Georgi-Maschler, T.; Friedrich, B.; Weyhe, R.; Heegn, H.; Rutz, M. Development of a recycling process for Li-ion batteries. *Journal of Power Sources* **2012**, *207*, 173-182.
429. Contestabile, M.; Panero, S.; Scrosati, B. A laboratory-scale lithium-ion battery recycling process. *Journal of Power Sources* **2001**, *92*, 65-69.

430. Song, D.; Wang, X.; Zhou, E.; Hou, P.; Guo, F.; Zhang, L. Recovery and heat treatment of the Li(Ni1/3Co1/3Mn1/3)O2 cathode scrap material for lithium ion battery. *Journal of Power Sources* **2013**, *232*, 348-352.
431. Song, D.; Wang, X.; Nie, H.; Shi, H.; Wang, D.; Guo, F.; Shi, X.; Zhang, L. Heat treatment of LiCoO2 recovered from cathode scraps with solvent method. *Journal of Power Sources* **2014**, *249*, 137-141.
432. Xu, Y.; Song, D.; Li, L.; An, C.; Wang, Y.; Jiao, L.; Yuan, H.T. A simple solvent method for the recovery of LixCoO2 and its applications in alkaline rechargeable batteries. *Journal of Power Sources* **2014**, *252*, 286-291.
433. Yang, L.; Xi, G.; Xi, Y. Recovery of Co, Mn, Ni, and Li from spent lithium ion batteries for the preparation of LiNixCoyMnzO2 cathode materials. *Ceramics International* **2015**, *41*, 11498-11503.
434. He, L.P.; Sun, S.Y.; Song, X.F.; Yu, J.G. Recovery of cathode materials and Al from spent lithium-ion batteries by ultrasonic cleaning. *Waste Manag* **2015**, *46*, 523-528.
435. Nayaka, G.P.; Zhang, Y.; Dong, P.; Wang, D.; Pai, K.V.; Manjanna, J.; Santhosh, G.; Duan, J.; Zhou, Z.; Xiao, J. Effective and environmentally friendly recycling process designed for LiCoO(2) cathode powders of spent Li-ion batteries using mixture of mild organic acids. *Waste Manag* **2018**, *78*, 51-57.
436. Liu, Y.-j.; Hu, Q.-y.; Li, X.-h.; Wang, Z.-x.; Guo, H.-j. Recycle and synthesis of LiCoO2 from incisors bound of Li-ion batteries. *Transactions of Nonferrous Metals Society of China* **2006**, *16*, 956-959.
437. Pinegar, H.; Smith, Y.R. Recycling of End-of-Life Lithium-Ion Batteries, Part II: Laboratory-Scale Research Developments in Mechanical, Thermal, and Leaching Treatments. *Journal of Sustainable Metallurgy* **2020**, *6*, 142-160.
438. Fouad, O.A.; Farghaly, F.I.; Bahgat, M. A novel approach for synthesis of nanocrystalline γ-LiAlO2 from spent lithium-ion batteries. *Journal of Analytical and Applied Pyrolysis* **2007**, *78*, 65-69.
439. Zhang, X.; Xie, Y.; Cao, H.; Nawaz, F.; Zhang, Y. A novel process for recycling and resynthesizing LiNi1/3Co1/3Mn1/3O2 from the cathode scraps intended for lithium-ion batteries. *Waste Manag* **2014**, *34*, 1715-1724.
440. Meng, Q.; Zhang, Y.; Dong, P. Use of glucose as reductant to recover Co from spent lithium ions batteries. *Waste Manag* **2017**, *64*, 214-218.
441. Natarajan, S.; Boricha, A.B.; Bajaj, H.C. Recovery of value-added products from cathode and anode material of spent lithium-ion batteries. *Waste Manag* **2018**, *77*, 455-465.
442. Sun, L.; Qiu, K. Vacuum pyrolysis and hydrometallurgical process for the recovery of valuable metals from spent lithium-ion batteries. *Journal of Hazardous Materials* **2011**, *194*, 378-384.
443. Zheng, R.; Zhao, L.; Wang, W.; Liu, Y.; Ma, Q.; Mu, D.; Li, R.; Dai, C. Optimized Li and Fe recovery from spent lithium-ion batteries via solution-precipitation method. *RSC Adv.* **2016**, *6*.
444. Huang, B.; Pan, Z.; Su, X.; An, L. Recycling of lithium-ion batteries: Recent advances and perspectives. *Journal of Power Sources* **2018**, *399*, 274-286.
445. Jena, K.K.; AlFantazi, A.; Mayyas, A.T. Comprehensive Review on Concept and Recycling Evolution of Lithium-Ion Batteries (LIBs). *Energy & Fuels* **2021**, *35*, 18257-18284.
446. Meshram, P.; Pandey, B.D.; Mankhand, T.R. Recovery of valuable metals from cathodic active material of spent lithium ion batteries: Leaching and kinetic aspects. *Waste Manag* **2015**, *45*, 306-313.
447. Shi, Y.; Chen, G.; Chen, Z. Effective regeneration of LiCoO₂ from spent lithium-ion batteries: a direct approach towards high-performance active particles. *Green Chemistry* **2018**, *20*, 851-862.
448. de Oliveira Demarco, J.; Cadore, J.; Oliveira, F.; Tanabe, E.; Bertuol, D. Recovery of metals from spent lithium-ion batteries using organic acids. *Hydrometallurgy* **2019**, *190*, 105169.

449. Zhao, Y.; Yuan, X.; Jiang, L.; Wen, J.; Wang, H.; Guan, R.; Zhang, J.; Zeng, G. Regeneration and reutilization of cathode materials from spent lithium-ion batteries. *Chemical Engineering Journal* **2020**, *383*, 123089.
450. Zhao, Y.; Yuan, X.; Jiang, L.; Li, X.; Zhang, J.; Wang, H. Reutilization of cathode material from spent batteries as a heterogeneous catalyst to remove antibiotics in wastewater via peroxymonosulfate activation. *Chemical Engineering Journal* **2020**, *400*, 125903.
451. Babbitt, C.W.; Althaf, S.; Cruz Rios, F.; Bilec, M.M.; Graedel, T.E. The role of design in circular economy solutions for critical materials. *One Earth* **2021**, *4*, 353-362.
452. Hanish C. , H.W., Kwade A. Recycling von Lithium-Ionen-Batterien. Braunschweig, 2012.
453. Vezzini, A. 23 - Manufacturers, Materials and Recycling Technologies. In *Lithium-Ion Batteries*, Pistoia, G., Ed.; Elsevier: Amsterdam, 2014; pp. 529-551.
454. Kotal, M.; Jakhar, S.; Roy, S.; Sharma, H.K. Cathode materials for rechargeable lithium batteries: Recent progress and future prospects. *Journal of Energy Storage* **2022**, *47*, 103534.
455. Ding, Y.-L.; Xie, J.; Cao, G.-S.; Zhu, T.-J.; Yu, H.-M.; Zhao, X.-B. Single-Crystalline LiMn2O4 Nanotubes Synthesized Via Template-Engaged Reaction as Cathodes for High-Power Lithium Ion Batteries. *Advanced Functional Materials* **2011**, *21*, 348-355.
456. Lee, S.; Cho, Y.; Song, H.-K.; Lee, K.T.; Cho, J. Carbon-Coated Single-Crystal LiMn2O4 Nanoparticle Clusters as Cathode Material for High-Energy and High-Power Lithium-Ion Batteries. *Angewandte Chemie International Edition* **2012**, *51*, 8748-8752.
457. Ohzuku, T.; Kitagawa, M.; Hirai, T. Electrochemistry of Manganese Dioxide in Lithium Nonaqueous Cell: III . X-Ray Diffractional Study on the Reduction of Spinel-Related Manganese Dioxide. *Journal of The Electrochemical Society* **1990**, *137*, 769.
458. Shin, Y.; Manthiram, A. Factors Influencing the Capacity Fade of Spinel Lithium Manganese Oxides. *Journal of The Electrochemical Society* **2004**, *151*, A204.
459. Zhang, X.; Cheng, F.; Zhang, K.; Liang, Y.; Yang, S.; Liang, J.; Chen, J. Facile polymer-assisted synthesis of LiNi0.5Mn1.5O4 with a hierarchical micro–nano structure and high rate capability. *RSC Advances* **2012**, *2*, 5669-5675.
460. Gummow, R.J.; de Kock, A.; Thackeray, M.M. Improved capacity retention in rechargeable 4 V lithium/lithium-manganese oxide (spinel) cells. *Solid State Ionics* **1994**, *69*, 59-67.
461. Rougier, A.; Saadoune, I.; Gravereau, P.; Willmann, P.; Delmas, C. Effect of cobalt substitution on cationic distribution in LiNi1 − y CoyO2 electrode materials. *Solid State Ionics* **1996**, *90*, 83-90.
462. Padhi, A.K.; Nanjundaswamy, K.S.; Goodenough, J.B. Phospho-olivines as Positive-Electrode Materials for Rechargeable Lithium Batteries. *Journal of The Electrochemical Society* **1997**, *144*, 1188.
463. Chung, S.Y.; Bloking, J.T.; Chiang, Y.M. Electronically conductive phospho-olivines as lithium storage electrodes. *Nat Mater* **2002**, *1*, 123-128.
464. Zhu, Y.; Yang, M.; Huang, Q.; Wang, D.; Yu, R.; Wang, J.; Zheng, Z.; Wang, D. V2O5 Textile Cathodes with High Capacity and Stability for Flexible Lithium-Ion Batteries. *Advanced Materials* **2020**, *32*, 1906205.
465. Nam, D.; Kwon, M.; Ko, Y.; Huh, J.; Cho, J. Aluminum textile-based binder-free nanostructured battery cathodes using a layer-by-layer assembly of metal/metal oxide nanoparticles. *Applied Physics Reviews* **2021**, *8*, 011405.
466. Qi, Z.; Xu, R.; Misra, S.; Wang, H.; Huang, J.; Zhao, K.; Wang, H. Ellipsometry-based failure analysis on translucent LiMn0.5Ni0.3Co0.2O2 in half-cell thin-film lithium-ion battery on glass substrates. *Materials Today Advances* **2021**, *10*, 100142.
467. You, Y.; Wu, X.-L.; Yin, Y.-X.; Guo, Y.-G. High-quality Prussian blue crystals as superior cathode materials for room-temperature sodium-ion batteries. *Energy & Environmental Science* **2014**, *7*, 1643-1647.

468. Gmitter, A.J.; Badway, F.; Rangan, S.; Bartynski, R.A.; Halajko, A.; Pereira, N.; Amatucci, G.G. Formation, dynamics, and implication of solid electrolyte interphase in high voltage reversible conversion fluoride nanocomposites. *Journal of Materials Chemistry* **2010**, *20*, 4149-4161.
469. Schmidt, J.P.; Chrobak, T.; Ender, M.; Illig, J.; Klotz, D.; Ivers-Tiffée, E. Studies on LiFePO4 as cathode material using impedance spectroscopy. *Journal of Power Sources* **2011**, *196*, 5342-5348.
470. Luo, C.; Xu, Y.; Zhu, Y.; Liu, Y.; Zheng, S.; Liu, Y.; Langrock, A.; Wang, C. Selenium@Mesoporous Carbon Composite with Superior Lithium and Sodium Storage Capacity. *ACS Nano* **2013**, *7*, 8003-8010.
471. Eftekhari, A. The rise of lithium–selenium batteries. *Sustainable Energy & Fuels* **2017**, *1*, 14-29.
472. Yang, C.P.; Xin, S.; Yin, Y.X.; Ye, H.; Zhang, J.; Guo, Y.G. An advanced selenium-carbon cathode for rechargeable lithium-selenium batteries. *Angew Chem Int Ed Engl* **2013**, *52*, 8363-8367.
473. Zhang, Z.; Zhang, Z.; Zhang, K.; Yang, X.; Li, Q. Improvement of electrochemical performance of rechargeable lithium–selenium batteries by inserting a free-standing carbon interlayer. *RSC Advances* **2014**, *4*, 15489-15492.
474. He, X.; Ren, J.; Wang, L.; Pu, W.; Jiang, C.; Wan, C. Expansion and shrinkage of the sulfur composite electrode in rechargeable lithium batteries. *Journal of Power Sources - J POWER SOURCES* **2009**, *190*, 154-156.
475. Ebner, M.; Marone, F.; Stampanoni, M.; Wood, V. Visualization and quantification of electrochemical and mechanical degradation in Li ion batteries. *Science* **2013**, *342*, 716-720.
476. Li, W.; Zheng, G.; Yang, Y.; Seh, Z.W.; Liu, N.; Cui, Y. High-performance hollow sulfur nanostructured battery cathode through a scalable, room temperature, one-step, bottom-up approach. *Proceedings of the National Academy of Sciences* **2013**, *110*, 7148-7153.
477. Jayaprakash, N.; Shen, J.; Moganty, S.S.; Corona, A.; Archer, L.A. Porous hollow carbon@sulfur composites for high-power lithium-sulfur batteries. *Angew Chem Int Ed Engl* **2011**, *50*, 5904-5908.
478. Wei Seh, Z.; Li, W.; Cha, J.J.; Zheng, G.; Yang, Y.; McDowell, M.T.; Hsu, P.-C.; Cui, Y. Sulphur–TiO2 yolk–shell nanoarchitecture with internal void space for long-cycle lithium–sulphur batteries. *Nature Communications* **2013**, *4*, 1331.
479. Wang, Y.L.; Sun, Q.L.; Zhao, Q.Q.; Cao, J.S.; Ye, S.H. Rechargeable lithium/iodine battery with superior high-rate capability by using iodine–carbon composite as cathode. *Energy & Environmental Science* **2011**, *4*, 3947-3950.
480. Yan, N.F.; Li, G.R.; Gao, X.P. Solar rechargeable redox flow battery based on Li2WO4/LiI couples in dual-phase electrolytes. *Journal of Materials Chemistry A* **2013**, *1*, 7012-7015.
481. Lu, K.; Hu, Z.; Ma, J.; Ma, H.; Dai, L.; Zhang, J. A rechargeable iodine-carbon battery that exploits ion intercalation and iodine redox chemistry. *Nature Communications* **2017**, *8*, 527.
482. Lyu, H.; Sun, X.-G.; Dai, S. Organic Cathode Materials for Lithium-Ion Batteries: Past, Present, and Future. *Advanced Energy and Sustainability Research* **2021**, *2*, 2000044.
483. Xie, J.; Zhang, Q. Recent progress in rechargeable lithium batteries with organic materials as promising electrodes. *Journal of Materials Chemistry A* **2016**, *4*, 7091-7106.
484. Yang, Z.; Wang, T.; Chen, H.; Suo, X.; Halstenberg, P.; Lyu, H.; Jiang, W.; Mahurin, S.M.; Popovs, I.; Dai, S. Surpassing the Organic Cathode Performance for Lithium-Ion Batteries with Robust Fluorinated Covalent Quinazoline Networks. *ACS Energy Letters* **2021**, *6*, 41-51.
485. Yang, D.-H.; Yao, Z.-Q.; Wu, D.; Zhang, Y.-H.; Zhou, Z.; Bu, X.-H. Structure-modulated crystalline covalent organic frameworks as high-rate cathodes for Li-ion batteries. *Journal of Materials Chemistry A* **2016**, *4*, 18621-18627.

486. Shadike, Z.; Lee, H.-S.; Tian, C.; Sun, K.; Song, L.; Hu, E.; Waluyo, I.; Hunt, A.; Ghose, S.; Hu, Y.; et al. Synthesis and Characterization of a Molecularly Designed High-Performance Organodisulfide as Cathode Material for Lithium Batteries. *Advanced Energy Materials* **2019**, *9*, 1900705.
487. Luo, C.; Ji, X.; Hou, S.; Eidson, N.; Fan, X.; Liang, Y.; Deng, T.; Jiang, J.; Wang, C. Azo Compounds Derived from Electrochemical Reduction of Nitro Compounds for High Performance Li-Ion Batteries. *Adv Mater* **2018**, *30*, e1706498.
488. Yang, Y.; Wang, C.; Yue, B.; Gambhir, S.; Too, C.O.; Wallace, G.G. Electrochemically Synthesized Polypyrrole/Graphene Composite Film for Lithium Batteries. *Advanced Energy Materials* **2012**, *2*, 266-272.
489. Zhu, Z.; Chen, J. Review—Advanced Carbon-Supported Organic Electrode Materials for Lithium (Sodium)-Ion Batteries. *Journal of The Electrochemical Society* **2015**, *162*, A2393.
490. Morita, Y.; Nishida, S.; Murata, T.; Moriguchi, M.; Ueda, A.; Satoh, M.; Arifuku, K.; Sato, K.; Takui, T. Organic tailored batteries materials using stable open-shell molecules with degenerate frontier orbitals. *Nat Mater* **2011**, *10*, 947-951.
491. Lee, S.; Kwon, G.; Ku, K.; Yoon, K.; Jung, S.-K.; Lim, H.-D.; Kang, K. Recent Progress in Organic Electrodes for Li and Na Rechargeable Batteries. *Advanced Materials* **2018**, *30*, 1704682.
492. Yuan, X.; Yuan, D.; Zeng, F.; Zou, W.; Tzorbatzoglou, F.; Tsiakaras, P.; Wang, Y. Preparation of graphitic mesoporous carbon for the simultaneous detection of hydroquinone and catechol. *Applied Catalysis B: Environmental* **2013**, *129*, 367-374.
493. Nzereogu, P.U.; Omah, A.D.; Ezema, F.I.; Iwuoha, E.I.; Nwanya, A.C. Anode materials for lithium-ion batteries: A review. *Applied Surface Science Advances* **2022**, *9*, 100233.
494. Guan, B.Y.; Lu, Y.; Wang, Y.; Wu, M.; Lou, X.W. Porous Iron–Cobalt Alloy/Nitrogen-Doped Carbon Cages Synthesized via Pyrolysis of Complex Metal–Organic Framework Hybrids for Oxygen Reduction. *Advanced Functional Materials* **2018**, *28*, 1706738.
495. J. Dai, J.L., Q. Zhang, M. Liao, T. Duan, W. Yao, . Microstructures fabricated from MOF template as advanced lithium-ion battery anode. *Mater. Lett* **2018**, *236*, 483–486.
496. Chen, D.; Ji, G.; Ding, B.; Ma, Y.; Qu, B.; Chen, W.; Lee, J.Y. Double Transition-Metal Chalcogenide as a High-Performance Lithium-Ion Battery Anode Material. *Industrial & Engineering Chemistry Research* **2014**, *53*, 17901-17908.
497. Sajjad, M.; Cheng, F.; Lu, W. Research progress in transition metal chalcogenide based anodes for K-ion hybrid capacitor applications: a mini-review. *RSC Advances* **2021**, *11*, 25450-25460.
498. Najam, T.; Shah, S.S.A.; Peng, L.; Javed, M.S.; Imran, M.; Zhao, M.-Q.; Tsiakaras, P. Synthesis and nano-engineering of MXenes for energy conversion and storage applications: Recent advances and perspectives. *Coordination Chemistry Reviews* **2022**, *454*, 214339.
499. Kong, F.; He, X.; Liu, Q.; Qi, X.; Sun, D.; Zheng, Y.; Wang, R.; Bai, Y. Enhanced reversible Li-ion storage in Si@Ti3C2 MXene nanocomposite. *Electrochemistry Communications* **2018**, *97*, 16-21.
500. Ding, W.; Wang, S.; Wu, X.; Wang, Y.; Li, Y.; Zhou, P.; Zhou, T.; Zhou, J.; Zhuo, S. Co0.85Se@C/Ti3C2Tx MXene hybrids as anode materials for lithium-ion batteries. *Journal of Alloys and Compounds* **2020**, *816*, 152566.
501. Logan, M.W.; Zhang, D.; Tan, B.; Gerasopoulos, K. A scalable aluminum niobate anode for high energy, high power practical lithium-ion batteries. *Journal of Materials Chemistry A* **2021**, *9*, 11228-11240.
502. Lou, X.; Li, R.; Zhu, X.; Luo, L.; Chen, Y.; Lin, C.; Li, H.; Zhao, X.S. New Anode Material for Lithium-Ion Batteries: Aluminum Niobate (AlNb11O29). *ACS Applied Materials & Interfaces* **2019**, *11*, 6089-6096.
503. Lu, X.; Jian, Z.; Fang, Z.; Gu, L.; Hu, Y.-S.; Chen, W.; Wang, Z.; Chen, L. Atomic-scale investigation on lithium storage mechanism in TiNb2O7. *Energy & Environmental Science* **2011**, *4*, 2638-2644.

504. Liu, W.; Zhi, H.; Yu, X. Recent progress in phosphorus based anode materials for lithium/sodium ion batteries. *Energy Storage Materials* **2019**, *16*, 290-322.
505. Gao, H.; Yang, F.; Zheng, Y.; Zhang, Q.; Hao, J.; Zhang, S.; Zheng, H.; Chen, J.; Liu, H.; Guo, Z. Three-Dimensional Porous Cobalt Phosphide Nanocubes Encapsulated in a Graphene Aerogel as an Advanced Anode with High Coulombic Efficiency for High-Energy Lithium-Ion Batteries. *ACS Applied Materials & Interfaces* **2019**, *11*, 5373-5379.
506. Wu, H.; Wei, K.; Tang, B.; Cui, Y.; Zhao, Y.; Xue, M.; Li, C.; Cui, Y. A novel Li3P-VP nanocomposite fabricated by pulsed laser deposition as anode material for high-capacity lithium ion batteries. *Journal of Electroanalytical Chemistry* **2019**, *841*, 21-25.
507. Wang, J.; Zhu, Y.; Zhang, C.; Kong, F.; Tao, S.; Qian, B.; Jiang, X. Bimetal phosphide Ni1.4Co0.6P nanoparticle/carbon@ nitrogen-doped graphene network as high-performance anode materials for lithium-ion batteries. *Applied Surface Science* **2019**, *485*, 413-422.
508. Doherty, C.M.; Caruso, R.A.; Drummond, C.J. High performance LiFePO4 electrode materials: influence of colloidal particle morphology and porosity on lithium-ion battery power capability. *Energy & Environmental Science* **2010**, *3*, 813-823.
509. Xing, Z.; Ju, Z.; Yang, J.; Xu, H.; Qian, Y. One-Step Hydrothermal Synthesis of ZnFe2O4 Nano-Octahedrons as a High Capacity Anode Material for Li-ion Batteries. *Nano Research* **2012**, *5*, 477-485.
510. Liu, J.; Conry, T.E.; Song, X.; Doeff, M.M.; Richardson, T.J. Nanoporous spherical LiFePO4 for high performance cathodes. *Energy & Environmental Science* **2011**, *4*, 885-888.
511. Poizot, P.; Laruelle, S.; Grugeon, S.; Dupont, L.; Tarascon, J.M. Nano-sized transition-metal oxides as negative-electrode materials for lithium-ion batteries. *Nature* **2000**, *407*, 496-499.
512. Xu, K. Li-ion battery electrolytes. *Nat Energy* **2021**, *6*
513. Huang, J.; Guo, Z.; Ma, Y.; Bin, D.; Wang, Y.; Xia, Y. Recent Progress of Rechargeable Batteries Using Mild Aqueous Electrolytes. *Small Methods* **2019**, *3*, 1800272.
514. Jia, X.; Liu, C.; Neale, Z.G.; Yang, J.; Cao, G. Active Materials for Aqueous Zinc Ion Batteries: Synthesis, Crystal Structure, Morphology, and Electrochemistry. *Chemical Reviews* **2020**, *120*, 7795-7866.
515. Huang, S.; Zhu, J.; Tian, J.; Niu, Z. Recent Progress in the Electrolytes of Aqueous Zinc-Ion Batteries. *Chemistry – A European Journal* **2019**, *25*, 14480-14494.
516. Wang, Y.; Liu, Y.; Liu, W.; Wu, J.; Li, Q.; Feng, Q.; Chen, Z.; Xiong, X.; Wang, D.; Lei, Y. Regulating the coordination structure of metal single atoms for efficient electrocatalytic CO2 reduction. *Energy & Environmental Science* **2020**, *13*, 4609-4624.
517. Cao, L.; Li, D.; Hu, E.; Xu, J.; Deng, T.; Ma, L.; Wang, Y.; Yang, X.-Q.; Wang, C. Solvation Structure Design for Aqueous Zn Metal Batteries. *Journal of the American Chemical Society* **2020**, *142*, 21404-21409.
518. Han, D.; Wu, S.; Zhang, S.; Deng, Y.; Cui, C.; Zhang, L.; Long, Y.; Li, H.; Tao, Y.; Weng, Z.; et al. A Corrosion-Resistant and Dendrite-Free Zinc Metal Anode in Aqueous Systems. *Small* **2020**, *16*, 2001736.
519. Suo, L.; Borodin, O.; Sun, W.; Fan, X.; Yang, C.; Wang, F.; Gao, T.; Ma, Z.; Schroeder, M.; von Cresce, A.; et al. Advanced High-Voltage Aqueous Lithium-Ion Battery Enabled by "Water-in-Bisalt" Electrolyte. *Angew Chem Int Ed Engl* **2016**, *55*, 7136-7141.
520. Chen, L.; Zhang, J.; Li, Q.; Vatamanu, J.; Ji, X.; Pollard, T.P.; Cui, C.; Hou, S.; Chen, J.; Yang, C.; et al. A 63 m Superconcentrated Aqueous Electrolyte for High-Energy Li-Ion Batteries. *ACS Energy Letters* **2020**, *5*, 968-974.
521. Hou, Z.; Dong, M.; Xiong, Y.; Zhang, X.; Zhu, Y.; Qian, Y. Formation of Solid–Electrolyte Interfaces in Aqueous Electrolytes by Altering Cation-Solvation Shell Structure. *Advanced Energy Materials* **2020**, *10*, 1903665.

522. CHEN Xiaoxia, L.K., WANG Baoguo. Research on high-safety electrolytes and their application in lithium-ion batteries. *Energy Storage Science and Technology* **2020**, *9*, 583-592.
523. Fan, X.; Wang, C. High-voltage liquid electrolytes for Li batteries: progress and perspectives. *Chemical Society Reviews* **2021**, *50*, 10486-10566.
524. Chen, J.; Naveed, A.; Nuli, Y.; Yang, J.; Wang, J. Designing an intrinsically safe organic electrolyte for rechargeable batteries. *Energy Storage Materials* **2020**, *31*, 382-400.
525. Liu, Z.; Huang, Y.; Huang, Y.; Yang, Q.; Li, X.; Huang, Z.; Zhi, C. Voltage issue of aqueous rechargeable metal-ion batteries. *Chemical Society Reviews* **2020**, *49*, 180-232.
526. Pan, Z.; Liu, X.; Yang, J.; Li, X.; Liu, Z.; Loh, X.J.; Wang, J. Aqueous Rechargeable Multivalent Metal-Ion Batteries: Advances and Challenges. *Advanced Energy Materials* **2021**, *11*, 2100608.
527. Zheng, Y.; Yao, Y.; Ou, J.; Li, M.; Luo, D.; Dou, H.; Li, Z.; Amine, K.; Yu, A.; Chen, Z. A review of composite solid-state electrolytes for lithium batteries: fundamentals, key materials and advanced structures. *Chemical Society Reviews* **2020**, *49*, 8790-8839.
528. Xu, L.; Lu, Y.; Zhao, C.-Z.; Yuan, H.; Zhu, G.-L.; Hou, L.-P.; Zhang, Q.; Huang, J.-Q. Toward the Scale-Up of Solid-State Lithium Metal Batteries: The Gaps between Lab-Level Cells and Practical Large-Format Batteries. *Advanced Energy Materials* **2021**, *11*, 2002360.
529. Hwang, J.; Matsumoto, K.; Chen, C.-Y.; Hagiwara, R. Pseudo-solid-state electrolytes utilizing the ionic liquid family for rechargeable batteries. *Energy & Environmental Science* **2021**, *14*, 5834-5863.
530. Ren, W.; Ding, C.; Fu, X.; Huang, Y. Advanced gel polymer electrolytes for safe and durable lithium metal batteries: Challenges, strategies, and perspectives. *Energy Storage Materials* **2021**, *34*, 515-535.
531. Wang, Z.; Li, H.; Tang, Z.; Liu, Z.; Ruan, Z.; Ma, L.; Yang, Q.; Wang, D.; Zhi, C. Hydrogel Electrolytes for Flexible Aqueous Energy Storage Devices. *Advanced Functional Materials* **2018**, *28*, 1804560.
532. Ma, C.; Cui, W.; Liu, X.; Ding, Y.; Wang, Y. In situ preparation of gel polymer electrolyte for lithium batteries: Progress and perspectives. *InfoMat* **2022**, *4*, e12232.
533. Wen, Z.; Li, Y.; Zhao, Z.; Qu, W.; Chen, N.; Xing, Y.; Ma, Y.; Li, L.; Wu, F.; Chen, R. A leaf-like Al2O3-based quasi-solid electrolyte with a fast Li+ conductive interface for stable lithium metal anodes. *Journal of Materials Chemistry A* **2020**, *8*, 7280-7287.
534. Fan, P.; Liu, H.; Marosz, V.; Samuels, N.T.; Suib, S.L.; Sun, L.; Liao, L. High Performance Composite Polymer Electrolytes for Lithium-Ion Batteries. *Advanced Functional Materials* **2021**, *31*, 2101380.
535. Zhang, Z.; Shao, Y.; Lotsch, B.; Hu, Y.-S.; Li, H.; Janek, J.; Nazar, L.F.; Nan, C.-W.; Maier, J.; Armand, M.; et al. New horizons for inorganic solid state ion conductors. *Energy & Environmental Science* **2018**, *11*, 1945-1976.
536. Jia, H.; Peng, L.; Yu, C.; Dong, L.; Cheng, S.; Xie, J. Chalcogenide-based inorganic sodium solid electrolytes. *Journal of Materials Chemistry A* **2021**, *9*, 5134-5148.
537. Liu, C.; Wang, H.-R.; Long, T.; Ma, Q.; Ning, P.; Dong, X.-R.; Zhou, C.-S.; Wu, X.-W.; Zeng, X.-X. Borosilicate Glass-Enabled Antifracture NASICON Solid Electrolytes for Lithium-Metal Batteries. *ACS Applied Energy Materials* **2022**, *5*, 3734-3740.
538. Yang, L.; Song, Y.; Liu, H.; Wang, Z.; Yang, K.; Zhao, Q.; Cui, Y.; Wen, J.; Luo, W.; Pan, F. Stable Interface between Lithium and Electrolyte Facilitated by a Nanocomposite Protective Layer. *Small Methods* **2020**, *4*, 1900751.
539. Che, H.; Chen, S.; Xie, Y.; Wang, H.; Amine, K.; Liao, X.-Z.; Ma, Z.-F. Electrolyte design strategies and research progress for room-temperature sodium-ion batteries. *Energy & Environmental Science* **2017**, *10*, 1075-1101.
540. Ma, Q.; Zeng, X.-X.; Yue, J.; Yin, Y.-X.; Zuo, T.-T.; Liang, J.-Y.; Deng, Q.; Wu, X.-W.; Guo, Y.-G. Viscoelastic and Nonflammable Interface Design–Enabled Dendrite-Free and Safe Solid Lithium Metal Batteries. *Advanced Energy Materials* **2019**, *9*, 1803854.

541. Wu, F.; Fang, S.; Kuenzel, M.; Mullaliu, A.; Kim, J.-K.; Gao, X.; Diemant, T.; Kim, G.-T.; Passerini, S. Dual-anion ionic liquid electrolyte enables stable Ni-rich cathodes in lithium-metal batteries. *Joule* **2021**, *5*, 2177-2194.
542. Hofmann, A.; Rauber, D.; Wang, T.M.; Hempelmann, R.; Kay, C.W.M.; Hanemann, T. Novel Phosphonium-Based Ionic Liquid Electrolytes for Battery Applications. *Molecules* **2022**, *27*.
543. Forsyth, M.; Porcarelli, L.; Wang, X.; Goujon, N.; Mecerreyes, D. Innovative Electrolytes Based on Ionic Liquids and Polymers for Next-Generation Solid-State Batteries. *Accounts of Chemical Research* **2019**, *52*, 686-694.
544. Xiong, S.; Liu, Y.; Jankowski, P.; Liu, Q.; Nitze, F.; Xie, K.; Song, J.; Matic, A. Design of a Multifunctional Interlayer for NASCION-Based Solid-State Li Metal Batteries. *Advanced Functional Materials* **2020**, *30*, 2001444.
545. Yu, L.; Guo, S.; Lu, Y.; Li, Y.; Lan, X.; Wu, D.; Li, R.; Wu, S.; Hu, X. Highly Tough, Li-Metal Compatible Organic–Inorganic Double-Network Solvate Ionogel. *Advanced Energy Materials* **2019**, *9*, 1900257.
546. Zhang, S.; Long, T.; Zhang, H.-Z.; Zhao, Q.-Y.; Zhang, F.; Wu, X.-W.; Zeng, X.-X. Electrolytes for Multivalent Metal-Ion Batteries: Current Status and Future Prospect. *ChemSusChem* **2022**, *15*, e202200999.
547. Heidari, A.A.; Mahdavi, H. Recent Development of Polyolefin-Based Microporous Separators for Li-Ion Batteries: A Review. *Chem Rec* **2020**, *20*, 570-595.
548. Palmer, R.J.; Staff, U.b. Polyamides, Plastics. In *Kirk-Othmer Encyclopedia of Chemical Technology*.
549. K. Chen, Y.L., H. Zhan. Advanced separators for Lithium-ion Batteries. *IOP Conference Series: Earth and Environmental Science* **2022**, *1011*, 012009.
550. Sun, Y.; Rohan, R.; Cai, W.; Wan, X.; Pareek, K.; Lin, A.; Yunfeng, Z.; Cheng, H. A Polyamide Single-Ion Electrolyte Membrane for Application in Lithium-Ion Batteries. *Energy Technology* **2014**, *2*, 698-704.
551. Li, C.; Qin, B.; Zhang, Y.; Varzi, A.; Passerini, S.; Wang, J.; Dong, J.; Zeng, D.; Liu, Z.; Cheng, H. Single-Ion Conducting Electrolyte Based on Electrospun Nanofibers for High-Performance Lithium Batteries. *Advanced Energy Materials* **2019**, *9*, 1803422.
552. Lee, M.J.; Kim, J.H.; Lim, H.S.; Lee, S.Y.; Yu, H.K.; Kim, J.H.; Lee, J.S.; Sun, Y.K.; Guiver, M.D.; Suh, K.D.; et al. Highly lithium-ion conductive battery separators from thermally rearranged polybenzoxazole. *Chem Commun (Camb)* **2015**, *51*, 2068-2071.
553. Lee, M.J.; Hwang, J.-K.; Kim, J.H.; Lim, H.-S.; Sun, Y.-K.; Suh, K.-D.; Lee, Y.M. Electrochemical performance of a thermally rearranged polybenzoxazole nanocomposite membrane as a separator for lithium-ion batteries at elevated temperature. *Journal of Power Sources* **2016**, *305*, 259-266.
554. Wang, H.-G.; Yuan, S.; Ma, D.-L.; Zhang, X.-B.; Yan, J.-M. Electrospun materials for lithium and sodium rechargeable batteries: from structure evolution to electrochemical performance. *Energy & Environmental Science* **2015**, *8*, 1660-1681.
555. Cai, M.; Yuan, D.; Zhang, X.; Pu, Y.; Liu, X.; He, H.; Zhang, L.; Ning, X. Lithium ion battery separator with improved performance via side-by-side bicomponent electrospinning of PVDF-HFP/PI followed by 3D thermal crosslinking. *Journal of Power Sources* **2020**, *461*, 228123.
556. Liu, J.; Liu, Y.; Yang, W.; Ren, Q.; Li, F.; Huang, Z. Lithium ion battery separator with high performance and high safety enabled by tri-layered SiO2@PI/m-PE/SiO2@PI nanofiber composite membrane. *Journal of Power Sources* **2018**, *396*, 265-275.
557. L. Wang, Z.W., Y. Sun, X. Liang, H. Xiang. Sb2O3 modified PVDF-CTFE electrospun fibrous membrane as a safe lithium-ion battery separator. *J. Membr. Sci* **2019**, *572*, 512-519.

558. Jang, J.; Oh, J.; Jeong, H.; Kang, W.; Jo, C. A Review of Functional Separators for Lithium Metal Battery Applications. *Materials (Basel)* **2020**, *13*.
559. Li, A.; Yuen, A.C.Y.; Wang, W.; De Cachinho Cordeiro, I.M.; Wang, C.; Chen, T.B.Y.; Zhang, J.; Chan, Q.N.; Yeoh, G.H. A Review on Lithium-Ion Battery Separators towards Enhanced Safety Performances and Modelling Approaches. *Molecules* **2021**, *26*, 478.
560. Ebensperger, A.; Maxwell, P.; Moscoso, C. The lithium industry: Its recent evolution and future prospects. *Resources Policy* **2005**, *30*, 218-231.
561. Prior, T.; Wäger, P.A.; Stamp, A.; Widmer, R.; Giurco, D. Sustainable governance of scarce metals: the case of lithium. *Sci Total Environ* **2013**, *461-462*, 785-791.
562. Wadia, C.; Albertus, P.; Srinivasan, V. Resource constraints on the battery energy storage potential for grid and transportation applications. *Journal of Power Sources* **2011**, *196*, 1593-1598.
563. Egbue, O.; Long, S.; Kim, S.D. Resource Availability and Implications for the Development of Plug-In Electric Vehicles. *Sustainability* **2022**, *14*, 1665.
564. Miao, Y.; Liu, L.; Zhang, Y.; Tan, Q.; Li, J. An overview of global power lithium-ion batteries and associated critical metal recycling. *J Hazard Mater* **2022**, *425*, 127900.
565. Gruber, P.W.; Medina, P.A.; Keoleian, G.A.; Kesler, S.E.; Everson, M.P.; Wallington, T.J. Global Lithium Availability. *Journal of Industrial Ecology* **2011**, *15*, 760-775.
566. Yaksic, A.; Tilton, J. Using the cumulative availability curve to assess the threat of mineral depletion: The case of lithium. *Resources Policy* **2009**, *34*, 185-194.
567. Shukla, A.K.; Kumar, T.P. Lithium Economy: Will It Get the Electric Traction? *J Phys Chem Lett* **2013**, *4*, 551-555.
568. Tabelin, C.B.; Dallas, J.A.; Casanova, S.; Pelech, T.M.; Bournival, G.; Saydam, S.; Canbulat, I. Towards a low-carbon society: A review of lithium resource availability, challenges and innovations in mining, extraction and recycling, and future perspectives. *Minerals Engineering* **2021**, *163*, 106743.
569. Speirs, J.; Contestabile, M.; Houari, Y.; Gross, R. The future of lithium availability for electric vehicle batteries. *Renewable and Sustainable Energy Reviews* **2014**, *35*, 183-193.
570. *Mineral commodity summaries 2021*; Reston, VA, 2021; p. 200.
571. Jiao, N.; Evans, S. Business Models for Sustainability: The Case of Second-life Electric Vehicle Batteries. *Procedia CIRP* **2016**, *40*, 250-255.
572. Panel, U.N.E.P.a.I.R. Recycling Rates of Metals: A Status Report. **(2011)**.
573. Kushnir, D.; Sandén, B.A. The time dimension and lithium resource constraints for electric vehicles. *Resources Policy* **2012**, *37*, 93-103.
574. Zhang, X.; Xie, Y.; Lin, X.; Li, H.; Cao, H. An overview on the processes and technologies for recycling cathodic active materials from spent lithium-ion batteries. *Journal of Material Cycles and Waste Management* **2013**, *15*, 420-430.
575. Silwamba, M.; Ito, M.; Hiroyoshi, N.; Tabelin, C.B.; Fukushima, T.; Park, I.; Jeon, S.; Igarashi, T.; Sato, T.; Nyambe, I.; et al. Detoxification of lead-bearing zinc plant leach residues from Kabwe, Zambia by coupled extraction-cementation method. *Journal of Environmental Chemical Engineering* **2020**, *8*, 104197.
576. Silwamba, M.; Ito, M.; Hiroyoshi, N.; Tabelin, C.; Hashizume, R.; Fukushima, T.; Park, I.; Jeon, S.; Igarashi, T.; Sato, T.; et al. Recovery of Lead and Zinc from Zinc Plant Leach Residues by Concurrent Dissolution-Cementation Using Zero-Valent Aluminum in Chloride Medium. *Metals* **2020**, *10*, 531.
577. Rosendahl, K.E.; Rubiano, D.R. How effective is lithium recycling as a remedy for resource scarcity? *Environmental and Resource Economics* **2019**, *74*, 985-1010.

578. DeRousseau, M.; Gully, B.; Taylor, C.; Apelian, D.; Wang, Y. Repurposing Used Electric Car Batteries: A Review of Options. *JOM - Journal of the Minerals, Metals and Materials Society* **2017**, *69*, 1575-1582.
579. Egbue, O.; Long, S. Barriers to widespread adoption of electric vehicles: An analysis of consumer attitudes and perceptions. *Energy Policy* **2012**, *48*, 717-729.
580. Ziemann, S.; Müller, D.B.; Schebek, L.; Weil, M. Modeling the potential impact of lithium recycling from EV batteries on lithium demand: A dynamic MFA approach. *Resources, Conservation and Recycling* **2018**.
581. Mohr, S.H.; Mudd, G.M.; Giurco, D. Lithium Resources and Production: Critical Assessment and Global Projections. *Minerals* **2012**, *2*, 65-84.
582. Maxwell, P.; Mora, M. Lithium and Chile: looking back and looking forward. *Mineral Economics* **2020**, *33*, 57-71.
583. Perspectives, I.E.A.E.T. IEA International Energy Agency: Paris, France. Available online: https://www.iea.org/reports/energy-technology-perspectives-2020